



UNIVERSITAT DE BARCELONA

Models and therapeutic approaches for Niemann-Pick (A/B and C) and other lysosomal storage disorders

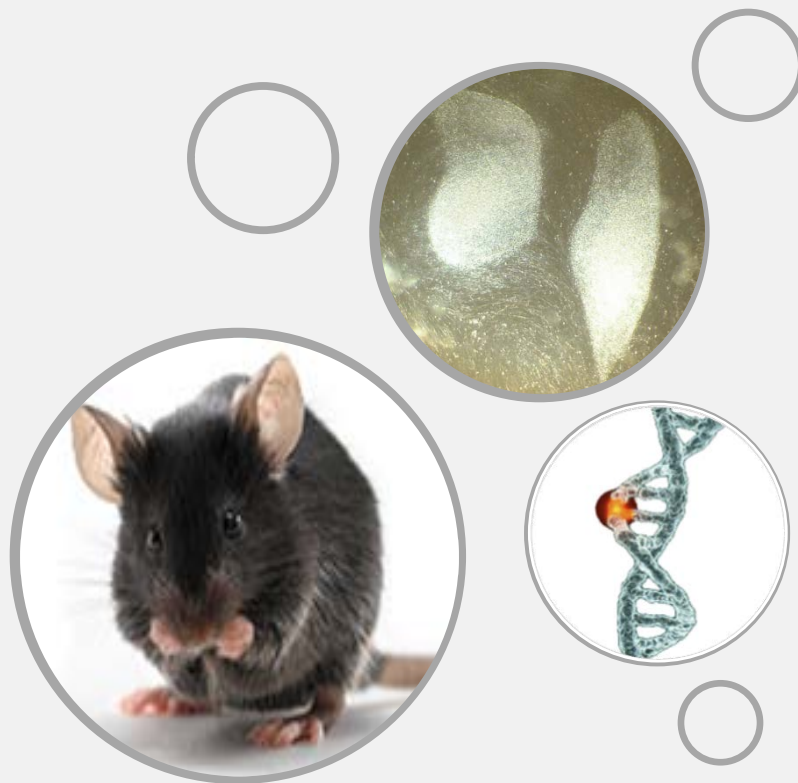
Marta Gomez Grau

ADVERTIMENT. La consulta d'aquesta tesi queda condicionada a l'acceptació de les següents condicions d'ús: La difusió d'aquesta tesi per mitjà del servei TDX (www.tdx.cat) i a través del Dipòsit Digital de la UB (diposit.ub.edu) ha estat autoritzada pels titulars dels drets de propietat intel·lectual únicament per a usos privats emmarcats en activitats d'investigació i docència. No s'autoritza la seva reproducció amb finalitats de lucre ni la seva difusió i posada a disposició des d'un lloc aliè al servei TDX ni al Dipòsit Digital de la UB. No s'autoritza la presentació del seu contingut en una finestra o marc aliè a TDX o al Dipòsit Digital de la UB (framing). Aquesta reserva de drets afecta tant al resum de presentació de la tesi com als seus continguts. En la utilització o cita de parts de la tesi és obligat indicar el nom de la persona autora.

ADVERTENCIA. La consulta de esta tesis queda condicionada a la aceptación de las siguientes condiciones de uso: La difusión de esta tesis por medio del servicio TDR (www.tdx.cat) y a través del Repositorio Digital de la UB (diposit.ub.edu) ha sido autorizada por los titulares de los derechos de propiedad intelectual únicamente para usos privados enmarcados en actividades de investigación y docencia. No se autoriza su reproducción con finalidades de lucro ni su difusión y puesta a disposición desde un sitio ajeno al servicio TDR o al Repositorio Digital de la UB. No se autoriza la presentación de su contenido en una ventana o marco ajeno a TDR o al Repositorio Digital de la UB (framing). Esta reserva de derechos afecta tanto al resumen de presentación de la tesis como a sus contenidos. En la utilización o cita de partes de la tesis es obligado indicar el nombre de la persona autora.

WARNING. On having consulted this thesis you're accepting the following use conditions: Spreading this thesis by the TDX (www.tdx.cat) service and by the UB Digital Repository (diposit.ub.edu) has been authorized by the titular of the intellectual property rights only for private uses placed in investigation and teaching activities. Reproduction with lucrative aims is not authorized nor its spreading and availability from a site foreign to the TDX service or to the UB Digital Repository. Introducing its content in a window or frame foreign to the TDX service or to the UB Digital Repository is not authorized (framing). Those rights affect to the presentation summary of the thesis as well as to its contents. In the using or citation of parts of the thesis it's obliged to indicate the name of the author.

Models and therapeutic approaches for Niemann-Pick (A/B and C) and other lysosomal storage disorders



Marta Gómez Grau
2015

MODELS AND THERAPEUTIC APPROACHES
FOR NIEMANN-PICK (A/B AND C)
AND OTHER LYSOSOMAL STORAGE DISORDERS

Memoria presentada por

MARTA GÓMEZ GRAU

para optar al grado de

DOCTORA POR LA UNIVERSITAT DE BARCELONA

Programa de Genética

Departamento de Genética

Curso 2014/2015

Tesis dirigida por la **Dra. Lluïsa Vilageliu Arqués** y el **Dr. Daniel Grinberg Vaisman** en el
Departamento de Genética de la Facultad de Biología de la Universitat de Barcelona

Dra. Lluïsa Vilageliu Arqués

Dr. Daniel Grinberg Vaisman

Marta Gómez Grau

Barcelona, 2015

七転び八起き

Agradecimientos

PRESENTATION

Lysosomal storage disorders (LSDs) are a group of more than 50 different genetic disorders due to the lack of degradation of substrates within lysosomes. Most of them are caused by mutations in genes coding for lysosomal hydrolases. LSDs are mainly inherited in an autosomal recessive manner.

Although in the last 25 years there has been much effort and progress to develop therapies aiming the correction of metabolic defects for these diseases, yet there is no effective therapy for many of them, and patients are exclusively treated with supportive care.

For several non-neurological LSDs, enzyme replacement therapy may be an option. However, this approach is not efficient, at the moment, for neurological patients. Thus, new therapeutic approaches need to be developed. One of these approaches is the use of drugs that are able to produce a read-through of premature stop codons. One advantage of this strategy is that, if successful, it can be applied to any disease, provided that the molecular cause is a nonsense mutation. The most extensively studied approach involves read-through by drugs affecting the ribosome-decoding site.

Niemann-Pick A/B (NPA/B) and Niemann-Pick C (NPC) are two rare inherited monogenic diseases. Although initially were defined as types of the same disease, subsequently they have been considered independent diseases due to the fact that they have different biochemical and molecular features. NPA/B disease is caused by mutations in the *SMPD1* gene, localized in chromosome 11, which codes for the enzyme acid sphingomyelinase, a soluble lysosome hydrolase. NPC disease is caused by mutations in the *NPC1* gene, localized in chromosome 18, which codes for a lysosomal membrane protein, involved in cholesterol transport. NPC disease also may be caused by mutations in the *NPC2* gene, localized in chromosome 14, which codes for a lysosomal soluble protein, involved in cholesterol transport too. The abnormal action of these proteins in patients promotes the accumulation of lipids, which differ in each disease, inside the lysosomes, causing their dysfunction.

This thesis makes contributions to the field of LSDs study. Various aspects have been addressed: therapeutic approaches have been tested as a first step in the achievement of a successful therapy for those LSDs bearing nonsense mutations. Important steps in the generation of a new cellular model for NPA/B have been achieved. This model would be helpful to understand the molecular processes that contribute to the development of this pathology and would be a valuable tool for the search of successful treatments. Finally, two new mouse models for NPC have been generated and characterized while one dies few days after birth, the other mimics the main characteristics of the disease and will be useful to probe specific treatments.

INDEX

INTRODUCTION	1
1. The lysosome	3
2. Lysosomal storage diseases	3
3. General therapeutic approaches for LSDs	7
Enzyme replacement therapy	8
Substrate reduction therapy	9
Hematopoietic stem cell therapy	10
Gene therapy	10
Pharmacological Chaperones	11
Nonsense suppressors	12
Combination therapies	13
4. LSDs models	14
Animal models	14
Cellular models	15
I. NONSENSE MUTATIONS: READ-THROUGH AS A THERAPEUTIC APPROACH	16
1. Translation and read-through. Nonsense mutations	16
2. Nonsense-Mediated mRNA Decay	17
3. Drugs	18
Aminoglycosides	18
Non-aminoglycosides	19
II. NIEMANN-PICK A/B DISEASE: GENERATION OF IPS CELLS (FOR A FUTURE NEURONAL CELLULAR MODEL)	21
1. The disease	21
Clinical features	21
Genetics	21
Laboratory diagnosis	22
Treatment	22
Animal models	22
2. Reprograming fibroblasts to iPSCs	23
3. The uses of iPSCs cells	24
4. iPSCs in Lysosomal storage disorders	25
III. NIEMANN-PICK TYPE C DISEASE: CHARACTERIZATION OF MOUSE MODELS	27
1. The disease	27
Clinical features	27
Genetics	28
Laboratory diagnosis	29
Treatment	29
2. Lipid accumulation	30
Cholesterol	30
Glycosphingolipids	31
Sphingomyelin	31
Sphingosine	31

3. Animal models	31
OBJECTIVES	35
I. NONSENSE SUPPRESSION THERAPY	37
II. GENERATION OF A CELLULAR MODEL FOR NIEMANN-PICK A/B	37
III. CHARACTERIZATION OF MOUSE MODELS OF NIEMANN-PICK C	37
MATERIAL AND METHODS	39
I. READ-THROUGH ANALYSIS	41
1. Samples and mutations	41
2. Site-directed mutagenesis	42
3. Drugs used	43
4. Coupled transcription/translation assay	43
5. COS7 cell culture and transfection	44
6. Enzyme assays	44
• Acid sphingomyelinase enzymatic activity	44
• Acetyl-CoA:α-glucosaminide N-acetyltransferase enzymatic activity	45
• N-acetylgalactosamine-4-sulfatase activity	45
• α-N-acetylglucosaminidase enzymatic activity	46
• β-hexosaminidase activity	46
7. Culture and treatments of patients' fibroblasts	47
8. mRNA quantification	47
9. Nonsense-mediated mRNA decay	47
10. Statistical analyses	48
II. GENERATION OF IPS CELLS	49
1. Cell samples	49
• Other cell lines used	49
2. Generation of iPSC	49
3. iPSCs characterization	50
• Alkaline Phosphatase staining	50
• Pluripotency immunocytochemistry	50
• DNA Extraction / genotyping	51
4. Protocol for the generation of a stock of irradiated HFF and MEF	51
5. Protocol for the conditioned Media	52
6. Plating of Inactivated Feeders	52
7. Enzyme activity (NPA/B)	52
III. GENERATION AND CHARACTERIZATION OF NPC MOUSE MODELS	53
1. Animals	53
2. Genotype analysis	53
3. RT-PCR transcript analysis	54
4. Liver Histology	54
5. Protein lysates and Western blot analysis	54
6. Cholesterol measurement	55

7. Sphingolipid Determination	55
8. Behavioural Phenotyping	56
• Grip strength	56
• Hot plate	56
• Circadian activity	56
• Rotarod	56
• Paw footprinting	56
• Elevated plus maze	57
• The novel object recognition	57
9. Statistics	58

RESULTS **59**

I. NONSENSE SUPPRESSION THERAPY	61
1. Mutations	61
2. Techniques used for the analysis	61
3. <i>In vitro</i> read-through (TNT)	61
4. Enzyme activity in transfected COS cells	64
5. Read-through treatment of patients' fibroblasts	65
II. GENERATION OF A CELLULAR MODEL FOR NIEMANN-PICK A/B	70
1. Reprogramming fibroblasts to iPSCs	70
2. Pluripotency of the iPSCs	71
3. Enzyme Activity in WT iPSCs and derived neurons	72
III. CHARACTERIZATION OF MOUSE MODELS OF NIEMANN-PICK C	73
1. Mice generation	73
2. Phenotyping of the mouse models	75
3. Pioneer	76
4. Imagine	76
5. Behavioural tests	77
Circadian activity	77
Novel object recognition	77
Elevated plus maze	79
Hot plate	79
Paw printing	79
6. Splicing pattern analysis	80
7. Western analysis	81
8. Lipid analysis in mice tissues	81
9. Histological analysis of liver tissue	83

DISCUSSION **85**

I. NON-SENSE MUTATIONS: READ-THROUGH AS A THERAPEUTIC APPROACH	87
II. GENERATION OF A CELLULAR MODEL FOR NIEMANN-PICK A/B	91
III. NIEMANN-PICK C: CHARACTERIZATION OF A MOUSE MODEL	94

CONCLUSIONS	99
BIBLIOGRAPHY	103
ANNEX	127

ABBREVIATIONS

AAV - Adeno-associated virus	KO - Knock-out
AMO - Antisense morpholino oligonucleotides	LacCer - Lactosylceramide
AP - Alkaline phosphatase	LDL - Low density lipoprotein
ARSB - Arylsulfatase B	LSDs - Lysosomal storage disorders
ASM - Acid sphingomyelinase	MEFs - Mouse embryonic fibroblasts
ASMKO - Acid sphingomyelinase Knock-out mice	MLD - Metachromatic leukodystrophy
ASOs - Antisense oligonucleotides	MPS - Mucopolysaccharidoses
BBB - Blood brain barrier	MPSI - Mucopolysaccharidosis I (Hurler / Scheie)
bFGF - basic fibroblast growth factor	MPSIII - Mucopolysaccharidosis III (Sanfilippo)
Cer - Ceramide	MPSVI - Mucopolysaccharidosis VI (Maroteaux-Lamy)
CF - Cystic fibrosis	NAGLU - N-Acetylglucosaminidase
CHX - Cycloheximide	NMD - Nonsense-mediated mRNA decay
CLNs - Neuronal ceroid lipofuscinoses	NPA/B - Niemann-Pick A/B
CNS - Central nervous system	NPC - Niemann-Pick C
dhCer - dihydroceramide	NTD - N-terminal domain
dhSM - dihydrosphingomyelin	OSKM - Oct4, Sox2, Klf4, and c-Myc
DMD - Duchenne muscular dystrophy	PC - Pharmacological chaperones
DMEM - Dulbecco's Modified Eagle's Medium	PFA - Paraformaldehyde
DMSO - Dimethyl sulfoxide	PTC - Premature termination codon
EJC - Exon junction complex	RF - Release factors
ER - Endoplasmic reticulum	RT - Room temperature
ERT - Enzyme replacement therapy	RT-PCR - Retro transcriptase PCR
FBS - Foetal bovine serum	SD - Standard deviation
GAG - Glycosaminoglycans	SEM - Standard error of the mean
GFP - Green fluorescence protein	SFB - Sanfilippo B
GlcCer - Glucosylceramide	SFC - Sanfilippo C
GSLs - Glycosphingolipids	SM - Sphingomyelin
hESC - human embryonic stem cells	SMPD1 - sphingomyelin phosphodiesterase 1
HFF - Human foreskin fibroblasts	SRT - Substrate reduction therapy
HGMD - Human Gene Mutation Databases	SSD - sterol-sensing domain
HGSNAT - Heparan- α -Glucosaminide N-Acetyltransferase	TBS - Tris-Buffered Saline
HSCT - Hematopoietic stem cell therapy	TNT - Transcription and translation
iPSCs - induced Pluripotent Stem Cells	WT - Wild-type

FIGURES

INTRODUCTION

Figure 1. The endolysosomal system.	3
Figure 2. A proposed model for the pathogenesis of lysosomal storage disorders (LSDs).	7
Figure 3. Therapies for lysosomal storage disorders (LSDs).	8
Figure 4. Schematic view of enzyme replacement therapy (ERT).	8
Figure 5. Schematic view of substrate reduction therapy (SRT).	9
Figure 6. Schematic view of hematopoietic stem cell therapy (HSC).	10
Figure 7. Schematic view of gene therapy.	11
Figure 8. Schematic view of pharmacological chaperones (PC) therapy.	12
Figure 9. Schematic view of read-through drugs therapy.	12
Figure 10. Schematic representation of the termination and read-through processes.	16
Figure 11. LSDs mutations grouped by type.	17
Figure 12. Nonsense-mediated mRNA decay (NMD) pathway.	18
Figure 13. <i>SMPD1</i> gene.	22
Figure 14. Medical applications of iPS cells.	25
Figure 15. Schematic representation of the clinical aspects of Niemann-Pick C disease.	27
Figure 16. <i>NPC1</i> gene and protein.	28
Figure 17. <i>NPC2</i> gene.	28
Figure 18. Proposed mechanism for transfer cholesterol.	29
Figure 19. Storage lipids and fold elevation in liver and brain from <i>Npc1</i> mouse.	30

MATERIAL AND METHODS

Figure 20. Chemical structure of the compounds used in this work.	43
Figure 21. Real-time PCR assay for <i>HGSNAT</i> and <i>NAGLU</i> genes, respectively.	47
Figure 22. Scheme of the digestion patterns.	48
Figure 23. Scheme of the reactions involved in the assay.	55

RESULTS

Figure 24. Positive read-through results with G418 and gentamicin.	63
Figure 25. Quantification of the read-through recovery.	63
Figure 26. Example of no full-length protein recovery.	64
Figure 27. Enzyme activity in COS7 cells.	65
Figure 28. Enzyme activity of Sanfilippo C treated fibroblasts in comparison to non-treated ones.	65
Figure 29. Enzyme activity of treated and non-treated Sanfilippo C fibroblasts in comparison to WT fibroblasts.	66
Figure 30. Enzyme activity of Sanfilippo B treated fibroblasts in comparison to non-treated ones.	66
Figure 31. Enzyme activity of treated and non-treated Sanfilippo B fibroblasts in comparison to WT fibroblasts.	67

Figure 32. Relative quantification of the mRNA levels of treated fibroblasts in comparison to non-treated ones.	67
Figure 33. Relative quantification of the mRNA amount of treated and non-treated fibroblasts in comparison to WT fibroblasts.	68
Figure 34. NMD analysis for Sanfilippo B fibroblasts.	69
Figure 35. NMD analysis for Sanfilippo C fibroblasts.	69
Figure 36. Schematic view of the reprogramming protocol.	70
Figure 37. Positive staining of alkaline phosphatase expression in each genotype.	71
Figure 38. Immunocytochemistry.	71
Figure 39. Chromatograms of <i>SMPD1</i> gene fragments of NPAB6 iPSCs.	72
Figure 40. ASM activity from different cell types.	72
Figure 41. NPC1 protein.	73
Figure 42. Pioneer mutation in humans and modifications introduced in mice to generate it.	74
Figure 43. Effect of the Imagine mutation in humans.	74
Figure 44. Schematic representation of the PCR results from the Imagine mutation genotyping.	75
Figure 45. Schematic representation of the PCR results from the Pioneer mutation genotyping.	75
Figure 46. Weight evolution and pathological symptoms.	76
Figure 47. Rotarod motor coordination test.	77
Figure 48. Circadian activity.	77
Figure 49. Habituation session.	78
Figure 50. Familiarization session.	78
Figure 51. Novel object recognition session.	78
Figure 52. Elevated plus maze.	79
Figure 53. Hot plate.	79
Figure 54. Paw printing.	80
Figure 55. RT-PCR transcript analysis.	80
Figure 56. Protein analysis.	81
Figure 57. Boxplot showing the distribution of brain lipid storage.	82
Figure 58. Histogram showing the brain lipid storage.	82
Figure 59. Total hepatic cholesterol.	83
Figure 60. Histological analysis of liver tissue.	83

TABLES

INTRODUCTION

Table 1 Classification of lysosomal storage diseases.	4
Table 2. Approved treatments and selected clinical trials for lysosomal storage disorders.	13
Table 3. Clinical features from NPA and NPB.	21
Table 4. Methods for reprogramming somatic cells to iPS cells.	24
Table 5. Disease modelling and drug testing of LSDs iPSCs.	25
Table 6. Mice model alleles.	33

MATERIAL AND METHODS

Table 7. Nonsense mutation studied in this work.	41
Table 8. Primers used in the site-directed mutagenesis.	42
Table 9. Drugs used.	43
Table 10. Acid sphingomyelinase protocol. (NPA/B).	45
Table 11. Acetyl-CoA: α -glucosaminide N-acetyltransferase protocol (MPSIIIC).	45
Table 12. N-acetylgalactosamine-4-sulfatase protocol (MPSVI).	45
Table 13. α -N-acetylglucosaminidase protocol (MPSIIIB).	46
Table 14. β -hexosaminidase protocol.	46
Table 15. Primers used for the nonsense-mediated mRNA decay assay.	48
Table 16. Primers used for genotyping.	51
Table 17. Primers used in the mouse genotyping analysis.	53
Table 18. Sequence of primers used in RT-PCR splicing analysis.	54

RESULTS

Table 19. Aminoglycosides concentrations used.	62
Table 20. Non-aminoglycosides concentrations used.	62

INTRODUCTION

1. The lysosome

Lysosomes are cytoplasmic acidic compartments, discovered by Christian de Duve in 1955 (De Duve *et al.*, 1955), that are found in all nucleated eukaryotic cells and are heterogeneous in size (100-500 nm in diameter), morphology (spherical to tubular) and distribution (often in a perinuclear pattern).

In each mammalian cell, there are normally several hundred lysosomes containing more than 50 hydrolytic enzymes for the degradation of different intracellular and extracellular macromolecules, such as protein, lipids, oligosaccharides and nucleic acids. Lysosomes have a single phospholipid-bilayer membrane where there are more than 25 lysosomal membrane proteins, some of them heavily glycosylated, helping in the transmembrane transport of substrates and digestion products, proton pumps and chloride ion channels to keep the pH at lower levels (pH4.5-5) for the appropriated performance of acidic hydrolases (Appelqvist *et al.*, 2013; Samie & Xu, 2014).

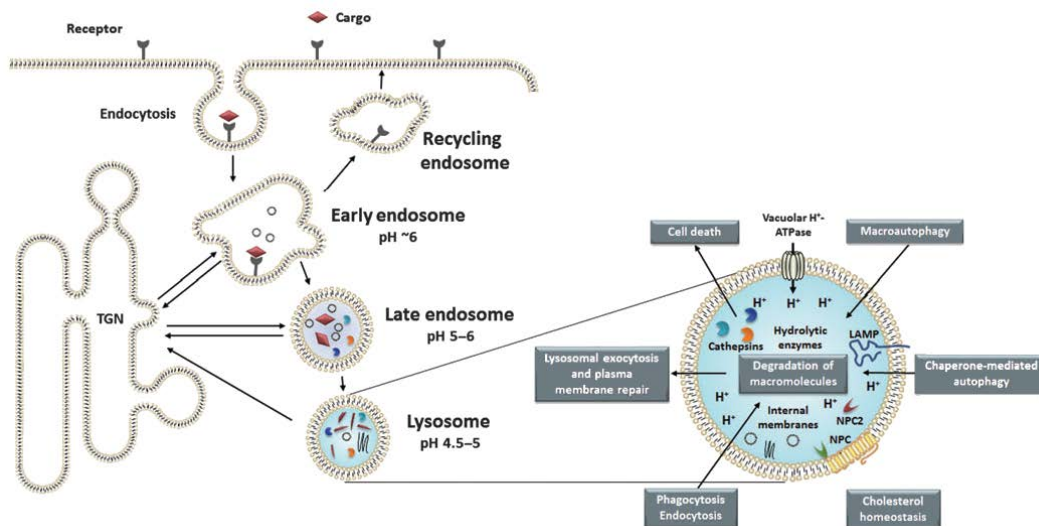


Figure 1. The endolysosomal system. Lysosomes represent the terminal for the degradative endocytic pathway, beginning with early endosomes budding from the plasma membrane. On the right there is a magnification of a lysosome, showing its critical involvement in many cellular processes, including endocytosis, autophagy, plasma membrane repair, cell death and cholesterol homeostasis. LAMP: lysosome-associated membrane protein. NPC: Niemann-Pick type C proteins. TGN: trans-Golgi network. (Appelqvist *et al.*, 2013).

Lysosomes are important for degradation of macromolecules and homeostasis of the cell, but they are also involved in many important cellular functions, including endocytosis, autophagy, apoptosis, cell death, endocytosis and exocytosis, receptor recycling, phagocytosis and membrane trafficking (Figure 1).

2. Lysosomal storage diseases

The lysosomal storage diseases (LSDs) are a diverse group of hereditary metabolic disorders mostly caused by dysfunctions in the enzymes responsible for the degradation of substrates for their removal or recycling. A minority is caused by defects in membrane proteins. When these enzymes or lysosomal proteins are defective, the lysosome accumulates substrates affecting signal transduction pathways at different levels and altering normal cellular processes (Figure 2) (Ballabio & Gieselmann, 2009).

Most LSDs are inherited in an autosomal recessive manner, although a few of them, such as Fabry and Hunter syndrome, are X-linked. All of them are monogenic diseases but some present allelic heterogeneity (Hurler and Scheie) or *locus* heterogeneity (Niemann-Pick C).

Even though as individual diseases LSDs are considered rare there are a large number of them, over 50, and their combined prevalence as a group is estimated to be 1:5000 to 1:8000 births (Boustany, 2013; Parenti *et al.*, 2015; Platt *et al.*, 2012; Schultz *et al.*, 2011; Segatori, 2014).

LSDs are frequently classified according to the major storage compound. The sphingolipidoses, diseases in which sphingolipids are stored, are the most prevalent LSD. There are also mucopolysaccharidoses (MPS), where glycosaminoglycans fragments accumulate; glycoproteinoses, oligosaccharidoses and others. However, since in most LSD more than one compound is accumulated, another way to classify them is by the defective enzyme/protein (Santra & Ramaswami, 2015).

LSDs also include diseases caused by defects in transport through the lysosomal membrane, in post-transcriptional processing of the lysosomal enzyme, in lysosome and lysosome-related organelle biogenesis or the neuronal ceroid lipofuscinoses (CLNs). In Table 1 all LSDs are classified.

Table 1 Classification of lysosomal storage diseases. Adapted from Winchester, 2013.

Disease (OMIM number)	Enzyme/Protein deficiency	Storage materials	Gene
SPHINGOLIPIDOSES INCLUDING SPHINGOLIPID ACTIVATOR DEFECTS			
GM1-gangliosidosis types I, II & III (230500, 230600, 230650)	β -Galactosidase	GM1, KS, oligos, glycolipids	<i>GLB1</i>
GM2-gangliosidosis Tay-Sachs (272800) Sandhoff (268800) GM2 activator defect (272750)	β -Hexosaminidase A β -Hexosaminidase B GM2 gangloside activator	GM2, oligos, globoside, glycolipids	<i>HEXA</i> <i>HEXB</i> <i>GM2A</i>
Fabry (301500)	α -Galactosidase A	Galactosylated glycolipids	<i>GLA</i>
Gaucher type I, II & III (230800, 230900, 231000)	β -Glucosidase	Glucosylceramide	<i>GBA</i>
Metachromatic leukodystrophy (MLD) (250100, 249900)	Arylsulfatase A Saposin B	Sulfatides	<i>ARSA</i> <i>PSAP</i>
Krabbe Disease (245200) (611722)	β -Galactocerebrosidase Saposin A	Galactosylceramide	<i>GALC</i> <i>PSAP</i>
Niemann-Pick type A & B (NPA/B) (257200, 607616)	Sphingomyelinase	Sphingomyelin	<i>SMPD1</i>
Farber (228000)	Acid ceramidase	Ceramide	<i>ASAH1</i>
Prosaposin deficiency (611721)	Prosaposin	Non-neuronal glycolipids, ubiquitinated material in neuron-lysosomes	<i>PSAP</i>
MUCOPOLYSACCHARIDOSES (MPS)			
MPSI Hurler/Scheie (607014, 607015, 607016)	α -L-iduronidase	DS, HS, and oligos	<i>IDUA</i>
MPSII Hunter (309900)	Iduronate-2-sulfatase	DS, HS, and oligos	<i>IDS</i>
MPSIIIA Sanfilippo A (252900)	Heparan N-sulfatase	HS and oligos	<i>SGSH</i>
MPSIIIB Sanfilippo B (252920)	α -N-acetyl-glucosaminidase	HS and oligos	<i>NAGLU</i>

Table 1. (Continued)

Disease (OMIM number)	Enzyme/Protein deficiency	Storage materials	Gene
MPSIIIC Sanfilippo C (252930)	Acetyl CoA: α -glucosamine N-acetyl transferase	HS and oligos	<i>HGSNAT</i>
MPSIIID Sanfilippo D (252940)	N-acetylglucosamine-6-sulfatase	HS and oligos	<i>GNS</i>
MPSIVA Morquio A (25300)	N-acetylgalactosamine-6-sulfatase	KS and oligos	<i>GALNS</i>
MPSIVB Morquio B (253010)	β -galactosidase	KS and oligos	<i>GLB1</i>
MPSVI Maroteaux-Lamy (253200)	N-acetylgalactosamine-4-sulfatase. (Arylsulfatase B)	DS and oligos	<i>ARSB</i>
MPSVII Sly (253220)	β -glucuronidase	CS, DS, HS and oligos	<i>GUSB</i>
MPSIX Natowicz (601492)	Hyaluronidase	Hyaluronan	<i>HYAL1</i>
GLYCOPROTEINOSES (OLIGOSACCHARIDOSES)			
Aspartylglucosaminuria (208400)	Aspartylglucosaminidase	Glycosyl-asparagines	<i>AGA</i>
Fucosidosis (230000)	α -L-fucosidase	Oligos, glycopeptides, glycolipids	<i>FUCA1</i>
α-mannosidosis (248500)	α -D-Mannosidase	Oligos	<i>MAN2B1</i>
β-mannosidosis (248510)	β -D-Mannosidase	Oligos	<i>MANBA</i>
Sialidosis I/II (Mucopolipidosis I) (565500)	Neuraminidase (Sialidase1)	Oligos glycopeptides	<i>NEU1</i>
Schindler\Kanzaki (609241 & 609242)	α -N-acetyl-galactosaminidase (α -Galactosidase B)	Oligos	<i>NAGA</i>
Galactosialidosis (256540)	Protective protein cathepsin A (PPCA)	Sialylated oligos and glycopeptides	<i>CTSA</i>
OTHER ENZYME DEFECTS			
Glycogenoses			
Pompe (232300)	α -Glucosidase (acid maltase)	Glycogen, oligos	<i>GAA</i>
Lipidoses			
Wolman (278000)	Acid lipase	Cholesterol esters	<i>LIPA</i>
Protease defects			
Papillon-Lefèvre	Cathepsin C, Dipeptidyl peptidase I (DPP I)	-	<i>CTSC</i>
Pyconodysostosis (265800)	Cathepsin k	Collagen, other bone proteins	<i>CTSK</i>
DEFECTS IN POST-TRANSCRIPTIONAL PROCESSING OF LYSOSOMAL ENZYME			
Multiple sulfatase deficiency, mucosulfatidosis (272200)	Formylglycine generating enzyme (SUMF1)	Sulfatides, glycolipids	GAGS, <i>SUMF1</i>
Mucopolipidosis IIα/β (ML II or I-cell) (252500)			
Mucopolipidosis IIIα/β (ML IIIA or pseudo-Hurler polydystrophy) (252600)	N-acetylglucosamine-1-phosphotransferase α / β subunit	Oligos, GAGS, lipids	<i>GNPTAB</i>
Mucopolipidosis IIIγ (ML III variant) (252605)	N-acetylglucosamine-1-phosphotransferase γ subunit	Oligos, GAGS, lipids	<i>GNPTG</i>
Stuttering (609261)	N-acetylglucosamine-1-phosphodiester α -N-acetylglucosaminidase (uncovering enzyme)	Oligos, GAGS, lipids	<i>GNPTAB</i> <i>GNPTG</i> <i>NAGPA</i>

Table 1. (Continued)

Disease (OMIM number)	Enzyme/Protein deficiency	Storage materials	Gene
LYSOSOMAL MEMBRANE AND TRANSPORT DEFECTS			
Cystinosis (219800, 219900, 219750)	Cystinosin (cysteine transporter)	Cystine	<i>CTNS</i>
Sialic acid storage disease Infantile (ISSD) (269920) Salla, adult form (604369)	Sialin (sialic acid transporter)	Sialic and uronic acids	<i>SLC17A5</i>
Cobalamin F disease (277380)	Cobalamin transporter	Cobalamin	<i>LMBRD1</i>
Danon (300257)	Lysosome-associated membrane protein 2 (LAMP-2)	Cytoplasmic debris and glycogen	<i>LAMP2</i>
LIMP-2 deficiency (254900)	LIMP-2 (lysosomal integral membrane protein 2 or SCARB2 Scavenger Receptor class B)	Not characterised	<i>SCARB2</i>
Malignant infantile Osteopetrosis (607649) (602727) Mucopolipidosis IV (252650)	Mucopolipin-1 (TRPML,transient receptor potential mucolipin) CLCN7, chloride channel 7 OSTM-1, osteopetrosis-associated transmembrane protein	Lipids	<i>MCOLN1</i> <i>CLCN7</i> <i>OSTM1</i>
Niemann-Pick type C1 (NPC) (257220) Niemann-Pick type C2 (607625)	NPC1 protein (proton-driven transporter) NPC2 protein (soluble lysosomal protein)	Cholesterol and other lipids	<i>NPC1</i> <i>NPC2</i>
NEURONAL CEROID LIPOFUSCINOSES (CLNs)			
CLN1 (256730)	Palmitoyl protein thioesterase 1 (PPT1)	Lipofuscin, Saposins	<i>PPT1</i>
CLN2 (204500)	Tripeptidyl peptidase I (TPP1)	Lipofuscin, subunit C of ATPase	<i>TPP1</i>
CLN3 (204200)	CLN3, lysosomal and/or Golgi transmembrane protein	Lipofuscin, subunit C of ATPase	<i>CLN3</i>
Recessive Adult NCL (ANCL Kufs) (204300)	CLN6 transmembrane protein in ER	Lipofuscin, subunit C of ATPase	<i>CLN6</i>
CLN4 (162350)	CSP α	Lipofuscin, subunit C of ATPase	<i>DNAJC5</i>
CLN5 (256731)	CLN5, soluble lysosomal protein	Lipofuscin, subunit C of ATPase	<i>CLN5</i>
CLN6 (601780)	CLN6 transmembrane protein in ER	Lipofuscin, subunit C of ATPase	<i>CLN6</i>
CLN7 (610951)	CLN7/MFSD8 (major facilitator superfamily domain-containing protein 8), transporter	Lipofuscin, subunit C of ATPase	<i>MSFD8</i>
CLN8 (600143)	CLN8 transmembrane protein in ER	Lipofuscin, subunit C of ATPase	<i>CLN8</i>
CLN9 (609055)	Unknown	Lipofuscin, subunit C of ATPase	-
CLN10 (610127)	Cathepsin D	Lipofuscin, subunit C of ATPase	<i>CTSD</i>
DEFECTS IN LYSOSOME AND LYSOSOME-RELATED ORGANELLE BIOGENESIS			
Chediak. Higashi syndrome (214500)	LYST		<i>CHS1</i> <i>LYST</i>
Griscelli syndrome type 1 (214450)	Myosin 5A	Melanin granules	<i>MYO5A</i>
Griscelli syndrome type 2 (607624)	Rab27A (soluble GTPase)	Melanin granules	<i>RAB27A</i>

Table 1. (Continued)

Disease (OMIM number)	Enzyme/Protein deficiency	Storage materials	Gene
Griscelli syndrome type 3 (609227)	Melanophilin	Melanin granules	<i>MLPH</i>
Hermansky-Pudlak syndrome type 1-9 (203300)		Lipofuscin/ceroid	

Abbreviations: CS, chondroitin sulfate; DS, dermatan sulfate; ER, endoplasmic reticulum; GAGs, glycosaminoglycans; HS, heparan sulfate; KS, keratin sulfate; oligos, oligosaccharides.

Although lysosomes are ubiquitously distributed, the accumulation of the material generally occurs in tissues and organs where the substrate turnover is high and lysosomal degradation is critical to maintain the homeostasis. The clinical consequence of this accumulation is the presence of visceral, hematological, skeletal, ocular and, in some cases, neurological manifestations. Some phenotypic overlap may exist among the different disorders. Symptoms can emerge at variable ages, from utero to late adulthood, and the disease progresses over time. Visceral manifestations (hepatosplenomegaly) and hematological abnormalities (enlarged, substrate-filled vacuoles visible in lymphocytes or histiocytes) are typical of LSDs. Skeletal involvement is characterized by generalized bone dysplasia, joint limitations and abnormalities in skeletal growth. Ocular manifestations include corneal or lenticular opacities, retinal involvement (cherry red spot, retinal dystrophy), optic nerve atrophy, glaucoma, and blindness. The most severe and important manifestation involves the central nervous system (CNS) and it happens on 75% of LSDs (Parenti *et al.*, 2015; Segatori, 2014).

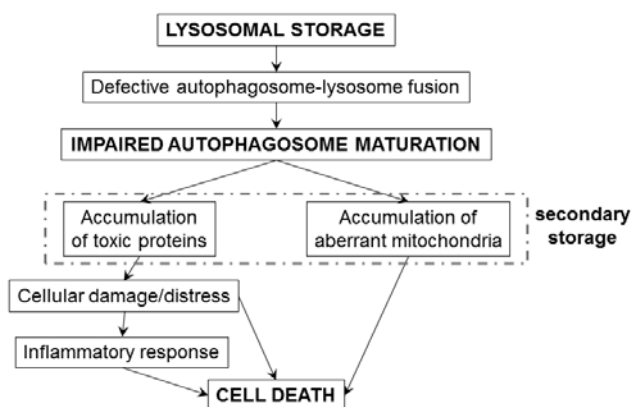


Figure 2. A proposed model for the pathogenesis of lysosomal storage disorders. Lysosomal storage leads to a reduced ability of lysosomes to fuse with autophagosomes. This results in a blockage (at least partial) of autophagy maturation and a defective degradation that promotes cell death. The inflammatory response to cell damage further contributes to cell death. Adapted from (Ballabio & Gieselmann, 2009)

3. General therapeutic approaches for LSDs

Although in the last 25 years there has been a lot of effort and progress to develop therapies aiming the correction of metabolic defects for these diseases, there is no effective therapy for many of them, and patients are exclusively treated with supportive care. The difficulty in finding an effective treatment for all LSDs is caused by significant variation in the response to treatment, not only between the different diseases, but also between sub-groups of patients with a specific disorder (Hollak & Wijburg, 2014).

The approaches developed to treat LSDs are based on two different strategies (Figure 3). Most of them aim to increase the functionality of the defective enzyme or protein by gene therapy, enzyme replacement, pharmacological chaperones, cell based therapy and premature stop codon read-through. Others are focused on the restoration of the equilibrium between the synthesis and the degradation of the involved substrate by synthesis reduction or by promoting

exocytosis of the unwanted storage molecules. However, the potential of enhanced exocytosis therapy has only been demonstrated in vitro (Medina *et al.*, 2011).

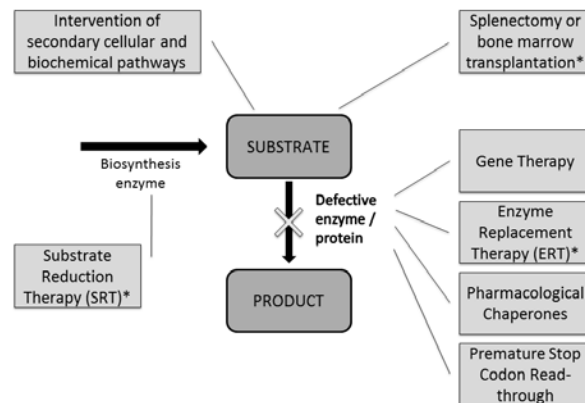


Figure 3. Therapies for lysosomal storage disorders (LSDs). LSDs treatments can be divided into those that restore the equilibrium between the synthesis and the degradation of the substrate (left) and those that aim to increase the functionality of the defective enzyme or protein (right). Treatments marked with * are in clinical use at present. Adapted from (Futerman & van Meer, 2004).

Enzyme replacement therapy

The concept of the enzyme replacement therapy (ERT) is to restore the deficient enzyme through exogenous administration of the functional, wild-type (WT) enzyme (Figure 4). In the early 1990's, it was demonstrated that human placental glucocerebrosidase (alglucerase) was efficient to reduce the organomegaly and to increase the quality of life in Gaucher disease type 1 patients, being the first ERT approved for a LSDs (Barton *et al.*, 1990).

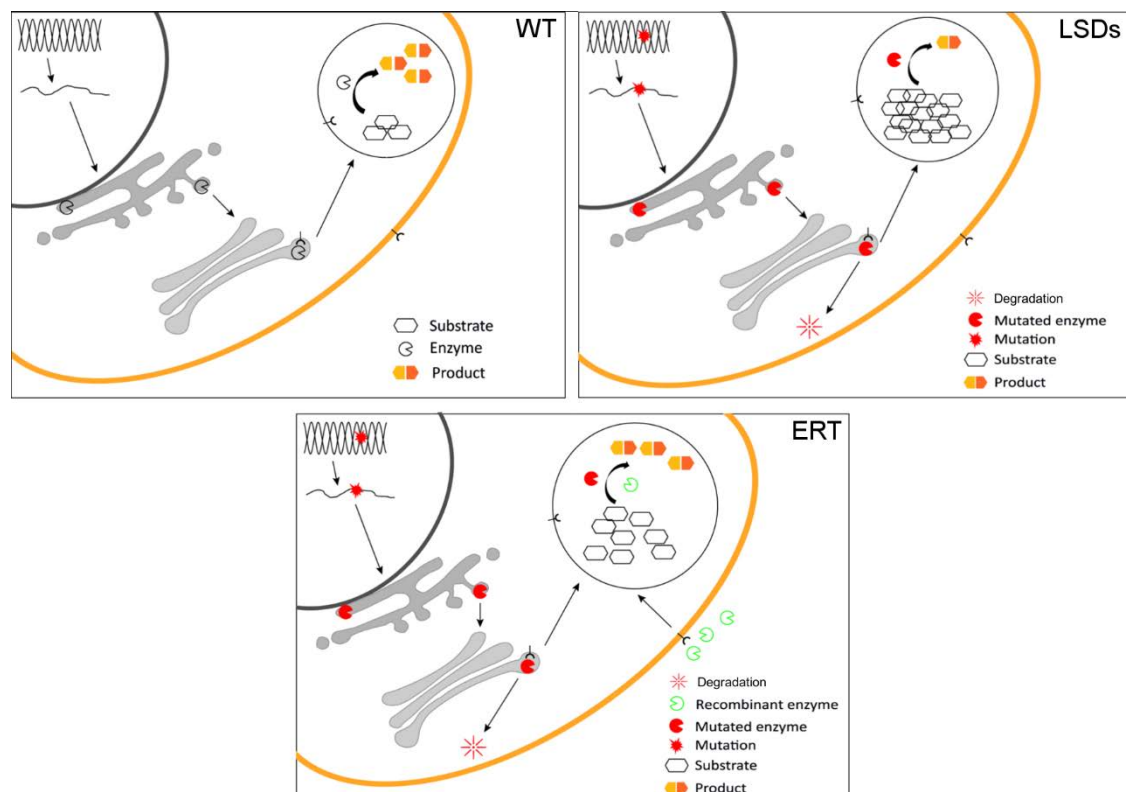


Figure 4. Schematic view of enzyme replacement therapy. In WT picture the enzyme arrives to the lysosome and works correctly. While in LSDs picture it is partially degraded and it does not work properly, so substrate accumulates. In ERT picture, recombinant enzyme is directly infused in patient bloodstream and taken up by cells through the receptor, here it traffics to the lysosome and hydrolyses accumulated substrates. WT, wild-type; LSD, lysosomal storage disorders; ERT, Enzyme replacement therapy.

5 years later, the first recombinant enzyme introduced in the market for this disease was Imiglucerase. Imiglucerase was produced in CHO cells and not long ago, this product was followed by Velaglucerase α and Taliglucerase α , produced in human cell line and plant cell line respectively. The next ERT to be on market was for Fabry disease, the recombinant enzyme Agalsidase β , produced in CHO cells, and quickly followed by the development of Agalsidase α , produced in a human cell line. After that, more ERT has been approved for other disorders, such as Laronidase for MPSI, Idursulfase for MPSII, Galsulfase for MPSVI, Alglucosidase α for Pompe disease and finally, in the last year, Elosulfase α for MPSIVA enzyme replacement treatment was approved (reviewed in Hollak & Wijburg, 2014; Ortolano *et al.*, 2014).

Nowadays, ERT has been approved for the seven LSDs mentioned above and it is under development for others. For more information see Table 2.

However, the ERT has several limitations: it is really costly, invasive and time consuming due to the short enzyme half-life; the requirement of frequent infusions; and the poor delivery to less accessible tissues such as bone or the brain. Recombinant enzymes are large molecules that cannot freely diffuse across membranes or the blood brain barrier (BBB) and are unable to reach the deep layers of many affected organs in the most severe phenotypes. For this reason, it has been shown that the ERT do not prevent or reverse neuronopathic symptoms in Gaucher disease type 2/3 or MPS. Nevertheless, many efforts are being addressed to the improvement of the delivery system. For example, by modifying the enzyme, inactivating chemically the carbohydrate-dependent receptor-mediated uptake in order to increase its plasma half-life (Grubb *et al.*, 2008; Huynh *et al.*, 2012); by fusing the recombinant enzyme with peptides that allow the penetration of BBB (reviewed in Ortolano *et al.*, 2014; Parenti *et al.*, 2015) or by the intrathecal administration of the enzyme (clinical trial ongoing, Table 2). Another drawback that reduces the efficiency of this therapy is that in some patients it may cause immune responses as it has been reported for Gaucher, Fabry, MPSI, MPSII, MPSIV, and Pompe (Desnick & Schuchman, 2012). New strategies to avoid this problem are needed (Hollak & Wijburg, 2014).

Substrate reduction therapy

The substrate reduction therapy (SRT) aims to restore the balance between the synthesis and the degradation of the storage material using inhibitors of the enzyme involved in the substrate synthesis (Figure 5). In this case, the therapeutic agent has the potential to cross the BBB, it does not generate immune reactions and it can be given orally.

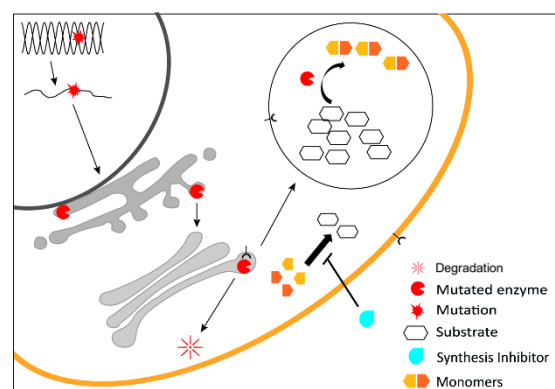


Figure 5. Schematic view of substrate reduction therapy (SRT). In SRT an inhibitor of the enzyme that synthesizes the substrate accumulated in patient's cells is administrated to patients and carried over by the cell, where it is able to reduce the synthesis of the storage material.

The first authorized product for LSDs was miglustat, an inminosugar able to partially inhibit the production of the substrate glucosylceramide but with modest effects on Gaucher type 1 patients and with frequent side effects (Cox *et al.*, 2000). Furthermore, it did not show convincing effectiveness in clinical trials of Gaucher type 3 patients (reviewed in Hollak & Wijburg, 2014; Schiffmann *et al.*, 2008). This inhibitor has also been assayed in Fabry, Sandhoff and Tay Sachs patients with no convincing results (reviewed in Hollak & Wijburg, 2014). However, it has been approved for treatment of NPC disease because of the beneficial effects achieved in patients (GM1 depletion, normalization of lipid-trafficking abnormality) (Lachmann *et al.*, 2004). A second generation product for SRT for Gaucher, eliglustat tartrate (Genz-112638, Genzyme), has been approved recently and it is being evaluated in phase III clinical trials (Lukina *et al.*, 2010).

Another compound for SRT, which is also on clinical trials (phase III) for MPS patients, is genistein, a flavonoid that has been reported to inhibit glycosaminoglycans synthesis in human MPSI, MPSII, MPSIIIA and MPSIIIB fibroblasts (Piotrowska *et al.*, 2008).

Hematopoietic stem cell therapy

This approach is based on supplying a continuous source of wild-type enzyme. It is expected that the donor-derived macrophages and microglia will populate the brain of the patient and will secrete functional lysosomal hydrolases to cross-correct the enzyme defect in affected cells (Figure 6). However, this approach involves a lot of risk and side effects. Hematopoietic stem cell therapy (HSCT) has been most extensively studied for MPSI (Hurler), but its efficacy depends on several factors such as the therapeutic window or the donor cell source. Less convincing results have been obtained for MPSII and MPSVI because, although there is a rapid improvement of visceral manifestations, the neurological and skeletal diseases are unresponsive to the treatment. For more than 2 decades HSCT has been applied in patients with MLD and also in others LSDs, including Gaucher type 1 and 3 (reviewed in Hollak & Wijburg, 2014). The success of HSCT approach made the LSDs attractive candidates for gene therapy.

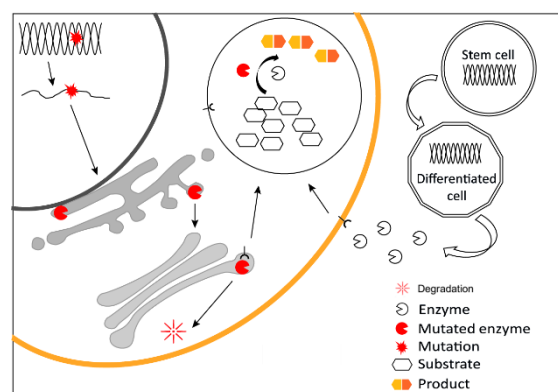


Figure 6. Schematic view of hematopoietic stem cell therapy (HSC). HSC expressing functional enzyme are differentiated and injected to the patient. The enzyme secreted by stem cells, together with modulating factors, is taken up by patient's cells through receptor.

Gene therapy

The aim of this approach is to increase or restore the defective enzyme activity by supplying a copy of the correct gene (Figure 7). LSDs appear to be excellent candidates for gene therapy, as they are monogenic diseases and the responsible enzymes are expressed ubiquitously; only a lower increase in the enzymatic activity is needed to ameliorate symptoms, and over expressions of the genes which code these enzymes do not seem to produce adverse effects. The controversy about this approach is the delivery: when a systematic delivery is used, it does not

produce positive effects in the CNS and when it is given by direct delivery it requires very invasive procedures.

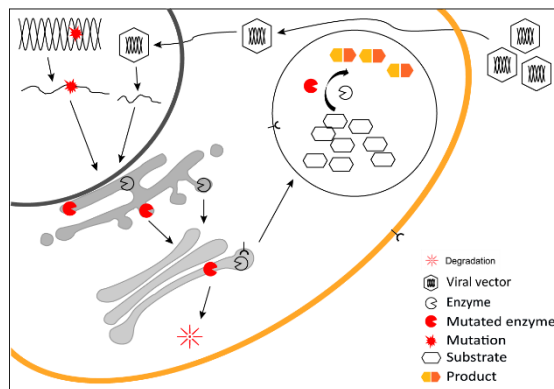


Figure 7. Schematic view of gene therapy. Transgenic viral vectors encoding a functional enzyme are injected to the patients to infect target cells. Once in the nucleus, viral DNA is transcribed and the functional enzyme is expressed in the endoplasmic reticulum and eventually traffics to the lysosome.

Different viral vectors such as lentivirus, retrovirus, adenovirus and adeno-associated virus (AAV) have already been tested in preclinical trials in the last decades for some LSDs and some more are in progress for the following diseases: MPSII, MPSIIIA, MPSVI, Pompe disease, CLNs, Gaucher and Fabry disease (Table 2).

Currently, AAVs are the vectors of choice for *in vivo* gene therapy, and lentiviruses for the *ex vivo* gene therapy. The *ex vivo* approach with lentivirus vectors has been successfully used in a clinical trial to treat MLD patients (NCT00633139) (Biffi *et al.*, 2013).

Retrovirus and AAV vectors have been reported for potential therapy in MPSVII with significant reduction of substrate storage in tissues. Moreover, promising preclinical tests were also undertaken in dog models of MPSI and MPSIII B to assay efficiency of AAV-based gene therapies in short to medium terms (reviewed in Ortolano *et al.*, 2014).

Also, it has been proved that if you contact an axonal ending of a neuron with a high titer AAV carrying a therapeutic transgene, the vector is axonally transported in a retrograde fashion and the product can be expressed distally to the administration site in animal model brains. However, additional studies are required (reviewed in Ortolano *et al.*, 2014).

Pharmacological Chaperones

Pharmacological chaperones (PC) are small molecules that bind to and stabilize the mutant lysosomal enzyme facilitating the correct protein folding and allowing its proper cellular trafficking to lysosome (Figure 8). One of the limitations of the use of PC as therapeutic agents is that these compounds are specific of mutation, and some mutations are totally insensitive to the treatment. The mutation must be a missense mutation located outside the enzyme's catalytic pocket, so it is still functional, but it has negative effects on protein folding efficiency and lysosomal trafficking (Smid *et al.*, 2010).

The majority of PC that has been identified binds to the catalytic domain of enzymes, as reversible inhibitors, to stabilize the enzyme. So the affinity of the inhibitor for the enzyme is also important, it has to bind tightly in the endoplasmic reticulum (ER) but weakly in the lysosome. Furthermore, there is a delicate balance between concentrations that enhance or inhibit activity (Ringe & Petsko, 2009). However, chaperones may also be allosteric, binding

outside the catalytic pocket. They have the advantage of avoiding inhibition but they must not interfere with protein-protein interactions (Boyd *et al.*, 2013).

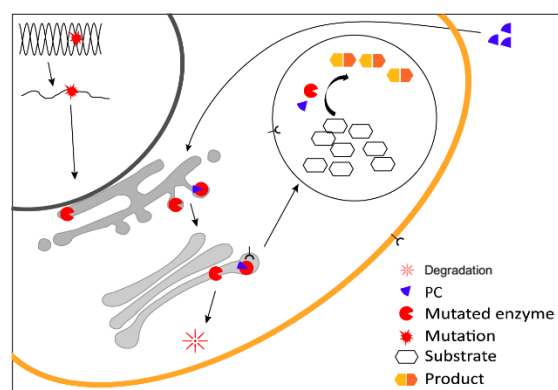


Figure 8. Schematic view of pharmacological chaperones (PC) therapy. PC binds the active site of a miss-folded enzyme at the endoplasmic reticulum and facilitates its transport to the lysosome, where the chaperone is released due to low pH. Once in the lysosome, the mutated enzyme can partially perform its catalytic function.

The first studies on PC therapy in LSDs were done for Fabry disease (Fan *et al.*, 1999) with the substrate analogue migalastat hydrochloride (DGJ). At present, this compound is under clinical trial phase III. Another PCs being on clinical trial are isofagomine (afegostat tartrate) and ambroxol, both in phase II for Gaucher type 1. As well as duvoglustat HCL for Pompe disease and pyrimethamine for GM2 disease (reviewed in (Hollak & Wijburg, 2014).

Nonsense suppressors

The nonsense suppressors are small molecules that enhance the suppression of a premature termination codon (PTC), caused by nonsense mutations, allowing the read-through and translation of the full-length protein (Figure 9). Nonsense mutations are approximately 10% of the total of mutations known to cause human inherited diseases (Mort *et al.*, 2008). So, this is a good approach to be assayed for these illnesses, as explained in more detail in section I (see page 16).

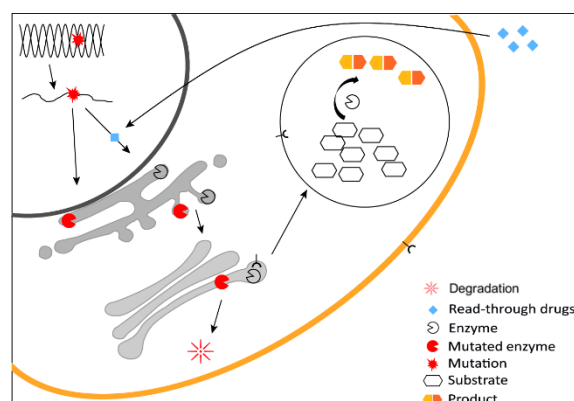


Figure 9. Schematic view of read-through drugs therapy. These drugs bind the ribosome allowing the read-through and translation of the full-length protein.

Suppressor effect of the aminoglycosides gentamicin and G418 was first shown in cystic fibrosis (CF) and Duchenne muscular dystrophy (DMD) patients but at therapeutic concentration they can produce side effects such as ototoxicity and nephrotoxicity (Forge & Schacht, 2000; Nagai & Takano, 2004).

New non aminoglycosides compounds, as PTC124, showed its potential in a murine model of Duchenne disease (Welch *et al.*, 2007). These exciting data *in vivo* were followed by clinical trials (phase II) in CF and DMD (Smid *et al.*, 2010) with positive changes for CF. There are currently no clinical trials to evaluate this kind of drugs in patients with LSDs (Pastores, 2010).

Combination therapies

Usually, the different therapeutic approaches are tested separately to assess if they are able to improve the patients' quality of life. However, the combined application of two different strategies has been assayed in order to enhance the therapeutic effect on patients.

It has been reported that the pre-treatment with ERT can improve the outcome of HSCT in MPSI patients (Cox-Brinkman *et al.*, 2006; Eisengart *et al.*, 2013). Moreover, it has been shown that some chaperones are able to enhance the effect of the wild-type exogenously administered enzyme in the ERT. This positive synergy has been demonstrated in preclinical studies for Pompe, Fabry and Gaucher diseases (Porto *et al.*, 2009, 2012).

In Table 2 a summary of the approved treatments and clinical trials for the LSDs is shown.

Table 2. Approved treatments and selected clinical trials for lysosomal storage disorders (LSDs). Adapted from Parenti *et al.*, 2015.

Disease	Type of treatment, Route of administration and Therapeutic agent
Fabry Disease	Clinical trial
	ERT, IV, PRX-102
	SRT, O, Genz682452
	PC, O, Miglustat HCL
	PC, O + ERT, IV, Miglustat HCL + agalsidase α / β
Approved treatment	
GT, IV, RV-GLA	
Gaucher type 1	Clinical trial
	PC, O, afegostat tartrate; Ambroxol
	GT, IV, RV-GBA
Approved treatment	
ERT, IV, Imiglucerase; Velaglucerase α ; Taliglucerase α	
SRT, O, Miglustat; Eliglustat tartrate	
GM1 and GM2	Clinical trial
SRT, O, Miglustat	
GM2	Clinical trial
PC, O, Pyrimethamine	
Lysosomal acid lipase deficiency	Clinical trial
ERT, IV, Sebelipase α	
α -mannosidosis	Clinical trial
ERT, IV, Lamazyn	
MLD	Clinical trial
	ERT, IV, Metazyn
	ERT, IT, HGT-1110
	GT, IV, LV-ARSA
	GT, IC, AAVrh.10-ARSA
MPSI	Clinical trial
	ERT, IT, Laronidase
Approved treatment	
ERT, IV, Laronidase	
MPSII	Clinical trial
	ERT, IV, Idursulfase β
	ERT, IV and IT Idursulfase
Approved treatment	
GT, IV, RV-IDS	
MPSIIIA	Clinical trial
	ERT, IT, HGT 1410
GT, IC, AAVrh.10-SGHS and SUMF1	
MPSIIIB	Clinical trial
GT, IC, AAV5-NAGLU	
MPSIII A,B,C	Clinical trial
SRT, O, Genistein aglycone	
MPSIVA	Approved treatment
ERT, IV, Elosulfase α	
MPSVI	Approved treatment
ERT, IV, Galsulfase	
MPSVII	Clinical trial
	ERT, IV, recombinant human β -glucuronidase
CLN2	Clinical trial
	GT, IC, AAVrh.10-CLN2
ERT, IC, BMN 190	
NPB	Clinical trial
ERT, IV, recombinant human ASM (olipudase α)	

Table 2. (Continued)

Disease	Type of treatment, Route of administration and Therapeutic agent	
NPC	Clinical trial	OTHER, IC, cyclodextrin
	Approved treatment	OTHER, O, Vorinostat
Pompe	Clinical trial	SRT, O, Miglustat
		ERT, IV, neoGAA
		ERT, IV, GILT-tagged recombinant human
		ERT, IV, alglucosidase α and albuterol
		ERT, IV, alglucosidase α and clenbuterol
		PC, O, duvoglustat HCL
		ERT, IV + PC, O, alglucosidase α and miglustat
		ERT, IV + PC, O, alglucosidase α and duvoglustat
Approved treatment	ERT, IV, Alglucosidase α	

Abbreviations: AAV, adeno-associated viral vector; ARSA, arylsulfatase A gene; CLN2, neuronal ceroid lipofuscinosis 2 gene; ERT, enzyme replacement therapy; GILT, glycosylation-independent lysosomal targeting; GAA, α -glucosidase gene; GBA, β -glucocerebrosidase gene; GLA, α -galactosidase A gene; GT, gene therapy; IC, intracerebral; ID, intradiaphragmatic; IDS, iduronase-2-sulfatase gene; IT, intrathecal; IV, intravenous; LV, lentiviral vector; NAGLU, N-acetylglucosaminidase gene; O, oral; PC, pharmacological chaperone; RV, retroviral vector; SGHS, N-sulfoglucosamine sulfohydrolase gene; SRT, substrate reduction therapy; SUMF-1, sulfatase-modifying factor 1 gene.

4. LSDs models

For LSDs there are different types of models, from cellular models such as fibroblast from animals or patients, which are easy to obtain and expand but have a limited use, to animal models, engineered and/or naturally occurred, that mimic key features of the disease.

Animal models

Animal models are essential to study the pathological pathways of the disease and to test new therapeutic strategies. Furthermore, well characterized animal models, which closely resemble the human disease, have been involved in establishing proof of therapeutic principle by demonstrating substrate clearance from tissues, with associated improvement in outcomes including increased survival. One example is the preclinical trial of ERT in the knock-out (KO) mouse model for Fabry disease or the gene therapy testing in MPSI mice (reviewed in Pastores *et al.*, 2013).

Small animals as mice are widely used as models because they have the advantage of being easy to breed and keep but also they offer the possibility to manipulate the mouse genome for generation of new models. Though not all mouse models which bear mutations identical to the ones seen in human patients express a phenotype that mimics the human conditions, as i.e. Gaucher disease N370S homozygosis mouse model (Xu *et al.*, 2003). Hence, the closer the symptoms are in a mouse to those observed in human patients, the more useful the mouse will be (G M Pastores *et al.*, 2013). Mouse models normally are genetically-engineered, bearing point mutations, knock down genes or being conditional knock-out or completely knock-out models. To date for sphingolipidoses there are 16 mouse models for Gaucher disease, 2 for Fabry disease, 4 for MLD, 3 for Krabbe disease, 3 for Niemann-Pick A/B, 3 for Farber disease, 2 for GM1 gangliosidosis and 5 for GM2 gangliosidosis (reviewed in Zigdon *et al.*, 2014). To date for MPS there are 1 mouse model for MPSI, 2 for MPSII, 1 for MPSIIIA, 3 for MPSIIIB, 2 for MPSIVA, 3 for MPSVI, 9 for MPSVII and 1 for MPSIX. For oligosaccharidosis, there are 2 mouse model for

aspartylglucosaminuria, 1 for α -mannosidosis, 1 for β -mannosidosis, 2 for sialidosis and 1 for galactosialidosis. For lysosomal membrane and transport defects, to date there are 1 mouse model for cystinosis, 1 for infantile sialic acid storage disease, 1 for Sall disease, 1 for Danon disease, 2 for mucopolipidosis IV, 16 for Niemann-Pick disease type C1 and 1 for Niemann-Pick disease type C2. For CNLs, to date there are 3 mouse model for CLN1, 4 for CLN2, 8 for CLN3, 1 for CLN5, 1 for CLN6, 1 for CLN7, 4 for CLN8 and 1 for CLN10. For the rest of LSDs, to date there are 5 for glycogen storage disease 2, 1 for lysosomal acid lipase deficiency, 3 for pycnodysostosis, 1 for multiple sulfatase deficiency, 2 for mucopolipidosis II, 8 for Chediak-Higashi syndrome, 2 for Griscelli syndrome type 1, 1 for Griscelli syndrome type 2 and 7 for Hermansky-Pudlak syndrome 1 (Mouse Genome Informatics, <http://www.informatics.jax.org/>). The majority of preclinical trials have been undertaken in the mouse models of LSDs.

For Niemann-Pick C disease there are several animal models (<http://www.informatics.jax.org/disease/models/257220>), which are explained in III.3 section (see page 31).

Larger animals are particularly used to test new therapies and strategies to overcome the challenge presented by the BBB. Some of them have been identified with spontaneous mutations in genes responsible for LSDs. These models are advantageous since they come from a heterogeneous genetic background more similar to that of humans; their size is more suitable for surgical manipulations and physiological and pathological measurements; and their longevity allows the evaluation of long-termed consequences of therapies. To date, LSD have been described in various breeds of cats (Krabbe, α -mannosidosis, GM1, GM2, MPSI, MPSVI, NPA/B, MLII, NPC), dogs (Krabbe, GM1, GM2, MPSI, MPSIIIA, MPSIIIB, MPSVII, α -fucosidosis, globoid cell leukodystrophy, Gaucher, NPA/B), pigs (GM2, Gaucher), sheeps (Krabbe, GM1, GM2, Gaucher, CLN) cows (α and β -mannosidosis, GM1, NPA/B) goats (MPSIIID), raccoons (NPA/B) flamingo, deer or rabbits (GM2) and non-human primate (Krabbe) (reviewed in Bradbury *et al.*, 2015; Haskins, 2009; Hemsley & Hopwood, 2010; Zigdon *et al.*, 2014).

Also invertebrate models, *Drosophila* and *C. elegans*, have been developed to identify the pathogenic signalling cascades to better understand the LSDs (reviewed in Hindle *et al.*, 2011).

Cellular models

Although, as stated, several animal models have been found or generated for the LSDs, these models are not able to mimic the whole spectrum of LSD conditions. So, to develop efficient therapies, a more detailed understanding of the pathophysiological development of LSD at the cellular level is essential. For this reason, induced pluripotent stem cells (iPSCs) derived from patients' somatic cells offer a valuable methodology to study *in vitro* the mechanisms involved in the initiation and progression of the diseases in those cell types not easily available, such as neurons, and to carry on investigating compounds with clinical treatment (Huang *et al.*, 2012). iPSCs models can be a valuable complement to mouse models. See section II.3, page 24 for further information.

In the case of the LSDs, several iPSCs-derived models have been generated and are reviewed in II.4 section (see page 25).

I. Nonsense mutations: read-through as a therapeutic approach

One of the emerging therapeutic strategies is based on the use of drugs that can induce the read-through of the premature stop codons. Several considerations have to be taken into account when assaying this kind of approach.

1. Translation and read-through. Nonsense mutations

In genetic systems, including humans, translation termination occurs when one of the 3 stop codons [UAA/UGA/UAG] enters the ribosomal site A. The recognition of these 3 codons is mediated by extra ribosomal proteins known as class I release factors (eRF1) and class II (eRF3) instead of the transferRNA (tRNA)

However, the mechanism of translation termination is not 100% efficient. There is a competition between stop codon recognition by RFs and stop codon decoding by a near-cognate tRNA (pairing with 2 of the 3 bases)(Bidou *et al.*, 2012; Karijolic & Yu, 2014). This decoding leads to a natural suppression of the stop codon, also called “read-through”, in which an amino acid is incorporated instead of the stop codon. Natural and premature termination codons exhibit low levels of translational read-through. Under normal conditions, natural read-through occurs at a rate of 0.01-1% at PTCs and 0.001-0.1% at normal stop codons (Keeling *et al.*, 2012) (Figure 10).

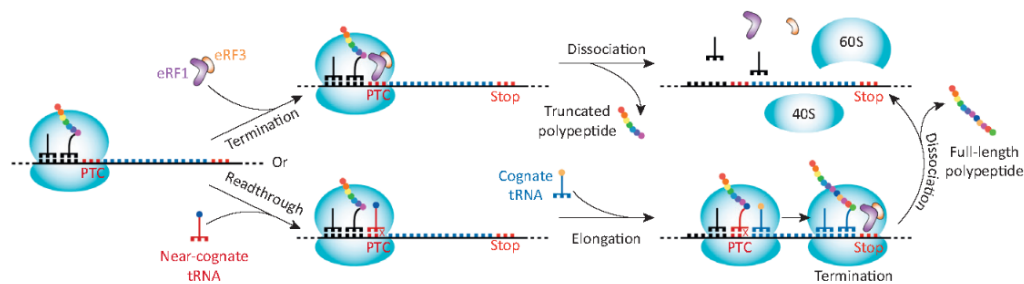


Figure 10. Schematic representation of the termination and read-through processes. When a ribosome encounters a premature termination codon (PTC) there are two possibilities: termination or read-through. In the first one, the release factors eRF1 and eRF3 enter the ribosomal A site to promote translation termination and dissociation of the two ribosomal subunits. In the second one, a near-cognate tRNA that forms a less-than-optimal interaction with a codon decodes the PTC, leading to read-through, and the ribosome carries on translating in the same reading frame until reaching the next stop codon. (Bidou *et al.*, 2012).

The efficiency of translation termination depends on the codon termination itself (UAA>UAG>UGA) and it is inversely correlated to the natural read-through. That means the codon with lowest termination fidelity (UGA) has the highest natural read-through potential (Bidou *et al.*, 2012; Karijolic & Yu, 2014).

The most common amino acid that decodes the read-through of UAA is glutamine, while for UAG is either glutamine or tryptophan and for UGA is tryptophan, but also is misread by arginine and cysteine tRNA (Lee & Dougherty, 2012).

It has been reported that termination signal strength can also be influenced by the immediately downstream nucleotide from the stop codon (position +4), being the C the most efficient one. However, conflicting rank orders in the other 3 nucleotides have been described using several mammalian systems. Moreover, it has been shown that several nucleotides upstream and

downstream of the stop codon also affect the read-through efficiency but the precise molecular mechanism involved is still unclear. So, taking all these considerations into account, it is difficult to predict the level of read-through for a given stop codon based purely on the surrounding nucleotide context (Bidou *et al.*, 2012; Karijolic & Yu, 2014).

In general, it has been estimated that nonsense mutations account for 5% to 15% of the genetic disorders. In a meta-analysis of the Human Gene Mutation Databases (HGMD), it was estimated that 11% of inherited disorders are caused by PTC mutations that lead to a degradation of the mRNA template and to the production of a non-functional, truncated polypeptide (Mort *et al.*, 2008). But the incidence of nonsense mutation in individual cases of genetic disorders can range from 5 to 70% (Lee & Dougherty, 2012).

In the case of LSDs, according to HGMD nonsense mutations represent, in general, a 10% of the mutations responsible of these diseases (Figure 11). However, the incidence of the nonsense mutations in each specific LSD can range from 2% to 34%.

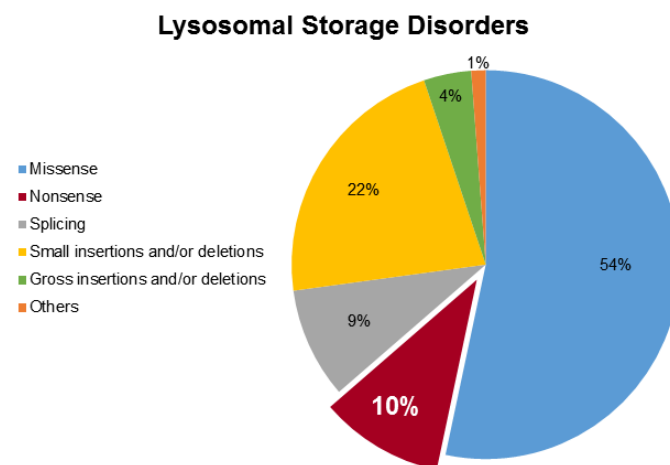


Figure 11. LSDs mutations grouped by type. Nonsense mutations represent the 10% of total mutated alleles.

2. Nonsense-Mediated mRNA Decay

The nonsense-mediated mRNA decay (NMD) is an mRNA quality control system evolutionary conserved that targets PTCs-containing transcripts for degradation. This elimination process is not 100% efficient and often results in the generation of low levels of truncated proteins (Karijolic & Yu, 2014).

There are 2 models that explain how NMD works: the exon junction complex (EJC) dependent model and the “faux” 3’ UTR model (Figure 12). In fact, it is believed that both models operate together. According to the first model, the EJC is formed 20-24 nucleotides upstream from an exon-exon junction, and these EJCs remain bound to the mRNA after splicing until they are displaced by the first round of translation. If no PTC is present, all the EJCs are removed leaving the mRNA resistant to degradation. However, if a PTC is present at least 50nt upstream of an EJC, the ribosome recognizes the stop codon by the eRF (1 and 3) and these proteins interact with the EJC proteins triggering the degradation.

In the second model it is proposed that eRFs interact with the poly A binding protein. If no PTC is present, the natural stop codon will be near the poly A binding protein. But if there is a PTC, the eRFs proteins could not interact with the 3’UTR binding proteins and this fact will trigger the

degradation of the mRNA. (reviewed in Bidou *et al.*, 2012; Lee & Dougherty, 2012; Linde & Kerem, 2008).

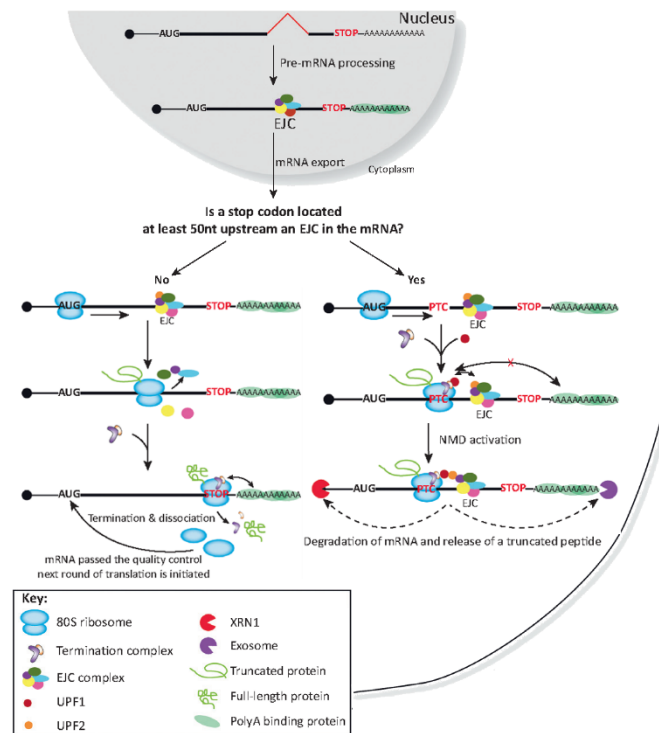


Figure 12. Nonsense-mediated mRNA decay (NMD) pathway. During pre-mRNA splicing, the EJC (exon junction complex) is formed at 20-24 nucleotides upstream from the exon-exon junction. If no PTC is present, all EJCs are removed during the first round of translation, rendering the mRNA resistant to degradation by NMD. Besides, the termination complex interacts with the poly A binding protein promoting termination. If a PTC is present at least 50 nucleotides upstream of the EJC, the ribosome stalls and the EJC remains stably associated with the mRNA. A bridge is formed between the terminated ribosome and the downstream EJC to form an active NMD complex that triggers rapid decay of the mRNA due to the termination complex cannot interact with the poly A binding protein (Bidou *et al.*, 2012).

3. Drugs

The goal of the suppression therapy is to enhance the ability of a near-cognate tRNA to compete against RFs in order to bind to a PTC and incorporate an amino acid at it. It will provide a full-length protein which may be fully functional or not.

The use of aminoglycosides as PTC-suppressors drugs to promote read-through *in vitro* has been explored for almost two decades. However, more recently, some non-aminoglycosides drugs have been discovered with nonsense suppression activities.

Aminoglycosides

These antibiotics can interact with the decoding centre of the ribosome (18S in eukaryotes), reducing the proof reading process in translation. The capacity to suppress PTCs was first demonstrated for the aminoglycoside streptomycin in *E. coli* in 1964 (Gorini & Kataja, 1964). After these initial observations, gentamicin, amikacin, paromomycin, G418 (geneticin), lividomycin and tobramycin have now been used in numerous cell lines and cell free extracts, including those derived from patients with various genetic disorders (reviewed in Karijolich & Yu, 2014; Lee & Dougherty, 2012), being tobramycin and amikacin the weakest at promoting read-through. Gentamicin and G418 are the two most commonly used aminoglycosides among all the studies performed to prove this approach. (reviewed in Lee & Dougherty, 2012). In general, G418 promotes read-through at lower concentrations and with higher efficiencies than gentamicin. Both of them have been shown to promote partial restoration of full-length functional protein using mouse models and in clinical trials for a variety of diseases such as CF, DMD; haemophilia A/B and Hailey-Hailey disease (Keeling *et al.*, 2014). It has been reported that half of the CF patients treated with gentamicin showed restoration of functional protein and

that there was also an increase of functional protein in a portion of DMD patients treated with gentamicin. However, gentamicin was unable to restore the protein activity in McArdle disease patients (Keeling *et al.*, 2014).

These studies reveal the main problems of using these drugs. Firstly, high concentrations of them are needed to achieve some read-through effect and the effectiveness has been shown to vary greatly according to the identity of the termination codon and its context. Besides, they display significant toxicity, such as ototoxicity and nephrotoxicity. The effects of the kidney damage can be reversed but the effects on the inner ear are irreversible.

In an effort to reduce aminoglycosides side effects, several aminoglycosides analogues were developed to identify molecules with enhanced nonsense suppression activity, such as TC compounds (derivatives of pyranmycin), JL compounds (derivatives of kanamycin B) or NB compounds (paromomycin-derivatives). Mattis *et al.* (2006) tested the new TC and JL drugs to evaluate their nonsense suppression ability in patient fibroblast but only six of the twenty compounds displayed effectiveness. Nudelman *et al.* (2006) synthesized novel paromomycin-derivatives where one of them, NB30, although with a lower suppression activity than paromomycin and gentamicin, was able to suppress numerous nonsense context sequences from a variety of genetic diseases *in vitro*, including Usher syndrome type 1, MPSI, CF, DMD and Rett syndrome. In an attempt to improve this compound Nudelman *et al.* synthesized the NB54 drug, whose potency was tested *in vitro* and in cell culture for the same diseases, exhibiting superior *in vitro* read-through efficiency to that of gentamicin and it exhibits far lower toxicity than that of gentamicin (Nudelman *et al.*, 2009). Nudelman's group, with the aim to enhance the potency and reduce the toxicity of the read-through compounds, generated a third-generation of drugs that includes NB74 and NB84. These compounds proved to be about 5 to 19-fold less toxic in HEK-293 cells; however, the toxicity in *in vivo* experiments have to be assessed (Nudelman *et al.*, 2010).

Non-aminoglycosides

In spite of all the work done with aminoglycosides and its positive results, it was necessary to look for new compounds that were structurally different from aminoglycosides, with higher efficiency in promoting read-through.

There is a number of non-aminoglycosides antibiotics that have also shown to suppress PTCs *in vitro* and *in vivo*, such as negamycin. This antibiotic is able to increase 38-fold the read-through in DMD mice, compared with untreated mice, and also is able to equal the read-through efficiency of gentamicin in *in vitro* analyses but no in *ex vivo* analysis (Allamand *et al.*, 2008). Negamycin seems to have less toxicity than gentamicin *in vivo* (Arakawa *et al.*, 2003), however it may induce other side-effects which should be further studied.

Other antibiotics with read-through activity are the macrolides, such as spiramycin, josamycin and tylosin. These antibiotics inhibit protein synthesis by binding to the large ribosomal unit (50S in prokaryotes), inhibiting the peptide bond formation during translation. Tylosin was able to achieve higher read-through levels in *in vitro* and in mice with a much lower concentration than G418 (Zilberberg *et al.*, 2010). The mechanism how macrolides promote read-through is unknown.

Welch *et al.* (2007) performed a study in which they screened 800000 low molecular weight compounds in an effort to find novel small molecules capable of selective suppression of PTCs. One of them, PTC124, demonstrated minimal toxicity as an orally bioavailable compound with potent read-through activity. Its efficiency has been proven by studies *in vitro*, *ex vivo* and *in vivo* with several different diseases, such as DMD, CF, Hurler syndrome or Usher syndrome. (reviewed in Karijolic & Yu, 2014). The good results in animal models of DMD and CF have brought this compound to phase II clinical trials with positive findings. Currently, it is in phase III clinical trial for both diseases. PTC124 promoted nonsense suppression of a PTC at lower concentration than gentamicin in tissue culture. It is believed that PTC124 binds to the highly conserved sites of large rRNA (28S) but more studies are needed to confirm this hypothesis.

Du *et al.* (2009) evaluated the ability to induce read-through in approximately 34000 compounds. Two of them, RTC13 and RTC14, were the best non-aminoglycosides with differing read-through activities. In *in vitro* analyses these compounds only had 10% of the aminoglycoside's activity but in *ex vivo* analyses both compounds induced a recovery of protein activity similar to that of G418 and gentamicin. Furthermore, both compounds demonstrated the ability to induce read-through in mice myotube cultures giving higher amounts of full-length protein at lower concentrations than gentamicin. Mechanistic studies for RTC13 have not yet been performed but the group that discovered them interpreted that RTC13 interact with the ribosomal 16S decoding region (Gatti, 2012). Du *et al.* (2013) continued with the effort to look for small molecular weight compounds (such as GJ071 and GJ072) active for all three premature stop codon in cells and synthesizing a second-generation of read-through compounds, RTC13-derivative, BZ16 and BZ6.

II. Niemann-Pick A/B disease: generation of iPSCs (for a future neuronal cellular model)

1. The disease

Niemann-pick type A/B is an autosomal recessive lipid storage disease resulting from mutations in the *SMPD1* gene (*sphingomyelin phosphodiesterase 1*, OMIM 607608) that cause a deficiency of acid sphingomyelinase (ASM, EC 3.1.4.12). This enzyme deficiency produces a progressive accumulation of sphingomyelin, which is the major structural component of all cell membranes, in systemic organs and in the brain.

Type A is the infantile, neurodegenerative form of the disorder, while type B patients generally have little or no neurological involvement and may survive until adolescence or adulthood.

Clinical features

In type A (OMIM 257200) the primary organs affected are the spleen, liver brain and lung. In the first months of life patients have diarrhea or vomits and they start failing to thrive and they usually have prominent hepatosplenomegaly at the 3rd month. At 5-10 months of life the hypotonia, the progressive loss of acquired motor skills and a reduction of spontaneous movements start. At 9 months, development plateaus and then it starts regressing. Macular cherry-red spots are typical feature but often not present until an advanced stage. Seizure may occur. Death classically occurs between 1.5 and 3 years. Type A is frequent in the Ashkenazi Jewish population and very rare in other populations. (2~3/100.000 among Ashkenazi Jewish individuals)(Vanier, 2013).

Type B (OMIM 607616) is a chronic panethnic disease that is clinically heterogeneous and the age of clinical onset, disease manifestations and severity vary considerably.

Splenomegaly and hepatomegaly constitute the main symptoms. Pulmonary involvement is common at all ages, retarded body growth, skeletal age and puberty are often delayed. Decreased bone mineral density and osteopenia occur in the majority of patients and only a 25% of patients can have macular halo and cherry-red spots.

Comparisons of the main characteristics of the two types of the disease are indicated in Table 3.

Table 3. Clinical features from NPA and NPB. Adapted from Winchester, 2013.

Feature	Type A	Type B
Age at onset	Early infancy	Childhood/Adolescence
Neurodegenerative course	+	±
Cherry-red macula	+	±
Hepatosplenomegaly	+	+
Marrow NPD cells	+	+
Pulmonary disease	±	+
Age at death	2-3 years	Childhood/adulthood
ASM activity	<5%	<10%

Genetics

The *SMPD1* gene is located on the short arm of chromosome 11 (11p15.4). The gene spans ~5kb and consists of 6 exons encoding the 629/631aa (depending on a six nucleotide-indel

polymorphism) of the full-length protein (Figure 13). It has genomic imprinting and there are two in-frame ATG, both functional (Schuchman, 2010). According to the HGMD (HGMD Professional 2015.2), over 150 mutations of the *SMPD1* gene are known (6.8% nonsense, 68.2% missense, 1.7% splicing, 17% small deletions, 5.1% small insertions and 1.1% small indel). In type A, 3 mutations (p.R496L, p.L302P and p.330fsX382) account for the 90% of mutated alleles in the Ashkenazi Jews. In the type B cases of the disease, the p.R608del mutation is considered to be neuro-protective. This mutation has a high frequency in the Maghreb region of North Africa, which includes Morocco, Algeria, and Tunisia (Vanier *et al.*, 1993), also in Gran Canaria Island (Fernández-Burriel *et al.*, 2003) and in Spain, where Rodríguez-Pascau *et al.* (2009) identified the mutation in 38% of the alleles from 21 Niemann-Pick patients.



Figure 13. *SMPD1* gene. *SMPD1* gene structure, with 4.57 Kb of length and containing six exons (www.ensembl.org)

Laboratory diagnosis

Diagnosis of Niemann-Pick A/B disease is established by a deficiency in the activity of ASM in white blood cells or cultured skin fibroblasts. Bone marrow usually reveals the presence of foamy histiocytes. Mutation analysis is currently used to confirm the enzymatic diagnosis and it can provide phenotype prediction. Therefore, it is useful for genetic counselling.

Treatment

Management of all types of ASM deficiency is still only symptomatic. Bone marrow transplantation has shown no evidence of neurological improvement. Splenectomy should be the last resort as it may worsen the pulmonary disease. Type B patients are appropriate candidate for ERT with human recombinant ASM. As preclinical studies in an ASM knock-out mouse model of Niemann-Pick demonstrated that administration of the recombinant enzyme reduced tissue substrate concentrations (Miranda *et al.*, 2000a), a phase I clinical trial has been carried out. In the treated patients an increase of ceramide in plasma, a product of sphingomyelin catabolism, has been observed. However, several side effects, such as elevated inflammatory biomarkers and constitutional symptoms (fever, pain nausea and/or vomiting), appear in the acute phase reaction (McGovern *et al.*, 2015).

Animal models

Before 1993 there were two naturally occurring mouse models of Niemann-Pick, the BALB/c-NPD mice (Pentchev *et al.*, 1980) and the *spm/spm* mice (Shigeki Miyawaki *et al.*, 1982). However, Horinouchi *et al.* (1993) sequenced the entire *SMPD1* gene and found no mutation, indicating that these models were not NPA/B models. Both of them were thought to be a NPC model. These models will be discussed in III.3 section (see page 31).

Otterbach & Stoffel (1995) achieved targeted disruption of the *SMPD1* gene in transgenic mice (*SMPD1*^{tm1Wst}) by homologous recombination in embryonic stem cells. This mouse model accumulates sphingomyelin in several tissues, such as liver, spleen, bone marrow, lung and brain. The same year Horinouchi *et al.* obtain similar results in ASM knock-out mice (ASMKO, *SMPD1*^{tm1Esc}) (Horinouchi *et al.*, 1995).

Marathe *et al.* (2000) created a mouse that stably expresses low levels of sphingomyelinase by using a novel transgenic/knock-out strategy. This mouse did not present the severe neurologic disease observed in ASMKO mouse but it has pathological intracellular inclusions, being a good model to study Niemann-Pick type B disease.

ASKMO mouse model has been used for preclinical trials of different therapies, such as SRT or ERT (Miranda *et al.*, 2000a). Also, it has been used to assay gene therapy combined with stem cells therapy (Miranda *et al.*, 2000b). However, the mice develop ataxia and die prematurely.

In order to investigate new therapies targeting the CNS is necessary to study in depth how disease develops in neurons. Therefore, the new strategy of modelling diseases with iPSCs is an interesting approach to test the therapies in different tissues and cell types as well as detect possible side effects before starting the animal trials.

2. Reprogramming fibroblasts to iPSCs

In 2006 Takahashi and Yamanaka found that a combination of just 4 transcription factors (Oct4, Sox2, Klf4, and c-Myc, known as the OSKM set) is sufficient to transform terminally differentiated mouse cells into iPSCs and one year later this was also achieved in human fibroblasts (Takahashi *et al.*, 2007; Takahashi & Yamanaka, 2006). iPSCs have the property of self-renewal and differentiation to many types of cell lineage like human embryonic stem cells (hESCs). These findings overcame the three main limitations of hESCs: lack of preimplantation genetic diagnoses for most diseases, the inefficiency of gene targeting in hESCs and ethical concerns regarding the use of hESCs for research (Seki & Fukuda, 2015; Tiscornia *et al.*, 2011).

In the following years, new sets of reprogramming factors and different delivery systems were developed (reviewed in Seki & Fukuda, 2015).

Delivery methods can be classified as integrative and non-integrative, viral and nonviral, DNA and RNA based. On the one hand, the integrative systems are those in which the vector gets integrated into the host cell genome, raising the risk of oncogenesis and potential disrupt of functional genes (retrovirus, lentivirus). Some improvements to these drawbacks are the use of cre-deletable systems (although the risk of gene breaks is still present because the Lox-P sequence remains) and the uses of piggyBac transposons that are completely eliminate with transposase. On the other hand, in the case of non-integrating systems the vectors do not integrate into the host genome but the efficiency of reprogramming was found to be very low (Sendai virus or adenovirus, episomal vectors, microRNA, or recombinant proteins). Small-molecules drugs are non-immunogenic cost-effective and easy to handle but further research is expected (Seki & Fukuda, 2015; Singh *et al.*, 2015).

iPSCs have been generated from a range of primary cell types. From fibroblasts, that are conveniently obtained, quickly expanded and easily reprogramed; keratinocytes, that are reprogramed with higher efficiency and speed than fibroblasts; lymphoblast to mesenchymal stem cells (Table 4).

Table 4. Methods for reprogramming somatic cells to iPSCs. Robinton & Daley, 2012.

Vector type	Cell types	Factors*	Efficiency (%)	Advantages	Disadvantages	
Retroviral	Fibroblasts, neural stem cells, stomach cells, liver cells, Keratinocytes, amniotic cells, blood cells and adipose cells	OSKM,CSK, OSK + VPA or OS + VPA	~0.001-1	Reasonably efficient	Genomic integration, incomplete proviral silencing and slow kinetics	
Integrating	Lentiviral	Fibroblasts and Keratinocytes	OSKM or <i>miR302/367 cluster</i> + VPA	~0.1-1.1	Reasonably efficient and transduces dividing and non-dividing cells	Genomic integration and incomplete proviral silencing
	Inducible lentiviral	Fibroblasts, β cells, keratinocytes, blood cells and melanocytes	OSKM or OSKMN	~0.1-2	Reasonably efficient and allows controlled expression of factors	Genomic integration and requirement for transactivator expression
Excisable	Transposon	Fibroblasts	OSKM	~0.1	Reasonably efficient and no genomic integration	Labour-intensive screening of excised lines
	<i>loxP</i> -flanked lentiviral	Fibroblasts	OSK	~0.1-1	Reasonably efficient and no genomic integration	Labour-intensive screening of excised lines, and <i>loxP</i> sites retained in the genome
Non-integrating	Adenovirus	Fibroblasts and liver cells	OSKM	~0.001	No genomic integration	Low efficiency
	Plasmid	Fibroblasts	OSNL	~0.001	Only occasional genomic integration	Low efficiency and occasional vector genomic integration
DNA free	Sendai virus	Fibroblasts	OSKM	~1	No genomic integration	Sequence-sensitive RNA replicase, and difficulty in purging cells of replicating virus
	Protein	Fibroblasts	OS	~0.001	No genomic integration, direct delivery of transcription factors and no DNA-related complications	Low efficiency, short half-life, and requirement for large quantities of pure proteins and multiple applications of protein
	Modified mRNA	Fibroblasts	OSKM or OSKML + VPA	~1-4.4	No genomic integration, bypasses innate antiviral response, faster reprogramming kinetics, controllable and high efficiency	Requirement for multiple rounds of transfection
	MicroRNA	Adipose stromal cells and dermal fibroblasts	miR-200c, miR-302s or miR-369s	~0.1	Efficient, faster reprogramming kinetics than commonly used lentiviral or retroviral vectors, no exogenous transcription factors and no risk of integration	Lower efficiency than other commonly used methods

*OSKM and similar factor names represent combinations of reprogramming factors: K, KLF4; L, LIN28; M, c-MYC; N, NANOG; O, OCT4; S, SOX2 and VPA, valproic acid.

3. The uses of iPSCs.

Due to the lack of information about the mechanism that plays a role in the disease progression or the molecular mechanism that underlies the disease, modelling diseases with iPSCs will help to improve our knowledge on the mechanisms causing the disease, so treatment could be developed aiming at the main cause of disease. iPSCs offer a new tool for basic studies, drug screening and toxicological testing to know the possible side effects of new drugs in somatic cells without animals or clinical trials, helping reducing the cost of drug production (Singh *et al.*, 2015).

Since 2009 when Lee *et al.* (2009) modelled familial dysautonomia, more than 40 iPSC disease models have been successfully generated from patients with genetic diseases and the list is still increasing (Huang *et al.*, 2012; Robinton & Daley, 2012; Yung *et al.*, 2013).

Studies with iPSCs from patients show that this model reproduced accurately several aspects of the phenotype seen in both human and animal models, though not all diseases are equally easy to model; iPSCs might reproduce some aspects of the disease better than others. These cell models have a great potential in orphan disease or in diseases for which mouse systems are not available. Moreover, iPSCs can be a valuable complement to the existing mouse models because animal and cell models do not exclude each other (Tiscornia *et al.*, 2011).

Besides, iPSCs technology could also be used as a cellular therapy itself, since it allows to transfer the patient its own differentiated iPSCs repaired by gene targeting to minimize the immune rejection (Figure 14).

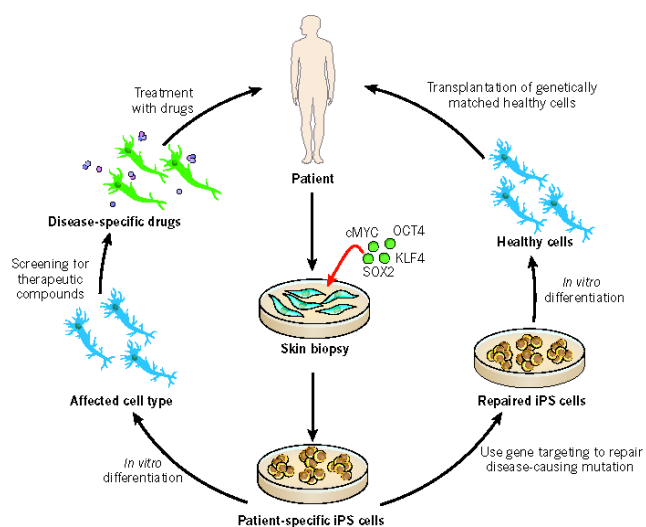


Figure 14. Medical applications of iPSCs. Reprogramming technology and iPSCs have the potential to be used to model and treat human disease (Robinton & Daley, 2012).

4. iPSCs in Lysosomal storage disorders

Since there is not a cure for most LSDs at present, specific iPSC may provide an exceptional opportunity for dissecting unexplored disease pathogenesis and identifying new drugs. As LSDs are monogenic diseases, a more carefully controlled comparison between diseased and wild-type cells can be done. This will help in the study of the disease phenotype caused by the patients' mutation and in the verification that drug-corrected cells reverse the disease phenotype. For these reasons, iPSCs from several LSDs have been generated (Table 5) and probably this list will increase in a near future (Huang *et al.*, 2012).

Table 5. Disease modelling and drug testing of LSDs iPSCs.

Disease	Species	Original cell type	Cell type of interest	Disease phenotype	Drug testing	Reference
Pompe	Mouse	Fibroblast	Skeletal muscle cells	Glycogen accumulation	No	(Kawagoe <i>et al.</i> , 2011)
Pompe	Human	Fibroblasts	Cardiomyocytes	Glycogen storage and abnormal morphology and function of mitochondria	Yes	(Huang <i>et al.</i> , 2011)
Fabry	Mouse	Fibroblasts	Cardiomyocytes	Gb3 accumulation	No	(Meng <i>et al.</i> , 2010)
Krabbe	Mouse	Fibroblasts	Neural stem cells	Reduced β -galactocerebrosidase activity	No	(Meng <i>et al.</i> , 2010)
Gaucher type 3	Human	Fibroblasts	ND	ND	No	(Park <i>et al.</i> , 2008)
MPSI	Human	Keranocytes and bone marrow mesenchymal stem cell	Hematopoietic cells	Lysosomal storage of glycosaminoglycan	No	(Tolar <i>et al.</i> , 2011)

Table 5. (Continued)

Disease	Species	Original cell type	Cell type of interest	Disease phenotype	Drug testing	Reference
MPSIIIB	Human	Fibroblasts	Neural stem cells	Storage vesicles associated with disorganized Golgi complex	Yes	(Lemonnier <i>et al.</i> , 2011)
MPSVII	Mouse	Fibroblasts	unknown	Elevated levels of hyaluronic acid and impaired formation of embryoid bodies	No	(Meng <i>et al.</i> , 2010)
NPC	Human	Fibroblasts	Neural progenitor	cholesterol accumulation	No	(Trilck <i>et al.</i> , 2013)
Fabry	Human	Fibroblasts	ND	Gb3 accumulation Abnormal differentiation	No	(Kawagoe <i>et al.</i> , 2013)
Sandhoff	Mouse	Neural stem cell	Cardiomyocytes Neural stem cell	GM2 accumulation impaired neuronal differentiation	Yes	(Ogawa <i>et al.</i> , 2013)
Gaucher type 1, 2, 3	Human	Fibroblasts	Macrophages Neurons	Low GC activity sphingolipids accumulation	Yes	(Panicker <i>et al.</i> , 2012)
NPC	Human	Fibroblasts	Hepatic cell neurons	Impairment autophagy flux, cholesterol accumulation	Yes	(Maetzel <i>et al.</i> , 2014a)
NPC	Human	Fibroblast	Neurons astrocytes	Early death of neurons, calcium and WNT signalling defects	Yes	(Efthymiou <i>et al.</i> , 2015)
MLD	Human	Fibroblasts	Neuroepithelial stem cell	Reduced ARSA activity	Yes	(Doerr <i>et al.</i> , 2015)
CLN2, CLN3	Human	Fibroblasts	Neurons	Abnormalities mitochondria, Golgi and RE	Yes	(Lojewski <i>et al.</i> , 2014)
Fabry	Human	Fibroblasts	Cardiomyocytes	GL3 accumulation	Yes	(Itier <i>et al.</i> , 2014)
NPC	Human	Fibroblasts	Neural stem cells	Cholesterol accumulation	Yes	(Yu <i>et al.</i> , 2014)
Danon	Human	N.D.	Cardiomyocytes	Impaired autophagy flux, increased cell size and apoptosis	Yes	(Hashem <i>et al.</i> , 2015)
GM1	Human	Fibroblasts	Neural progenitor	Low β -galactosidase activity, GM1 accumulation	Yes	(Son <i>et al.</i> , 2015)
MPSVII	Human	Fibroblasts	Neural Stem cells	Decreased GUSB activity	Yes	(Griffin <i>et al.</i> , 2015)
Gaucher type 2	Human	Fibroblasts	Neurons macrophages	Low β -glucosidase activity and protein levels	Yes	(Tiscornia <i>et al.</i> , 2013)
Gb3, globotriaosylceramide; ND, not described						

III. Niemann-Pick type C disease: characterization of mouse models

1. The disease

Niemann-Pick type C disease (NPC) (OMIM 257220) is an autosomal recessive lysosomal lipid storage disorder due to mutations in one of two genes, either *NPC1* (95% of the cases) or *NPC2*, with extreme clinical heterogeneity. In about 90% of the patients, a progressive neurodegenerative involvement is the dominant feature. NPC is a panethnic disease and has an estimated incidence of approximately 1/100.000 live births.

The cellular pathology of this disease is characterised by an impaired egress of cholesterol from the late endosomal/lysosomal compartment, but other lipids, especially sphingolipids, are also involved.

The study of NPC provided clues of the cellular cholesterol homeostasis and molecular mechanism leading to NPC disease have also been discussed, but there are still many questions that remain unanswered (Vanier & Patterson, 2013; Vanier, 2015). For further information see III.2 section (page 30).

Clinical features

NPC has a highly variable clinical phenotype with a wide-ranging age of onset and with a life span from few days of life to 60 years. However, the majority of patients die between 10 and 25 years old. Visceral involvement (liver, spleen and lung) and neurological manifestation arise in different times.

The patients gradually develop neurologic abnormalities, which are initially manifested by ataxia, grand mal seizures, and loss of previously learned speech (dysarthria). Other features include dystonia, dysphagia and progressive dementia.

There are four clinical forms of the disease, classified by the age of onset of the neurological manifestations: the early infantile onset form, before 2 years, where most patients never learn to walk and survival rarely exceeds 5 years of life; the late infantile onset form, between 2 and 5 years old, where impairment in mental development becomes very obvious and death often occurs between 7 and 12 years of life; the juvenile onset form, between 5 and 15 years old, that constitutes the large majority of cases and lifespan varies from late teens until 30 or later, and finally the adolescent and adult onset form, which is an attenuated juvenile form. In Figure 15 a schematic representation of the clinical signs of the different forms is shown (Vanier & Latour, 2015).

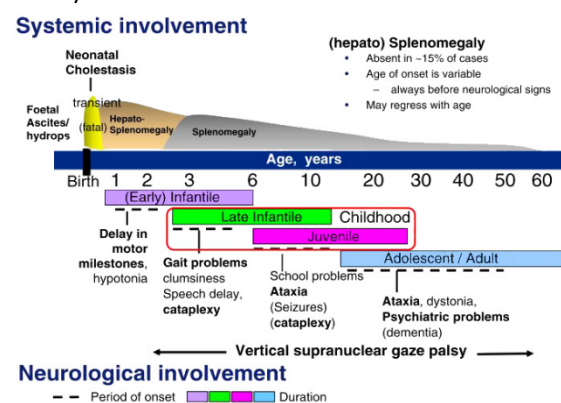


Figure 15. Schematic representation of the clinical aspects of Niemann-Pick C disease. Vanier, 2015.

Genetics

The *NPC1* gene (OMIM 257220) is located on the large arm of the chromosome 18 (18q11-q12). The gene spans ~56kb and consists of 25 exons encoding a 1278 aminoacids glycoprotein with 13 transmembrane domains, a sterol-sensing domain (SSD) and a cytoplasmatic C-terminal lysosomal targeting motif (Figure 16). More than 350 mutations have been reported to date in the HGMD (Professional 2015.2) (7.5% nonsense, 60.3% missense, 7.2% splicing, 13.9% small deletions, 8% small insertions, 0.5% small indel, 2.3% gross deletions and 0.3% gross insertions). The most frequent mutation is p.I1061T accounting for 20% of mutated alleles among France and the United Kingdom (Millat *et al.*, 1999). It is very common in Spanish-American patients (McKay Bounford & Gissen, 2014) but no so frequent in Portugal, Spain or Italy (Fancello *et al.*, 2009; Fernandez-Valero *et al.*, 2005; Macías-Vidal *et al.*, 2011; Ribeiro *et al.*, 2001). This mutation makes that the NPC1 protein do not become fully glycosylated and have a decreased half-life compared to wild-type (Gelsthorpe *et al.*, 2008).

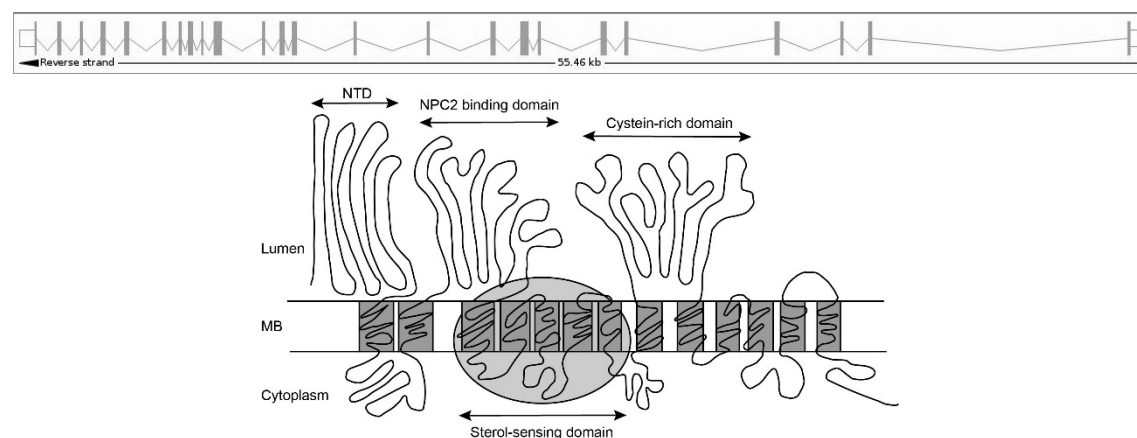


Figure 16. *NPC1* gene and protein. *NPC1* gene structure, with 55.46 Kb of length and containing 25 exons (www.ensembl.org) and schematic *NPC1* protein model, with N-terminal domain (NTD), NPC2 binding domain, sterol-sensing domain and cysteine-rich domain. Adapted from Millat *et al.*, 2001.

The *NPC2* gene (OMIM 607625) is located on the large arm of chromosome 14 (14q24.3). The gene spans ~14kb and consists of 5 exons encoding a 151aminoacids soluble glycoprotein that binds to cholesterol with high affinity (Figure 17). Over 20 different mutations are known to date, being all of them “private” (Vanier, 2015). According to HGMD (Professional 2015.2) 26.1% nonsense, 47.8% missense, 13% splicing and 13% small deletions.

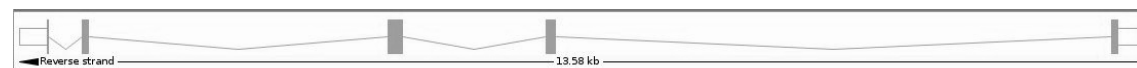


Figure 17. *NPC2* gene. *NPC2* gene structure, with 13.58 Kb of length and containing five exons (www.ensembl.org)

NPC1 structural characteristics are associated with cholesterol transport. Sterol-sensing domain is involved in cholesterol metabolism and N-terminal domain (NTD) is able to bind cholesterol by surrounding the 3 β -hydroxyl end with high affinity. *NPC2* specifically binds cholesterol with nanomolar affinity by recognizing the isoocetyl side chain and leaving the 3 β -hydroxyl end exposed, in an orientation opposite to the NTD of *NPC1*. *NPC2* also rapidly transfers cholesterol but no glycosphingolipid, ceramide, phospholipids or fatty acids directly to membrane. It has been shown that the second large luminal loop of *NPC1* is a binding site for *NPC2* protein, this

protein-protein interaction only occurs at acidic conditions and requires that cholesterol to be bound to NPC2 (reviewed in Klein *et al.*, 2014; Yu *et al.*, 2014a).

Mutations in either protein led to the same pattern of lipid accumulations and have the same clinical phenotype, indicating that both proteins work cooperatively to facilitate the egress of free cholesterol and other lipid cargo from the lysosomes (Vanier, 2015).

Thus, a model was proposed for the concerted transfer of cholesterol from NPC2 to NPC1 within lysosomes (Figure 18). Endocytosed unesterified cholesterol is derived to lysosome and then transferred via NPC2 from membranes of the internal vesicles of lysosomes to NPC1 in the limiting membrane. The molecular mechanism by which cholesterol is exported from NPC1 to the ER and plasma membrane has not been elucidated yet, although vesicular transport, transport via carrier proteins and direct membrane contact have been proposed (Vance & Karten, 2014).

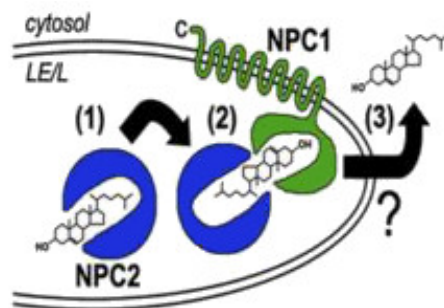


Figure 18. Proposed mechanism for transfer cholesterol mediated by NPC1 and NPC2 proteins. NPC2 binds endocytosed cholesterol in the lysosomal lumen (1). NPC2 shuttles the cholesterol to the cholesterol binding pocket of NPC1 without direct contact of the hydrophobic cholesterol molecule with the aqueous lysosomal lumen (2). The mechanism by which NPC1-associated cholesterol is exported from the outer lysosomal membrane to the endoplasmic reticulum and plasma membrane has not been established (3). (Vance & Karten, 2014).

Laboratory diagnosis

Foam cells are often present in bone marrow. Demonstration of impaired intracellular cholesterol transport in cultured cells is the primary laboratory diagnosis for NPC. The filipin test is the most sensitive assay, due to the fact that filipin is a polyene antibiotic that binds to cholesterol but not to esterified sterols. It detects the accumulation of cholesterol and in the 85% of cases filipin show numerous strongly fluorescent perinuclear vesicles. Molecular genetic study is very useful to confirm an NPC diagnosis and is the preferred strategy for prenatal diagnosis. Oxysterols are significantly elevated in patients' plasma and can be used as a diagnostic tool (Vanier, 2015; Vanier, 2010).

Treatment

Therapy for Niemann-pick C disease remains largely symptomatic. Bone marrow transplantation has been unsuccessful and among the therapies tested in animal models, cyclodextrin and SRT with miglustat were the ones that gave best results. In this regard, nowadays Niemann-Pick C patients can be treated by SRT with miglustat.

Miglustat, a drug previously approved for the treatment of Gaucher disease, was approved in 2009 for the treatment of neurological manifestations of NPC. It has been proved that it stabilizes neurological disease and patients improve swallowing over 12 months, 24 months or 2 years of miglustat treatment (Patterson *et al.*, 2015; Patterson *et al.*, 2010; Pineda *et al.*, 2009; Wraith *et al.*, 2010). In the feline model of NPC, miglustat decreased GM2 ganglioside accumulation and slightly delayed development of neurological symptoms (Stein *et al.*, 2012). In

mice models miglustat also reduced ganglioside storage and extended the life span of the animals (Zervas *et al.*, 2001).

Another treatment that is currently being assayed is the use of 2-hydroxypropyl- β -cyclodextrin. In fact, phase I clinical trials are ongoing (NTC01747135). Many studies, in cells and in animal models, have been conducted where cyclodextrin treatment decreased cholesterol and all other lipids in excess, such as glycosphingolipids. Similarly, the excess of GM2 and GM3 in brain was decreased but there were no changes in the normal profiles of other gangliosides (Davidson *et al.*, 2009).

2. Lipid accumulation

The storage material in NPC patients is highly complex and includes multiple different classes of lipids. The lipids that progressively accumulate in this disease include cholesterol, sphingomyelin (SM), multiple glycosphingolipids (GSLs) and sphingosine (Figure 19). In NPC patient's cells and animal models, cholesterol and SM are the most abundant storage lipids in peripheral tissues whereas in brain, GSLs storage is more significant with no changes in cholesterol or SM. An unusual lipid only stored in NPC disease and not in other LSDs is sphingosine (reviewed in Lloyd-Evans & Platt, 2010). There is some controversy about which of the lipids is the one that really causes the disease.

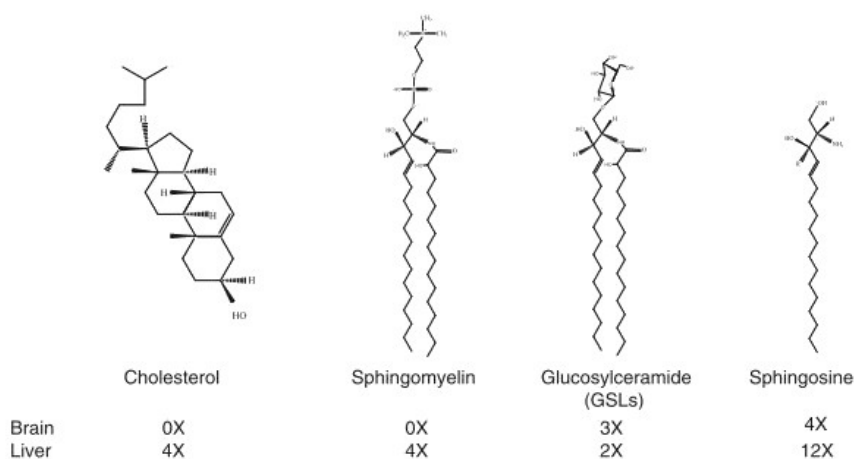


Figure 19. Storage lipids and fold elevation in liver and brain from Npc1 mouse. (Lloyd-Evans & Platt, 2010).

Cholesterol

Cholesterol is the most dominant storage lipid and both NPC1 and NPC2 proteins can bind this molecule. Low density lipoprotein (LDL)-derived cholesterol is transported via the endocytic system to lysosomes where it is trapped and the free cholesterol begins to accumulate. LDL also contains significant levels of ceramide and GSLs. For this reason, further work is needed to make it clear which one of the lipids requires reduction to correct the phenotype.

Another issue that needs further study is to know if cholesterol accumulation is due to a direct transport role of NPC1 protein or if NPC1 is a cholesterol-regulated protein that transports cargo other than cholesterol.

However, there are some studies showing that cholesterol maybe is not the primary cause in NPC disease. Several reasons support this hypothesis: it has been shown that therapies that

lower cholesterol have no clinical benefit in patients and in animal models; genetic manipulation of the NPC mice model in order not to capture LDL does not improve the phenotype of the animal; there are NPC patients that do not store LDL-derived cholesterol but have accumulation of other lipids; cholesterol can be transported out of lysosomes through other pathways and the only approved drug for therapy of NPC, miglustat, reduces GSL biosynthesis without reducing cholesterol levels.

Glycosphingolipids

In brain, the major storage material is GSLs, instead of cholesterol. Mainly glucosylceramide (GlcCer), lactosylceramide (LacCer) and gangliosides, GM2 and GM3.

Just as the accumulation of gangliosides in other LSD results in severe neuropathology, in the case of NPC these lipids may also cause the neurodegeneration effect on patients. This hypothesis was ruled out when (Liu *et al.*, 2000) crossed NPC mice with mice that could not synthesize GSLs and no correction was observed. However, cholesterol levels were decreased in neurons with no GM1/GM2 indicating that the accumulation of cholesterol is dependent on the accumulation of gangliosides. Conversely, miglustat produced a reduction of the GSLs accumulated and not cholesterol levels, promoting clinical benefits in both mice and humans.

Developmental ganglioside studies conducted in the murine or feline models showed that GM2 increases first followed by GM3 (Maue *et al.*, 2012). In human disease, GM2 and GM3 was not present in brains of 24 week-old foetus but it was present in patients who died in their 3 first months of life (Vanier, 1999).

In *Npc1*^{nih} mouse there are decreased levels of galactosylceramide, the most specific myelin lipid (Weintraub *et al.*, 1985), as in *Npc1*^{D1005G} mouse and the NPC1 cat model. This lipid has also been found particularly low in brain of patients with the most severe early infantile neurological form of the disease (Vanier, 2015).

Sphingomyelin

Although sphingomyelin is the main sphingolipid that accumulates in Niemann-Pick types A/B, in type C the localization of the ASM protein has been shown to be abnormal and is also less active. Interestingly, SM, like cholesterol, is not elevated in the brain either. It has been shown that there is a close biophysical relationship between SM and cholesterol, because the restoration of ASM in NPC patient's fibroblasts causes a reduction of cholesterol (Devlin *et al.*, 2010).

Sphingosine

Among all storage lipids in NPC disease, sphingosine is the only one that induces a NPC phenotype in normal cells when added. It has been demonstrated that sphingosine is the first lipid that accumulates, followed by cholesterol, SM and GSLs. In peripheral tissues, as spleen or liver, there is a differential increase of 12-fold, but in brain the increase is only of 4-fold (reviewed in Lloyd-Evans & Platt, 2010).

3. Animal models

Two murine (BALB/c-*Npc1*^{nih} or *m1N* and C57BLKS/J-*Npc1*^{spm}), one feline and one canine spontaneous models of NPC disease have been reported (Morris *et al.*, 1982; Miyawaki *et al.*, 1982; Lowenthal *et al.*, 1990; Kuwamura *et al.*, 1993) showing clinical and pathological features

quite similar to those in humans. Light and electron microscopic features of these models closely resemble human NPC disease. In both, canine and feline models, infiltration of foamy macrophages is extensive in the lung, liver, spleen, and lymph nodes. Hepatosplenomegaly is absent in the canine model. These models had an essential role in defining the biochemical basis for NPC and proved to be useful to progress on the understanding of the cellular and molecular mechanisms underlying neurodegeneration and to test general therapies, such as substrate reduction therapy, or to study the effects of treatments in liver and brain.

The study of these models has allowed to find enzymatic markers for lysosomes, mitochondria and peroxisomes in brain and liver. Also, it has been shown that it is the cholesterol carried in low density lipoprotein and chylomicrons that is sequestered in tissues, and not new synthesised sterol (Xie *et al.*, 1999).

One of the main benefits of mouse models is that they can be easily genetically manipulated to create new models such as the KO mutant mice (*Npc1*^{tm1.2Apl or delta}), the conditional KO mice (*Npc1*^{tm1.1Apl or flox}) (Elrick *et al.*, 2010) or the chemical-induced mice (*Npc1*^{nmf164}) (Maue *et al.*, 2012) to study the effect of the mutation in specific tissues or/and to study the effect of some particular human mutations.

In 1977, Morris *et al.* found a strain of BALB/c mice producing offspring which develops a lack of locomotion coordination and loss of weight leading to death at 10 weeks of age. These mice had a 5-fold increase of total cholesterol in liver and spleen at the first weeks of life, arriving at 10-15 fold increase at later stages. That was the first mouse model of NPC disease. This mouse carries the allele *Npc1*^{m1N or nih}, which is a spontaneous mutation due to the insertion of a transposon (Morris *et al.*, 1982). Most of the studies in mice have been done in this model.

In 1982, Miyawaki *et al.* also found a strain of C57BL mice with neurological symptoms and weight loss beginning in the 7 week of age and died at 12 weeks. It showed a marked enlargement of the liver and spleen. That is why this mouse was first known as the “sphingomyelinosis” mouse. However, four years later Miyawaki *et al.* (1986) reclassified the C57BLKS/J-*Npc1*^{SPM} mouse as a model of NPC rather than of NPA/B. The allele *Npc1*^{SPM} is a spontaneous point mutation in the intron 19 leading to a frameshift and a truncated protein.

Sleat *et al.* (2004) generated an *Npc2* mouse model and a double mutant *Npc1/Npc2* mouse model. The *Npc2* mouse model (*Npc2*^{tm1Plob}) was done by an aberrant recombination leading to a miss-splicing mRNA with a 4% of wild-type levels of correctly spliced *Npc2* mRNA and protein. With this study it has been shown that *Npc1* and *Npc2* have no redundant functions in a common pathway for lipid transport. Moreover, the phenotypes of the *Npc1* or *Npc2* single mutant and of the *Npc1/Npc2* double mutant are similar or identical in the disease onset, progression, pathology and type of lipid accumulation.

Elrick *et al.* (2010) generated an *Npc1* conditional KO mutant mice, using gene targeting. Deletion of *Npc1* in mature cerebellar Purkinje cells led to an age-dependent impairment in motor tasks, including rotarod at 15 weeks and balance beam performance at 10 weeks; tremors starts at 13 weeks of life. These mice did not show the early death or weight loss characteristic of global *Npc1*-null mice that live no longer than 9 weeks. These findings suggest that Purkinje cell degeneration is sufficient to cause motor impairment but no other features of the disease.

Histologic examination revealed the progressive loss of Purkinje cells in an anterior-to-posterior gradient in a similar pattern to that of global knock-out mice. The authors concluded that *Npc1* deficiency leads to cell-autonomous selective neurodegeneration and suggested that the ataxic symptoms of NPC disease may arise from Purkinje cell death rather than cellular dysfunction.

Xie *et al.* (2011) generated a mouse model with two different point mutations, p.P202A and p.F203A, near the N-terminal domain of the *Npc1* protein to abolish its cholesterol binding activity. Mutation was introduced by homologous recombination (*Npc1*^{tm1Mb/jg or pf}) and the mice reproduced the phenotype of *Npc1*^{nih} confirming the physiologic relevance of the cholesterol binding site on *Npc1*. These mice exhibited neurodegeneration at 7 weeks and died at 10 weeks. Liver and other organs accumulated cholesterol in lysosomes but after cyclodextrins treatment the hepatic cholesterol accumulation was reduced.

Maue *et al.* (2012) generated an *Npc1* mouse model with a point mutation, D1005G, by mutagenesis. The mutation corresponds to a site in the large cysteine-rich luminal loop of the *Npc1* protein, where approximately one-third of the identified human mutations have been located. Even though, this mouse had relatively normal levels of mRNA, it had dramatically reduced levels of *Npc1* protein, as well as abnormal cholesterol metabolism and altered glycolipid expression. This model survived longer, almost 20 weeks, and the loss of weight was later and gradually than the *Npc1* KO model which only lived 9 weeks. This model was made to study the common late-onset forms of humans NPC disease.

Recently, Praggastis *et al.* (2015) generate a Knock-in model bearing the most prevalent mutation in NPC patients, p.I1061T. This mutation encodes a misfolded protein which reduced its half-life. This *Npc1*^{I1061T or tm1.1Dso} model displays a less severe, delayed form of NPC disease with regard to weight loss, decreased motor coordination, Purkinje cell death, lipid storage, and premature death. The murine *Npc1*^{I1061T} protein has a reduced half-life *in vivo*, consistent with protein misfolding and rapid ER-associated degradation, and can be stabilized by histone deacetylase inhibition. This novel mouse model faithfully recapitulates human NPC disease and provides a powerful tool for preclinical evaluation of therapies targeting NPC1 protein variants with compromised stability.

A comparison of NPC mice models are shown in Table 6.

Table 6. Mice model alleles.

Alleles	Allele type	Mutation	Genetic Background	Reference
<i>Npc1</i> ^{m1N or nih}	Spontaneous	Transposon insertion results in premature truncation of the protein.	BALB/c	(Morris <i>et al.</i> , 1982)
<i>Npc1</i> ^{spm}	Spontaneous	Single point mutation intron 19. 43 base pair insertion generates a frame shift.	C57BLKS/J	(Miyawaki <i>et al.</i> , 1982)
<i>Npc2</i> ^{tm1plob}	Targeted	Aberrant recombination	129S1/Sv * BALB/c * C57BL/6	(Sleat <i>et al.</i> , 2004)

Table 6. (Continued)

Alleles	Allele type	Mutation	Genetic Background	Reference
<i>Npc1</i> ^{tm1.1Apl} or flox	Targeted (Conditional ready, No functional change)	Exon 9 was floxed	B6.Cg	(Elrick <i>et al.</i> , 2010)
<i>Npc1</i> ^{tm1.2Apl} or delta	Targeted (Null/knock-out)	Cre mediated recombination removed exon 9	B6.Cg	(Elrick <i>et al.</i> , 2010)
<i>Npc1</i> ^{tm1Mbjg} or pf	Targeted	Nucleotide substitutions. p.P202A and p.F203A	129S6/SvEvTac * C57BL/6J	(Xie <i>et al.</i> , 2011)
<i>Npc1</i> ^{nmf164}	Chemically induced	Single point mutation. p.D1005G	C57BL/6J	(Maue <i>et al.</i> , 2012)
<i>Npc1</i> ^{tm1.1Dso} or I1061T	Targeted (Conditional ready, Humanized sequence)	Nucleotide substitution. C.3179A>C (p.I1061T)	B6.129	(Praggastis <i>et al.</i> , 2015)

OBJECTIVES

The current aims of the group where this thesis has been performed are to develop new therapeutic strategies for different lysosomal storage disorders and to generate cellular and animal models for these diseases.

The main objectives of this thesis, included in the aims of the group, are to assay the nonsense suppression therapy in several lysosomal storage diseases and to generate and characterize cellular and animal models for Niemann-Pick A/B and Niemann-Pick C, respectively.

Specific objectives:

I. Nonsense suppression therapy

- To test the effect of several read-through drugs, aminoglycosides (gentamicin and G418) and non-aminoglycosides drugs (PTC124, RTC13, RTC14, BZ6 and BZ16), on different nonsense mutations found in patients of four LSDs, using different approaches.

II. Generation of a cellular model for Niemann-Pick A/B

- To obtain iPSCs from fibroblasts of three different NPA/B patients and a healthy control, to further be differentiated to neurons.

III. Characterization of mouse models of Niemann-Pick C

- To obtain two different mouse models of NPC: one homozygous for a pseudoexon-generating mutation and another homozygous for a 1-bp deletion, from the heterozygous mice generated by *OZ-Gene*.

- To assess the effect of the pseudoexon-generating mutation on the splicing process in the mice bearing this mutation.

- To perform the biochemical and histological characterization of the two lines of homozygous mice through the analyses of substrate accumulation in different tissues.

- To perform a neurobehavioral characterization of the mice through a battery of behavioural tests.

MATERIAL AND METHODS

I. Read-through analysis

1. Samples and mutations

In this work, 19 primary nonsense mutations, corresponding to 4 LSD-responsible genes, were analysed. They are listed in Table 7. Several of them were found in Spanish patients. In the case of *ARSB* (*Arylsulfatase B*), mutations p.R160X and p.W322X were found in two Spanish Maroteaux-Lamy patients (Garrido *et al.*, 2007). The three *SMPD1* mutations were found in Spanish Niemann-Pick patients (Rodriguez-Pascau *et al.*, 2009a). Two of the three *NAGLU* (*N-Acetylglucosaminidase*) mutations, p.R168X and p.Q566X, were present in the same Spanish Sanfilippo B patient, SFB1, named as P5 in Matalonga *et al.* (Matalonga *et al.*, 2014). While mutation p.R168X was found in several other Spanish patients (Coll *et al.*, 2001), mutation p.Q566X was found only in this patient. Regarding to the *HGSNAT* (*Heparan- α -Glucosaminide N-Acetyltransferase*) mutations, p.R384X was found in a French Sanfilippo C patient, SFC13, who was referred to us. All other mutations were obtained from the literature.

Fibroblasts from a Spanish SFB patient (patient SFB1, genotype p.W168X/p.Q566X), and from a French SFC patient (patient SFC13, genotype p.R384X/c.1542+4dupA) were available.

Table 7. Nonsense mutation studied in this work.

Gene	Disease	Mutation		Exon ¹	Stop codon ²	References
		c.DNA	Protein			
<i>ARSB</i>	Maroteaux-Lamy	c.438G>A	p.W146X	2 (8)	(A)UGA(C)	(Voskoboeva <i>et al.</i> , 2000)
		c.478C>T	p.R160X	3 (8)	(C)UGA(G)	(Voskoboeva <i>et al.</i> , 1994)
		c.966G>A	p.W322X	5 (8)	(G)UGA(G)	(Garrido <i>et al.</i> , 2007)
		c.1507C>T	p.Q503X	8 (8)	(A)UAG(U)	(Villani <i>et al.</i> , 1999)
<i>SMPD1</i>	Niemann-Pick A/B	c.509G>A	p.W170X (W168X) ³	2 (6)	(C)UGA(G)	(Rodriguez-Pascau <i>et al.</i> , 2009a)
		c.945C>A	p.Y315X (Y313X) ³	2 (6)	(G)UAA(C)	(Rodriguez-Pascau <i>et al.</i> , 2009a)
		c.1327C>T	p.R443X (R441X) ³	4 (6)	(C)UGA(A)	(Schuchman, 1995)
<i>NAGLU</i>	Sanfilippo B	c.503G>A	p.W168X	2 (6)	(C)UAG(A)	(Coll <i>et al.</i> , 2001)
		c.1674C>G	p.Y558X	6 (6)	(G)UAG(G)	(Ouesleti <i>et al.</i> , 2011)
		c.1696C>T	p.Q566X	6 (6)	(G)UAG(G)	(Matalonga <i>et al.</i> , 2014)
<i>HGSNAT</i>	Sanfilippo C	c.607C>T	p.R203X	6 (18)	(U)UGA(G)	(Ruijter <i>et al.</i> , 2008)
		c.887C>A	p.S296X	10 (18)	(A)UAG(A)	(Feldhammer <i>et al.</i> , 2009)
		c.947G>A	p.W316X	10 (18)	(A)UAG(A)	(Hrebícek <i>et al.</i> , 2006)
		c.962T>G	p.L321X	10 (18)	(G)UGA(A)	(Hrebícek <i>et al.</i> , 2006)
		c.1150C>T	p.R384X	12 (18)	(U)UGA(G)	(Hrebícek <i>et al.</i> , 2006)
		c.1209G>A	p.W403X	12 (18)	(G)UGA(C)	(Ouesleti <i>et al.</i> , 2011)
		c.1516C>T	p.R506X	15 (18)	(U)UGA(U)	(Hrebícek <i>et al.</i> , 2006)
		c.1530G>A	p.W510X	15 (18)	(U)UGA(U)	(Ruijter <i>et al.</i> , 2008)
		c.1674C>G	p.Y558X	17 (18)	(G)UAG(C)	(Feldhammer <i>et al.</i> , 2009)

¹Exon bearing the nonsense mutation (total number of exons of the corresponding gene)

²In brackets the nucleotides at 5' and 3' of the stop codon

³In brackets alternative nomenclature considering a six nucleotide-indel polymorphism

2. Site-directed mutagenesis

The nonsense mutations were introduced in the wild-type full-length cDNA of the corresponding gene cloned in the pcDNA3.1 expression vector by PCR-based site-directed mutagenesis using the *QuikChange II XL™ Site-Directed Mutagenesis Kit* (Stratagene Cloning Systems), according to the manufacturer's instructions.

Specific manufacturer characteristics were taken into account for primers design. Table 8 shows the sequence of the primers used indicating the changes introduced in grey shadow.

Table 8. Primers used in the site-directed mutagenesis.

Gene	Mutation		Primer 5'-3'	%CG Nts	°C
SMPD1	p.W168X	Forward	CACCTGTGGGCACTGAGACATTTTCTCATCTTGG	50 34	79.2
		Reverse	CCAAGATGAGAAAATGTCTCAGTGCCACAGGTG		
	p.Y313X	Forward	CCAGTGCCAGTGTAACCTGCTGTGGTAACC	58 31	80.3
		Reverse	GGTTACCCACAGCAGGTTACTGACTGGCACTGG		
	p.R441X	Forward	GCTGGAGCTGGAATTACTGAATTGTAGCCAGG	46 35	78.1
		Reverse	CCTGGCTACAATTCAGTAATAATTCCAGCTCCAGC		
NAGLU	p.W168X	Forward	AACCTGGCACTGGCCTAGAGCGGCCAGGAGGCC	70 33	86.6
		Reverse	GGCCTCCTGGCCGCTCTAGGCCAGTGCCAGGTT		
	p.Y558X	Forward	CCCCGCTTCCGCTAGGACCTGCTGGACC	72 29	84.5
		Reverse	GGTCCAGCAGGTCCTAGCGGAAGGCGGGG		
	P.Q566X	Forward	GCTGGACCTCACTCGGTAGGCAGTGCAAGGAGCT	64 33	84.1
		Reverse	AGCTCCTGCACTGCCTACCGAGTGAGGTCCAGC		
HGSNAT	p.R203X	Forward	GCCATAAGTTCTTGAGAACTGATCGCCTCATCAATTCTG	43 40	79.6
		Reverse	CAGAATTGATGAGGCGATCAGTTTCTCAAGAACTTATGGC		
	p.S296X	Forward	CTCCATTTTCTATAGATGACTTCTATACTGCAACGGGGG	41 41	79.6
		Reverse	CCCCGTTGCAGTATAGAAGTCATCTATAGAAAAATGGAAG		
	p.W316X	Forward	GCTGGGGAAGATTGCATAGAGGAGTTTCTGTAA	46 35	78.1
		Reverse	TTAACAGGAACTCCTCTATGCAATCTTCCCCAGC		
	p.L321X	Forward	GCATGGAGGAGTTTCTGTGAATCTGCATAGGAATTATC	44 39	79.5
		Reverse	GATAATTCCTATGCAGATTCACAGGAACTCCTCCATGC		
	p.R384X	Forward	GAGCTGCCTTCTCTTTGAGACATCACGTCCAG	52 33	79.1
		Reverse	CTGGACGTGATGTCTCAAAGAGAAAGGCAGCTC		
	p.W403X	Forward	GCTGGAAGGCCTGTGACTGGGCTTGACATTCC	59 32	81.6
		Reverse	GGAATGTCAAGCCAGTCACAGGCCTTCCAGC		
	p.R506X	Forward	GGACCAAAGACATCCTGATTTGATTCAGTCTTGGTG	46 37	79.4
		Reverse	CACCAAGCAGTGAATCAATCAGGATGTCTTTGGTCC		
	p.W510X	Forward	CCTGATTCGATTCAGTCTTGTGTTGTATTCTTGGGC	45 38	79.4
		Reverse	GCCCAAGAATAACAACATCAAGCAGTGAATCGAATCAGG		
	p.Y558X	Forward	GGTCTGTAGCCAGTTGTGGATGTGAAGGGGC	59 32	81.6
		Reverse	GCCCTTCACATCCACAACCTGGCTACAGGACC		

Nts, nucleotides

E.coli JM109 aliquots were transformed with vectors bearing each mutation and the transformed colonies were selected by ampicillin resistance. Colonies were grown in Luria-Bertani (LB) medium with ampicillin and vectors were isolated by *Kit Wizard Plus SV Minipreps DNA Purification System* (Promega). The DNA from each sample was quantified using a NanoDrop ND-1000 spectrophotometer (NanoDrop Technologies).

All the constructs were resequenced to ensure that no spurious mutations had been introduced, following the manufacturer instructions of *BigDye Terminator v3.1 Cycle Sequencing Kit* (Applied Biosystems).

The sequence analyses were performed in the "Servei de Genòmica" of PCB (Parc Científic de Barcelona). To visualize and compare the sequences Seqman software was used.

3. Drugs used

Seven different read-through compounds were used. Two of them were aminoglycosides, gentamicin and G418, and five were non-aminoglycosides, PTC124, RTC13, RTC14, BZ6 and BZ16 (Figure 20). Aminoglycoside compounds were dissolved in ddH₂O whereas non-aminoglycoside were dissolved in dimethyl sulfoxide (DMSO). In Table 9 it is summarised the different drugs and the range of concentration used in all the experiments.

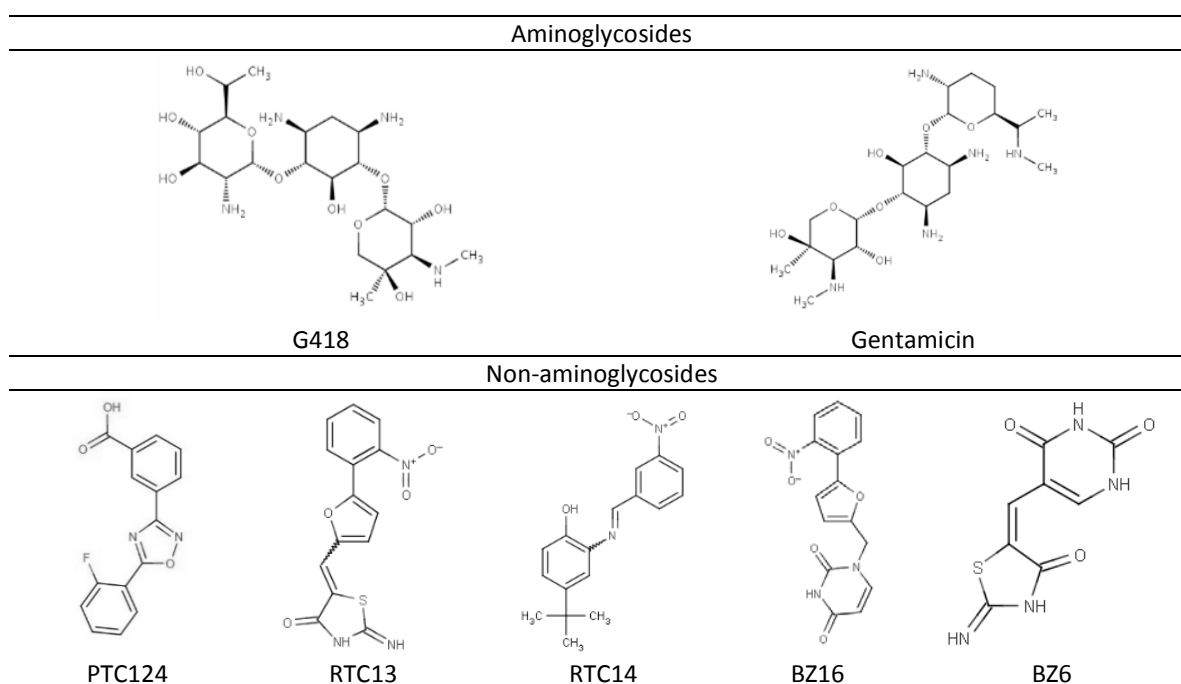


Figure 20. Chemical structure of the compounds used in this work.

Table 9. Drugs used

Drug	Trading house	Concentrations	Dissolved in
Gentamicin	Gibco, Carlsbad, CA, USA	2.5-1000 µl/ml	ddH ₂ O
G418	Gibco, Carlsbad, CA, USA	0.25-100 µl/ml	ddH ₂ O
PTC124	Excenen Pharmatech Co., Ltd, Guangzhou City, China	1.5-60 µl/ml	DMSO
RTC13	Gift Dr. Gatti	10-40 µl/ml	DMSO
RTC14	(Departments of Pathology & Laboratory Medicine and	10-40 µl/ml	DMSO
BZ6	Human Genetics, UCLA School of Medicine)	10-40 µl/ml	DMSO
BZ16		10-40 µl/ml	DMSO

4. Coupled transcription/translation assay

The *TNT Quick Coupled Transcription/Translation System* (Promega) was used for *in vitro* protein synthesis, as described by (Sanchez-Alcudia *et al.*, 2012). Briefly, each reaction was done at 30°C for 90 min and contained 250ng of plasmid, 10 µl of *TNT T7 Quick Master Mix* (Promega), and 1

μl of L-[^{35}S]-methionine-cysteine (EasyTag EXPRESS ^{35}S Protein Labeling Mix, [^{35}S], 7mCi; PerkinElmer). The ranges of concentrations used were: G418 (0.25-10 $\mu\text{g}/\text{ml}$), gentamicin (2.5-20 $\mu\text{g}/\text{ml}$), PTC124 (1.5-10 μM), RTC13 (10-40 μM) and RTC14 (10-40 μM) [(Du *et al.*, 2009), BZ6 (10-40 μM) and BZ16 (10-40 μM) (Du *et al.*, 2013; Jung *et al.*, 2011; Kuschal *et al.*, 2013). The [^{35}S]-labelled proteins resulting from these reactions were separated by SDS-PAGE and then revealed after overnight exposure at -70°C in autoradiography films. As HGSNAT protein is a homo-oligomer, denaturalization buffer contains urea 8M. Quantification of the electrophoretic bands was performed using *Discovery Series Quantity One 1D Analysis Software Protein* (Bio-Rad).

Mutation p.Y313X of the *SMPD1* gene was used to choose the best concentrations for each product. Read-through efficiency was calculated as the amount of full-length protein produced divided by the sum of the truncated protein plus the full-length protein, expressed as percentages.

5. COS7 cell culture and transfection

COS7 cells (CV-1 in Origin with SV40 genes) were cultured in Dulbecco's Modified Eagle's Medium (DMEM) supplemented with 10% Foetal bovine serum (FBS) and 1% penicillin/streptomycin (Gibco) at 37°C and 5% CO_2 . For transfection with the cDNAs, COS7 cells were seeded on 6-well plates. When the cells were at 80%-90% confluence, $1\mu\text{g}$ of the plasmid bearing either the wild-type or the mutant cDNA (corresponding to the genes *ARSB*, *SMPD1* or *HGSNAT*) was introduced using lipofectamine 2000 (Invitrogen, Life Technologies, Paisley, UK), following the manufacturer's instructions. As a negative control, the pcDNA3.1 empty vector was transfected. Different concentrations of G418 (50, 75, 100 $\mu\text{g}/\text{ml}$), gentamicin (500, 700, 1000 $\mu\text{g}/\text{ml}$) and PTC124 (20, 40, 60 μM) were added 4h post-transfection. Fresh media and drugs were replaced every 24h. Cells were harvested 48h after treatment for *ARSB* and *SMPD1* and 72h after treatment for *HGSNAT*, and centrifuged. The pellets were washed twice with PBS and stored at -80°C until enzyme activity analyses were performed. Two independent transfection experiments (with two replicates each) were performed for each mutation, as well as for the wild-type construct and the negative control).

6. Enzyme assays

Cellular pellets were resuspended in 100-300 μl of ddH₂O and sonicated afterwards for a minute. Protein concentration was determined by the Lowry method. The activity measurements were performed in duplicate (at least) in all the cases.

- **Acid sphingomyelinase enzymatic activity**

This enzyme activity was measured using fluorogenic substrate, 6-hexadecanoylamino-4-methylumbelliferyl-phosphorylcholine (HMU-PC, Moscerdam). The reaction mixture containing 50 μl of cell homogenate, 100 μl of 0.66mM HMU-PC in substrate buffer (0.1M sodium acetate buffer pH 5.2, with 0.2% (w/v) synthetic sodium taurocholate (Sigma) and 0.02% sodium azide) was incubated at 37°C for 1h. The reaction was ended by adding 1.1ml of stop buffer (0.5M NaHCO_3 / Na_2CO_3 buffer pH 10.7, containing 0.25% (w/v) Triton X-100) and fluorescence was measured in a Modulus™ Microplate Multimode Reader (Turner Biosystems), (excitation 365 nm, emission 450 nm). The protocol of the analysis is shown in Table 10.

Table 10. Acid sphingomyelinase protocol. (NPA/B).

	Blank (x2)	Samples (x2)
Substrate buffer	50 µl	--
Sample (1mg/ml)	--	50 µl
Substrate HMU-PC	100 µl	100 µl
Incubation	1h at 37°C in agitation	
Stop buffer	1'1 ml	1'1 ml

HMU-PC: 6-hexadecanoylamino-4-methylumbelliferyl-phosphorylcholine
Each sample and blank were measured in duplicate.

- **Acetyl-CoA:α-glucosaminide N-acetyltransferase enzymatic activity**

It was measured using fluorogenic substrate, 4-methylumbelliferyl-β-d-glucosaminide (4MU-βGlcN, Moscerdam). The reaction mixture containing 10µl of cell homogenate, 25µl of 6 mM acetyl-CoA, 15µl of 0.25% Triton X-100 and 25µl of 3mM 4MU-βGlcN in Mcllvain buffer (0.2M Na₂HPO₄, 0.1M citric-acid buffer, pH 5.7) was incubated at 37°C for 17h. The reaction was ended by adding 1ml of stop buffer (0.5M Na₂CO₃/NaHCO₃, pH 10.7), and fluorescence was measured in a Modulus™ Microplate Multimode Reader (excitation 365 nm, emission 450 nm). The protocol of the analysis is shown in Table 11.

Table 11. Acetyl-CoA:α-glucosaminide N-acetyltransferase protocol (MPSIIC).

	Blank (x2)	Samples (x2)
Triton X-100 0.25%	--	15 µl
6 mM acetyl-CoA	--	25 µl
ddH ₂ O	40 µl	--
Sample (1mg/ml)	10 µl	10 µl
Substrate 4MU-βGlcN	25 µl	25 µl
Incubation	17h at 37°C in agitation	
Stop buffer	1 ml	1 ml

4MU-βGlcN: 4-methylumbelliferyl-β-d-glucosaminide
Each sample and blank were measured in duplicate

- **N-acetylgalactosamine-4-sulfatase activity**

It was determined by spectrophotometric quantification of 4-nitrocatecol produced by hydrolysis of the substrate 4-nitrocatecol sulphate dipotassium salt (Sigma-Aldrich). The reaction mixture containing 50µl of cell homogenate, 50µl of ddH₂O and 100µl of substrate (50mM 4-nitrocatecol sulphate and 10mM barium acetate in 0.5M sodium acetate buffer, pH 6) was incubated at 37°C for 30-90min. The reaction was ended by adding 300µl of stop buffer (NaOH 1N) and absorbance was measured in a spectrophotometer (absorbance 515nm). The protocol of the analysis is shown in Table 12.

Table 12. N-acetylgalactosamine-4-sulfatase protocol (MPSVI).

	Samples (x2)
Sample	50 µl
ddH ₂ O	50 µl
Substrate*	100 µl
Incubation	30' and 90' at 37°C in agitation
Stop buffer	300 µl

* 4-nitrocatecol sulphate dipotassium salt

Each sample and blank were measured in duplicate

- **α -N-acetylglucosaminidase enzymatic activity**

The measurement of the α -N-acetylglucosaminidase enzymatic activity was performed by Dr. Victor Rodriguez Sureda in the CIBBIM (Centre d'Investigacions en Bioquímica i Biologia Molecular) of Vall d'Hebron hospital of Barcelona.

This enzyme activity was measured using fluorogenic substrate, 4-methylumbelliferyl-N-acetyl- α -D-glucosaminide (4MU- α GlcNAc, Calbiochem, Merck). The reaction mixture contained 20 μ l of 0.2 M sodium acetate buffer, pH 4.3, 40 μ l of the 2 mM 4MU- α GlcNAc resuspended in ddH₂O and 20 μ l of cell lysate. The mixture was incubated for 2 hours at 37°C and the reaction was stopped with 1ml of stop buffer (glycine buffer 0.1 M pH 10.4). Measurements were performed in a fluorometer (excitation 365nm, emission 450nm).

The protocol of the analysis is shown in Table 13.

Table 13. α -N-acetylglucosaminidase protocol (MPSIIIB).

	Blank (x2)	Samples (x2)
0.2 M sodium acetate buffer	20 μ l	20 μ l
ddH ₂ O	20 μ l	--
Sample (1mg/ml)	--	20 μ l
Substrate 4MU- α GlcNAc	40 μ l	40 μ l
Incubation	2h at 37°C in agitation	
Stop buffer	1ml	1ml

4MU- α GlcNAc: 4-methylumbelliferyl-N-acetyl- α -D-glucosaminide

Each sample and blank were measured in duplicate

In all the cases, the residual enzyme activity of the mutant alleles was expressed as a percentage of the mean of the activity values of the wild-type construct transfected in the same experiment. The activity of the negative control was subtracted.

- **β -hexosaminidase activity**

Each time that enzyme activity assay was performed; the activity of another lysosomal enzyme (β -hexosaminidase) was also measured, as a control. The β -hexosaminidase activity was measured using fluorogenic substrate, 4-methylumbelliferyl-2-acetomido-2-deoxy- β -D-Glucopiranoside (4MU, Sigma-Aldrich). The reaction mixture containing 10 μ l of cell homogenate, 10 μ l of 0.5 M citrate buffer, pH4.4 and 50 μ l of 3 mM 4MU resuspended in ddH₂O was incubated at 37°C for 2 and 17 minutes. The reaction was ended by adding 1 ml of stop buffer (0.5 M Na₂CO₃/NaHCO₃ buffer, pH 10.7), and fluorescence was measured in a Modulus™ Microplate Multimode Reader (excitation 365 nm, emission 450 nm).

The protocol of this assay is shown in Table 14.

Table 14. β -hexosaminidase protocol.

	Blank (x2)	Samples (x2)
Substrate 4MU	50 μ l	50 μ l
Citrate buffer	10 μ l	10 μ l
Sample	--	10 μ l
ddH ₂ O	10 μ l	--
Incubation	2' and 17' at 37°C in agitation	
Stop buffer	1 ml	1 ml

4MU: 4-methylumbelliferyl-2-acetomido-2-deoxy- β -D-Glucopiranoside

Each sample and blank were measured in duplicate

7. Culture and treatments of patients' fibroblasts

Fibroblasts were cultured in DMEM supplemented with 10% FBS and 1% penicillin/streptomycin (Gibco) at 37°C and 5% CO₂, in 6-well plates, except for the NAGLU activity measurements, for which 100 mm plates were used.

G418 (75 µg/ml), gentamicin (300 µg/ml), PTC124 (20 µM), RTC13, RTC14, BZ6 and BZ16 (30 µM) were added to the medium without antibiotics. Fresh media and drugs were replaced every 24h and cells were harvested after 3 days of treatment, for mRNA quantification and enzyme analyses.

8. mRNA quantification

The levels of *HGSNAT* and *NAGLU* transcripts in patients' fibroblasts were analysed by qRT-PCR in a LightCycler® 480 instrument (Roche Applied Sciences). For RNA isolation, cultured patients' fibroblasts were harvested and RNA was obtained using a High Pure RNA Isolation Kit (Roche Applied Sciences), following the manufacturer's recommendations. Concentrations were determined using the NanoDrop ND-1000 spectrophotometer (NanoDrop). RNA samples were stored at -80°C until analysed. The RNA obtained was retrotranscribed using a High-Capacity cDNA Archive Kit (Applied Biosystems) and real time-PCR was performed using the LightCycler® 480 II system and the Universal Probe Library (Roche Applied Science). Gene assays were designed using Universal ProbeLibrary Assay Design Center software (Roche Applied Science) (Figure 21). Human-specific Taqman Gene Expression assays for *SDHA* (*succinate dehydrogenase complex, Hs00417200_m1*) and *HPRT1* (*hypoxanthine phosphoribosyltransferase 1, Hs99999909_m1*) genes were used as endogenous controls to normalize the relative amounts of mRNA. These genes were selected because they were stably expressed under the experimental conditions. The Roche LightCycler® 480 software was used to perform advanced relative quantification analysis of gene expression, according to the LightCycler® 480 instrument operator's manual.

Gene:	<i>HGSNAT</i>	<i>NAGLU</i>
Probe:	#18	#27
Primer Forward:	TGATCGCCTCATCAATTCTG	CCTCCTGGCACATCAAGC
Primer Reverse:	GCTGGCTGAACATCACCAT	GAGGGAACACCCTGGTGAC
Length amplicon:	72 nucleotides	129 nucleotides
Length intron spanned:	1341 nucleotides	177 nucleotides
Position probe:		

Figure 21. Real-time PCR assay for *HGSNAT* and *NAGLU* genes, respectively. Number of probe, sequence of primers, length of amplicon, length of intron spanned and position of the probe in genomic DNA is shown for each gene.

9. Nonsense-mediated mRNA decay

For nonsense-mediated mRNA decay experiments, fibroblasts from SFB1 and SFC13 patients were seeded on 6-well plates and cultured in the absence or presence of 1 mg/ml of cycloheximide (CHX) for 6 h. Total RNA was isolated and retrotranscribed as described above. A

specific PCR amplification reaction was performed to obtain fragments including mutations p.W168X (*NAGLU*) and p.R384X (*HGSNAT*), respectively. Primers used are listed in Table 15.

Table 15. Primers used for the nonsense-mediated mRNA decay assay.
Mismatch is indicated with a grey shadow

Primer 5'-3'		
NAGLU	Forward	CCGCTATTACCAGAATGTG
	Reverse	CCGGTGCTGCAGGTAAG
HGSNAT	Forward_mismatch	AGAGGAGCTGCCTTTCTCCT
	Reverse	CCCAGGACCAAGATAACCAG
GAPDH	Forward	GGTCATCCCTGAGCTGAAC
	Reverse	GGGGTCTACATGGCAACTG

In the p.W168X-*NAGLU* PCR amplification, a 298bp fragment was obtained. After digestion with *BmpI* restriction enzyme, the fragment bearing the p.W168X mutation will not be digested while the fragment not bearing that mutation (WT for this mutation), which corresponds to the allele bearing the p.Q566X mutation, will be digested in two fragments of 162bp and 136bp, respectively. These fragments were separated in a 2.5% agarose gel electrophoresis (Figure 22 SFB). In the case of p.R384X-*HGSNAT* amplification, the forward primer had a mismatch in order to create a *XhoI* restriction site, indicated in grey shadow in Table 10. The 140bp amplification fragment was digested with *XhoI* restriction enzyme. If the allele bore the p.R384X mutation, it will not be digested while if not (i.e. the allele wearing the c.1542+4dupA mutation), it will be digested in two fragments of 121bp and 19bp, respectively. Fragments were separated in a 12% polyacrylamide gel electrophoresis (Figure 22 SFC).

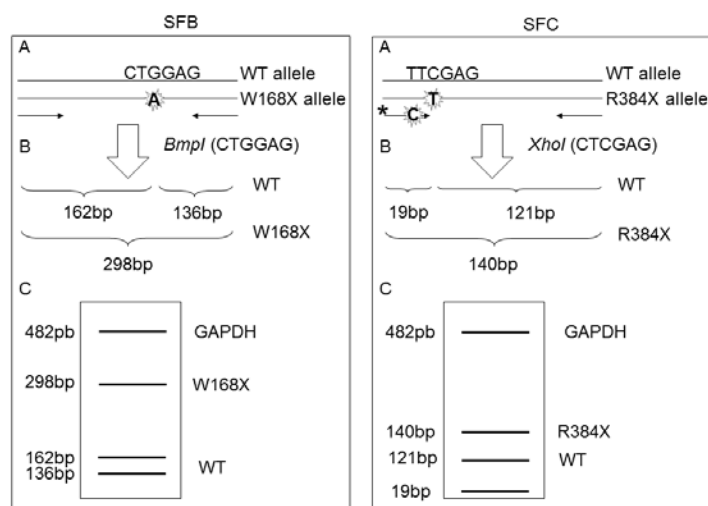


Figure 22. Scheme of the digestion patterns. A) Restriction site affected by the mutation (in bold). Arrows indicated primers used for the PCR amplification. * indicates mismatch primer
B) Restriction enzyme used (restriction site in brackets) and length of the expected fragments is indicated.
C) Scheme of results obtained in a gel.

Quantification of the relative intensity of the electrophoretic bands was performed using Image Lab 5.1 Analysis Software (Bio-Rad). Amplification of a 482bp fragment of the *GAPDH* cDNA was used as a control. Obviously, this fragment did not contain any restriction site for the enzymes used.

10. Statistical analyses

Statistical analyses were performed using the Student's t-test. In some experiments we had only two replicates. However, it should be noted that this test was recently validated for extremely small sample sizes (Winter, 2013). A p-value < 0.05 was predetermined as significant.

II. Generation of iPSC cells

1. Cell samples

To generate iPSCs, fibroblasts from three Niemann-Pick type A/B patients were used. The three patients, NPAB2, NPAB4 and NPAB6 have been previously described (named patient 2 (A), 4(B) and 6(B), respectively in supplementary table 2 (Rodriguez-Pascau *et al.*, 2009a)). Patient NPAB2 carries the mutation p.Y313X in homozygosity which produce the most severe phenotype of the disease (type A), while the other 2 patients, NPAB4 and NPAB6, are compound heterozygotes carrying the genotypes p.R441X/p.R474W and p.R608del/p.A482E, respectively, which produce milder phenotypes (type B).

- **Other cell lines used**

To produce the retroviruses, the Phoenix Amphotropic retrovirus producer cell line was used. Phoenix Amphotropic is a second-generation retrovirus producer cell line for the generation of helper-free ecotropic and amphotropic retroviruses. This cell line has been extensively tested for helper virus production and established as being helper-virus free. Phoenix Amphotropic cells are HEK293T/17 cells that have been transformed with adenovirus E1a carrying a temperature sensitive T antigen co-selected with neomycin. The unique feature of this cell line is that it is highly transfectable with lipid-based transfection protocols up to 50% or higher of cells can be transiently transfected.

Human foreskin fibroblasts (HFFs) can be used as a feeder layer to support the growth of iPSCs and for the maintenance of iPSCs in the undifferentiated state. However, the growth of these cells should be arrested before being used as a feeder layer by irradiating them (iHFF). This method is explained in II.4 section (page 51).

Mouse embryonic fibroblasts (MEFs) can be used for conditioning iPSC media. This media is used when iPSCs need to be grown without a feeder layer. However, the growth of these cells should be arrested before being used. This method is explained in II.4 section (page 51).

All these cell lines were kindly provided by Dr. Raya group, at the Institut of Bioenginyeria de Catalunya (IBEC), Barcelona.

2. Generation of iPSC

Fibroblasts from one healthy two years old individual (Advancell) and fibroblasts from three patients were infected with retroviruses carrying human cDNA coding for KLF4, SOX2, and OCT4 or these three cDNAs plus c-Myc as previously described (Raya *et al.*, 2009).

Fibroblasts were cultured in DMEM (Sigma) supplemented with 10% FBS (Gibco) and 1% Penicillin-Streptomycin (Gibco) at 37°C, 5% CO₂, 5% O₂ and used between 2 and 6 passages. Retroviruses for the four factors and a green fluorescence protein (GFP) control were independently produced after transfecting the cell line Phoenix Amphotropic using XtremeGENE 9 reagent (Roche) according to the manufacturer's directions. After 24h, the medium was replaced, cells were incubated at 32°C because viruses are more stable at 32°C; hence, higher retroviral titers are obtained, and the viral supernatant was harvested after 24 and 48h. These supernatant were filtered through 0.45µm filter units to make cell-free infective

supernatants. About 10^6 fibroblasts were seeded per well of a 6-well plate and infected with a 1:1:1:1 mix of retroviral supernatants of Flag-tagged OCT4, SOX2, KLF4 and c-MYC in the presence of $1\mu\text{g ml}^{-1}$ polybrene. For transduction control, GFP supernatant with polybrene was added to the fibroblast. Infection consisted of a 45 min centrifuge at 750g after which supernatants were left in contact with the cells for 24h at 37°C, 5% CO₂. Two infections on consecutive days were performed. Four days after beginning the infection, fibroblasts were seeded on iHFF in the same culture medium. After 24h, the medium was changed to iPSC medium, consisting of KO-DMEM (Gibco) supplemented with 20% KO-Serum Replacement (Gibco), 0.5% Penicillin-Streptomycin (Gibco), 2 mM Glutamax (Gibco), 50 μM 2-mercaptoethanol (Gibco), 1 mM non-essential aminoacids (Gibco) and 10 ng ml⁻¹ basic fibroblast growth factor (bFGF, Peprotech). Cultures were maintained at 37°C, 5% CO₂, with media changes every other day, for 4-12 weeks until iPSC colonies appeared. Clones from each cell line were grown on iHFF until pass 15, when all the validation experiments begin.

When iPSCs colonies of one genotype did not appear, some improvements to the protocol were done. To overexpress the ASM gene in HFF, transfection of the cDNA with Lipofectamine 2000 Transfection Reagent (Sigma) following the manufacturer's instructions was done.

Also, after infection, 24h later from seeding the fibroblast onto iHFF layer, medium was replaced with iPSC medium supplemented with 0.5 mM valproic acid to further increase the efficiency of reprogramming. Medium was changed daily and valproic acid was omitted after seven days.

iPS cells were maintained by mechanical dissociation of colonies and splitting 1:3 onto iHFF layer in iPSC medium or by 0.05% trypsin digestion and passaging onto Matrigel-coated plates with conditioned media (explained in II.5 section, page 52).

3. iPSCs characterization

- **Alkaline Phosphatase staining**

Alkaline phosphatase (AP) staining was performed using the Alkaline Phosphatase Blue Membrane Substrate Solution (Sigma) according to the manufacturer's protocol.

Cells were fixed with a 1/10 dilution of formaldehyde 37% in PBS for 4 minutes. A mixture 1:1 of the two-component buffered solutions was added to cells; after 15 minutes they were washed with PBS and the slides were kept at 4°C until photos were taken. The two-component mixture develops a bluish-purple product when reacting with alkaline phosphatase in membrane type assays.

- **Pluripotency immunocytochemistry**

Patient-specific iPS cells were grown on plastic cover slide chambers with HFF feeders layer for 6-10 days and then fixed in 4% paraformaldehyde (PFA) for 10 minutes. Cells were washed 3 times during 15 minutes with TBS+ (Tris 50 mM, NaCl 150 mM pH 7.4 and 0.1% X-Triton) and blocked during 2h with TBS++ (Tris 50 mM, NaCl 150 mM pH 7.4, 0.3% X-Triton and 3% donkey serum). The following primary antibodies were used at 4°C overnight: TRA1-81 (dil. 1:200, Millipore), SOX2 (dil. 1:100, Fisher Scientific), OCT3/4 (dil. 1:60, Santa Cruz biotechnology), NANOG (dil. 1:25, R&D Systems) diluted in TBS++. The next day, the cells were washed 3 times during 10 minutes with TBS+ and blocked 1h RT with TBS+. Incubation with secondary antibodies

diluted in TBS++ for 2h at dark was done. Secondary antibodies with Cy2 and Cy3 (1:200) from Jackson ImmunoResearch were used. The cells were washed twice during 10 minutes with TBS+ and for nucleus staining DAPI (Invitrogen) at 0.5 µg/ml was used diluted in TBS++ for 10 minutes. The slides before being mounted with PVA:DABCO mounting medium, were washed 10 minutes twice with TBS. Before images were acquired with an SP2 confocal system (Leica) and analysed with ImageJ software, slides were stored at 4°C in the dark.

- **DNA Extraction / genotyping**

Patients' iPS cells were split with trypsin 0.05% (Gibco) and seeded into plates previously treated with Matrigel (BD Biosciences) for 1 hour at room temperature. After 2 passes, when iPSCs had the best morphological shape and were at 80% confluence, iPSCs were harvested to extract DNA using Wizard® Genomic DNA Purification Kit (Promega) following the manufacturer's protocol.

Genomic DNA was amplified by PCR, and PCR products were sequenced with Big Dye Terminator Cycle Sequencing Kit. The sequence analysis was performed in the "Servei de Genòmica" of PCB (Parc Científic de Barcelona). To visualize and compare the sequences Seqman software was used.

Table 16 show the primers used to analyse the fragments where p.Y313X, p.R441X, p.R474W, p.A482E and p.R608del mutations lie.

Table 16. Primers used for genotyping.

Primers 5'-3'		
SMPD1_313	Forward	CCGGCCCTTTTGATATGGTG
	Reverse	GGGTTTCCACGGACGATAAG
SMPD1_400	Forward	GAAAGCCTTCATTAGTCCCC
	Reverse	CCAACCTCCTCCCCTATCC
SMPD1_608	Forward	TCTACAGGGCTCGAGAAACC
	Reverse	GAGAAGGTCCTGTTTCCCCG

4. Protocol for the generation of a stock of irradiated HFF and MEF

Thaw one vial of HFFs/MEFs into a 150 mm dish with fibroblast medium and change medium after 48 h. 8-10 days later, when cells are confluent, wash with PBS and trypsinize the cells with 3 ml of 0.25% trypsin/EDTA (Gibco) for 5 min at 37°C. Split the cells in the ratio 1:6 into 6 x 150 mm dishes with fibroblast medium and add fresh medium after 48 h. 8-10 days later, again split the cells into 1:6 to generate 36 150 mm dishes with fibroblast medium and add fresh medium after 48 h. 8-10 days later, when cells are confluent trypsinize and collect the cells from all 36 dishes. Working in groups of 9 dishes, aspirate the medium, wash twice with PBS and add 3 ml of 0.25% trypsin/EDTA to each plate, incubate for 5 min at 37°C and collect the cells of each plate with 7 ml of fibroblast medium. Collect the cell suspension of the 36 dishes into various 50 ml conical tubes. Centrifuge the eight 50 ml conical tubes at 1200 g for 5 minutes at 4°C and discard the supernatant. Resuspend the cell pellet of each tube with 5 ml of fibroblast medium and combine all of them to finally have one 50 ml conical tube. Count the total number of viable cells and split them in 2 conical tubes. Centrifuge at 1200 g for 5 minutes at 4°C and discard the supernatant. Irradiate the pellets at 70 Gy and resuspend the cells in freezing medium (90% HyClone FBS and 10% DMSO) to obtain 4x10⁶ or 2 x10⁶ cells per ml. aliquot 1 ml of cell

suspension into each cryovial. Freeze the cells overnight using a Mr. Frosty™ and storage into liquid N₂ after 24h.

5. Protocol for the conditioned Media

Thaw a 4x10⁶ iMEFs onto 5 x 100 mm 0.1% gelatin-coated (EmbryoMax. Millipore). MEFs are plated overnight in fibroblast media. The following day the media is removed and iPSCs media for conditioning added. Each day media is collected and replaced, after 20 days media is collected and the cells discarded. Before using it, media has to be filtered and hFGF has to be added.

6. Plating of Inactivated Feeders

Irradiated cells are plated on wells/dishes coated with Matrigel. To coat dishes with Matrigel add enough Matrigel solution (Matrigel diluted 1:40 in KO-DMEM) to cover the dish/well. Incubate the dishes overnight at 4°C or for 1h at room temperature. Immediately before plating the cells, aspirate the Matrigel solution. Irradiated cells were left overnight in the incubator in fibroblast media before being used. If cells were not used within 3 days of plating, they were discarded.

7. Enzyme activity (NPA/B)

Acid sphingomyelinase activity was analysed using the fluorogenic substrate 6-hexadecanoylamino-4-methylumbelliferyl-phosphorylcholine as explained in I.6 section (page 44). Measurements were performed in a Modulus™ Microplate Multimode Reader (Turner Biosystems), following the manufacturer's instructions.

III. Generation and characterization of NPC mouse models

1. Animals

Throughout the work presented in this thesis, two mice models have been used: the *Npc1*^{Imagine} mice and the *Npc1*^{Pioneer} mice as Niemann-Pick type C models.

The heterozygous *Npc1*^{Imagine/+} mice are mice with a C57BL/6 genetic background, which were generated by homologous recombination by OZgene company. They have one allele in which the mouse intron 9 of the *Npc1* gene has been replaced by the whole human intron 9 of the *NPC1* gene with the mutation c.1554-1009G>A and a WT allele (containing the wild-type mouse intron 9), which gives a normal phenotype. Mutation c.1554-1009G>A produces in the NPC patients an aberrant splicing process that generates a 194bp pseudoexon. Heterozygous *Npc1*^{Imagine/+} mice were interbred to generate litters with genotypes *Npc1*^{Imagine/Imagine}, *Npc1*^{Imagine/+} and NPC^{+/+}.

The heterozygous mice *Npc1*^{Pioneer/+} mice are mice with a C57BL/6 genetic background, which were generated by homologous recombination by OZgene company. The heterozygous mice *Npc1*^{Pioneer/+} have one allele with a modified *Npc1* exon 12 containing the c.1920delG mutation and a stop codon in the position where translation terminates in the human *NPC1* gene bearing the c.1920delG mutation and a wild-type allele which gives a normal phenotype. Heterozygous *Npc1*^{Pioneer/+} mice were interbred to generate litters with genotypes *Npc1*^{Pioneer/Pioneer}, *Npc1*^{Pioneer/+} and NPC^{+/+} mice.

Animals were fed and maintained in the Parc de Recerca Biomédica (PRBB) animal facility. Animals were housed in standard macrolon cages (40 cm long x 25 cm wide x 20 cm high) under a 12h light/dark schedule (lights on 08:00 to 20:00) in controlled environmental conditions of humidity (50%-70%) and temperature (22±2°C) with food and water supplied *ad libitum*. All experimental procedures were approved by the local ethical committee and carried out according to the guidelines of the local and European regulations.

2. Genotype analysis

To determine the mice genotype, a tail fragment of 1 mm of length was cut with a cautery and genomic DNA was extracted to be used it as a template for PCR amplification.

The tail fragment was digested in 300 µl of NaOH 50 mM at 98°C during 30 minutes. The samples were vortexed and 30 µl of Tris-HCl 1 M, pH 8 were added to neutralize the tissue digestion. Afterwards, samples were centrifuged for 6 minutes at 13.2rpm to separate the non-digested part. One µl of the supernatant was used to perform the PCR amplification with the specific primers listed in Table 17.

Table 17. Primers used in the mouse genotyping analysis.

Primers 5'-3'		
NPC_Imagine	Forward_human	GCCCATGTTGTCCTTAGAA
	Forward_mouse	GCCCAAGTGACTTGATTTC
	Reverse	GAGCAAACCTCGTATCATTC
NPC_Pioneer	Forward	CAAGAATCCAAATCTGAC
	Reverse	GAGGAAGGTCTGACTGAG

A specific PCR amplification reaction with 3 primers was designed to detect the presence of the c.1554-1009G>A mutation (*Npc1*^{Imagine} mice). Detection of the wild-type allele is done by Forward_mouse NPC_Imagine primer and reverse NPC_Imagine primer that hybridize in mouse intron 9 and a homologous part of exon 9, (leading to a 151bp fragment). Detection of the mutated allele is done by Forward_human NPC_Imagine primer that hybridize in human intron 9 and the same reverse NPC_Imagine primer (leading to an 185bp fragment). Fragments were separated in a 2% agarose gel electrophoresis.

The mutation (c.1920delG) present in *Npc1*^{Pioneer} mice generates an *Nla*III restriction site that allows to distinguish the mutant allele from the wild-type allele by digestion. NPC_Pioneer primers (Table 17) were used to generate 229bp fragments from the exon 12 of the *Npc1* gene. DNA fragments were digested with *Nla*III restriction enzyme during 2h a 37°C, and the results were analysed in a 2.5% agarose gel electrophoresis. Wild-type allele produces a 193bp and a 36bp fragment, meanwhile the mutated allele gives a 144bp, a 48bp and a 36bp fragment.

3. RT-PCR transcript analysis

Mice were euthanized with CO₂ followed by cervical dislocation. Brain and liver were dissected and immediately frozen with liquid nitrogen and stored until the experiments were performed.

Approximately 100 milligrams of frozen mouse brain and 30 mg of frozen mouse liver were homogenized using TissueRuptor (QIAgen) in QIAzol Lysis reagent (QIAgen) and RNeasy Lipid Tissue Mini Kit (QIAgen) was used, following the manufacturer's recommendations for total RNA isolation. Total RNA was quantified using the NanoDrop ND-1000 spectrophotometer (NanoDrop Technologies). Reverse transcription was performed using the High-Capacity cDNA Reverse Transcription Kit (Applied Biosystems) according to the manufacturer's instructions.

The RT-PCR splicing analysis was performed using the primers shown in Table 18:

Table 18. Sequence of primers used in RT-PCR splicing analysis.

Primers 5'-3'	
Fm_ex9	GAGTGTGTTAAATTACTTCC
Rm_ex11	TGTAGTAATTATTCACGGGG

Different fragments are expected depending on the kind of splicing: normal splicing gives a 296bp fragment, inclusion of the pseudoexon would give a 463bp fragment and if exclusion of exon 10 occurs, a 168bp fragment would be produced. The RT-PCR products were sequenced to confirm their identity.

4. Liver Histology

Mice were killed with CO₂ and rapidly transcardially perfused with PBS solution, followed by fixation with 4% (wt/vol) paraformaldehyde. Brains and livers were removed and postfixed in the same fixative for 24-48h, respectively. Fixed samples were paraffin-embedded, sectioned, and stained with hematoxylin and eosin (H&E).

5. Protein lysates and Western blot analysis

Tissue lysates were obtained by the addition of ice-cold RIPA buffer (Desoxycolate 0.25% w/v, NP40 1% v/v, Tris pH 7.5 1 M, EDTA 500 mM, NaCl 5 M and protease inhibitor) (500µl/100mg

tissue) and passing the tissues through a 5ml syringe equipped with a 21xG needle. Subsequent sonication for two minutes (10 seconds on/off intervals) was applied to ensure that homogenization was complete. Protein concentration was determined using the Lowry method, and 50µg of lysate were loaded on 7.5% SDS-PAGE gels, transferred onto Immobilon-P transfer membrane (Millipore, Billerica, MA, USA) and blocked with 5% non-fat milk in PBS containing 0.2% Tween-20 (PBST) for 1h. The blotted membranes were incubated overnight at 4°C with primary antibody against NPC1 (ab36983, abcam) diluted 1:1000, and then washed. Antirabbit IgG antibody (A0545, Sigma-Aldrich, UK) was used as a secondary antibody (dilution 1:10.000). For normalization and quantification, immunodetection (dilution 1/8.000) against α -Tubulin (T5168, Sigma-Aldrich, UK) was used. Bands were detected with a LAS-4000 mini system (Fujifilm). Multigauge software was used for band quantification, followed by statistical analysis with Microsoft excel 2013.

6. Cholesterol measurement

Cholesterol was measured by the Amplex[®]Red cholesterol assay kit (Invitrogen) following the manufacturer's protocol. This assay utilizes enzyme-coupled reactions to produce highly fluorescent resorufin for quantitation (excitation 571 nm, emission 585nm). Resorufin is produced by the reaction of the Amplex[®] Red reagent with H₂O₂ produced from the cholesterol oxidase-catalysed oxidation of cholesterol (Figure 23). 50 mg of liver tissue were homogenized in Reaction Buffer and sonicated for two minutes (10 seconds on/off intervals). As cholesterol can be in the form of cholesteryl esters, cholesterol esterase is used to produce free cholesterol from cholesterol esters. Total and unesterified cholesterol were determined using the same kit with or without esterase, respectively. Protein concentration was determined using the Lowry method.

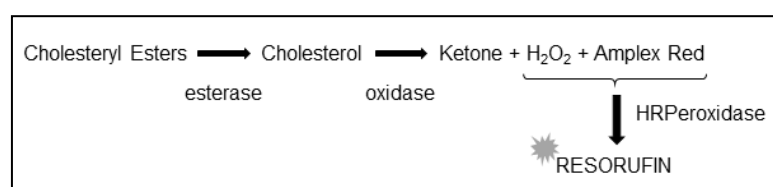


Figure 23. Scheme of the reactions involved in the assay.

7. Sphingolipid Determination

Brain tissue was homogenate by TissueRuptor (QIAGEN) in 0.2 M sucrose at 5% w/v. Protein concentration was determined using the Lowry method and a 400ug protein aliquot was taken for protein quantification. Sphingolipid extracts, fortified with internal standards, were prepared as described (Shaner *et al.*, 2009) and analysed as reported previously (Canals *et al.*, 2009), with minor modifications. The LC/MS analysis consisted of a Waters Acquity UPLC system connected to a Waters LCT Premier orthogonal accelerated time of flight mass spectrometer (Waters), operated in positive electrospray ionization mode. Full scan spectra from 50 to 1500 Da were acquired, and individual spectra were summed to produce data points each of 0.2 s. Mass accuracy and reproducibility were maintained by using an independent reference spray via the LockSpray interference. The analytical column was a 100 × 2.1-mm inner diameter, 1.7-µm C8 Acquity UPLC bridged ethylene hybrid (Waters). The two mobile phases were phase A: MeOH/HCOOH (998:2, v/v) and phase B: water/HCOOH (998:2, v/v); both contained 2 mm ammonium formate. The column was held at 30°C. Quantification was carried out using the extracted ion chromatogram of each compound, using 50 mDa windows. The linear dynamic

range was determined by injecting standard mixtures. Positive identification of compounds was based on the accurate mass measurement with an error of <5 ppm and its LC retention time, compared with that of a standard ($\pm 2\%$).

8. Behavioural Phenotyping

- **Grip strength**

On the test day, each mouse was weighed and singly housed in a holding cage for the duration of the experiment. A 3 mm diameter metal wire was used as the grip bar. The mouse was held near the base of its tail and lowered toward the bar until it gripped the bar with both forepaws first and all limbs afterwards. The mouse was then gently pulled away from the bar at a steady rate of about 2.5 cm/second until the bar was released. Peak force disturbance was automatically registered in Newtons by the apparatus. Data were recorded, and four additional trials were immediately given. Finally, the mean of maximal grip force was calculated as Newtons per grams of body weight.

- **Hot plate**

To assess nociception mice were placed on a hot plate at $52 \pm 0.1^\circ\text{C}$ surrounded by a plastic cylinder (19 cm diameter, 19 cm high) and latency to paw licking and jump were manually registered by the experimenter. A maximum latency of 180 s was set up to avoid tissue damage.

- **Circadian activity**

Circadian activity (CA) was measured using activity cages (TSE, Germany) that consist of infrared detection photobeams for analysis of horizontal activity. The test was performed under low non-aversive lighting conditions (50 lux.) to avoid stressful stimuli. Total distance travelled each 30 min was recorded for 24h. Mice were individually housed in standard macrolon cages (40 cm long x 25 cm wide x 20 cm high) during 24h for 2 consecutive days.

- **Rotarod**

The protocol consisted of a training session at a constant speed (4 rpm) for a maximum of 60 seconds. Next, the animals were tested for each of 6 different velocities (4, 7, 14, 19, 24 and 34 rpm) for a maximum of 120 seconds, with a 10 min interval between each trial. The latency to fall off the rotarod was registered. One hour later, mice received two trials of accelerating conditions at increasing speed levels, ranging from 4 to 40 rpm over a 1-min period. The mean latency to fall off the rotarod (for the two trials at each speed level) was recorded and used in subsequent analysis.

- **Paw footprinting**

To obtain footprints, the hind feet of the mice were coated with black nontoxic paint. The animals were allowed to walk along 50-cm-long, 10-cm-wide runway (with 10-cm-high walls) into an enclosed box. All mice performed the test 2 times and the average between trials was calculated. A clean sheet of white paper was placed on the floor of the runway for each run. The footprint patterns were analysed for three parameters (all measured in cm). (1) Stride length was measured as the average distance of forward movement between each stride. (2) Hind-base width was measured as the average distance between left and right hind footprints. These values were determined by measuring the perpendicular distance of a given step to a line connecting its opposite preceding and proceeding steps. (3) Distance from left or right front

hind-footprint overlap was used to measure uniformity of step alternation. When the centre of the hind footprint fell on top of the centre of the preceding front footprint, a value of zero was recorded. When the footprints did not overlap, the distance between the centres of the footprints was recorded. For each step parameter, three values were measured from each run, excluding footprints made at the beginning and at the end of the run, where the animal was initiating and finishing movement, respectively. The mean value of each set of three values was used in subsequent analysis.

- **Elevated plus maze**

Mice were placed on an elevated plus maze that consist of a black Plexiglas apparatus with four arms (29 cm long x 5 cm wide) set in cross from a neutral square (5 cm x 5 cm). Two opposite arms are delimited by vertical walls (closed arms) and the other two arms have unprotected edges (open arms). The maze was elevated 40 cm above the floor and placed under indirect light (100 lx.). At the beginning of a 5-min session each mouse was placed in the central zone, facing one of the open arms. A video-tracking camera allowed registering time spent, number of entries, speed and distance in the different zones.

- **The novel object recognition**

Novel object recognition was examined in a Y maze apparatus. It consists of three adjacent arms (each arm is 30 cm x 5 cm x 6 cm) delineating a Y shape, and thus restricted the zone where mice are allowed to move, increasing the amount of exploration in all groups of mice. The protocol consists of three sessions:

1) *Habituation session* Animals were habituated for 10 min to the Y maze. During this habituation session the number of entries in the three arms was manually recorded by the experimenter. Moreover, the percentage of spontaneous alternation was also measured. Spontaneous alternation is considered when mice consecutively entered non-previously explored arms. The percentage of spontaneous alternation is mathematically estimated as the number of consecutive entrances divided by the maximum alternation (total number of entries divided by 3) and x 100.

2) *Familiarization session* 4h later, mice were placed to the Y maze that contained two identical plastic-made objects and located on two of the arm ends. All mice were placed at the end of the arm that does not contain any object. Time exploring the two objects was recorded for 10 minutes.

3) *Test session* After 24 h, mice were presented to two objects for 10 minutes, one was the same used in the familiarization session and the other was a novel one. The discrimination index is calculated as time exploring the novel object – time exploring the familiar object / total time of exploration x 100. The position of the novel object was counterbalanced between animals.

The arena and objects were deeply cleaned between animals to avoid olfactory cues. All measures of exploration were registered manually by the experimenter blind to genotype or treatment. Exploratory behaviour is defined as the animal directing its nose towards the object at a distance of < 2 cm. Sitting on or resting against the object is not considered as exploration.

9. Statistics

All data passed the normality test of Kolmogorov–Smirnov. For comparisons between two groups, the homozygous imagine mice and their WT control littermates unpaired t-tests were performed. Significant threshold was set for $p < 0.05$. The results are expressed as means \pm Standard deviation (SD) or Standard error of the mean (SEM). All statistical analyses were performed using Statistical Package for the Social Sciences (SPSS) software 21, unless otherwise stated.

RESULTS

I. Nonsense suppression therapy

1. Mutations

Most of the mutations included in this study were found in Spanish patients. Some others were obtained from the literature (see Table 7, on page 41).

2. Techniques used for the analysis

We have used different techniques for the analysis of the read-through of the nonsense mutations. One of them was the transcription and translation assay (TNT) for the *in vitro* analysis of the recovery of the full-length protein. This technique can be applied to any mutation, once introduced in the wild-type full-length cDNA of the corresponding gene cloned in a proper expression vector. We set up this technique with the *SMPD1* mutations, testing a wide range of concentrations of the different drugs. Afterwards, it was applied to all the mutations using all the drugs.

Another technique used was the analysis of the recovery of the enzyme activity. We had previously set up the measurements of the activity for most of the enzymes in our laboratory. Only the analyses of the NAGLU enzyme activity (for the SFB mutations) were performed in collaboration with the group of Dr. Carmen Domínguez of the CIBBIM-Nanomedicina in Vall d'Hebron Institut de Recerca (VHIR).

This approach was performed using either COS7 cells transfected with the cDNAs of interest or patients' fibroblasts when available. With COS7 cells we tested gentamicin, G418 and PTC124 in three different concentrations, reported in the literature. With the fibroblasts (from one SFB and one SFC patient), we only tested one concentration of each compound.

On the patients' fibroblasts, we also checked the level of mRNA after the treatments and analysed the NMD involvement.

3. *In vitro* read-through (TNT)

We tested the effect of the seven different products using a mammalian-coupled TNT assay on the cDNAs which bore the nonsense mutations indicated in Table 7. In the absence of treatment, truncated proteins of the expected size for most of the mutations were synthesized. The truncated proteins derived from mutations p.W146X and p.R160X of the *ARSB* gene were not clearly seen, probably due to their small size, precluding the good performance of quantification. That is the reason why they were excluded of this assay.

We have tested a wide range of drug concentration for the aminoglycosides gentamicin and G418, as listed in Table 19. For the non-aminoglycosides drugs, only three concentrations (based on the reported literature) were assayed for each mutation, since the amount of drugs were limited. In Table 20 the concentrations used for non-aminoglycosides are shown.

Table 19. Aminoglycosides concentrations used.

Disease	Mutation	Gentamicin ($\mu\text{g/ml}$)							G418 ($\mu\text{g/ml}$)									
		2.5	5	10	20	30	40	50	0.25	0.5	1	1.5	2	3	4	5	7.5	10
<i>NPA/B</i>	W168X	X	X	X	X	X	X		X	X	X		X	X		X	X	X
	Y313X	X	X	X	X		X	X	X	X	X		X	X	X	X	X	X
	R441X	X	X	X	X	X	X	X	X	X	X	X	X	X	X	X	X	X
	R203X	X	X	X	X	X		X	X	X	X	X	X		X	X		X
	S296X	X	X	X					X	X	X							
	W316X	X	X	X					X	X	X							
<i>SFC</i>	L321X	X	X	X					X	X	X							
	R384X	X	X	X					X	X	X		X			X	X	X
	W403X	X	X	X					X	X	X							
	R506X	X	X	X					X	X	X							
	W510X	X	X	X					X	X	X							
	Y558X	X	X	X					X	X	X							
<i>SFB</i>	W168X	X	X	X					X	X	X							
	Q566X	X	X	X					X	X	X							
	Y558X	X	X	X	X	X		X	X	X	X	X	X	X	X	X	X	X
<i>ML</i>	W322X		X	X	X	X		X	X	X	X	X	X		X	X	X	X
	Q503X		X	X	X	X	X		X	X		X	X		X	X	X	X

Table 20. Non-aminoglycosides concentrations used.

Drug	Concentrations (μM)		
PTC124	2.5	5	10
RTC13	3	6	12
RTC14	3	6	12
BZ16	3	6	12
BZ6	2	5	10

Recovery of the full-length protein was observed for some of the mutants with G418 (geneticin) or gentamicin (Figure 24), while no recovery was observed with PTC124, RTC13, RTC14, BZ6 and BZ16.

In particular, for the three *SMPD1* mutations, clear recovery was observed with G418 treatment at different concentrations, while gentamicin had a lower effect on mutations p.W168X and p.Y313X and no effect on p.R441X (Figure 24). The best results were around 35% recovery for the p.W168X mutation with 0.25 $\mu\text{g/ml}$ of G418, and around 18% recovery for mutation p.R441X after treatment with 2 $\mu\text{g/ml}$ G418 (Figure 25). Additionally, positive results were obtained for the two *HGSNAT* mutations (p.R203X and p.W403X), the latter showing better results (Figure 24), with recovery of around 25% with G418 at 0.5 and 1 $\mu\text{g/ml}$ (Figure 25). Positive results with gentamicin were also observed for these two *HGSNAT* mutations, with a maximum of 16% recovery for p.W403X with 5 $\mu\text{g/ml}$ of gentamicin (Figure 25).

A faint band corresponding to the full-length protein was detected for mutation p.Y558X of the *NAGLU* gene, both with G418 and gentamicin (Figure 24), corresponding to a maximum of less than 10% recovery after G418 treatment at 1 mg/ml (Figure 25).

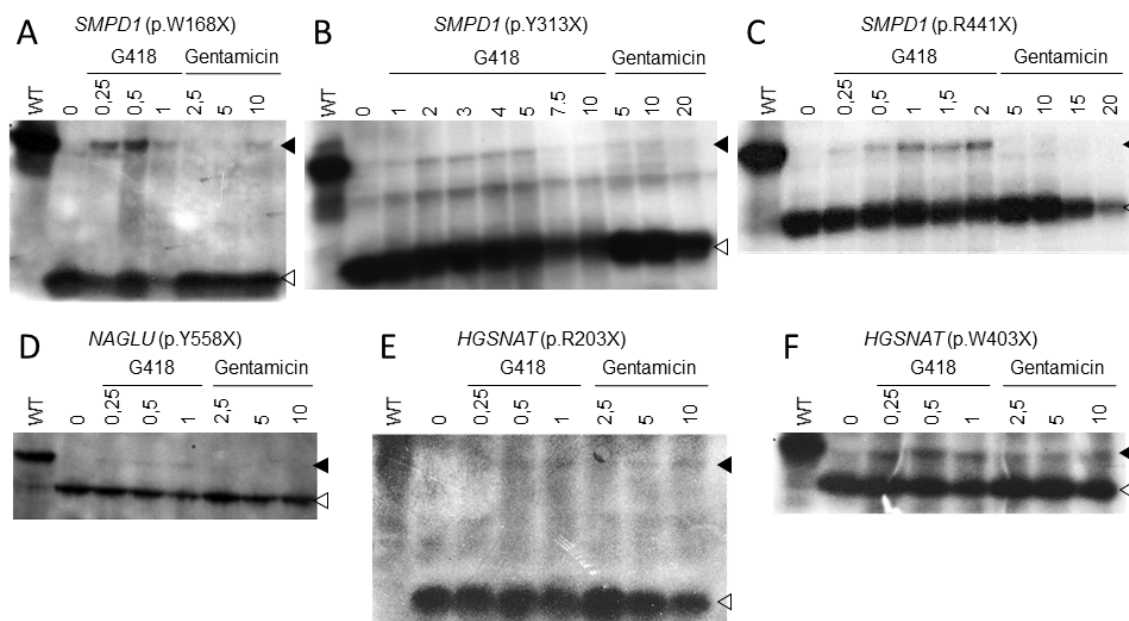


Figure 24. Positive read-through results with G418 and gentamicin. The figure shows representative experiments for the indicated *SMPD1* (A-C), *NAGLU* (D) and *HGSNAT* (E-F) nonsense mutations. WT, wild-type construct. Black arrowhead, full-length protein. White arrowhead, truncated protein. Concentrations are in $\mu\text{g/ml}$.

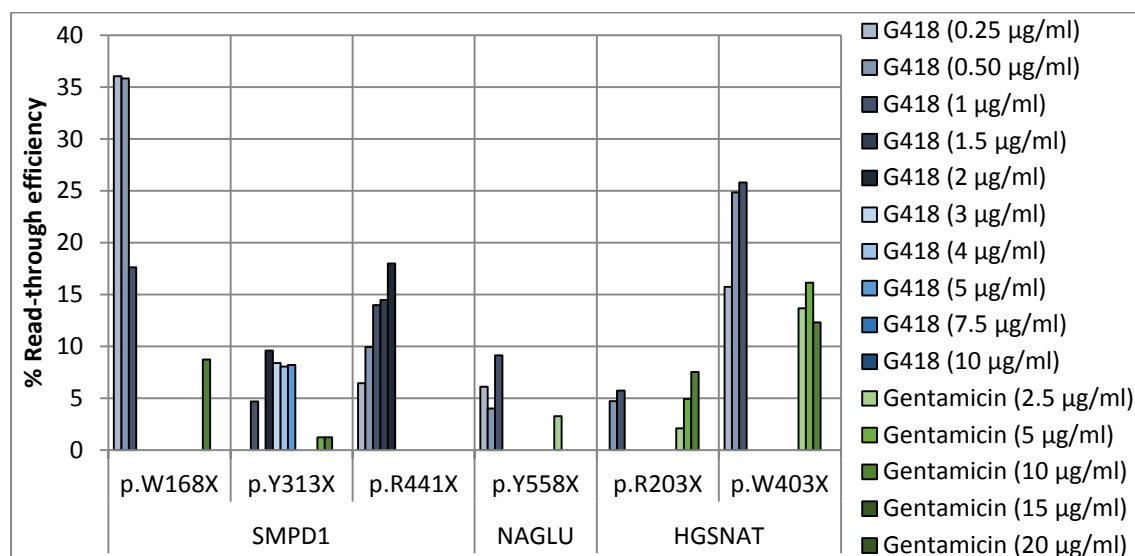


Figure 25. Quantification of the read-through recovery. The figure shows the quantification of the full-length protein synthesized from each mutant construct. The percentage of full-length protein relative to the sum of full-length plus truncated proteins is shown for each aminoglycoside treatment and for the indicated concentration.

In some cases, no recovery of the full-length was observed. In Figure 26 we show an example of negative results for the treatment of the *HGSNAT*-p.S296X mutation with different read-through compounds, where the truncated protein is clearly visible but there is no recovery of the full-length protein.

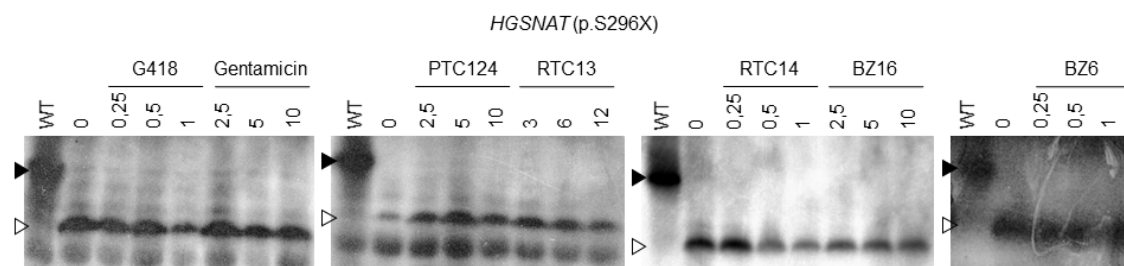


Figure 26. Example of no full-length protein recovery. An example for the indicated *HGSNAT* nonsense mutation is shown. WT, wild-type construct. Black arrowhead, full-length protein. White arrowhead, truncated protein. Concentrations of G418 and gentamicin are in $\mu\text{g/ml}$ and for the non-aminoglycoside drugs are in μM .

4. Enzyme activity in transfected COS7 cells

Acid sphingomyelinase (NPA/B) activity was measured according to (Rodríguez-Pascau *et al.*, 2009a) and we tried three concentrations of the aminoglycosides drugs and PTC124. N-acetylgalactosamine-4-sulfatase (MPSVI) activity was measured according to Dr. Domínguez (personal communication). As two out of four mutations were not suitable for TNT, we tried all four with gentamicin and PTC124 in 3 different concentrations. Acetyl-CoA: α -glucosaminide N-acetyltransferase (MPSIIIC, SFC) activity was measured according to (Canals *et al.*, 2011). Instead of analysing all mutations, we prioritized p.R384X mutation because we had fibroblast containing it and we wanted to see the possible effect of treatment; and p.R203X and p.W403X mutations because they gave us some recovery at TNT assay (*in vitro* level). We only used 2 different amounts of the aminoglycoside drugs.

The possible recovery of enzyme activity was analysed in COS7 cells transfected with the mutated cDNA. For this assay, only gentamicin, G418 and PTC124 were used. The best results were for the *ARSB* p.W146X mutation with gentamicin and an almost two-fold increase was obtained (Figure 27). A positive result for this mutation was also found with PTC124 treatment, although to a lesser extent. A moderate increase in activity (around 20 to 50%, with borderline significance) was found for the following mutations and treatments: *SMPD1* p.W168X treated with G418; *SMPD1* p.Y313X treated with gentamicin; *ARSB* p.R160X, p.W322X and p.Q503X treated with PTC124; and *HGSNAT* p.R203X; p.R384X and p.W403X treated with gentamicin (Figure 27).

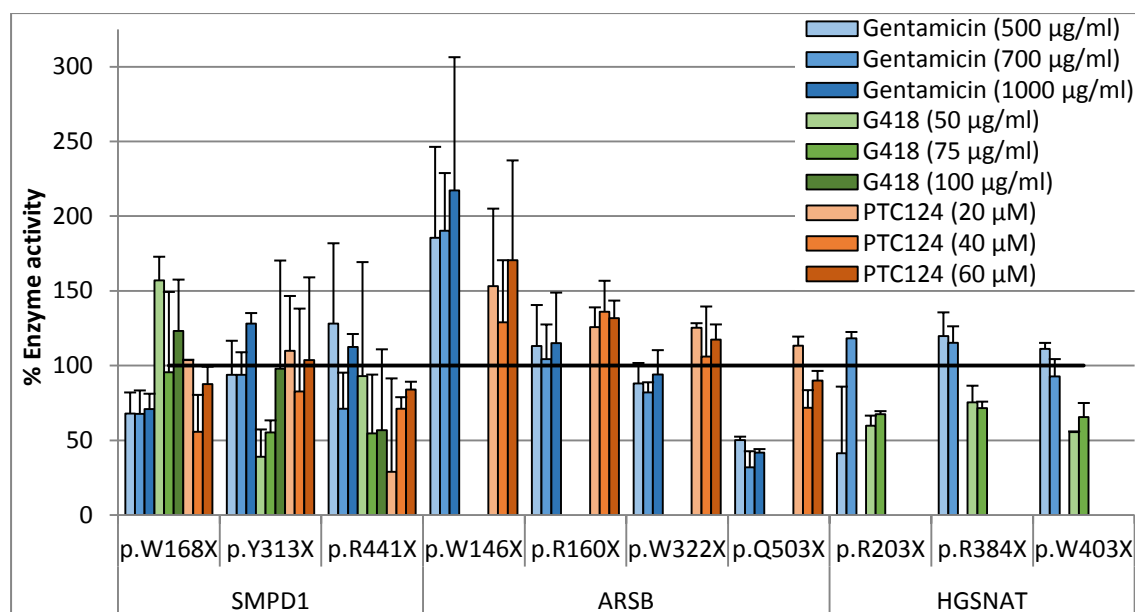


Figure 27. Enzyme activity in COS7 cells. Effect of different read-through compounds on the enzyme activity in COS7 cells transfected with cDNAs bearing the indicated nonsense mutation in the X-axis. Data are expressed as the mean \pm SD of at least two experiments performed in duplicate. Pattern codes for compounds and concentrations are indicated in the inset.

5. Read-through treatment of patients' fibroblasts

We treated fibroblasts from a Sanfilippo C patient with the seven different read-through compounds, only at one concentration each (Gentamicin at 300 μ g/ml, G418 at 75 μ g/ml, PTC124 at 20 μ M and RTC13, RTC14, BZ6, BZ16 at 30 μ M). Gentamicin gave a 3-fold increase on the enzyme activity compared with the non-treated fibroblasts (Figure 28). However, when the enzyme increasing activity of the treated fibroblasts was compared to the activity of wild-type fibroblasts, it did not reach the 1% of the WT activity (Figure 29). The other compounds showed no effect on the enzyme activity (Figure 28).

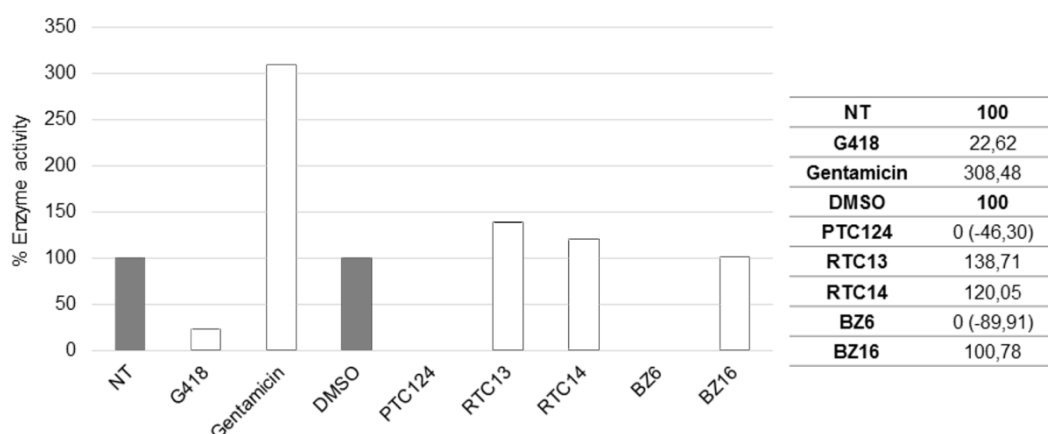


Figure 28. Enzyme activity of Sanfilippo C treated fibroblasts in comparison to non-treated ones. The Y-axis represents the percentage of enzyme activity compared to the untreated fibroblasts (NT, grey bars). Different bars indicated the different treatments performed. For PTC124, RTC13, RTC14, BZ6 and BZ16 the untreated samples included DMSO, since these products were dissolved in it. Values are indicated in the table on the right; only one experiment was performed.

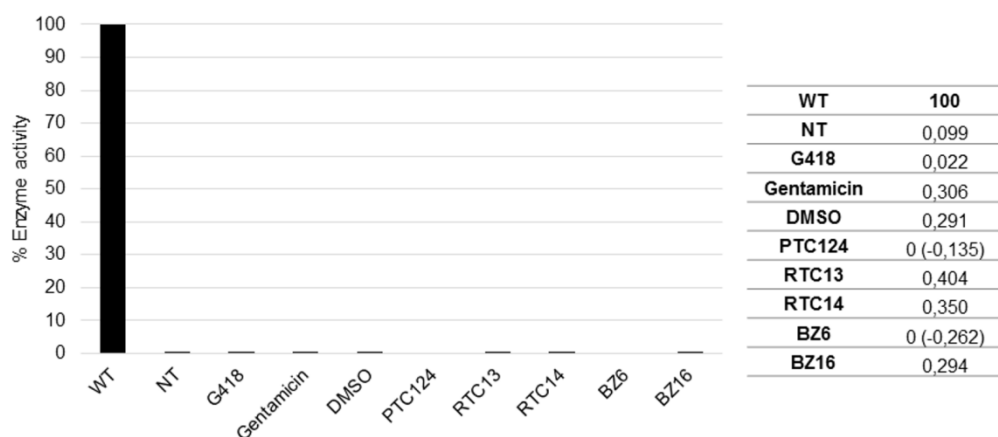


Figure 29. Enzyme activity of treated and non-treated Sanfilippo C fibroblasts in comparison to WT fibroblasts. The Y-axis represents the percentage of enzyme activity compared to the wild-type fibroblasts (black bar). Different bars indicated the different treatments performed. Values are indicated in the table on the right; only one experiment was performed. WT, wild-type; NT, non-treated.

The fibroblasts from a Sanfilippo B patient were also treated with the seven different read-through compounds at one concentration each (Gentamicin at 300 μ g/ml, G418 at 75 μ g/ml, PTC124 at 20 μ M and RTC13, RTC14, BZ6, BZ16 at 30 μ M) to check the increase in enzyme activity, but no positive result was obtained for any of the products. First, we performed the assay in 6-well plates, and afterwards we repeated it for the aminoglycosides and the RTC13 and PCT124 drugs on 75cm² flasks. In this case, we obtained a small increase with G418 compared to the non-treated fibroblasts (Figure 30). However, when this value is compared to that of wild-type fibroblasts, it does not reach the 1% of the WT activity (Figure 31).

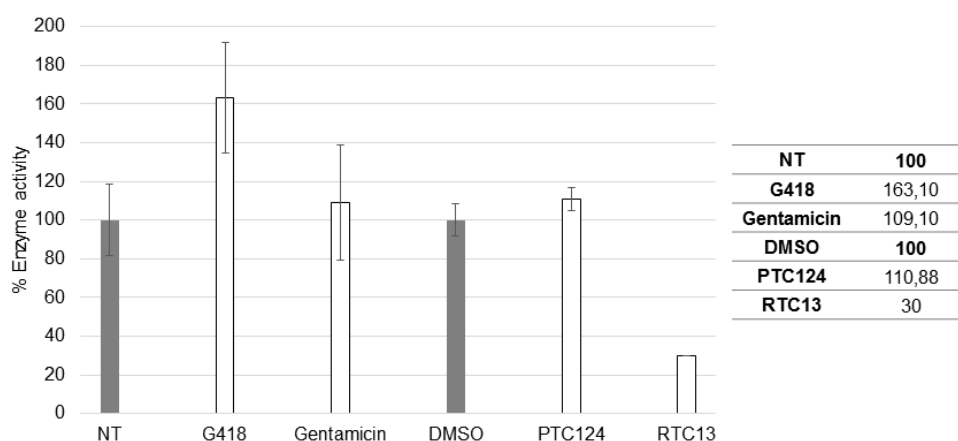


Figure 30. Enzyme activity of Sanfilippo B treated fibroblasts in comparison to non-treated ones. The Y-axis represents the percentage of enzyme activity compared to the untreated fibroblasts (NT, grey bars). Different bars indicated the different treatments performed. For PTC124 and RTC13 the untreated samples included DMSO, since these products were dissolved in it. Data are expressed as mean \pm SD of two experiments and values are indicated in the table on the right.

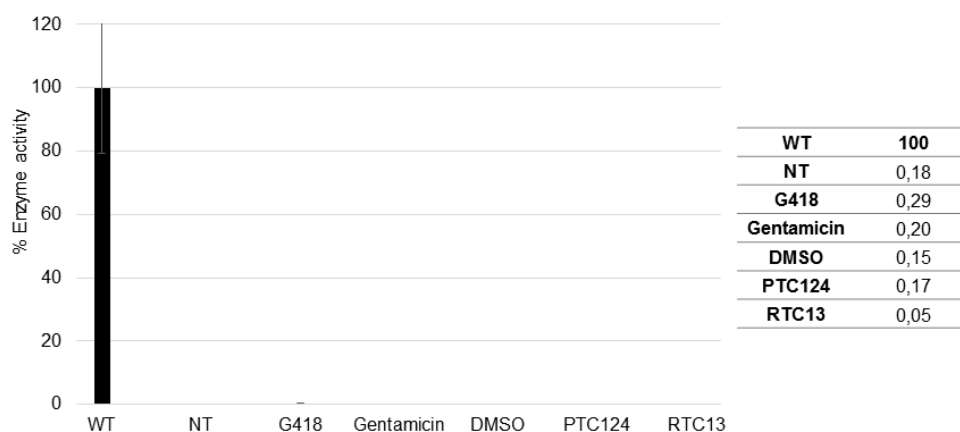


Figure 31. Enzyme activity of treated and non-treated Sanfilippo B fibroblasts in comparison to WT fibroblasts. The Y-axis represents the percentage of enzyme activity compared to the wild-type fibroblasts (black bar). Different bars indicated the different treatments performed. Data are expressed as mean \pm SD of two experiments and values are indicated in the table on the right. WT, wild-type; NT, non-treated.

On the fibroblasts from the SFC and the SFB patients, mRNA levels (of the *NAGLU* and *HGSNAT* gene, respectively) were quantified after the treatment with the seven compounds mentioned above at the same concentrations as in the enzyme activity assay.

We first set up the technique by doing standard curves of the genes in study (*HGSNAT* and *NAGLU* genes) to check the amount of cDNA needed to do the experiment. The endogenous genes (*HPRT* and *SDHA*) had already been analysed.

As shown in Figure 32, Sanfilippo C fibroblasts did not show any increase of the RNA level after the treatment either with G418 or with gentamicin (compared to non-treated fibroblasts). Patient's fibroblasts treated with some non-aminoglycosides read-through drugs show a 1.5-fold increase in the mRNA level when compared to non-treated fibroblasts (in this case treated with DMSO as it is the vehicle for these drugs).

In the case of Sanfilippo B fibroblasts, the treatment with G418 increased the amount of RNA by almost 2-fold when compared to non-treated fibroblasts. Treatments with all other compounds did not increase the amount of RNA, and even lowered it by half.

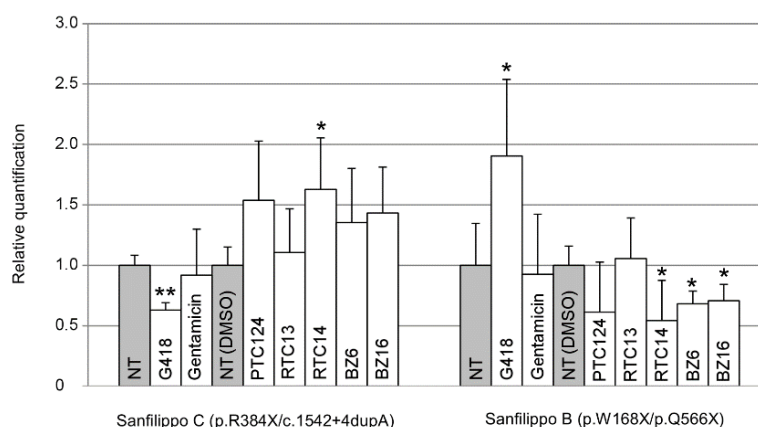


Figure 32. Relative quantification of the mRNA levels of treated fibroblasts in comparison to non-treated ones. The Y-axis represents the results of the relative quantification of mRNA levels, normalized with respect to the untreated

fibroblasts (NT, grey bars). Different bars indicated the different treatments performed. For PTC124, RTC13, RTC14, BZ6 and BZ16 the untreated samples included dimethyl sulfoxide (DMSO), since these products were dissolved in it. Data are expressed as mean \pm SD of three experiments. Syndromes and genotypes of the different fibroblasts are indicated in the X-axis. * $p < 0.05$, ** $p < 0.01$, compared to untreated cells. (Note that only increases in mRNA level were considered).

It is interesting to compare the increase in the amount of the RNA of the mutated fibroblasts after treatment with the RNA of the WT fibroblasts in order to evaluate if this increment could reach the therapeutic threshold.

In our case, the amount of mRNA from Sanfilippo C fibroblasts treated with non-aminoglycosides drugs reached a 45-50% of the WT levels. (Figure 33). The best results were for Sanfilippo B fibroblasts treated with G418, where RNA levels are similar to WT levels with no significant differences (Student's t-test). The amount of mRNA in fibroblasts treated with RTC13 seem to be a 70% of the WT levels, but it should be noted that it is probably due to the effect of the vehicle in which the drug is dissolved, DMSO (Figure 33).

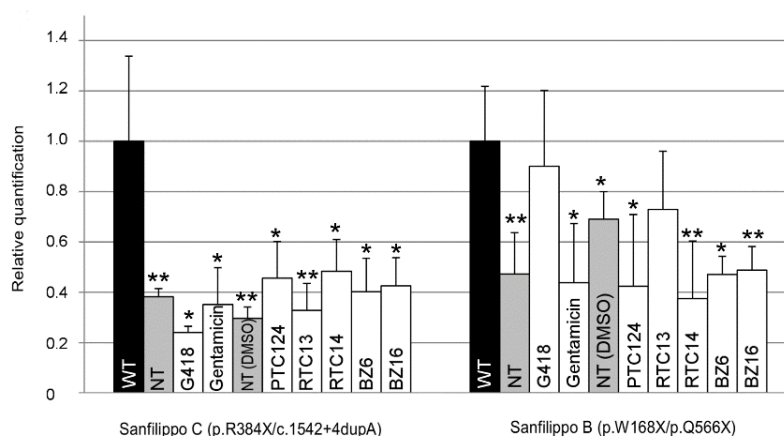


Figure 33. Relative quantification of the mRNA amount of treated and non-treated fibroblasts in comparison to WT fibroblasts. The Y-axis represents the results of the relative quantification of mRNA levels, normalized with respect to the wild-type fibroblasts (black bars). Different bars indicated the different treatments performed. Data are expressed as mean \pm SD of three experiments. Syndromes and genotypes of the different fibroblasts are indicated in the X-axis. * $p < 0.05$, ** $p < 0.01$, compared to WT. (Note that the relevant results are those that reached RNA levels similar to those of WT, i.e., that are not significantly different from those of WT).

It would have been interesting to assess the level of translation of these mRNAs, but the lack of appropriate antibodies or the technical problems with those available, precluded having data on this issue.

To test whether the stop codon mutations could cause a decrease in mRNA levels through the nonsense-mediated mRNA decay mechanism (NMD), fibroblasts were grown in the presence of cycloheximide (CHX), a protein synthesis inhibitor, and RT-PCR was performed.

We analysed a cDNA fragment of the *NAGLU* gene (298bp) which included position c.503, corresponding to mutation p.W168X, amplified from WT fibroblasts and SFB fibroblasts, with genotype p.W168X/p.Q.566X, grown in the absence or presence of CHX and digested with *Bmpl* restriction enzyme. As shown in Figure 34A, alleles not bearing the mutation p.W168X were digested yielding two fragments of 162bp and 136bp respectively. *GAPDH* was used as a control

gene. In Sanfilippo B fibroblasts a significant increase (p -value < 0.05) in the mRNA levels of the allele bearing the stop mutation *NAGLU* p.W168X was observed after CHX treatment. The allele bearing the *NAGLU* Q566X mutation did not show any significant increase, as expected, since it lies in the last exon of the gene (Figure 34B). The experiment was repeated 3 times.

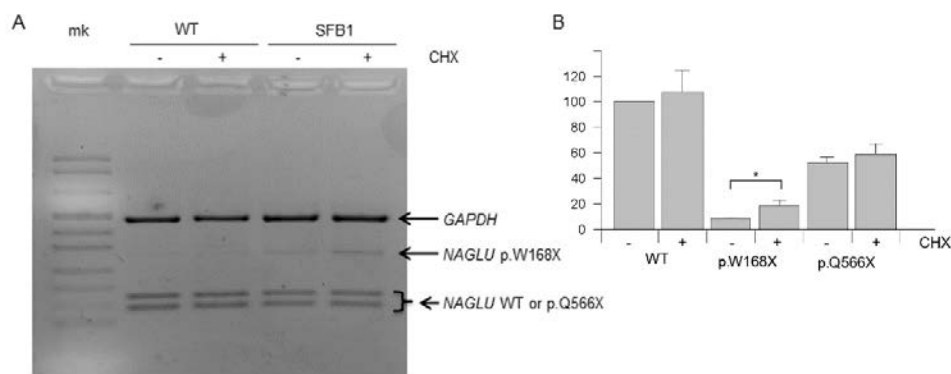


Figure 34. NMD analysis for Sanfilippo B fibroblasts. A) Agarose gel electrophoresis analysis of a cDNA fragment of the *NAGLU* gene (298-bp long), which includes position c.503 (corresponding to mutation p.W168X), amplified from WT fibroblasts or fibroblasts from patient SFB1 (genotype: p.W168X/p.Q566X), grown in the absence (-) or presence (+) of cycloheximide (CHX) and digested with *BmpI*. Alleles not bearing the mutation (WT or p.Q566X) were digested, yielding two fragments of 162 and 136 bp. *GAPDH* was used as a control gene. The experiment was repeated three times, one of which is shown. mk: marker. B) Quantification of the relative amounts of the bands shown in A and in two additional replicates. * $p < 0.05$.

For the *HGSNAT* p.R384X mutation, we analysed a cDNA fragment (140bp) which included position c.1150, corresponding to that mutation, amplified from WT fibroblasts and SFC fibroblasts, with genotype p.R384X/c.1542+4dupA, grown in the absence or presence of CHX and digested with *XhoI* restriction enzyme. As shown in Figure 35A, alleles not bearing the mutation p.R384X were digested, yielding two fragments of 121 and 19bp respectively. *GAPDH* was used as control gene. In Sanfilippo C fibroblasts, a clear increase with borderline significance (p -value = 0.07) was observed after CHX treatment in the mRNA levels of the allele bearing the stop mutation p.R384X (Figure 35B). The experiment was repeated 3 times.

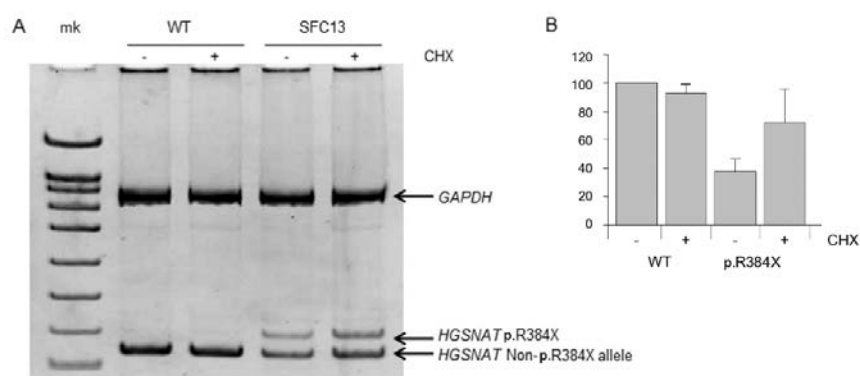


Figure 35. NMD analysis for Sanfilippo C fibroblasts. A) Agarose gel electrophoresis analysis of a cDNA fragment of the *HGSNAT* gene (140-bp long), which includes position c.1150 (corresponding to mutation p.R384X), amplified from WT fibroblasts or fibroblasts from patient SFC13 (genotype: p.R384X/c.1542+4dupA), grown in the absence (-) or presence (+) of cycloheximide (CHX) and digested with *XhoI*. Alleles not bearing the mutation (WT or c.1542+4dupA) were digested, yielding two fragments of 121 and 19 bp (not shown in the gel). *GAPDH* was used as a control gene. The experiment was repeated three times, one of which is shown. mk: marker. B) Quantification of the relative amounts of the bands shown in A and in two additional replicates.

II. Generation of a cellular model for Niemann-Pick A/B

1. Reprogramming fibroblasts to iPSCs

Fibroblasts from 3 patients of Niemann-Pick A/B disease (NPAB2, NPAB4 and NPAB6) and one healthy control were used. Patient NPAB2 was carrying the mutation p.Y313X in homozygosity which causes the most severe phenotype of the disease (type A) while the other 2 patients, NPAB4 and NPAB6, were compound heterozygotes carrying the genotypes p.R441X/p.R474W and p.R608del/p.A482E respectively, which give milder phenotype (type B).

WT and NPB fibroblasts were reprogrammed at early passages (p.5) with retroviral delivery of OCT4, SOX2, KLF4, and c-MYC (4f) or without c-MYC (3f) to generate independent iPSC lines for each individual and for each combination (Figure 36). After three to four weeks, the first iPSC colonies appeared, but the vast majority of colonies appear after 2 months. We obtained from 3 to 6 colonies from WT and NPAB6 in the first round of reprogramming. In the second attempt, 5 colonies of NPAB4 appeared. Mechanically isolated colonies were expanded on iHFF until passage 15 when the validation tests were done.

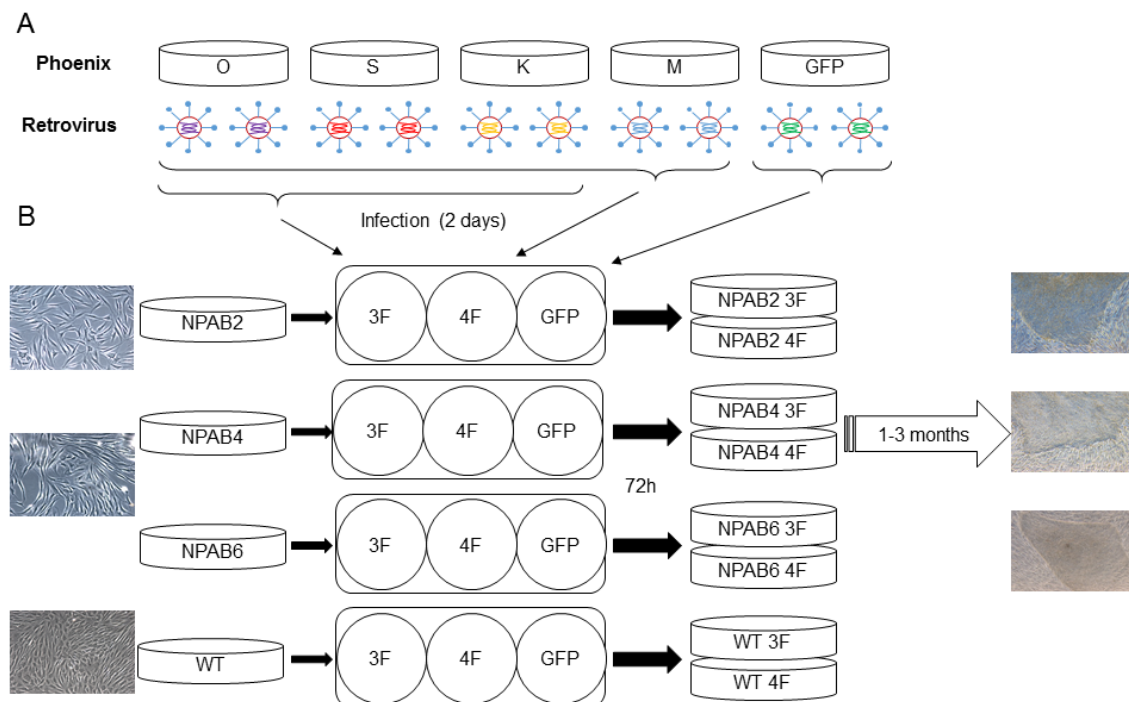


Figure 36. Schematic view of the reprogramming protocol. A) Transfection of Phoenix cells with cDNA coding for OCT4 (O), SOX2 (S), KLF4 (K), c-Myc (M) and GFP for the collection of retroviruses. B) Fibroblasts of each patient and a healthy control were seeded onto a 6-well plate and infected with the retroviruses twice. After 72h, fibroblasts were seeded on iHFF and iPSC colonies appeared from 1 to 3 months. 3F, three factors; 4F, four factors.

However, we did not obtain iPSCs colonies from NPAB2 fibroblasts. These fibroblasts were successfully reprogrammed only when valproic acid was added to the reprogramming protocol. We previously tried to overexpress the *SMPD1* gene in the HFF so that the enzyme excreted could help to achieve NPAB2 reprogramming but transfected HFF did not present an increase in the ASM activity.

2. Pluripotency of the iPSCs

iPSCs derived from NPA/B and WT human fibroblasts were characterized regarding to their pluripotency. All iPSC colonies showed alkaline phosphatase expression (Figure 37).

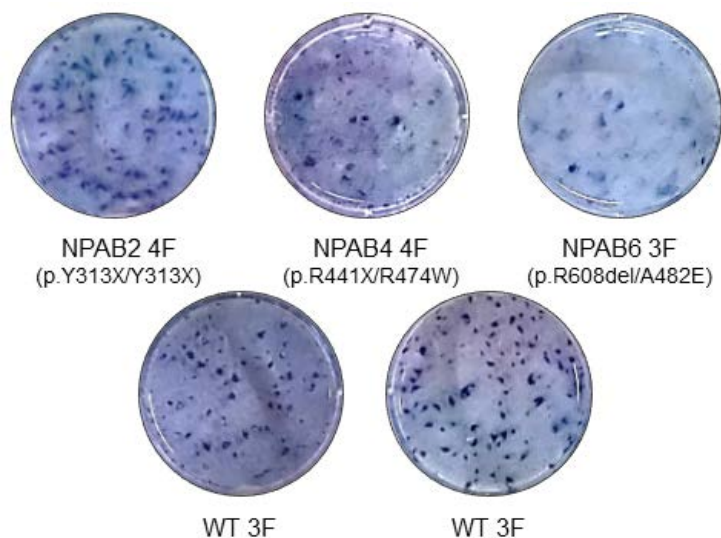


Figure 37. Positive staining of alkaline phosphatase expression in each genotype.

Immunocytochemistry assays with several pluripotent markers, such as transcription factors or ESC specific surface antigens, were performed in NPAB4 and NPAB6 iPSCs. As seen in Figure 38, Nanog, Oct4, SSEA3-4 and Tra-1-81 were strongly expressed in the iPSC, confirming their pluripotency state. It was not possible to perform the immunocytochemistry assays for NPAB2 iPSCs due to an important contamination by mycoplasma in our laboratory.

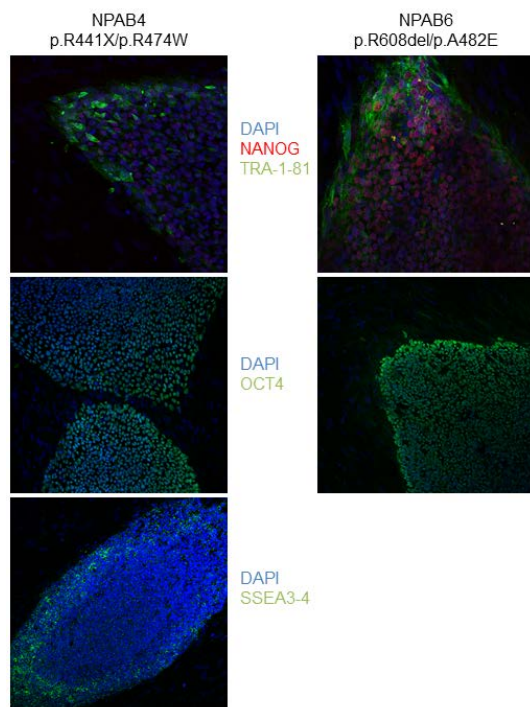


Figure 38. Immunocytochemistry. Representative colonies of NPAB4- and NPAB6-iPSCs stained positive for the pluripotency markers OCT4, TRA-1-81, and SSEA3-4 (green) and NANOG (red).

In NPAB6 iPSCs we checked for the presence of the patient's mutations. The cells were seeded onto matrigel-coated plates, and DNA was obtained. The sequence of the *SMPD1* gene confirmed that, as expected, both mutations of the NPAB6 patient were maintained (Figure 39).

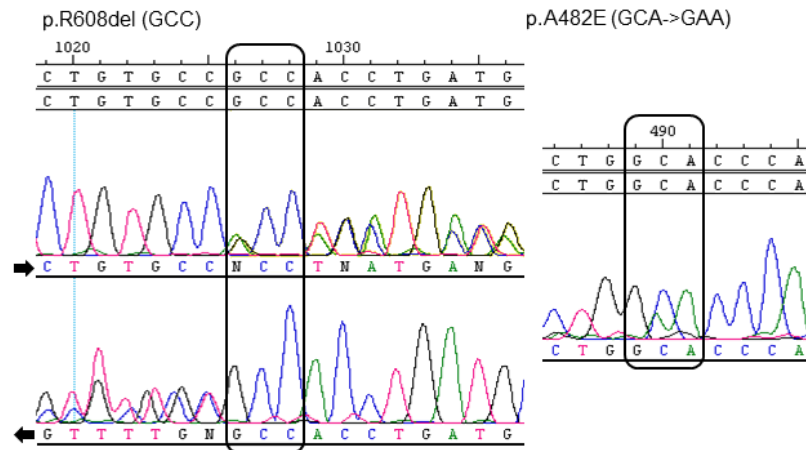


Figure 39. Chromatograms of *SMPD1* gene fragments of NPAB6 iPSCs. NPAB6 mutations are marked with a box. In the p.R608del allele forward and reverse strands are shown.

3. Enzyme Activity in WT iPSCs and derived neurons

To set up the technique, we measured the ASM activity in WT iPSCs and in WT iPSCs-derived neurons (which were a gift from Dr. Canals). We found a decreased enzyme activity of WT-iPSCs compared to WT fibroblasts. However, the activity of ASM was higher in the WT iPSC-derived neurons giving a value of about 2-fold that of WT fibroblasts (Figure 40). It should be noted that this experiment was done only once, first to assess whether we could detect ASM activity in iPSC-derived neurons.

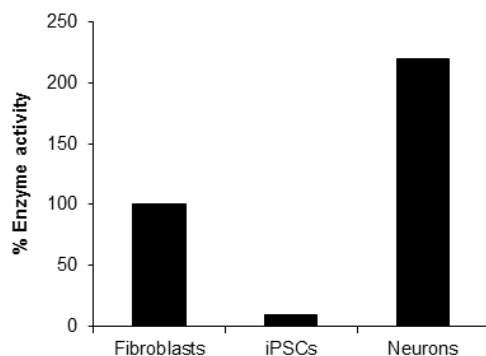


Figure 40. ASM activity from different cell types. The Y-axis represents the percentage of enzyme activity compared to the wild-type fibroblasts, considered as 100. Only one experiment was performed.

It was not possible to carry on with this project due to an important contamination by mycoplasma in our laboratory. Contaminated iPSCs did not grow well on matrigel-coated plates and it precluded the validations. Unfortunately, although the contaminated iPSCs were treated with antimycoplasma drugs for several weeks, we could not get rid of the contamination. Besides, if the antimycoplasma treatment is used for a long time, no iPSCs colonies grow up after few passages

III. Characterization of mouse models of Niemann-Pick C

1. Mice generation

The murine *Npc1* gene contains 25 exons and shares a high homology at the DNA level (83.4% identity and similarity) as well as protein level (86.4% identity and 93.5% similarity) (EMBOSS Stretcher) with human *NPC1* gene. In order to generate a humanized mouse model that could mimic the phenotype of the NPC patients with genotype c.1554-1009G>A/c.1920delG, the OZ Gene Company generated two strains of mice bearing one of these two *Npc1* mutations each in heterozygosity and named them “Imagine” and “Pioneer” respectively (Figure 41). So, the *Npc1*^{Pioneer} mice carry the human mutation c.1920delG and the *Npc1*^{Imagine} mice carry the human mutation c.1554-1009G>A.

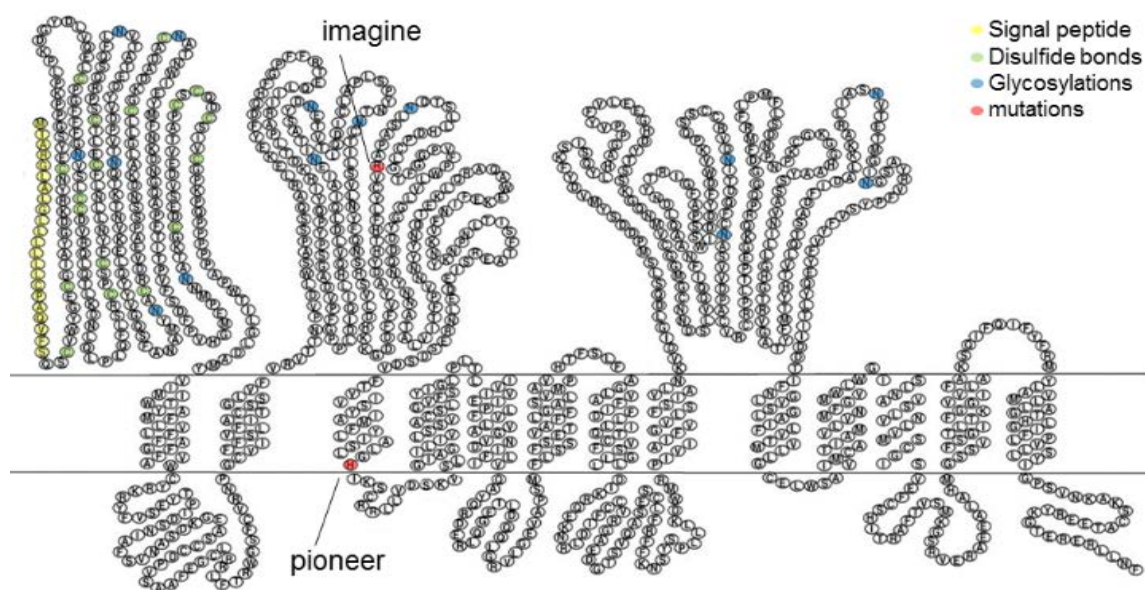


Figure 41. NPC1 protein. Imagine and Pioneer mutations are indicated in red. Signal peptide is indicated in yellow and disulfide bonds and glycosylations are indicated in green and blue, respectively. Adapted from Davies & Ioannou, 2000.

The c.1920delG mutation in the *Npc1* exon 12 causes a truncated protein due to a frameshift. Since the coding sequence surrounding the target nucleotide is not the same in the human gene as in the mouse gene, 2 nucleotides downstream of the introduced change were modified in the mouse genome to generate the stop codon mutation in the same position as in humans (Figure 42). This mutation is situated at the beginning of SSD domain which is important for the binding of cholesterol (Figure 41).

Pioneer
c.1920delG

Wild-type	CTA	GCC	TTG	GG	CAC	ATG	AAA	
	Leu	Ala	Leu	Gly	His	Met	Lys	humans
1920ΔG	CTA	GCC	TTG	GGC	ACA	TGA	AA	
	Leu	Ala	Leu	Gly	Thr	stop		
Wild-type	CTC	GCC	CTG	GG	CAC	ATC	CAG	
	Leu	Ala	Leu	Gly	His	Ile	Gln	mice
Modified	CTC	GCC	CTG	GGC	ACA	TGA	AG	
	Leu	Ala	Leu	Gly	Thr	stop		

Figure 42. Pioneer mutation in humans and modifications introduced in mice to generate it. The deleted nucleotide is marked in red shadow and in green shadow the additional modifications done in mice to generate the premature stop codon.

To generate the c.1554-1009G>A mutation in mice, the whole mouse *Npc1* intron 9 was replaced with the human *NPC1* intron 9 containing the mutation. The change of a G to an A in humans generates an alternative donor splice site which gives rise to an aberrant splicing that includes a pseudoexon of 194bp and produces a frameshift (Figure 43). In Figure 41 it is indicated on the WT protein the first amino acid that changes due to this mutation.

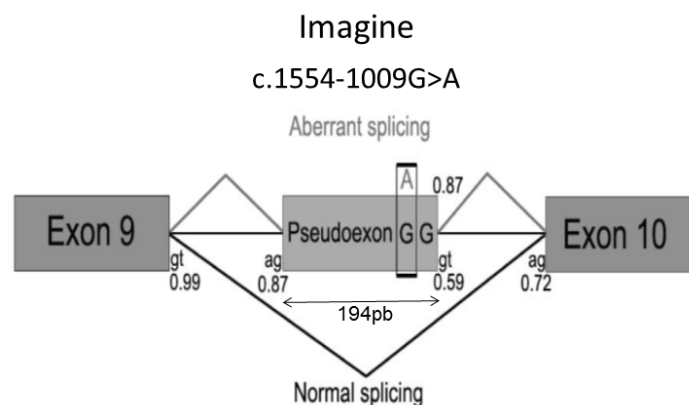


Figure 43. Effect of the Imagine mutation in humans. Scheme of part of the *NPC1* gene, showing the 194pb pseudoexon inclusion. Calculated splice scores are indicated below the corresponding 5' and 3' splice sites. The mutant score for the G-to-A mutation is stated above denoted by a box. Adapted from Rodríguez-Pascau *et al.*, 2009b.

Once we got the heterozygous *Npc1*^{Imagine/+} and *Npc1*^{Pioneer/+} mice generated by OZgene, they were mated with C57BL/6 mice to expand the colony. Heterozygous male and female F1 littermates were bred to obtain homozygous animals for both strains, *Npc1*^{Imagine} and *Npc1*^{Pioneer}. Mutations in both strains were assessed by a specific PCR amplification followed by restriction analysis. In Figure 44 the schematic protocol for the identification of the *Npc1*^{Imagine} mice is shown. The DNA including the human intron will produce a 151bp fragment while the DNA bearing the mouse intron will produce an 185bp fragment. By separating those fragments in an agarose gel electrophoresis, we could easily identify the mice bearing the Imagine mutation in homozygosity, the heterozygous mice or the mice bearing no mutations.



Figure 44. Schematic representation of the PCR results from the Imagine mutation genotyping. Situation of the primers and Imagine mutation (*) in genomic DNA. Schematic representation in a gel (left) and photo of the results given by this protocol (right). White arrowheads indicates the length of the bands (in bp).

In Figure 45 the schematic protocol for the identification of the *Npc1*^{Pioneer} mice is shown. The DNA bearing the Pioneer mutation and digested by *Nla*III restriction enzyme gives rise to three fragments (144, 48 and 36bp), while the DNA not bearing this mutation, but also digested with *Nla*III restriction enzyme, produces only two fragments (193 and 36bp). When those fragments are separated in a polyacrylamide gel electrophoresis it is easy to differentiate the mice bearing the Pioneer mutation in homozygosity, the heterozygous mice or the mice bearing no mutations. Sequencing of the genomic DNA confirmed the identity of each genotype.

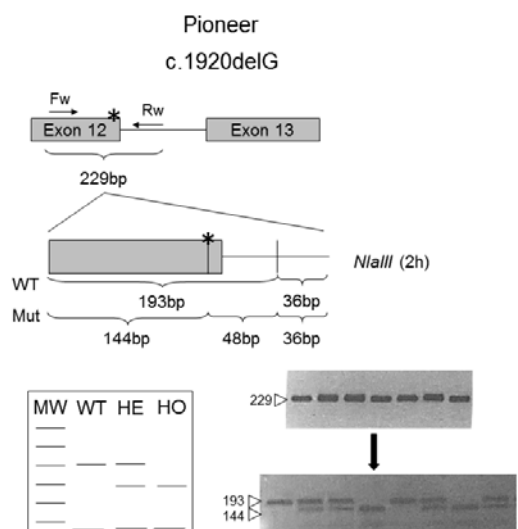


Figure 45. Schematic representation of the PCR results from the Pioneer mutation genotyping. Situation of the primers and Pioneer mutation (*) in genomic DNA. Representation of *Nla*III cutting pattern of WT and mutated fragments. Schematic representation in a gel (left) and photo of the results given by this protocol (right). White arrowheads indicate the length of the bands (in bp).

2. Phenotyping of the mouse models

The segregation ratio of *Npc1*^{Pioneer} and *Npc1*^{Imagine} mice model shows a marked deficiency of homozygotes. A 2% (72:98:5) and 18% (65:125:43) respectively were obtained instead of the 25% expected.

Motor coordination and behavioural tests to phenotype the NPC mouse model were performed in collaboration with Mara Dierssen's group at the Cellular and Systems Neurobiology laboratory in the Centre for Genomic Regulation (CRG).

3. Pioneer

The *Npc1*^{Pioneer} mice had a very low rate of birth. Only a few homozygous animals were born from all the crosses and most of them were females. As 12 male homozygous animals are needed to perform the behavioural phenotyping, it was not possible to phenotype this mouse model.

4. Imagine

About 14 wild-type and 14 *Npc1*^{Imagine} (homozygous for the mutation (HO)) male mice were studied from 21 to 60 days of age.

When compared to the WT, *Npc1*^{Imagine} mice lived less, with an average lifespan of 9 weeks. Imagine mice, at 30 days of age, had a similar body weight to that of their WT littermates, but after day 35 it started to decrease progressively being significantly different from that of WT mice in the final weeks of their life (Figure 46A). At approximately 7 weeks of age, there is an onset of visible tremors and ataxia in mice (Figure 46B) that hinder the performance of psychomotor tests, such as rotarod, showing impaired motor coordination compared to WT.

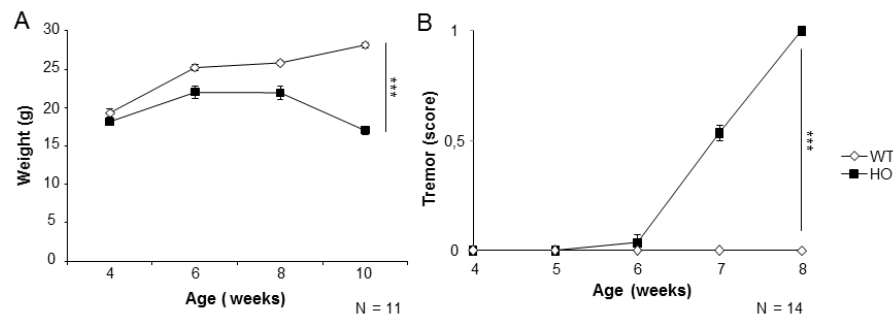


Figure 46. Weight evolution and pathological symptoms. A) Body weight of mice during the observation period. B) Appearance of tremors during the observation period. WT, Wild-type; HO, homozygous. *** $p < 0.001$.

In the rotarod training session mice were habituated to the apparatus and they had to stay on the moving cylinder at 4 rpm for 2 minutes. In this session, the number of times falling from the apparatus was significantly higher in *Npc1*^{Imagine} mice than in WT ($p < 0.001$) (Figure 47A). In our experiment mice were given trials on the rotarod, from 7 to 34 rpm during 1 minute period each velocity. Transgenic mice were unable to learn through sessions, while WT efficiently learned the task until 34 rpm ($p < 0.001$) (Figure 47B). *Npc1*^{Imagine} mice fall more often than WT mice during the training session and fell down earlier from the wheel in each velocity during the learning curve.

In the rotarod acceleration test mice were exposed to velocity acceleration from 4 to 40 rpm in 1 minute and latency to fall down was measured. In this session, which presents the maximum difficulty, *Npc1*^{Imagine} mice also fall down earlier and with less acceleration of the wheel when compared to controls ($p < 0.001$) (Figure 47 C and D).

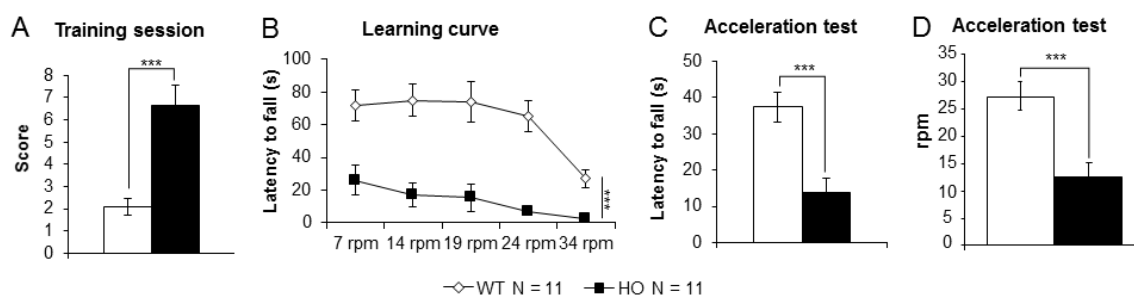


Figure 47. Rotarod motor coordination test. A) Training session. Score given to number of times falling from the apparatus at 4rpm. B) Latency to fall of animals at different velocities. C) Acceleration session. Latency to fall of mice on rotarod increasing velocity from 4 to 40 rpm in 1 minute. D) Acceleration session. Revolutions per minute (rpm) when falling from the apparatus. Data are expressed as mean \pm SEM. WT, Wild-type; HO, homozygous. *** $p < 0.001$.

5. Behavioural tests

Some of the tests were performed when the pathological symptoms were already detected at 7-8 weeks of age. Thus, tremor and ataxia may have affected the performance in motor coordination tests

Circadian activity

The circadian activity was performed at 5 weeks and at 8 weeks of age. A distinct pattern of locomotor activity was established for the diseased animals. Both WT and *Npc1*^{Imagine} mice during the first three to four hours of exposition to the new environment showed novelty-related hyperactivity. During this initial period 8 weeks old mice of both genotypes travelled more distance compared to 5 weeks old mice ($p=0.001$) indicating an increase according to the age in the activity. Moreover, transgenic mice showed hyperactivity during the habituation period compared to controls ($p=0.002$). This hyperactivity was also detected during the active phase of the circadian cycle in transgenic animals and increased with age ($p=0.034$) (Figure 48).

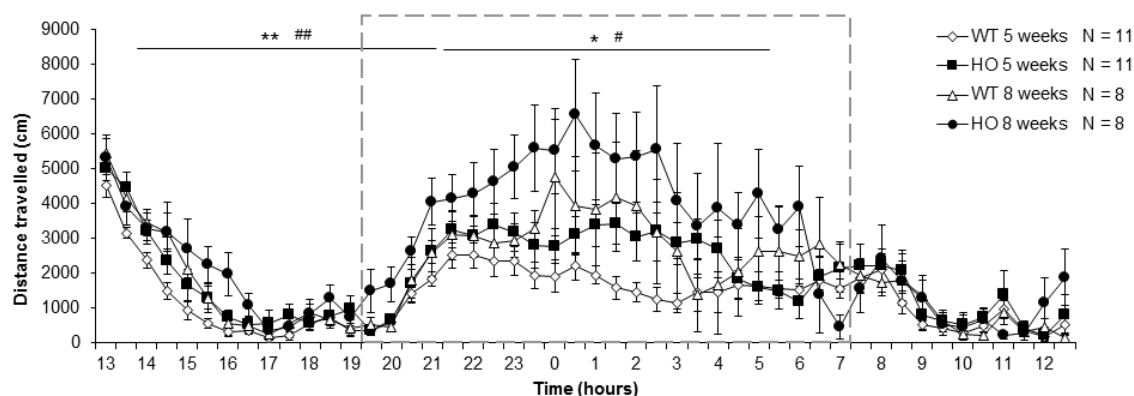


Figure 48. Circadian activity. Distance travelled (in cm) each 30 min for 24h, starting the test around 13 a.m. Grey dashed box represents the active phase of the circadian cycle. Data are expressed as mean \pm SEM. WT, Wild-type; HO, homozygous. Genotype effect: ** $p < 0.01$; * $p < 0.05$. Age effect: ## $p < 0.01$; # $p < 0.05$.

Novel object recognition

In the habituation session, transgenic mice performed the task with no significant differences in the spontaneous alternation and in the number of entries in any arm of the maze (Figure 49).

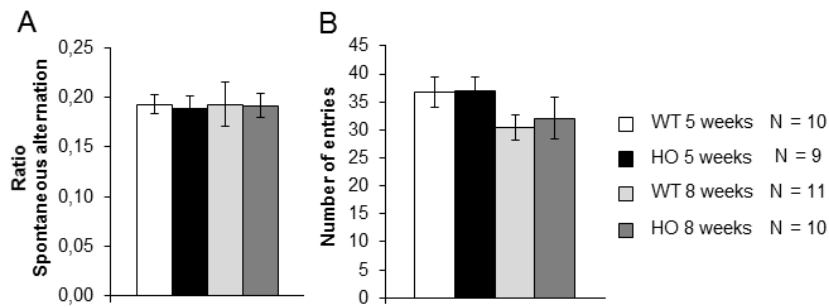


Figure 49. Habituation session. A) Number of total entries in the arms of the Y-maze. B) Spontaneous alternation expressed as n° of alternations divided by total number of entries minus 2. Data are expressed as mean \pm SEM. WT, Wild-type; HO, homozygous.

In the familiarization session, mice were presented with two identical objects for 10 minutes. At 5 weeks no differences were detected between WT and *Npc1*^{Imagine}. However, at 8 weeks, WT explored more time both objects than *Npc1*^{Imagine} mice at 8 weeks of age and also WT explored more time both object than WT mice at 5 weeks of age ($p=0.003$) and this increase associated to the age in the exploration was not detected in *Npc1*^{Imagine} mice (Figure 50).

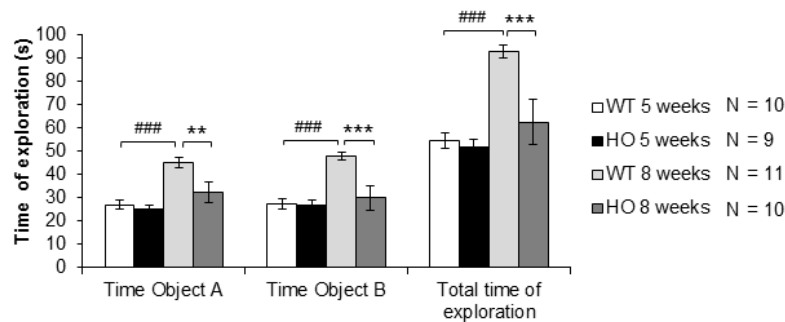


Figure 50. Familiarization session. Time of exploration. Data are expressed as mean \pm SEM. WT, Wild-type; HO, homozygous. Genotype effect: *** $p < 0.001$, ** $p < 0.01$. Age effect: ### $p < 0.001$.

In the recognition session, mice were exposed to a familiar and a new object in order to measure the capacity to discriminate novelty. There is no difference between genotypes concerning about the amount of time exploration (Figure 51A) suggesting an habituation of WT, and a slight increase in exploration through sessions in *Npc1*^{Imagine} mice. Nevertheless, the discrimination index indicates that *Npc1*^{Imagine} mice at 8 weeks of age presented an impairment in memory recognition compared to their WT littermates ($p=0.033$) (Figure 51B).

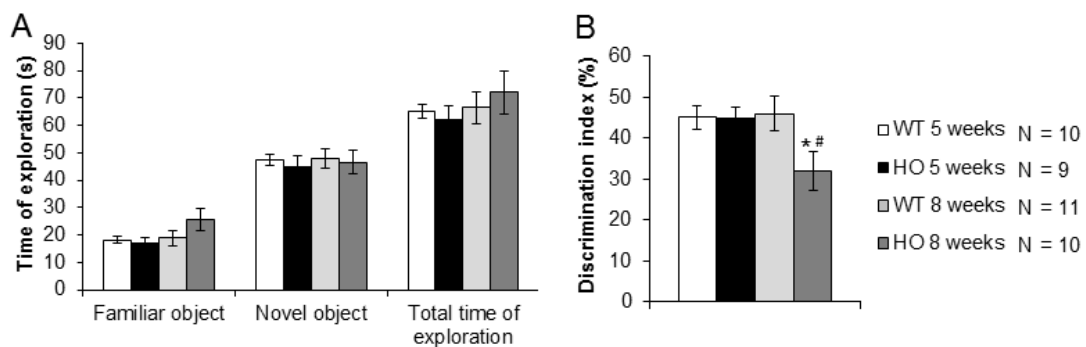


Figure 51. Novel object recognition session. A) Time of exploration. B) Discrimination index measured as time of exploration towards the novel object minus time of exploration towards familiar object divided to the total time of

exploration, expressed as percentage. Data are expressed as mean \pm SEM. WT, Wild-type; HO, homozygous. Genotype effect: * $p < 0.05$. Age effect: # $p < 0.05$.

Elevated plus maze

Npc1^{Imagine} mice spent more time than WT in the open arms suggesting that they are less anxious or present more impulsive phenotype (% time open arms $p=0.05$) (ratio open/closed $p=0.01$) (Figure 52 A and B). Regarding to the activity in elevated plus maze (EPM), *Npc1*^{Imagine} mice presented higher distance travelled in open arms than in closed arms (Distance travelled in open arms: $p=0,009$; distance travelled in closed arms: $p=0.040$) (Figure 52D). Also, *Npc1*^{Imagine} mice entered more times into the open arms compared to controls (entries in open arms: $p=0.032$) (Figure 52C).

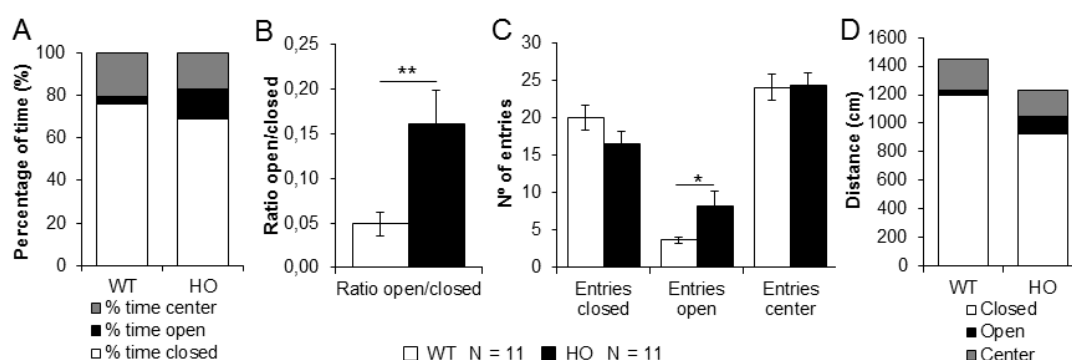


Figure 52. Elevated plus maze. A) Stacked bar chart showing the percentage of time spent in open, closed or in the centre of the maze. B) Ratio calculated by the time spent in the open arms divided to the time spent in closed arms. C) Number of entries into arms. D) Stack bar charts showing distance travelled in centimetres in open, closed or in the centre of the maze. Data are expressed as mean \pm SEM. WT, Wild-type; HO, homozygous. * $p < 0.05$; ** $p < 0.01$.

Hot plate

Diseased animals seemed to have a slightly higher pain threshold compared to controls, therefore they lasted more time to lick their front paws ($p=0.041$) (Figure 53).

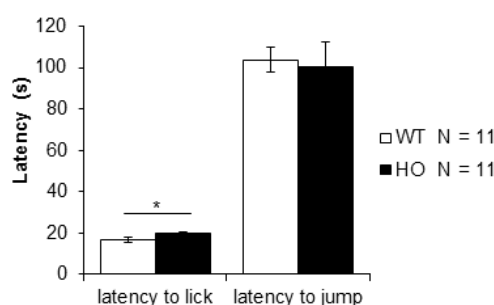


Figure 53. Hot plate. Latency to lick the front paws and to jump. Data are expressed as mean \pm SEM. WT, Wild-type; HO, homozygous. * $p < 0.05$.

Paw printing

There was no difference between genotypes regarding to the number of steps or the stride and step distance, but transgenic mice showed reduced angles of hind prints compared to controls ($p=0.000$) (Figure 54).

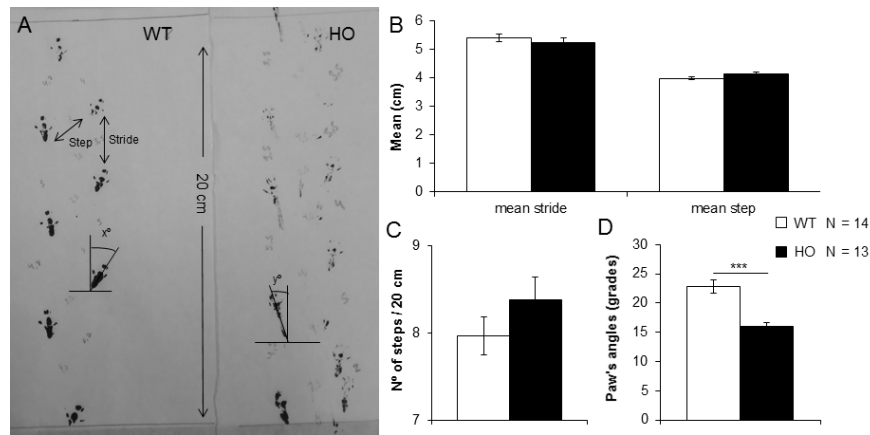


Figure 54. Paw printing. A) Schematic representation of footprints analysed. B) Mean of distance between steps and stride (cm). C) Number of steps measured in 20 cm of walking. D) Paw's angles measured as degrees. Data are expressed as mean ± SEM. WT, Wild-type; HO, homozygous. *** p < 0.001.

6. Splicing pattern analysis

To determine if the replacement of a complete murine intron by the complete homologous human one causes the same pattern of alternative aberrant splicing in the mice as the one seen in human patients, RNA was extracted from liver and brain cortex, and a RT-PCR experiment was done using primers flanking exon 9 and 11.

As seen in Figure 55, in both tissues, a multiple band pattern was observed. These bands were excised and sequenced, and were shown to correspond to different alternatively spliced transcripts. In brain, WT mice only had the transcript corresponding to the normal splicing (Figure 55 C2). However, in the transgenic mice, two alternative transcripts were seen and not the WT transcript. It was confirmed by sequencing that the larger band (Figure 55 C1) included a 194bp pseudoexon and the smaller band (Figure 55 C3) corresponded to a transcript with the exon 10 skipped. In the liver, WT mice presented only the WT transcript, but in the transgenic mice two additional bands were also seen as well as the WT transcript. The alternative splicing-produced transcripts gives rise to non-functional proteins.

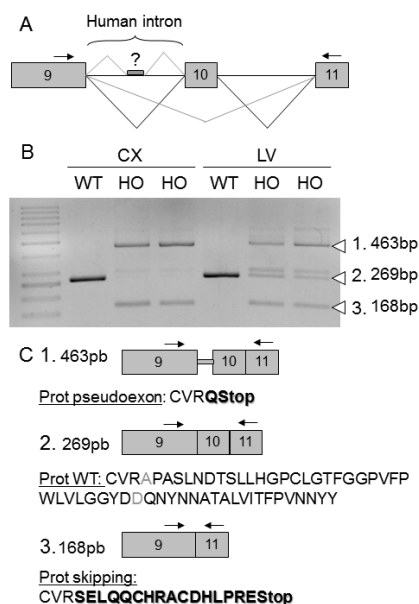


Figure 55. RT-PCR transcript analysis.

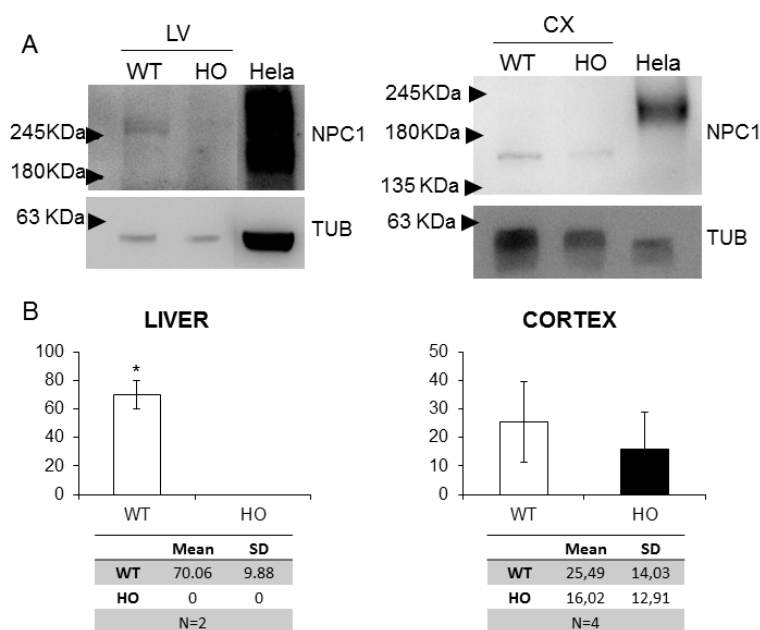
A) Schematic representation of the correct splicing (in black) and the alternative splicing processes (in grey).

B) Agarose gel electrophoresis analysis of a cDNA fragment from exon 9 to 11 from *Npc1*^{Imagine} mouse brain cortex (CX) and liver (LV). White arrowheads indicate the length of bands (in bp). C) Schematic interpretation of the different bands. WT, Wild-type; HO, homozygous.

7. Western analysis

To check for the presence of the Npc1 protein in the liver and brain cortex of the *Npc1*^{Imagine} mice, we performed a western blot analysis with NPC1 antibody. Human and mice NPC1 protein has a predicted molecular weight of 142KDa. However, there is a glycosylated form of approximately 180KDa that can be also detected in western analysis.

In the *Npc1*^{Imagine} cortex tissue there is a slight reduction of Npc1 protein whereas the in liver tissue, transgenic mice have a significant reduction of the protein ($p=0.03$) (Figure 56).



8. Lipid analysis in mice tissues

To determine whether the Imagine mutation led to a similar lipid storage phenotype as NPC patients or another mice models, we surveyed sphingolipids and cholesterol in brain and liver tissue from WT and *Npc1*^{Imagine} littermates respectively.

Liquid chromatography–mass spectrometry was used for the quantification of the different classes of lipid, including ceramides, sphingomyelins and gangliosides in collaboration with Dr. Casas from Department of Biomedical Chemistry of “Institut de Química Avançada de Catalunya” (IQAC-CSIC). The analyses were performed on brain samples of ten transgenic and ten WT mice in duplicate.

In WT mice brain there are some storage of lipids, such as sphingomyelin (SM), ceramide (Cer) and Glucosylceramide (GlcCer), to a lesser extent, there is also storage of total gangliosides, dihydrosphingomyelin (dhSM) or dihydroceramide (dhCer). However, there is no storage of other types of lipids such as lactosylceramide (LacCer) or the gangliosides GM2 and GM3 (Figure 57). However, in *Npc1*^{Imagine} mice brain there is a broad range of lipids, where the most significant increases are the gangliosides and LacCer. GlcCer in *Npc1*^{Imagine} mice brain is the only lipid whose storage is reduced instead of being increased (Figure 57).

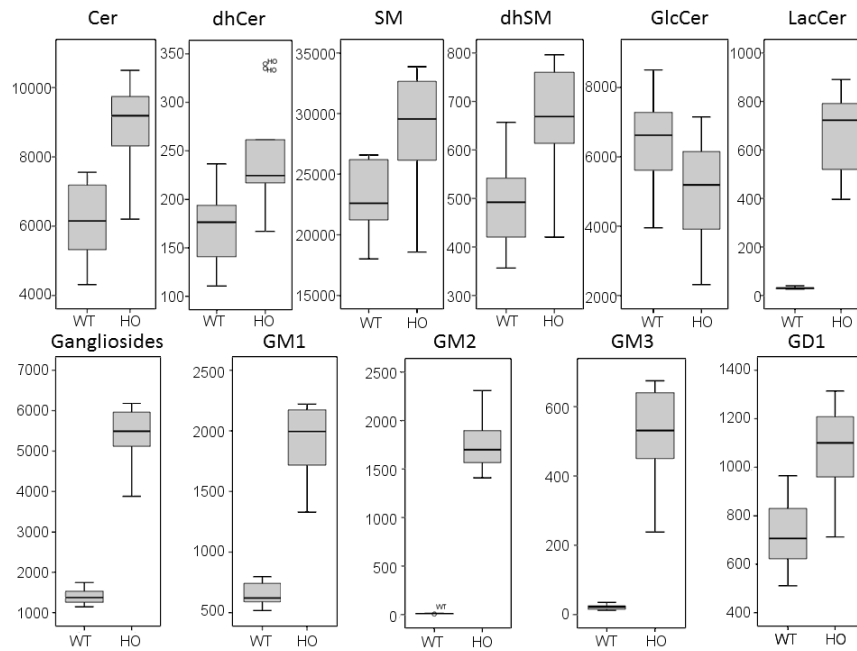


Figure 57. Boxplot showing the distribution of brain lipid storage. The X-axis shows the phenotype and the Y-axis shows the quantification level of the lipid indicated, expressed in pmol/mg prot. The top and bottom of each box in the box plots indicates the upper and lower limit of the 95% confidence interval, respectively; and the bar inside the box is the median. The whiskers extend out to the most extreme data point. Cer: Ceramide; dhCer: dihydroceramide; SM: sphingomyelin; dhSM: dihydrosphingomyelin; GlcCer: glucosylceramide, LacCer: lactosylceramide; WT, Wild-type; HO, homozygous. N = 10 WT; N = 10 HO.

As seen in Figure 58 the lipid accumulation in *Npc1*^{Imagine} and WT mice was significantly different for all the classes (Cer: $p < 0.001$, SM: $p = 0.003$, dhCer: $p = 0.007$, dhSM: $p = 0.002$, GlcCer: $p = 0.029$, LacCer, Gangliosides, GM1, GM2, GM3 and GD1: $p < 0.001$).

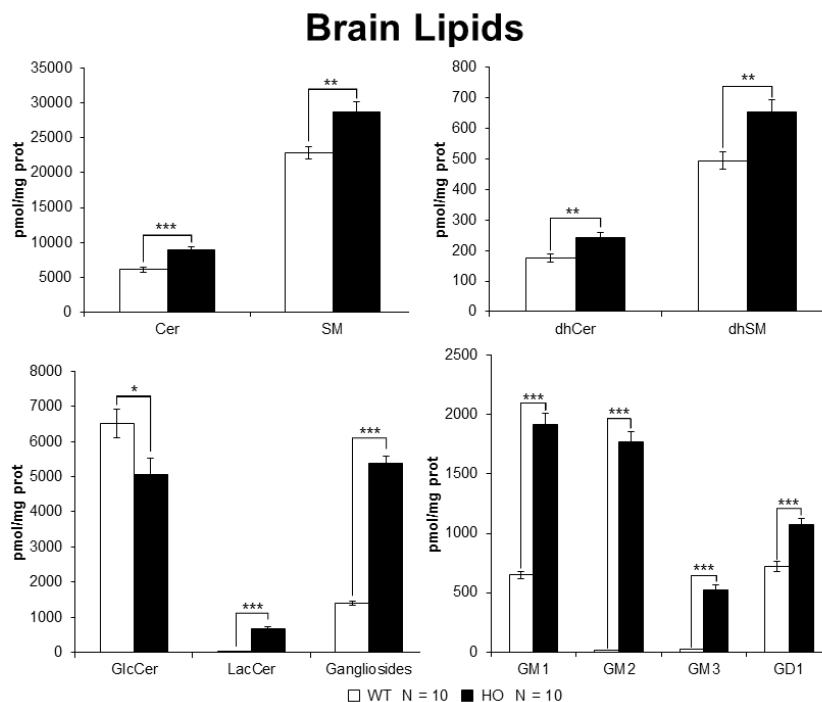


Figure 58. Histogram showing the brain lipid storage. Data are expressed as mean \pm SD. WT, Wild-type; HO, homozygous. * $p < 0.05$, ** $p < 0.01$ and *** $p < 0.001$.

Cholesterol levels in the liver tissue of WT and *Npc1^{Imagine}* mice were evaluated by the *Amplex Red Cholesterol assay* that gives quantitative values of esterified and unesterified cholesterol. The analyses were performed on samples of 5 WT and 5 *Npc1^{Imagine}* mice at 8 weeks of age. As shown in Figure 59, the levels of total cholesterol, as a sum of esterified and unesterified cholesterol, were statistically higher in transgenic mice than in WT ($p=0.006$).

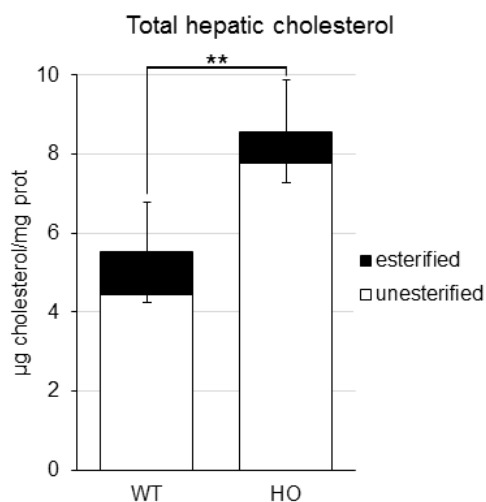


Figure 59. Total hepatic cholesterol. Stacked bar chart showing the quantification of esterified and unesterified cholesterol in μg cholesterol / mg protein. Data are represented as mean \pm SD. **= $p < 0.01$.

9. Histological analysis of liver tissue

Histological analyses of liver tissue were also used to evaluate the lipid accumulation in *Npc1^{Imagine}* and WT mice. *Npc1^{Imagine}* mice had accumulation of lipid in vacuole-like inclusions (Figure 60 black arrows), accompanied by infiltration of macrophages (Figure 60 black circle), different organization of hepatocytes and swelling of sinusoids (Figure 60).

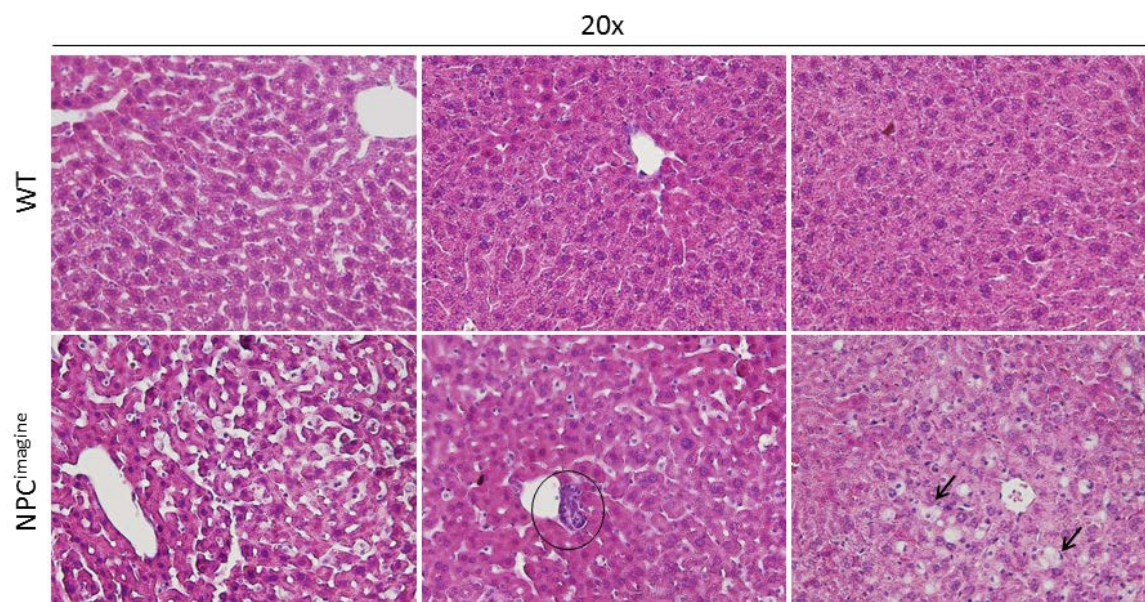


Figure 60. Histological analysis of liver tissue. Foamy macrophages in *Npc1^{Imagine}* hepatocytes are indicated by black arrows. Neutrophil infiltration is marked with a black circle.

DISCUSSION

I. Nonsense mutations: read-through as a therapeutic approach

Correction of nonsense mutations with small molecules that interfere with ribosomal function and modify the translation of mRNA by bypassing PTCs could be an interesting therapeutic option for monogenic diseases caused by this type of DNA mutation. Such correction has been reported as being successful for several diseases and compounds besides several studies have validated this strategy using animal models.

In 1985, Burke and Mogg were the first to demonstrate that the aminoglycosides G418 and paromomycin antibiotics could restore the synthesis of a full-size protein in cultured mammalian cells (COS7) up to a 20% of wildtype levels (Burke & Mogg, 1985). Similar results had been obtained before in yeast and *E.coli* cell free system (Gorini & Kataja, 1964)

Later, G418 and gentamicin were shown to restore the expression of the full-length cystic fibrosis transmembrane conductance regulator (CFTR) protein in a bronchial epithelial cell line carrying a nonsense mutation in the CFTR gene, genotype F508del/W128X (Bedwell *et al.*, 1997).

The ability of gentamicin to promote protein translation was first demonstrated *in vivo*, in 1999, in a *mdx* mouse which is a model of Duchenne muscular dystrophy (DMD) carrying a point mutation that generates a premature stop codon. It has been shown that there is a window in the gentamicin dosage where misreading can lead to the restoration of the full-length protein. This mistranslation cannot completely restore normal levels of protein. Moreover, excessive levels of drugs can interfere with protein translation to such an extent that cell proliferation and differentiation is prevented. (Barton-Davis *et al.*, 1999).

Nowadays several groups have reported good recovery results with aminoglycosides in different disease animal models; CFTR^{-/-} mice treated with gentamicin (Du *et al.*, 2002), nephrogenic diabetes insipidus mice with G418 (Sangkuhl *et al.*, 2004), haemophilia mice with gentamicin and G418 (Yang *et al.*, 2007), retinitis mice with gentamicin (Guerin *et al.*, 2008). Also, some pilot clinical trials detected restoration of functional protein in CF patients (Clancy *et al.*, 2001; Wilschanski *et al.*, 2003) and in DMD patients treated with gentamicin (Malik *et al.*, 2010; Politano *et al.*, 2003). Another pilot study found that intravenously administered gentamicin restored coagulation factor function in a fraction of haemophilia patients (James *et al.*, 2005).

However, a critical point to be taken into account is whether the efficacy of read-through is clinically relevant. In this regard, lysosomal storage disorders could be a good option since it has been reported that small amounts of functional protein (around 10% of WT enzyme activity) may be considered therapeutically relevant in several LSDs (Suzuki *et al.*, 2009).

In 2001, two groups tested gentamicin in patients' fibroblasts from CLN2 and MPSI diseases obtaining restoration of 3 to 5% of normal levels of protein activity (Keeling, 2001; Sleat *et al.*, 2001). Later, gentamicin read-through effect was tested in CHO cells carrying different stop mutations from MPSI disease, suggesting a codon-specific effect. Gentamicin had less effect on the TAG codons when compared to the other two stop codons constructs (TAA and TGA) (Hein *et al.*, 2004). In the last 5 years, several papers have been published where the read-through capability of gentamicin and PTC124 were tested in patients fibroblasts from MPSVI, Fabry, NPA/B, MPSI, MPSII, MPSIIIB with an increase of up to 3-fold enzyme activity (Bartolomeo *et al.*,

2013; Matalonga *et al.*, 2015). Moreover, the read-through capability of different aminoglycosides and non-aminoglycosides compounds as NB84 or NB54 was tested in fibroblasts from MPSI disease mice model. NB84 was the drug which most effectively suppressed the stop codon, *in vitro* and *in vivo*, resulting in a significant attenuation of the primary biochemical defects associated with MPSI (Wang *et al.*, 2012). Recently, it has been obtained 1.2 and 20-fold enzyme activity increase when CLN1 and MPSI mice model were treated with PTC124 and NB84 respectively (Gunn *et al.*, 2014; Miller *et al.*, 2015). Furthermore, the combination of read-through drugs, gentamicin and NB84, with inhibitors of NMD enhanced the enzyme activity by an additional 50% more than treatment with read-through drugs alone (Keeling *et al.*, 2013).

In our work we have analysed a considerable number of PTC mutations responsible for different LSDs (Niemann-Pick types A/B, Sanfilippo syndrome types B and C, and Maroteaux-Lamy syndrome) with different identity and context. Two aminoglycoside (G418 and gentamicin) and five non-aminoglycoside (PTC124, RTC13, RTC14, BZ6 and BZ16) read-through compounds have been tested using several techniques. Although some positive results were found for specific methods they were not generally confirmed by the other methods. In this regard, we found some correction by TNT analyses that were not confirmed by enzyme activity assays, i.e. p.R203X or p.W403X mutations of the *HGSNAT* gene or the *SMPD1* gene mutations. This could be due to the fact that in the read-through process, the amino acid incorporated on the stop codon provoked the incorrect folding of the protein or that the protein containing the missense change was not active. On the contrary, we observed an increased enzyme activity for some mutations that presented no recovery of the full-length protein in the TNT assays after some of the treatments. This is the case of *ARSB* p.W146X mutation that presents the highest increase of enzyme activity detected but does not correlate with the TNT result. This could be explained by technical difficulties of the TNT technique (for instance, small truncated proteins are difficult to detect).

In the early papers of the 1960s, describing "nonsense suppression" a variable response to treatments and, in general, a not very robust response was already reported. A possible explanation for the variability in the results could be the different identity of the PTCs involved and the context surrounding them (basically, the fourth nucleotide). The UGA codon followed by a C has been reported to be the best combination for a high read-through efficiency (Bidou *et al.*, 2004; Manuvakhova *et al.*, 2000). In the present study, only two out of the 19 mutations had this optimal combination (see Table 7). One of them, *HGSNAT* p.W403X, showed one of the best results in the TNT assay with gentamicin and G418, and the other one, *ARSB* p.W146X, showed the best recovery of activity in transfected COS7 cells after treatment with gentamicin and PTC124. Some authors suggested that in the stop codon context, the first nucleotide 5' of the PTC is also important, with U being more susceptible to promote read-through, independent of the stop codon itself (Floquet *et al.*, 2011). In the present study, 4 out of the 19 mutations bear a U in this position (all in the *HGSNAT* gene: p.R203X, p.R384X, p.R506X and p.W510X). While they also carry the UGA stop codon (reported to be the best by several authors), none of them carries the C in the 4th position, which should make them all sub-optimal, according to Floquet *et al.* (2011). Only p.R203X gives some recovery in the TNT assay with gentamicin and G418. Mutations p.R203X and p.R384X give some recovery with gentamicin but not with G418 in the activity assay in transfected COS7 cells.

Sánchez-Alcudia *et al.* (2012) and Matalonga *et al.* (2015) performed mRNA analyses on different patients' fibroblasts. All patients' fibroblasts showed decreased levels of mRNA expression compared to those of WT but after read-through drug treatments no significant increase of mRNA expression was observed, except for cells treated with G418 and PTC124 in the study by Sánchez-Alcudia *et al.* and in samples treated with gentamicin in one case described by Matalonga *et al.*

We assayed gentamicin, G418 and six additional read-through drugs on fibroblasts of the Sanfilippo B (p.W168X/p.Q566X) and the Sanfilippo C (p.R384X/c.1542+4dupA) patients. Treatment with non-aminoglycoside RTC14 gave slightly recovery of the mRNA levels for Sanfilippo C fibroblasts when compared to mRNA levels of non-treated fibroblasts, although this recovery remains significantly different compared to mRNA levels on WT fibroblasts. Treatment with aminoglycoside G418 gave good recovery of the mRNA levels for Sanfilippo B fibroblasts, but a negligible increase in enzyme activity was observed compared to non-treated fibroblasts, suggesting that the protein with the missense change (generated by the read-through) was not active. The increase in mRNA levels could be due to an improved stability of the mutant RNA as a consequence of a reduction in the efficacy of the NMD process. We were able to demonstrate that the NMD mechanism was partially responsible for the reduction in RNA levels in the alleles bearing nonsense mutations located in the NMD-competent region of the gene (p.W168X). This suggests that the read-through efficacy could be enhanced with the additional use of NMD inhibitors. This possible strategy, a treatment combining read-through drugs with NMD inhibitors, was already suggested by Bordeira-Carrico *et al.* (2012). However, the toxicity of the different compounds, including G418 and NMD inhibitors, argues against their therapeutic potential. On the other hand, the G418 drug showed no recovery with Sanfilippo C fibroblasts neither in mRNA levels nor in enzyme activity.

Gentamicin and G418 are the most widely used PTC-specific compounds. A lot of works have been published using these compounds and good recovery results reported (Lee & Dougherty, 2012; Lai *et al.*, 2004; Sanchez-Alcudia *et al.*, 2012).

PTC124 was identified as a read-through drug over 10 years ago and was reported as non-toxic and orally bioavailable (Welch *et al.*, 2007). It appeared as the most promising compound for the correction of nonsense mutations, but there was also controversy about the results. Also, it does not cross the blood–brain barrier efficiently and it is a poor candidate for adjunctive read-through therapy with replacement proteins for LSDs (Miller *et al.*, 2015). Even so, PTC124 was approved for DMD and CF disease and two phase III clinical trials are ongoing for these diseases (NCT01826487, NCT02139306) (Ryan, 2014). In the present study, we have also tried the PTC124 drug and found some recovery of the ARSB activity in transfected COS7 cells with p.W146X and p.R160X mutations and also on RNA levels of the Sanfilippo C fibroblasts. The effect of PTC124 on one of the *ARSB* mutations studied here, p.Q503X, was previously analysed in patients' fibroblasts by Bartolomeo *et al.* (2013), who found no recovery of enzyme activity. Whereas Peltz *et al.* (2013), from PTC Therapeutics Inc., consider that there are multiple, independent demonstrations of Ataluren's (PTC124) nonsense suppressing activity, other authors question this statement. McElroy *et al.* (2013) failed to find evidence of activity for PTC124 in a thorough and systematic investigation of the proposed mechanism of action of PTC124 in a wide array of cell-based assays. They found no evidence of translational read-through activity for PTC124

while G418 exhibited varying activity in every read-through assay done. The slight effects found in our study are consistent with those who found that this compound is, at least, not as effective as it was claimed when it was discovered. The result of the ongoing clinical trials will be very interesting to clarify this issue.

We also assayed several compounds generated by Dr. Gatti group at the University of California, Los Angeles (UCLA): RTC13 and RTC14, BZ6 and BZ16 (Du *et al.*, 2009; Jung *et al.*, 2011). Positive results for RTC13 and RTC14 have been found for numerous mutations in the ATM gene and in ATM patients' fibroblasts (Du *et al.*, 2009; Nakamura *et al.*, 2012). Moreover, there were also positive results with both compounds in *in vitro* and *in vivo* experiments with a DMD mouse model (Du *et al.*, 2009; Kayali *et al.*, 2012). BZ16 (a derivative of RTC13) and RTC14 were also probed in numerous mutation of ATM gene (Jung *et al.*, 2011) and in skin fibroblast from xeroderma pigmentosum (Group C) patients with an increase of mRNA levels (Kuschal *et al.*, 2013).

We found some recovery of RNA levels with RTC14 and BZ16 in Sanfilippo C fibroblasts (particularly with the former). However, our results are rather modest compared to the published data.

In summary, our results and those of others on read-through treatment for nonsense mutations show a certain degree of recovery either in protein levels, mRNA levels or enzyme activity. The results are sometimes inconsistent between groups, mutations, compounds and techniques. However, the positive results are promising and, in some cases, they have led to clinical trials, whose results will have important implications for the field. The small molecule read-through (SMRT) chemicals also can be promising for systemic use, including for treatment of central nervous system involvement. Novel compounds are being generated by different groups in the search for more efficient and less toxic drugs. The fact that slight recovery of protein levels could be enough to cure LSDs, and that any good compound could be used for many diseases, is sufficient to encourage further research.

II. Generation of a cellular model for Niemann-Pick A/B

No effective therapy for NPA/B patients has been developed till now. However, a clinical trial of ERT for NPB has been set up very recently (NCT02292654). Regarding to animal models, there are two ASM mice, one with the features of NPA and the other one with NPB features. Differences in the brains of the two mice have been detected, NPB mice cerebellar Purkinje cell layer is preserved for at least 8 months whereas in NPA mice is lost by 4 months.

Induced pluripotent stem cells (iPSCs) technology has been successfully used to model a considerable number of monogenic diseases, including those in which the central nervous system is involved (Singh *et al.*, 2015; Yung *et al.*, 2013). Several LSDs have been modelled using iPSCs (see Table 5, on page 25). In these studies, disease-relevant cells differentiated from patient-derived iPSC lines were generated.

For those LSDs that have neuronal degeneration as an important feature of the disease, iPSCs were differentiated to neuronal progenitors or neurons to study in deep the disease, i.e. MPSIIIB (Lemonnier *et al.*, 2011), MPSIIIC (Canals *et al.*, 2015), MPSVII (Griffin *et al.*, 2015), NPC (Efthymiou *et al.*, 2015; Maetzel *et al.*, 2014b; Trilck *et al.*, 2013; Yu *et al.*, 2014b), MLD (Doerr *et al.*, 2015), CLN2 and CLN3 (Lojewski *et al.*, 2014), GM1 (Son *et al.*, 2015) and Gaucher type 2 (Panicker *et al.*, 2012; Tiscornia *et al.*, 2013).

There are some LSDs whose the main affected cells are of mesoderm origin such as cardiomyocytes and hematopoietic cells, i.e. Pompe (Huang *et al.*, 2011), Fabry (Itier *et al.*, 2014), Danon (Hashem *et al.*, 2015), MPSI (Tolar *et al.*, 2011) and Gaucher disease (Panicker *et al.*, 2012; Tiscornia *et al.*, 2013). In these cases, the iPSCs were differentiated to the affected cell types.

One of the preliminary objectives of this thesis was to obtain iPSCs from NPA and NPB patients' cells and then differentiate them to neurons in order to search for differences between type A and type B neurons, and WT neurons. These differences have been shown in the animal models or in post-mortem brain stains (Ledesma *et al.*, 2011), but the possibility to study the alterations of the neurons *in vitro* and to test treatments at different time points of the disease makes the iPSC model an appealing approach. Therefore, the use of iPSCs gives us the advantage of providing an inexhaustible source of neurons without resorting to invasive procedures.

As a preliminary experiment, we analyse the ASM activity on WT iPSCs and WT iPSCs-derived neurons to see if we were able to detect the enzyme activity in these cells. At the iPSCs step we detected low ASM activity, but in neurons the activity was higher.

Probably, WT-iPSC cells have less ASM activity compared to WT fibroblasts due to its low lysosome charge. This has been reported for other LSDs such as Sanfilippo C syndrome (Canals *et al.*, 2015). As a reduction in ASM activity in patients' fibroblasts correlated with phenotypic characteristics of the disease, the possible activity decrease in neurons may explain the differences in the neuronal traits among NPA/B patients.

We started with fibroblasts from 3 patients carrying different genotypes. Two of them, named NPAB4 and NPAB6, have been reported to be type B patients (Rodriguez-Pascau *et al.*, 2009a). NPAB4 patient bears the genotype p.R441X/p.R474W whereas genotype of the NPAB6 patient is

p.R608del/p.A482E. The third patient, NPAB2, with p.Y313X/p.Y313X genotype, has been reported to have NPD type A (Rodriguez-Pascau *et al.*, 2009a). The choice of the patients was due to sample availability and phenotype.

Retroviruses were used to introduce OCT4, SOX2, KLF4 and c-Myc (or without c-Myc) in the patient's fibroblasts. Differences in the efficacy and in the reprogramming time were observed between control and the different patients' cells, being NPAB6 (p.R608del/p.A482E) the first ones whose colonies were obtained, followed by NPAB4 (p.R441X/p.R474W). For NPAB2 (p.Y313X/p.Y313X), we did not succeed in getting colonies. So, we decided to supply the patients' fibroblasts with the lacking enzyme in order to achieve reprogramming, as described in Huang *et al.* (2011) and Lemonnier *et al.* (2011) for Pompe and MPSIIIB respectively. However, no positive results were obtained. Finally, we achieved reprogramming using acid valproic (a histone deacetylase inhibitor), which was reported to enhance the reprogramming efficiency with four factors (OSKM) in mouse fibroblasts (Huangfu *et al.*, 2008a; Huangfu *et al.*, 2008b).

The different efficiency in reprogramming may be due to the genotype. NPAB6 fibroblasts bear the p.R608del mutation, which has been reported to have a neuroprotective role and to be associated with the type B of the disease. On the contrary, NPAB2 bear the p.Y313X mutation in homozygosity and was diagnosed as type A. In our hands, the more severe p.Y313X mutation was found to produce more trouble in the reprogramming process.

In 2008, Maherali & Hochedlinge (2008) exposed several criteria to determine whether a genuine iPSC, a cell fully reprogrammed, has been achieved. These criteria include an array of features associated with pluripotency, including morphological, molecular, and functional characteristics.

Morphologically iPSCs must appear identical to ESCs and must demonstrate unlimited self-renewal. On the molecular level, iPSCs must display gene expression profiles that are indistinguishable from ESCs and other associated features, including protein-level expression of key pluripotency factors (e.g., Oct4, Nanog) and ESC-specific surface antigens (SSEA- 3/-4, Tra-1-60/-81 in human); expression of genes involved in retroviral silencing, such as Trim28. At the functional level, iPSCs should demonstrate their ability to differentiate into lineages from all three embryonic germ layers, either *in vitro* or/and teratoma formation. In addition, it should be checked that the resulting iPSCs are free from genetic aberrations and have a normal karyotype (Maherali & Hochedlinger, 2008).

However, human iPSCs/ESCs survive poorly as single cells, and initial passaging of new colonies must be done mechanically; several passages (approximately five to ten) are required before the cells can be adapted to enzymatic dissociation (Lerou *et al.*, 2008) and start doing all the validations. As each passage has to be done every 6-10 days, more than 3 months are needed from the appearance of the first iPSC colonies until the validation tests can be performed. During this period of time our laboratory underwent major mycoplasma contamination that precluded the growing of iPSCs onto matrigel matrix, and further work for several months.

Mycoplasmas are small bacteria (0.3µm in diameter) lacking a cell wall. There are several species which are known to occur in 98% of the laboratory infections of cell cultures (Nikfarjam & Farzaneh, 2012). The effects of mycoplasma infection are more insidious than those produced by

other bacteria, fungi and yeast. They may remain undetected by microscopic observation but can cause an alteration of growth rate, induction of apoptosis, morphological changes, chromosomal aberrations and alterations in the amino acid and nucleic acid metabolism (Nikfarjam & Farzaneh, 2012).

We realized that when contaminated iPSCs were on a feeder layer, they grew faster than mycoplasma-free iPSCs. Contaminated iPSCs were treated with antimycoplasma drugs. But, as iPSC colonies had a 3D formation only the most exterior layer were in-touch with the treatment and when we give them a passage mechanically, the mycoplasma that was in the inner parts of the colony spread out, giving again a positive result in mycoplasma tests. When antimycoplasma treatment, which is really aggressive with iPSCs, was used for a prolonged time no iPSCs colonies grew up after few passages.

The antimycoplasma treatment was BM-Cyclin (Appplychem). This treatment includes BM-Cyclin I containing the macrolide tiamulin for 3 days followed by BM-Cyclin II containing the tetracycline minocycline for 4 days. This alternating cycles were applied three times, for a total of 21 days of treatment. The mechanism of action of macrolides and tetracyclines is the inhibition of protein synthesis, by binding different subunits of ribosomes.

Uphoff *et al.* (2012) tested the efficiency of various mycoplasma treatments. BM-Cyclin cured 38/44 (86%) of the cell lines tested, but 3 cell lines had resistant mycoplasmas and the last 3 cell lines were killed during the treatment period.

As we did not have time to perform a new reprogramming experiment (2 months till the appearance of the first colonies) and validation tests (3 months to have the cells ready, and 3 months more to differentiate them into the three embryonic germ layers), unfortunately, we had to stop this project.

However, it would be interesting to finish all the iPSCs validation and to carry on with the neuronal differentiation to study in deep the degeneration in patients of different types of NPA/B disease. Also, it would be interesting to probe the efficiency of read-through compounds to restore enzyme activity in NPAB2 cells and NPAB4 cells at iPSC stage and neuron stage. Both patients carry a nonsense mutation in their genotype p.Y313X and p.R441X, respectively.

III. Niemann-Pick C: characterization of a mouse model

Niemann-Pick C disease and other LSDs, have naturally occurring mammalian models that may recapitulate the main features of human pathology. In the case of NPC disease, the BALB/c NPC1^{nih} mouse (Morris *et al.*, 1982) presents the very severe phenotype of the human pathology. Besides, some others cellular (Bergamin *et al.*, 2013; Efthymiou *et al.*, 2015; Rodríguez-Pascau *et al.*, 2012; Soga *et al.*, 2015; Trilck *et al.*, 2013) and mouse models have been generated (Elrick *et al.*, 2010; Maue *et al.*, 2012; Praggastis *et al.*, 2015; Sleat *et al.*, 2004; Xie *et al.*, 2011). These models have proven to be useful to improve the understanding of the cellular and molecular mechanisms underlying neurodegeneration and to test general therapies, such as substrate reduction therapy.

Some specific mutations may benefit from targeted mutation therapies, as well as the general ones. This is the case of the pseudoexon-generating mutations, usually located deep within introns, which create cryptic splice sites that are used by the splicing machinery, resulting in the aberrant inclusion of intron sequences known as “pseudoexons” in the mRNA. This kind of mutations can be targeted with antisense oligonucleotides (ASOs) that bind by complementarity to the sequence of the cryptic splice site and, thus, the aberrant splice sites will be blocked allowing the restoration of normal splicing and the generation of a wild-type protein (Kole *et al.*, 2012).

In a previous work of our group, positive results for the correction of a *NPC1* pseudoexon-generating mutation on NPC fibroblasts, using antisense morpholino oligonucleotides (AMO) were reported (Rodríguez-Pascau *et al.*, 2009b). This mutation, identified in a Spanish patient, is the c.1554-1009G>A and results in the incorporation of 194bp of the intron 9 of the *NPC1* gene in the mRNA. The same mutation was also found later in some other Spanish patients (Macías-Vidal *et al.*, 2011). Afterwards, our interest focused on the generation of a mouse model bearing this human mutation since there had not been performed *in vivo* studies to assess this kind of therapy for NPC disease.

Fortunately, a mouse bearing this mutation in heterozygosity (*Npc1*^{Imagine/+}) had been generated by OZgene on demand of the Addi and Cassi Fund (<http://addiandcassi.com/>). The knock-in mice bore the human *NPC1* intron 9 (instead of mouse intron 9) with the deep intronic mutation described above. Moreover, they had also demanded another heterozygous mouse bearing the human c.1920delG mutation (*Npc1*^{Pioneer/+}). In this case, the *NPC1* exon 12 had been modified in order to contain a stop codon in the position where translation terminates in the human *NPC1* gene bearing the c.1920delG mutation. The Addi and Cassi Fund kindly sent us these two heterozygous mice. The name of the Fund corresponds to the names of the two NPC sisters who bear the two mutations described above.

In this project we generated the two homozygous mice and fully characterized them to verify if they presented the mainly pathogenic features of the disease, with the aim to test therapy based on AMOs on the mice carrying the pseudoexon-generating mutation.

Although there are mice models commercially available, these new two mice models, *Npc1*^{Imagine} and NPC^{Pioneer}, will be useful to better understand NPC disease. Some of the existing NPC mice models are complete KO (Sleat *et al.*, 2004) and other are conditional KO (Elrick *et al.*, 2010).

Moreover, two new models with point mutations have been recently obtained (Maue *et al.*, 2012; Praggastis *et al.*, 2015). The KO mice represents the most severe form of the disease and the conditional KO or the mice with point mutations may present a late-onset form of the disease. *Npc1*^{Imagine} mice model is, to our knowledge, the first NPC and LSD mice model bearing an aberrant splicing mutation. It will be useful to study the role of alternative splicing in this disease and to test the efficiency of splicing-targeted therapy approaches. The *Npc1*^{Pioneer} mouse model could be interesting in order to investigate the effect of a deletion in the beginning of the SSD domain and its clinical effect on the disease. Both models mimic the severe form of the disease. In Figure 41 (page 73) we can see the positions of the “Imagine” and “Pioneer” mutations in the NPC1 protein.

We could not perform the behavioural phenotyping on *Npc1*^{Pioneer} model because we could not get the 12 male mice needed for the tests. The frequency of homozygous *Npc1*^{Pioneer} mice from the crossing of the heterozygous mice was much lower than expected. While in *Npc1*^{nih} mice, the homozygous mutants compromised 16-18% of the pups born (Maue *et al.*, 2012), in *Npc1*^{Pioneer} only the 3% were born. The cause of this decrease in the birth rate could be the type of the mutation. The deletion of a base pair in the exon 12 leads to a change in the reading frame and, consequently, a premature stop codon is generated two amino acids further. This deletion is located in the third transmembrane domain, at the beginning of the SSD domain. It is known that mutations affecting the SSD domain of the NPC1 protein are particularly deleterious, since they correspond to the most severe neurological form of the disease (Millat *et al.*, 2001). The SSD domain was also identified on several other proteins involved in cholesterol homeostasis and it is an important binding site between cholesterol and NPC1 (Yu *et al.*, 2014). According to our results, carrying a mutation like this in homozygosity provokes severe damage leading to death before birth or in the first days of life.

Further investigations have to be done. A good approach to study this mutation could be in heterozygosity with an allele that gives a less severe form of the disease.

The birth rate of the *Npc1*^{Imagine} homozygous mice was the same as the rate of birth of *Npc1*^{nih} mice. Thus, it was possible to gather a group of several males for the phenotyping, and perform the behavioural and molecular tests. These mice had a progressive and fast impairment that started at 6 weeks of life with a decreased body weight, tremors and ataxia leading to death before the 10 weeks of life, consistent with the late infantile onset form of the human disease. These mice were not able to perform successfully the rotarod test showing an impairment of the motor coordination and balance.

They showed some degree of anxiety when doing the elevated plus maze test, revealing an impulsive behaviour of diseased animals, and they presented hyperactivity when compared to their WT littermates during the active phase of the circadian cycle. This hyperactivity could be considered as an index of cortical dysfunction that would be a sign of impulsivity. *Npc1*^{Imagine} mice may have cortico-hippocampal deficits because of impairment in recognition memory. This memory is a cognitive domain that depends on hippocampal functional integrity. All this features are in concordance with the clinical signs of the of NPC patients.

At the molecular level, we first checked if the deep intronic mutation caused the same aberrant splicing in mice than that observed in humans (incorporation of a pseudoexon into the mRNA).

We did not know beforehand if the mouse splicing machinery would work equally. We realised that, in the mouse mRNA, the pseudoexon was also included as a consequence of the alternative splicing performed due to the presence of the mutation. However, an additional alternative splicing band was also observed and it was confirmed that it corresponded to the excision of the exon near the mutation.

In the RT-PCR transcript analysis, it was evident that cerebral cortex of *Npc1*^{Imagine} homozygous animals showed both aberrant splicing bands. This could be the reason why these mice presented a really severe form of the disease. However, in these livers, we observed both aberrant splicing bands and, also, a small amount of the WT transcript that gives the mice the opportunity to survive. A reduction of Npc1 protein was observed in the mutant mice in both tissues. However, the reduction was larger in the liver than in the cortex, which is in disagreement with our RT-PCR results.

NPC disease is mainly characterised by an impaired egress of the cholesterol from the late endosomal/lysosomal compartment but also includes multiples different classes of lipids.

Previous studies have shown that multiple cholesterol metabolites and sphingolipid species accumulate in liver and brain of the NPC-/- mouse model, and abundance of many species increases with disease progression (Fan *et al.*, 2013; Goldin *et al.*, 1992; Pentchev *et al.*, 1980; Porter *et al.*, 2010). In NPC patients' cells and animal models, cholesterol is the most abundant storage lipid in peripheral tissues, such as the liver, whereas in the brain there is accumulation of other lipids rather than cholesterol. That is the reason why we checked the accumulation of cholesterol in liver and performed a lipidomics assay in brain.

Cholesterol can be bound by the N-terminal domain of NPC1 protein (Kwon *et al.*, 2009) and previous studies demonstrated that in the mouse liver there is an increase of this lipid (Butler *et al.*, 1993). In our mouse model we observed a significant, albeit small, increase of cholesterol (1.5-fold), while other studies reach a 4-fold increase (Lloyd-Evans & Platt, 2010). A lipidomic study in liver could be useful to confirm the levels of cholesterol accumulation since it is a more precise quantification assay.

Previous studies showed an increase of sphingomyelin only in peripheral tissues and not in the brain (Vanier, 2015). Our results show that there is a significance increase of SM in the brain that could be due to an abnormal function of ASM, as seen in some NPC patients (Devlin *et al.*, 2010). SM is a phospholipid found in cell membranes and especially in the myelin sheath that surrounds nerve cell axons. A change of lipid membrane composition is thought to alter cell signalling, neuronal polarization, calcium homeostasis and immune response. Recently, SM accumulation in neurons was shown to be involved in the decrease of dendritic spines (Sabourdy *et al.*, 2015).

Historically, the first lipid abnormalities described in NPC brain were those relating to gangliosides and glycosphingolipids. In autopsy brains, GM2 and GM3 gangliosides showed a more than ten-fold increase (Vanier, 2015). Our mouse model significantly accumulates different gangliosides, such as GM1, GM2 and GM3. These gangliosides were described to accumulate in fibroblasts of patients (Watanabe *et al.*, 1998), in cellular models created by shRNA (Rodríguez-Pascau *et al.*, 2012) and by stem cells (Bergamin *et al.*, 2013) and in other mouse models (Sleat *et al.*, 2004).

A secondary accumulation of glycosphingolipids, normally present in minimal amounts, is particularly prominent in NPC, and it is also a common feature of neuropathology in a number of other lysosomal storage diseases (Vanier, 2015). Moreover, others NPC mouse models, as those generated by Praggastis *et al.* (2015) and by Maue *et al.* (2012), have the same pattern of storage in brain tissue as that previously reported in mice by Fan *et al.* including the reduction of specific sphingolipids species in brain tissues such as glucosylceramide and galactosylceramide (Fan *et al.*, 2013). This decrease may reflect demyelination that accompanies NPC disease (Ahmad *et al.*, 2005).

In addition to the biochemical analyses, histological analyses also provided evidence of abnormal lipid accumulation in the liver of *Npc1*^{Imagine} mutant mice. In our study, we clearly showed the presence of foamy cytoplasm cells and macrophages infiltration in livers of NPC mice, while these cells were not detected in WT livers. This is in agreement with the fact that in less severe forms of the disease, a progression in hepatic damage is observed along with structural alterations in all of the hepatic cell types (Vázquez *et al.*, 2011).

As future work, it would be interesting to fully characterise the compound heterozygote *Npc1*^{Imagine/Pioneer} mouse model which carries the genotype of the two siblings of the family who originated the Addi and Cassi Fund and compare the lipid accumulation pattern in brain and liver tissue with the *Npc1*^{Imagine} and the WT mice. The characterization of the compound heterozygotes is underway and the first behavioural tests are in progress.

Also, it would be interesting to use both mouse models, *Npc1*^{Imagine/Pioneer} and *Npc1*^{Imagine}, to further assess the application of the therapy based on AMOs. This therapy was proved to be efficient by Rodriguez-Pascau *et al.* (2009b) in patient fibroblasts. These new models could be useful to study the NPC disease in deep and to try on new therapeutic approaches.

CONCLUSIONS

-
- The read-through aminoglycoside drugs gentamicin and G418 showed positive results in the TNT assays for the p.W168X, p.Y313X and p.R441X mutations of the *SMPD1* gene, for the p.Y558X mutation of the *NAGLU* gene and for the p.R203X and p.W403X mutations of the *HGSNAT* gene, achieving up to 35% of read-through efficiency.
 - No positive results have been obtained with the non-aminoglycosides PTC124, RTC13, RTC14, BZ16 and BZ6 in the *in vitro* (TNT) analysis for any of the mutations studied in this thesis.
 - In the *in vitro* expression assays using transfected COS7 cells, G418 gave positive results for the p.W168X mutation of the *SMPD1* gene, gentamicin for the p.W146X mutation of the *ARSB* gene and PTC124 for all 4 studied mutations of the *ARSB* gene.
 - No positive results have been obtained with the 7 drugs tested on the two patients' fibroblasts, one of SFB and the other of SFC disease, in enzyme activity assays.
 - Increased mRNA levels (up to the wild-type level) have been recovered after G418 and RTC13 treatment on SFB patient's fibroblasts.
 - Putative cells from three different Niemann-Pick A/B patients and one healthy control have been obtained, although the validation could not be completed due to mycoplasma contamination for which iPSCs are very sensitive.
 - A mouse model, *Npc1*^{Imagine}, with the c.1554-1009G>A mutation (a splicing mutation) in homozygosity has been generated and characterized.
 - It has been proven that the humanized *Npc1*^{Imagine} model presents the same aberrant splicing process than the human patients' fibroblasts carrying the same mutation and it would be a good model to assay aberrant-splicing therapies.
 - *Npc1*^{Imagine} is a good model for Niemann-Pick C disease as it presents the main features of the disease, such as lipid accumulation, shorter lifespan and abnormal behaviour.
 - The *Npc1*^{Pioneer} mouse model bearing the c.1920delG mutation in homozygosity has been generated. However, it could not be characterized due to the very low rate of birth of the animals carrying this frameshift mutation.

BIBLIOGRAPHY

- Ahmad, I., Lope-Piedrafita, S., Bi, X., Hicks, C., Yao, Y., Yu, C., Chaitkin, E., Howison, C. M., Weberg, L., Trouard, T. P., and Erickson, R. P. (2005). Allopregnanolone treatment, both as a single injection or repetitively, delays demyelination and enhances survival of Niemann-Pick C mice. *Journal of Neuroscience Research*, 82(6), 811–821.
- Allamand, V., Bidou, L., Arakawa, M., Floquet, C., Shiozuka, M., Paturneau-Jouas, M., Gartioux, C., Butler-Browne, G. S., Mouly, V., Rousset, J.-P., Matsuda, R., Ikeda, D., and Guicheney, P. (2008). Drug-induced readthrough of premature stop codons leads to the stabilization of laminin alpha2 chain mRNA in CMD myotubes. *The Journal of Gene Medicine*, 10(2), 217–224.
- Appelqvist, H., Waster, P., Kagedal, K., Ollinger, K., Wäster, P., Kågedal, K., and Öllinger, K. (2013). The lysosome: from waste bag to potential therapeutic target. *Journal of Molecellar Cell Biology*, 5(4), 214–226.
- Arakawa, M., Shiozuka, M., Nakayama, Y., Hara, T., Hamada, M., Kondo, S., Ikeda, D., Takahashi, Y., Sawa, R., Nonomura, Y., Sheykholeslami, K., Kondo, K., Kaga, K., Kitamura, T., Suzuki-Miyagoe, Y., Takeda, S., and Matsuda, R. (2003). Negamycin restores dystrophin expression in skeletal and cardiac muscles of mdx mice. *Journal of Biochemistry*, 134(5), 751–758.
- Ballabio, A., and Gieselmann, V. (2009). Lysosomal disorders: From storage to cellular damage. *Biochimica et Biophysica Acta - Molecular Cell Research*, 1793(4), 684–696.
- Bartolomeo, R., Polishchuk, E. V., Volpi, N., Polishchuk, R. S., and Auricchio, A. (2013). Pharmacological read-through of nonsense ARSB mutations as a potential therapeutic approach for mucopolysaccharidosis VI. *Journal of Inherited Metabolic Disease*, 36(2), 363–371.
- Barton, N. W., Furbish, F. S., Murray, G. J., Garfield, M., and Brady, R. O. (1990). Therapeutic response to intravenous infusions of glucocerebrosidase in a patient with Gaucher disease. *Proceedings of the National Academy of Sciences of the United States of America*, 87(5), 1913–1916.
- Barton-Davis, E. R., Cordier, L., Shoturma, D. I., Leland, S. E., and Sweeney, H. L. (1999). Aminoglycoside antibiotics restore dystrophin function to skeletal muscles of mdx mice. *The Journal of Clinical Investigation*, 104(4), 375–381.
- Bedwell, D. M., Kaenjak, A., Benos, D. J., Bebok, Z., Bubien, J. K., Hong, J., Tousson, A., Clancy, J. P., and Sorscher, E. J. (1997). Suppression of a CFTR premature stop mutation in a bronchial epithelial cell line. *Nature Medicine*, 3(11), 1280–1284.
- Bergamin, N., Dardis, A., Beltrami, A., Cesselli, D., Rigo, S., Zampieri, S., Domenis, R., Bembi, B., and Beltrami, C. A. (2013). A human neuronal model of Niemann Pick C disease developed from stem cells isolated from patient's skin. *Orphanet Journal of Rare Diseases*, 8, 34.

- Bidou, L., Allamand, V., Rousset, J. P., and Namy, O. (2012). Sense from nonsense: therapies for premature stop codon diseases. *Trends in Molecular Medicine*, *18*(11), 679–688.
- Bidou, L., Hatin, I., Perez, N., Allamand, V., Panthier, J.-J., and Rousset, J.-P. (2004). Premature stop codons involved in muscular dystrophies show a broad spectrum of readthrough efficiencies in response to gentamicin treatment. *Gene Therapy*, *11*(7), 619–627.
- Biffi, A., Montini, E., Lorioli, L., Cesani, M., Fumagalli, F., Plati, T., Baldoli, C., Martino, S., Calabria, A., Canale, S., Benedicenti, F., Vallanti, G., Biasco, L., Leo, S., Kabbara, N., Zanetti, G., Rizzo, W. B., Mehta, N. A. L., Cicalese, M. P., Casiraghi, M., Boelens, J. J., Del Carro, U., Dow, D. J., Schmidt, M., Assanelli, A., Neduva, V., Di Serio, C., Stupka, E., Gardner, J., von Kalle, C., Bordignon, C., Ciceri, F., Rovelli, A., Roncarolo, M. G., Aiuti, A., Sessa, M., and Naldini, L. (2013). Lentiviral hematopoietic stem cell gene therapy benefits metachromatic leukodystrophy. *Science (New York, N.Y.)*, *341*(6148), 1233158.
- Bordeira-Carrico, R., Pego, A. P., Santos, M., Oliveira, C., Bordeira-Carriço, R., Pêgo, A. P., Santos, M., and Oliveira, C. (2012). Cancer syndromes and therapy by stop-codon readthrough. *Trends in Molecular Medicine*, *18*(11), 667–678.
- Boustany, R.-M. N. M. (2013). Lysosomal storage diseases--the horizon expands. *Nature Reviews. Neurology*, *9*(10), 583–598.
- Boyd, R. E., Lee, G., Rybczynski, P., Benjamin, E. R., Khanna, R., Wustman, B. A., and Valenzano, K. J. (2013). Pharmacological chaperones as therapeutics for lysosomal storage diseases. *Journal of Medicinal Chemistry*, *56*(7), 2705–2725.
- Bradbury, A. M., Gurda, B. L., Casal, M. L., Ponder, K. P., Vite, C. H., and Haskins, M. E. (2015). A review of gene therapy in canine and feline models of lysosomal storage disorders. *Human Gene Therapy. Clinical Development*, *26*(1), 27–37.
- Burke, J. F., and Mogg, A. E. (1985). Suppression of a nonsense mutation in mammalian cells in vivo by the aminoglycoside antibiotics G-418 and paromomycin. *Nucleic Acids Research*, *13*(17), 6265–6272.
- Butler, J. D., Vanier, M. T., and Pentchev, P. G. (1993). Niemann-Pick C disease: cystine and lipids accumulate in the murine model of this lysosomal cholesterol lipidosis. *Biochemical and Biophysical Research Communications*, *196*(1), 154–159.
- Canals, D., Mormeneo, D., Fabriàs, G., Llebaria, A., Casas, J., and Delgado, A. (2009). Synthesis and biological properties of Pachastrissamine (jaspine B) and diastereoisomeric jaspines. *Bioorganic & Medicinal Chemistry*, *17*(1), 235–241.
- Canals, I., Elalaoui, S. C., Pineda, M., Delgadillo, V., Szlago, M., Jaouad, I. C., Sefiani, A., Chabás, A., Coll, M. J., Grinberg, D., and Vilageliu, L. (2011). Molecular analysis of

- Sanfilippo syndrome type C in Spain: seven novel HGSNAT mutations and characterization of the mutant alleles. *Clinical Genetics*, 80(4), 367–374.
- Canals, I., Soriano, J., Orlandi, J. G., Torrent, R., Richaud-Patin, Y., Jiménez-Delgado, S., Merlin, S., Follenzi, A., Consiglio, A., Vilageliu, L., Grinberg, D., and Raya, A. (2015). Activity and High-Order Effective Connectivity Alterations in Sanfilippo C Patient-Specific Neuronal Networks. *Stem Cell Reports*.
- Clancy, J. P., Bebök, Z., Ruiz, F., King, C., Jones, J., Walker, L., Greer, H., Hong, J., Wing, L., Macaluso, M., Lyrene, R., Sorscher, E. J., and Bedwell, D. M. (2001). Evidence that systemic gentamicin suppresses premature stop mutations in patients with cystic fibrosis. *American Journal of Respiratory and Critical Care Medicine*, 163(7), 1683–1692.
- Coll, M. J., Antón, C., and Chabás, A. (2001). Allelic heterogeneity in Spanish patients with Sanfilippo disease type B. Identification of eight new mutations. *Journal of Inherited Metabolic Disease*, 24(1), 83–84.
- Cox, T., Lachmann, R., Hollak, C., Aerts, J., van Weely, S., Hrebíček, M., Platt, F., Butters, T., Dwek, R., Moyses, C., Gow, I., Elstein, D., and Zimran, A. (2000). Novel oral treatment of Gaucher's disease with N-butyldeoxynojirimycin (OGT 918) to decrease substrate biosynthesis. *Lancet*, 355(9214), 1481–1485.
- Cox-Brinkman, J., Boelens, J.J., Wraith, J. E., O'meara, A., Veys, P., Wijburg, F. A., Wulffraat, N., and Wynn, R. F. (2006). Haematopoietic cell transplantation (HCT) in combination with enzyme replacement therapy (ERT) in patients with Hurler syndrome. *Bone Marrow Transplantation*, 38(1), 17–21.
- Davidson, C. D., Ali, N. F., Micsenyi, M. C., Stephney, G., Renault, S., Dobrenis, K., Ory, D. S., Vanier, M. T., and Walkley, S. U. (2009). Chronic cyclodextrin treatment of murine Niemann-Pick C disease ameliorates neuronal cholesterol and glycosphingolipid storage and disease progression. *PLoS One*, 4(9), e6951.
- Davies, J. P., and Ioannou, Y. A. (2000). Topological analysis of Niemann-Pick C1 protein reveals that the membrane orientation of the putative sterol-sensing domain is identical to those of 3-hydroxy-3-methylglutaryl-CoA reductase and sterol regulatory element binding protein cleavage-activating. *The Journal of Biological Chemistry*, 275(32), 24367–24374.
- De Duve, C., Pressman, B. C., Gianetto, R., Wattiaux, R., and Appelmans, F., (1955). Tissue fractionation studies. 6. Intracellular distribution patterns of enzymes in rat-liver tissue. *Biochemical Journal*, 60(4), 604–617.
- Desnick, R. J., and Schuchman, E. H. (2012). Enzyme replacement therapy for lysosomal diseases: lessons from 20 years of experience and remaining challenges. *Annual Review of Genomics and Human Genetics*, 13, 307–335.

- Devlin, C., Pipalia, N. H., Liao, X., Schuchman, E. H., Maxfield, F. R., and Tabas, I. (2010). Improvement in lipid and protein trafficking in Niemann-Pick C1 cells by correction of a secondary enzyme defect. *Traffic*, *11*(5), 601–615.
- Doerr, J., Böckenhoff, A., Ewald, B., Ladewig, J., Eckhardt, M., Gieselmann, V., Matzner, U., Brüstle, O., and Koch, P. (2015). Arylsulfatase A Overexpressing Human iPSC-derived Neural Cells Reduce CNS Sulfatide Storage in a Mouse Model of Metachromatic Leukodystrophy. *Molecular Therapy: The Journal of the American Society of Gene Therapy*, *23*(9), 1519–1531.
- Du, L., Damoiseaux, R., Nahas, S., Gao, K., Hu, H., Pollard, J. M., Goldstine, J., Jung, M. E., Henning, S. M., Bertoni, C., and Gatti, R. a. (2009). Nonaminoglycoside compounds induce readthrough of nonsense mutations. *The Journal of Experimental Medicine*, *206*(10), 2285–2297.
- Du, L., Jung, M. E., Damoiseaux, R., Completo, G., Fike, F., Ku, J.-M. M., Nahas, S., Piao, C., Hu, H., and Gatti, R. a. (2013). A new series of small molecular weight compounds induce read through of all three types of nonsense mutations in the ATM gene. *Molecular Therapy*, *21*(9), 1653–1660.
- Du, M., Jones, J. R., Lanier, J., Keeling, K. M., Lindsey, J. R., Tousson, A., Bebök, Z., Whitsett, J. A., Dey, C. R., Colledge, W. H., Evans, M. J., Sorscher, E. J., and Bedwell, D. M. (2002). Aminoglycoside suppression of a premature stop mutation in a *Cftr*^{-/-} mouse carrying a human *CFTR*-G542X transgene. *Journal of Molecular Medicine*, *80*(9), 595–604.
- Efthymiou, A. G., Steiner, J., Pavan, W. J., Wincovitch, S., Larson, D. M., Porter, F. D., Rao, M. S., and Malik, N. (2015). Rescue of an in vitro neuron phenotype identified in Niemann-Pick disease, type C1 induced pluripotent stem cell-derived neurons by modulating the WNT pathway and calcium signaling. *Stem Cells Translational Medicine*, *4*(3), 230–238.
- Eisengart, J. B., Rudser, K. D., Tolar, J., Orchard, P. J., Kivisto, T., Ziegler, R. S., Whitley, C. B., and Shapiro, E. G. (2013). Enzyme replacement is associated with better cognitive outcomes after transplant in Hurler syndrome. *The Journal of Pediatrics*, *162*(2), 375–380.e1.
- Elrick, M. J., Pacheco, C. D., Yu, T., Dadgar, N., Shakkottai, V. G., Ware, C., Paulson, H. L., and Lieberman, A. P. (2010). Conditional Niemann-Pick C mice demonstrate cell autonomous Purkinje cell neurodegeneration. *Human Molecular Genetics*, *19*(5), 837–847.
- Fan, J. Q., Ishii, S., Asano, N., and Suzuki, Y. (1999). Accelerated transport and maturation of lysosomal alpha-galactosidase A in Fabry lymphoblasts by an enzyme inhibitor. *Nature Medicine*, *5*(1), 112–115.
- Fan, M., Sidhu, R., Fujiwara, H., Tortelli, B., Zhang, J., Davidson, C., Walkley, S. U., Bagel, J. H., Vite, C., Yanjanin, N. M., Porter, F. D., Schaffer, J. E., and Ory, D. S. (2013).

- Identification of Niemann-Pick C1 disease biomarkers through sphingolipid profiling. *Journal of Lipid Research*, 54(10), 2800–2814.
- Fancello, T., Dardis, A., Rosano, C., Tarugi, P., Tappino, B., Zampieri, S., Pinotti, E., Corsolini, F., Fecarotta, S., D'Amico, A., Di Rocco, M., Uziel, G., Calandra, S., Bembi, B., and Filocamo, M. (2009). Molecular analysis of NPC1 and NPC2 gene in 34 Niemann-Pick C Italian patients: identification and structural modeling of novel mutations. *Neurogenetics*, 10(3), 229–239.
- Feldhammer, M., Durand, S., Mrázová, L., Boucher, R.-M., Laframboise, R., Steinfeld, R., Wraith, J. E., Michelakakis, H., van Diggelen, O. P., Hrebíček, M., Kmoč, S., and Pshezhetsky, A. V. (2009). Sanfilippo syndrome type C: mutation spectrum in the heparan sulfate acetyl-CoA: alpha-glucosaminide N-acetyltransferase (HGSNAT) gene. *Human Mutation*, 30(6), 918–925.
- Fernández-Burriel, M., Peña, L., Ramos, J. C., Cabrera, J. C., Marti, M., Rodríguez-Quiñones, F., and Chabás, A. (2003). The R608del mutation in the acid sphingomyelinase gene (SMPD1) is the most prevalent among patients from Gran Canaria Island with Niemann-Pick disease type B. *Clinical Genetics*, 63(3), 235–236.
- Fernandez-Valero, E. M., Ballart, A., Iturriaga, C., Lluch, M., Macias, J., Vanier, M. T., Pineda, M., and Coll, M. J. (2005). Identification of 25 new mutations in 40 unrelated Spanish Niemann-Pick type C patients: genotype-phenotype correlations. *Clinical Genetics*, 68(3), 245–254.
- Floquet, C., Deforges, J., Rousset, J. P., and Bidou, L. (2011). Rescue of non-sense mutated p53 tumor suppressor gene by aminoglycosides. *Nucleic Acids Research*, 39(8), 3350–3362.
- Forge, A., and Schacht, J. (2000). Aminoglycoside antibiotics. *Audiology & Neuro-Otology*, 5(1), 3–22.
- Futerman, A. H., and van Meer, G. (2004). The cell biology of lysosomal storage disorders. *Nature Reviews Molecular Cell Biology*, 5(7), 554–565.
- Garrido, E., Chabás, A., Coll, M. J., Blanco, M., Domínguez, C., Grinberg, D., Vilageliu, L., and Cormand, B. (2007). Identification of the molecular defects in Spanish and Argentinian mucopolysaccharidosis VI (Maroteaux-Lamy syndrome) patients, including 9 novel mutations. *Molecular Genetics and Metabolism*, 92(1-2), 122–130.
- Gatti, R. a. (2012). SMRT compounds correct nonsense mutations in primary immunodeficiency and other genetic models. *Annals of the New York Academy of Sciences*, 1250(1), 33–40.
- Gelsthorpe, M. E., Baumann, N., Millard, E., Gale, S. E., Langmade, S. J., Schaffer, J. E., and Ory, D. S. (2008). Niemann-Pick type C1 I1061T mutant encodes a functional protein that is selected for endoplasmic reticulum-associated degradation due to protein misfolding. *The Journal of Biological Chemistry*, 283(13), 8229–8236.

- Goldin, E., Roff, C. F., Miller, S. P., Rodriguez-Lafrasse, C., Vanier, M. T., Brady, R. O., and Pentchev, P. G. (1992). Type C Niemann-Pick disease: a murine model of the lysosomal cholesterol lipidosis accumulates sphingosine and sphinganine in liver. *Biochimica et Biophysica Acta*, *1127*(3), 303–311.
- Gorini, L., and Kataja, E. (1964). Phenotypic repair by streptomycin of defective genotypes in *E. Coli*. *Proceedings of the National Academy of Sciences of the United States of America*, *51*, 487–493.
- Griffin, T. A., Anderson, H. C., and Wolfe, J. H. (2015). Ex vivo gene therapy using patient iPSC-derived NSCs reverses pathology in the brain of a homologous mouse model. *Stem Cell Reports*, *4*(5), 835–846.
- Grubb, J. H., Vogler, C., Levy, B., Galvin, N., Tan, Y., and Sly, W. S. (2008). Chemically modified beta-glucuronidase crosses blood-brain barrier and clears neuronal storage in murine mucopolysaccharidosis VII. *Proceedings of the National Academy of Sciences of the United States of America*, *105*(7), 2616–2621.
- Guerin, K., Gregory-Evans, C. Y., Hodges, M. D., Moosajee, M., Mackay, D. S., Gregory-Evans, K., and Flannery, J. G. (2008). Systemic aminoglycoside treatment in rodent models of retinitis pigmentosa. *Experimental Eye Research*, *87*(3), 197–207.
- Gunn, G., Dai, Y., Du, M., Belakhov, V., Kandasamy, J., Schoeb, T. R., Baasov, T., Bedwell, D. M., and Keeling, K. M. (2014). Long-term nonsense suppression therapy moderates MPS I-H disease progression. *Molecular Genetics and Metabolism*, *111*(3), 374–381.
- Hashem, S. I., Perry, C. N., Bauer, M., Han, S., Clegg, S. D., Ouyang, K., Deacon, D. C., Spinharney, M., Panopoulos, A. D., Izpisua Belmonte, J. C., Frazer, K. A., Chen, J., Gong, Q., Zhou, Z., Chi, N. C., and Adler, E. D. (2015). Brief Report: Oxidative Stress Mediates Cardiomyocyte Apoptosis in a Human Model of Danon Disease and Heart Failure. *Stem Cells (Dayton, Ohio)*, *33*(7), 2343–2350.
- Haskins, M. (2009). Gene Therapy for Lysosomal Storage Diseases (LSDs) in Large Animal Models. *ILAR Journal*, *50*(2), 112–121.
- Hein, L. K., Bawden, M., Muller, V. J., Sillence, D., Hopwood, J. J., and Brooks, D. A. (2004). alpha-L-iduronidase premature stop codons and potential read-through in mucopolysaccharidosis type I patients. *Journal of Molecular Biology*, *338*(3), 453–462.
- Hemsley, K. M., and Hopwood, J. J. (2010). Lessons learnt from animal models: Pathophysiology of neuropathic lysosomal storage disorders. *Journal of Inherited Metabolic Disease*, *33*(4), 363–371.
- Hindle, S., Hebbar, S., and Sweeney, S. T. (2011). Invertebrate models of lysosomal storage disease: what have we learned so far? *Invertebrate Neuroscience*, *11*(2), 59–71.

- Hollak, C. E. M., and Wijburg, F. A. (2014). Treatment of lysosomal storage disorders: successes and challenges. *Journal of Inherited Metabolic Disease*, 37(4), 587–598.
- Horinouchi, K., Erlich, S., Perl, D. P., Ferlinz, K., Bisgaier, C. L., Sandhoff, K., Desnick, R. J., Stewart, C. L., and Schuchman, E. H. (1995). Acid sphingomyelinase deficient mice: a model of types A and B Niemann-Pick disease. *Nature Genetics*, 10(3), 288–293.
- Horinouchi, K., Sakiyama, T., Pereira, L., Lalley, P. A., and Schuchman, E. H. (1993). Mouse models of Niemann-Pick disease: mutation analysis and chromosomal mapping rule out the type A and B forms. *Genomics*, 18(2), 450–451.
- Hrebíček, M., Mrázová, L., Seyrantepe, V., Durand, S., Roslin, N. M., Nosková, L., Hartmannová, H., Ivánek, R., Cízkova, A., Poupětová, H., Sikora, J., Urinová, J., Stranecký, V., Zeman, J., Lepage, P., Roquis, D., Verner, A., Ausseil, J., Beesley, C. E., Maire, I., Poorthuis, B. J. H. M., van de Kamp, J., van Diggelen, O. P., Wevers, R. A., Hudson, T. J., Fujiwara, T. M., Majewski, J., Morgan, K., Knoch, S., and Pshezhetsky, A. V. (2006). Mutations in TMEM76* cause mucopolysaccharidosis IIIC (Sanfilippo C syndrome). *American Journal of Human Genetics*, 79(5), 807–819.
- Huang, H.-P., Chen, P.-H., Hwu, W.-L., Chuang, C.-Y., Chien, Y.-H., Stone, L., Chien, C.-L., Li, L.-T., Chiang, S.-C., Chen, H.-F., Ho, H.-N., Chen, C.-H., and Kuo, H.-C. (2011). Human Pompe disease-induced pluripotent stem cells for pathogenesis modeling, drug testing and disease marker identification. *Human Molecular Genetics*, 20(24), 4851–4864.
- Huang, H.-P., Chuang, C.-Y., and Kuo, H.-C. (2012). Induced pluripotent stem cell technology for disease modeling and drug screening with emphasis on lysosomal storage diseases. *Stem Cell Research & Therapy*, 3(4), 34.
- Huangfu, D., Maehr, R., Guo, W., Eijkelenboom, A., Snitow, M., Chen, A. E., and Melton, D. A. (2008a). Induction of pluripotent stem cells by defined factors is greatly improved by small-molecule compounds. *Nature Biotechnology*, 26(7), 795–797.
- Huangfu, D., Osafune, K., Maehr, R., Guo, W., Eijkelenboom, A., Chen, S., Muhlestein, W., and Melton, D. A. (2008b). Induction of pluripotent stem cells from primary human fibroblasts with only Oct4 and Sox2. *Nature Biotechnology*, 26(11), 1269–1275.
- Huynh, H. T., Grubb, J. H., Vogler, C., and Sly, W. S. (2012). Biochemical evidence for superior correction of neuronal storage by chemically modified enzyme in murine mucopolysaccharidosis VII. *Proceedings of the National Academy of Sciences of the United States of America*, 109(42), 17022–17027.
- Itier, J.M., Ret, G., Viale, S., Sweet, L., Bangari, D., Caron, A., Le-Gall, F., Bénichou, B., Leonard, J., Deleuze, J.-F., and Orsini, C. (2014). Effective clearance of GL-3 in a human iPSC-derived cardiomyocyte model of Fabry disease. *Journal of Inherited Metabolic Disease*, 37(6), 1013–1022.

- James, P. D., Raut, S., Rivard, G. E., Poon, M.C., Warner, M., McKenna, S., Leggo, J., and Lillicrap, D. (2005). Aminoglycoside suppression of nonsense mutations in severe hemophilia. *Blood*, *106*(9), 3043–3048.
- Jung, M. E., Ku, J. M., Du, L., Hu, H., and Gatti, R. a. (2011). Synthesis and evaluation of compounds that induce readthrough of premature termination codons. *Bioorganic & Medicinal Chemistry Letters*, *21*(19), 5842–5848.
- Karijolic, J., and Yu, Y. T. (2014). Therapeutic suppression of premature termination codons: mechanisms and clinical considerations (review). *International Journal of Molecular Medicine*, *34*(2), 355–362.
- Kawagoe, S., Higuchi, T., Meng, X.L., Shimada, Y., Shimizu, H., Hirayama, R., Fukuda, T., Chang, H., Nakahata, T., Fukada, S., Ida, H., Kobayashi, H., Ohashi, T., and Eto, Y. (2011). Generation of induced pluripotent stem (iPS) cells derived from a murine model of Pompe disease and differentiation of Pompe-iPS cells into skeletal muscle cells. *Molecular Genetics and Metabolism*, *104*(1-2), 123–128.
- Kawagoe, S., Higuchi, T., Otaka, M., Shimada, Y., Kobayashi, H., Ida, H., Ohashi, T., Okano, H. J., Nakanishi, M., and Eto, Y. (2013). Morphological features of iPS cells generated from Fabry disease skin fibroblasts using Sendai virus vector (SeVdp). *Molecular Genetics and Metabolism*, *109*(4), 386–389.
- Kayali, R., Ku, J.M., Khitrov, G., Jung, M. E., Prikhodko, O., and Bertoni, C. (2012). Read-through compound 13 restores dystrophin expression and improves muscle function in the mdx mouse model for Duchenne muscular dystrophy. *Human Molecular Genetics*, *21*(18), 4007–4020.
- Keeling, K. M. (2001). Gentamicin-mediated suppression of Hurler syndrome stop mutations restores a low level of alpha-L-iduronidase activity and reduces lysosomal glycosaminoglycan accumulation. *Human Molecular Genetics*, *10*(3), 291–299.
- Keeling, K. M., Wang, D., Conard, S. E., and Bedwell, D. M. (2012). Suppression of premature termination codons as a therapeutic approach. *Critical Reviews in Biochemistry and Molecular Biology*, *47*(5), 444–463.
- Keeling, K. M., Wang, D., Dai, Y., Murugesan, S., Chenna, B., Clark, J., Belakhov, V., Kandasamy, J., Velu, S. E., Baasov, T., and Bedwell, D. M. (2013). Attenuation of nonsense-mediated mRNA decay enhances in vivo nonsense suppression. *PloS One*, *8*(4), e60478.
- Keeling, K. M., Xue, X., Gunn, G., and Bedwell, D. M. (2014). Therapeutics Based on Stop Codon Readthrough. *Annual Review of Genomics and Human Genetics*, 1–24.
- Klein, A. D., Alvarez, A. R., and Zanlungo, S. (2014). The Unique case of the Niemann-Pick Type C Cholesterol Storage Disorder, *Pediatric endocrinology reviews*, 166–175.

- Kole, R., Krainer, A. R., and Altman, S. (2012). RNA therapeutics: beyond RNA interference and antisense oligonucleotides. *Nature Reviews. Drug Discovery*, *11*(2), 125–140.
- Kuschal, C., DiGiovanna, J. J., Khan, S. G., Gatti, R. A., and Kraemer, K. H. (2013). Repair of UV photolesions in xeroderma pigmentosum group C cells induced by translational readthrough of premature termination codons. *Proceedings of the National Academy of Sciences of the United States of America*, *110*(48), 19483–19488.
- Kuwamura, M., Awakura, T., Shimada, A., Umemura, T., Kagota, K., Kawamura, N., and Naiki, M. (1993). Type C Niemann-Pick disease in a boxer dog. *Acta Neuropathologica*, *85*(3), 345–348.
- Kwon, H. J., Abi-Mosleh, L., Wang, M. L., Deisenhofer, J., Goldstein, J. L., Brown, M. S., and Infante, R. E. (2009). Structure of N-terminal domain of NPC1 reveals distinct subdomains for binding and transfer of cholesterol. *Cell*, *137*(7), 1213–1224.
- Lachmann, R. H., te Vruchte, D., Lloyd-Evans, E., Reinkensmeier, G., Sillence, D. J., Fernandez-Guillen, L., Dwek, R. A., Butters, T. D., Cox, T. M., and Platt, F. M. (2004). Treatment with miglustat reverses the lipid-trafficking defect in Niemann-Pick disease type C. *Neurobiol Dis*, *16*(3), 654–658.
- Lai, C.H., Chun, H. H., Nahas, S. A., Mitui, M., Gamo, K. M., Du, L., and Gatti, R. A. (2004). Correction of ATM gene function by aminoglycoside-induced read-through of premature termination codons. *Proceedings of the National Academy of Sciences of the United States of America*, *101*(44), 15676–15681.
- Ledesma, M. D., Prinetti, A., Sonnino, S., and Schuchman, E. H. (2011). Brain pathology in Niemann Pick disease type A: insights from the acid sphingomyelinase knockout mice. *Journal of Neurochemistry*, *116*(5), 779–788.
- Lee, G., Papapetrou, E. P., Kim, H., Chambers, S. M., Tomishima, M. J., Fasano, C. A., Ganat, Y. M., Menon, J., Shimizu, F., Viale, A., Tabar, V., Sadelain, M., and Studer, L. (2009). Modelling pathogenesis and treatment of familial dysautonomia using patient-specific iPSCs. *Nature*, *461*(7262), 402–406.
- Lee, H. L. R., and Dougherty, J. P. (2012). Pharmaceutical therapies to recode nonsense mutations in inherited diseases. *Pharmacology & Therapeutics*, *136*(2), 227–266.
- Lemonnier, T., Blanchard, S., Toli, D., Roy, E., Bigou, S., Froissart, R., Rouvet, I., Vitry, S., Heard, J. M., and Bohl, D. (2011). Modeling neuronal defects associated with a lysosomal disorder using patient-derived induced pluripotent stem cells. *Human Molecular Genetics*, *20*(18), 3653–3666.
- Lerou, P. H., Yabuuchi, A., Huo, H., Miller, J. D., Boyer, L. F., Schlaeger, T. M., and Daley, G. Q. (2008). Derivation and maintenance of human embryonic stem cells from poor-quality in vitro fertilization embryos. *Nature Protocols*, *3*(5), 923–933.

- Linde, L., and Kerem, B. (2008). Introducing sense into nonsense in treatments of human genetic diseases. *Trends in Genetics*, *24*(11), 552–563.
- Liu, Y., Wu, Y. P., Wada, R., Neufeld, E. B., Mullin, K. A., Howard, A. C., Pentchev, P. G., Vanier, M. T., Suzuki, K., and Proia, R. L. (2000). Alleviation of neuronal ganglioside storage does not improve the clinical course of the Niemann-Pick C disease mouse. *Human Molecular Genetics*, *9*(7), 1087–1092.
- Lloyd-Evans, E., and Platt, F. M. (2010). Lipids on trial: the search for the offending metabolite in Niemann-Pick type C disease. *Traffic*, *11*(4), 419–428.
- Lojewski, X., Staropoli, J. F., Biswas-Legrand, S., Simas, A. M., Haliw, L., Selig, M. K., Coppel, S. H., Goss, K. A., Petcherski, A., Chandrachud, U., Sheridan, S. D., Lucente, D., Sims, K. B., Gusella, J. F., Sondhi, D., Crystal, R. G., Reinhardt, P., Sternecker, J., Schöler, H., Haggarty, S. J., Storch, A., Hermann, A., and Cotman, S. L. (2014). Human iPSC models of neuronal ceroid lipofuscinosis capture distinct effects of TPP1 and CLN3 mutations on the endocytic pathway. *Human Molecular Genetics*, *23*(8), 2005–2022.
- Lowenthal, A. C., Cummings, J. F., Wenger, D. A., Thrall, M. A., Wood, P. A., and de Lahunta, A. (1990). Feline sphingolipidosis resembling Niemann-Pick disease type C. *Acta Neuropathologica*, *81*(2), 189–197.
- Lukina, E., Watman, N., Arreguin, E. A., Dragosky, M., Iastrebner, M., Rosenbaum, H., Phillips, M., Pastores, G. M., Kamath, R. S., Rosenthal, D. I., Kaper, M., Singh, T., Puga, A. C., and Peterschmitt, M. J. (2010). Improvement in hematological, visceral, and skeletal manifestations of Gaucher disease type 1 with oral eliglustat tartrate (Genz-112638) treatment: 2-year results of a phase 2 study. *Blood*, *116*(20), 4095–4098.
- Macías-Vidal, J., Rodríguez-Pascau, L., Sánchez-Ollé, G., Lluch, M., Vilageliu, L., Grinberg, D., and Coll, M. J. (2011). Molecular analysis of 30 Niemann-Pick type C patients from Spain. *Clinical Genetics*, *80*(1), 39–49.
- Maetzel, D., Sarkar, S., Wang, H., Abi-Mosleh, L., Xu, P., Cheng, A. W., Gao, Q., Mitalipova, M., and Jaenisch, R. (2014a). Genetic and chemical correction of cholesterol accumulation and impaired autophagy in hepatic and neural cells derived from niemann-pick type C patient-specific iPSC cells. *Stem Cell Reports*, *2*(6), 866–880.
- Maherali, N., and Hochedlinger, K. (2008). Guidelines and techniques for the generation of induced pluripotent stem cells. *Cell Stem Cell*, *3*(6), 595–605.
- Malik, V., Rodino-Klapac, L. R., Viollet, L., Wall, C., King, W., Al-Dahhak, R., Lewis, S., Shilling, C. J., Kota, J., Serrano-Munuera, C., Hayes, J., Mahan, J. D., Campbell, K. J., Banwell, B., Dasouki, M., Watts, V., Sivakumar, K., Bien-Willner, R., Flanigan, K. M., Sahenk, Z., Barohn, R. J., Walker, C. M., and Mendell, J. R. (2010). Gentamicin-induced readthrough of stop codons in Duchenne muscular dystrophy. *Annals of Neurology*, *67*(6), 771–780.

- Manuvakhova, M., Keeling, K., and Bedwell, D. M. (2000). Aminoglycoside antibiotics mediate context-dependent suppression of termination codons in a mammalian translation system. *RNA (New York, N.Y.)*, 6(7), 1044–1055.
- Marathe, S., Miranda, S. R., Devlin, C., Johns, A., Kuriakose, G., Williams, K. J., Schuchman, E. H., and Tabas, I. (2000). Creation of a mouse model for non-neurological (type B) Niemann-Pick disease by stable, low level expression of lysosomal sphingomyelinase in the absence of secretory sphingomyelinase: relationship between brain intra-lysosomal enzyme activity and central. *Human Molecular Genetics*, 9(13), 1967–1976.
- Matalonga, L., Arias, A., Coll, M. J., Garcia-Villoria, J., Gort, L., and Ribes, A. (2014). Treatment effect of coenzyme Q(10) and an antioxidant cocktail in fibroblasts of patients with Sanfilippo disease. *Journal of Inherited Metabolic Disease*, 37(3), 439–446.
- Matalonga, L., Arias, Á., Tort, F., Ferrer-Cortés, X., Garcia-Villoria, J., Coll, M. J., Gort, L., and Ribes, A. (2015). Effect of Readthrough Treatment in Fibroblasts of Patients Affected by Lysosomal Diseases Caused by Premature Termination Codons. *Neurotherapeutics: The Journal of the American Society for Experimental NeuroTherapeutics*.
- Mattis, V. B., Rai, R., Wang, J., Chang, C.-W. T., Coady, T., and Lorson, C. L. (2006). Novel aminoglycosides increase SMN levels in spinal muscular atrophy fibroblasts. *Human Genetics*, 120(4), 589–601.
- Maue, R. a., Burgess, R. W., Wang, B., Wooley, C. M., Seburn, K. L., Vanier, M. T., Rogers, M. a., Chang, C. C., Chang, T. Y., Harris, B. T., Graber, D. J., Penatti, C. A. a, Porter, D. M., Szwergold, B. S., Henderson, L. P., Totenhagen, J. W., Trouard, T. P., Borbon, I. a., and Erickson, R. P. (2012). A novel mouse model of Niemann-Pick type C disease carrying a D1005G-Npc1 mutation comparable to commonly observed human mutations. *Human Molecular Genetics*, 21(4), 730–750.
- McElroy, S. P., Nomura, T., Torrie, L. S., Warbrick, E., Gartner, U., Wood, G., and McLean, W. H. I. (2013). A lack of premature termination codon read-through efficacy of PTC124 (Ataluren) in a diverse array of reporter assays. *PLOS Biology*, 11(6), e1001593.
- McGovern, M. M., Wasserstein, M. P., Kirmse, B., Duvall, W. L., Schiano, T., Thurberg, B. L., Richards, S., and Cox, G. F. (2015). Novel first-dose adverse drug reactions during a phase I trial of olipudase alfa (recombinant human acid sphingomyelinase) in adults with Niemann-Pick disease type B (acid sphingomyelinase deficiency). *Genetics in Medicine : Official Journal of the American College of Medical Genetics*.
- McKay Bounford, K., and Gissen, P. (2014). Genetic and laboratory diagnostic approach in Niemann Pick disease type C. *Journal of Neurology*, 261 Suppl (S2), S569–75.

- Medina, D. L., Fraldi, A., Bouche, V., Annunziata, F., Mansueto, G., Spampanato, C., Puri, C., Pignata, A., Martina, J. A., Sardiello, M., Palmieri, M., Polishchuk, R., Puertollano, R., and Ballabio, A. (2011). Transcriptional activation of lysosomal exocytosis promotes cellular clearance. *Developmental Cell*, *21*(3), 421–430.
- Meng, X.L. L., Shen, J.S. S., Kawagoe, S., Ohashi, T., Brady, R. O., and Eto, Y. (2010). Induced pluripotent stem cells derived from mouse models of lysosomal storage disorders. *Proc Natl Acad Sci U S A*, *107*(17), 7886–7891.
- Millat, G., Marçais, C., Rafi, M. A., Yamamoto, T., Morris, J. A., Pentchev, P. G., Ohno, K., Wenger, D. A., and Vanier, M. T. (1999). Niemann-Pick C1 disease: the I1061T substitution is a frequent mutant allele in patients of Western European descent and correlates with a classic juvenile phenotype. *American Journal of Human Genetics*, *65*(5), 1321–1329.
- Millat, G., Marçais, C., Tomasetto, C., Chikh, K., Fensom, A. H., Harzer, K., Wenger, D. A., Ohno, K., and Vanier, M. T. (2001). Niemann-Pick C1 disease: correlations between NPC1 mutations, levels of NPC1 protein, and phenotypes emphasize the functional significance of the putative sterol-sensing domain and of the cysteine-rich luminal loop. *American Journal of Human Genetics*, *68*(6), 1373–1385.
- Miller, J. N., Kovács, A. D., and Pearce, D. A. (2015). The novel Cln1(R151X) mouse model of infantile neuronal ceroid lipofuscinosis (INCL) for testing nonsense suppression therapy. *Human Molecular Genetics*, *24*(1), 185–196.
- Miranda, S. R., He, X., Simonaro, C. M., Gatt, S., Dagan, A., Desnick, R. J., and Schuchman, E. H. (2000a). Infusion of recombinant human acid sphingomyelinase into niemann-pick disease mice leads to visceral, but not neurological, correction of the pathophysiology. *FASEB Journal : Official Publication of the Federation of American Societies for Experimental Biology*, *14*(13), 1988–1995.
- Miranda, S. R., Erlich, S., Friedrich, V. L., Gatt, S., and Schuchman, E. H. (2000b). Hematopoietic stem cell gene therapy leads to marked visceral organ improvements and a delayed onset of neurological abnormalities in the acid sphingomyelinase deficient mouse model of Niemann-Pick disease. *Gene Therapy*, *7*(20), 1768–1776.
- Miyawaki, S., Mitsuoka, S., Sakiyama, T., and Kitagawa, T. (1982). Sphingomyelinosis, a new mutation in the mouse: A model of Niemann-Pick disease in humans. *Journal of Heredity*, *73*(4), 257–263.
- Miyawaki, S., Yoshida, H., Mitsuoka, S., Enomoto, H., and Ikehara, S. (1986). A mouse model for Niemann-Pick disease. Influence of genetic background on disease expression in spm/spm mice. *Journal of Heredity*, *77*(6), 379–384.
- Morris, M. D., Bhuvaneshwaran, C., Shio, H., and Fowler, S. (1982). Lysosome lipid storage disorder in NCTR-BALB/c mice. I. Description of the disease and genetics. *The American Journal of Pathology*, *108*(2), 140–149.

- Mort, M., Ivanov, D., Cooper, D. N., and Chuzhanova, N. A. (2008). A meta-analysis of nonsense mutations causing human genetic disease. *Human Mutation*, 29(8), 1037–1047.
- Nagai, J., and Takano, M. (2004). Molecular aspects of renal handling of aminoglycosides and strategies for preventing the nephrotoxicity. *Drug Metabolism and Pharmacokinetics*, 19(3), 159–170.
- Nakamura, K., Du, L., Tunuguntla, R., Fike, F., Cavalieri, S., Morio, T., Mizutani, S., Brusco, A., and Gatti, R. A. (2012). Functional characterization and targeted correction of ATM mutations identified in Japanese patients with ataxia-telangiectasia. *Human Mutation*, 33(1), 198–208.
- Nikfarjam, L., and Farzaneh, P. (2012). Prevention and detection of mycoplasma contamination in cell culture. *Cell Journal*, 13(4), 203–212.
- Nudelman, I., Glikin, D., Smolkin, B., Hainrichson, M., Belakhov, V., and Baasov, T. (2010). Repairing faulty genes by aminoglycosides: development of new derivatives of geneticin (G418) with enhanced suppression of diseases-causing nonsense mutations. *Bioorganic & Medicinal Chemistry Letters*, 18(11), 3735–3746.
- Nudelman, I., Rebibo-Sabbah, A., Cherniavsky, M., Belakhov, V., Hainrichson, M., Chen, F., Schacht, J., Pilch, D. S., Ben-Yosef, T., and Baasov, T. (2009). Development of novel aminoglycoside (NB54) with reduced toxicity and enhanced suppression of disease-causing premature stop mutations. *Journal of medicinal chemistry*, 52(9), 2836–2845.
- Nudelman, I., Rebibo-Sabbah, A., Shallom-Shezifi, D., Hainrichson, M., Stahl, I., Ben-Yosef, T., and Baasov, T. (2006). Redesign of aminoglycosides for treatment of human genetic diseases caused by premature stop mutations. *Bioorganic & Medicinal Chemistry Letters*, 16(24), 6310–6315.
- Ogawa, Y., Tanaka, M., Tanabe, M., Suzuki, T., Togawa, T., Fukushige, T., Kanekura, T., Sakuraba, H., and Oishi, K. (2013). Impaired neural differentiation of induced pluripotent stem cells generated from a mouse model of Sandhoff disease. *PLoS One*, 8(1), e55856.
- Ortolano, S., Viéitez, I., Navarro, C., Spuch, C., Vieitez, I., Navarro, C., and Spuch, C. (2014). Treatment of lysosomal storage diseases: recent patents and future strategies. *Recent Patents on Endocrine, Metabolic and Immune Drug Discovery*, 8(1), 9–25.
- Otterbach, B., and Stoffel, W. (1995). Acid sphingomyelinase-deficient mice mimic the neurovisceral form of human lysosomal storage disease (Niemann-Pick disease). *Cell*, 81(7), 1053–1061.
- Ouesleti, S., Brunel, V., Ben Turkia, H., Dranguet, H., Miled, A., Miladi, N., Ben Dridi, M. F., Lavoine, A., Saugier-Veber, P., and Bekri, S. (2011). Molecular characterization of MPS IIIA, MPS IIIB and MPS IIIC in Tunisian patients. *Clinica Chimica Acta; International Journal of Clinical Chemistry*, 412(23-24), 2326–2331.

- Panicker, L. M., Miller, D., Park, T. S., Patel, B., Azevedo, J. L., Awad, O., Masood, M. A., Veenstra, T. D., Goldin, E., Stubblefield, B. K., Tayebi, N., Polumuri, S. K., Vogel, S. N., Sidransky, E., Zambidis, E. T., and Feldman, R. A. (2012). Induced pluripotent stem cell model recapitulates pathologic hallmarks of Gaucher disease. *Proceedings of the National Academy of Sciences of the United States of America*, 109(44), 18054–18059.
- Parenti, G., Andria, G., and Ballabio, A. (2015). Lysosomal Storage Diseases : From Pathophysiology to Therapy. *Annual Review of Medicine*, 66, 471–486.
- Park, I.-H., Arora, N., Huo, H., Maherali, N., Ahfeldt, T., Shimamura, A., Lensch, M. W., Cowan, C., Hochedlinger, K., and Daley, G. Q. (2008). Disease-specific induced pluripotent stem cells. *Cell*, 134(5), 877–886.
- Pastores, G. M. (2010). Therapeutic approaches for lysosomal storage diseases. *Therapeutic Advances in Endocrinology and Metabolism*, 1(4), 177–188.
- Pastores, G. M., Torres, P. a, and Zeng, B.-J. (2013). Animal models for lysosomal storage disorders. *Biochemistry. Biokhimiia*, 78(7), 721–725.
- Patterson, M. C., Mengel, E., Vanier, M. T., Schwierin, B., Muller, A., Cornelisse, P., and Pineda, M. (2015). Stable or improved neurological manifestations during miglustat therapy in patients from the international disease registry for Niemann-Pick disease type C: an observational cohort study. *Orphanet Journal of Rare Diseases*, 10(1), 65.
- Patterson, M. C., Vecchio, D., Jacklin, E., Abel, L., Chadha-Boreham, H., Luzy, C., Giorgino, R., and Wraith, J. E. (2010). Long-term miglustat therapy in children with Niemann-Pick disease type C. *Journal of Child Neurology*, 25(3), 300–305.
- Peltz, S. W., Morsy, M., Welch, E. M., and Jacobson, A. (2013). Ataluren as an agent for therapeutic nonsense suppression. *Annual Review of Medicine*, 64, 407–425.
- Pentchev, P. G., Gal, A. E., Booth, A. D., Omodeo-Sale, F., Fouks, J., Neumeyer, B. A., Quirk, J. M., Dawson, G., and Brady, R. O. (1980). A lysosomal storage disorder in mice characterized by a dual deficiency of sphingomyelinase and glucocerebrosidase. *Biochimica et Biophysica Acta*, 619(3), 669–679.
- Pineda, M., Wraith, J. E., Mengel, E., Sedel, F., Hwu, W. L., Rohrbach, M., Bembi, B., Walterfang, M., Korenke, G. C., Marquardt, T., Luzy, C., Giorgino, R., and Patterson, M. C. (2009). Miglustat in patients with Niemann-Pick disease Type C (NP-C): a multicenter observational retrospective cohort study. *Molecular Genetics and Metabolism*, 98(3), 243–249.
- Piotrowska, E., Jakóbkiewicz-Banecka, J., Tylki-Szymanska, A., Liberek, A., Maryniak, A., Malinowska, M., Czartoryska, B., Puk, E., Kloska, A., Liberek, T., Baranska, S., Wegrzyn, A., and Wegrzyn, G. (2008). Genistin-rich soy isoflavone extract in substrate reduction therapy for Sanfilippo syndrome: An open-label, pilot study in 10 pediatric patients. *Current Therapeutic Research, Clinical and Experimental*, 69(2), 166–179.

- Platt, F. M., Boland, B., and van der Spoel, A. C. (2012). Lysosomal storage disorders: The cellular impact of lysosomal dysfunction. *Journal of Cell Biology*, 199(5), 723–734.
- Politano, L., Nigro, G., Nigro, V., Piluso, G., Papparella, S., Paciello, O., and Comi, L. I. (2003). Gentamicin administration in Duchenne patients with premature stop codon. Preliminary results. *Acta Myologica: Myopathies and Cardiomyopathies: Official Journal of the Mediterranean Society of Myology / Edited by the Gaetano Conte Academy for the Study of Striated Muscle Diseases*, 22(1), 15–21.
- Porter, F. D., Scherrer, D. E., Lanier, M. H., Langmade, S. J., Molugu, V., Gale, S. E., Olzeski, D., Sidhu, R., Dietzen, D. J., Fu, R., Wassif, C. A., Yanjanin, N. M., Marso, S. P., House, J., Vite, C., Schaffer, J. E., and Ory, D. S. (2010). Cholesterol oxidation products are sensitive and specific blood-based biomarkers for Niemann-Pick C1 disease. *Science Translational Medicine*, 2(56), 56ra81.
- Porto, C., Cardone, M., Fontana, F., Rossi, B., Tuzzi, M. R., Tarallo, A., Barone, M. V., Andria, G., and Parenti, G. (2009). The pharmacological chaperone N-butyldeoxynojirimycin enhances enzyme replacement therapy in Pompe disease fibroblasts. *Molecular Therapy: The Journal of the American Society of Gene Therapy*, 17(6), 964–971.
- Porto, C., Pisani, A., Rosa, M., Acampora, E., Avolio, V., Tuzzi, M. R., Visciano, B., Gagliardo, C., Materazzi, S., la Marca, G., Andria, G., and Parenti, G. (2012). Synergy between the pharmacological chaperone 1-deoxygalactonojirimycin and the human recombinant alpha-galactosidase A in cultured fibroblasts from patients with Fabry disease. *Journal of Inherited Metabolic Disease*, 35(3), 513–520.
- Praggastis, M., Tortelli, B., Zhang, J., Fujiwara, H., Sidhu, R., Chacko, a., Chen, Z., Chung, C., Lieberman, a. P., Sikora, J., Davidson, C., Walkley, S. U., Pipalia, N. H., Maxfield, F. R., Schaffer, J. E., and Ory, D. S. (2015). A Murine Niemann-Pick C1 I1061T Knock-In Model Recapitulates the Pathological Features of the Most Prevalent Human Disease Allele. *Journal of Neuroscience*, 35(21), 8091–8106.
- Raya, A., Rodríguez-Pizà, I., Guenechea, G., Vassena, R., Navarro, S., Barrero, M. J., Consiglio, A., Castellà, M., Río, P., Sleep, E., González, F., Tiscornia, G., Garreta, E., Aasen, T., Veiga, A., Verma, I. M., Surrallés, J., Bueren, J., and Izpisua Belmonte, J. C. (2009). Disease-corrected haematopoietic progenitors from Fanconi anaemia induced pluripotent stem cells. *Nature*, 460(7251), 53–59.
- Ribeiro, I., Marcão, A., Amaral, O., Sá Miranda, M. C., Vanier, M. T., and Millat, G. (2001). Niemann-Pick type C disease: NPC1 mutations associated with severe and mild cellular cholesterol trafficking alterations. *Human Genetics*, 109(1), 24–32.
- Ringe, D., and Petsko, G. A. (2009). What are pharmacological chaperones and why are they interesting? *Journal of Biology*, 8(9), 80.
- Robinton, D. a., and Daley, G. Q. (2012). The promise of induced pluripotent stem cells in research and therapy. *Nature*, 481(7381), 295–305.

- Rodríguez-Pascau, L., Coll, M. J., Casas, J., Vilageliu, L., and Grinberg, D. (2012). Generation of a human neuronal stable cell model for niemann-pick C disease by RNA interference. *JIMD Reports*, 4, 29–37.
- Rodríguez-Pascau, L., Gort, L., Schuchman, E. H., Vilageliu, L., Grinberg, D., Chabas, A., Rodríguez-Pascau, L., Gort, L., Schuchman, E. H., Vilageliu, L., Grinberg, D., and Chabás, A. (2009a). Identification and characterization of SMPD1 mutations causing Niemann-Pick types A and B in Spanish patients. *Human Mutation*, 30(7), 1117–1122.
- Rodríguez-Pascau, L., Coll, M. J., Vilageliu, L., Grinberg, D., Rodríguez-Pascau, L., Coll, M. J., Vilageliu, L., and Grinberg, D. (2009b). Antisense oligonucleotide treatment for a pseudoexon-generating mutation in the NPC1 gene causing Niemann-Pick type C disease. *Human Mutation*, 30(11), E993–E1001.
- Ruijter, G. J. G., Valstar, M. J., van de Kamp, J. M., van der Helm, R. M., Durand, S., van Diggelen, O. P., Wevers, R. A., Poorthuis, B. J., Pshezhetsky, A. V, and Wijburg, F. A. (2008). Clinical and genetic spectrum of Sanfilippo type C (MPS IIIC) disease in The Netherlands. *Molecular Genetics and Metabolism*, 93(2), 104–111.
- Ryan, N. J. (2014). Ataluren: First Global Approval. *Drugs*, 74(14), 1709–1714.
- Sabourdy, F., Astudillo, L., Colacios, C., Dubot, P., Mrad, M., Ségui, B., Andrieu-Abadie, N., Levade, T., Segui, B., Andrieu-Abadie, N., Levade, T., Ségui, B., Andrieu-Abadie, N., and Levade, T. (2015). Monogenic neurological disorders of sphingolipid metabolism. *Biochimica et Biophysica Acta (BBA) - Molecular and Cell Biology of Lipids*, 1851(8), 1040–1051.
- Samie, M. A., and Xu, H. (2014). Lysosomal exocytosis and lipid storage disorders. *Journal of Lipid Research*, 55(6), 995–1009.
- Sanchez-Alcudia, R., Perez, B., Ugarte, M., Desviat, L. R., Sánchez-Alcudia, R., Pérez, B., Ugarte, M., and Desviat, L. R. (2012). Feasibility of nonsense mutation readthrough as a novel therapeutical approach in propionic acidemia. *Human Mutation*, 33(6), 973–980.
- Sangkuhl, K., Schulz, A., Römler, H., Yun, J., Wess, J., and Schöneberg, T. (2004). Aminoglycoside-mediated rescue of a disease-causing nonsense mutation in the V2 vasopressin receptor gene in vitro and in vivo. *Human Molecular Genetics*, 13(9), 893–903.
- Santra, Saikat; Ramaswami, U. (2015). Lysosomal disorders. *Paediatrics and Child Health*, 25(3), 123–132.
- Schiffmann, R., Fitzgibbon, E. J., Harris, C., DeVile, C., Davies, E. H., Abel, L., van Schaik, I. N., Benko, W., Timmons, M., Ries, M., and Vellodi, A. (2008). Randomized, controlled trial of miglustat in Gaucher's disease type 3. *Annals of Neurology*, 64(5), 514–522.

- Schuchman, E. H. (1995). Two new mutations in the acid sphingomyelinase gene causing type a Niemann-pick disease: N389T and R441X. *Human Mutation*, 6(4), 352–354.
- Schuchman, E. H. (2010). Acid sphingomyelinase, cell membranes and human disease: lessons from Niemann-Pick disease. *FEBS Letters*, 584(9), 1895–1900.
- Schultz, M. L., Tecedor, L., Chang, M., and Davidson, B. L. (2011). Clarifying lysosomal storage diseases. *Trends in Neurosciences*, 34(8), 401–410.
- Segatori, L. (2014). Impairment of homeostasis in lysosomal storage disorders. *IUBMB Life*, 66(7), 472–477.
- Seki, T., and Fukuda, K. (2015). Methods of induced pluripotent stem cells for clinical application. *World Journal of Stem Cells*, 7(1), 116–125.
- Shaner, R. L., Allegood, J. C., Park, H., Wang, E., Kelly, S., Haynes, C. A., Sullards, M. C., and Merrill, A. H. (2009). Quantitative analysis of sphingolipids for lipidomics using triple quadrupole and quadrupole linear ion trap mass spectrometers. *Journal of Lipid Research*, 50(8), 1692–1707.
- Singh, V. K., Kalsan, M., Kumar, N., Saini, A., and Chandra, R. (2015). Induced pluripotent stem cells: applications in regenerative medicine, disease modeling, and drug discovery. *Frontiers in Cell and Developmental Biology*, 1–18.
- Sleat, D. E., Sohar, I., Gin, R. M., and Lobel, P. (2001). Aminoglycoside-mediated suppression of nonsense mutations in late infantile neuronal ceroid lipofuscinosis. *European Journal of Paediatric Neurology: EJPN: Official Journal of the European Paediatric Neurology Society*, 5 Suppl A, 57–62.
- Sleat, D. E., Wiseman, J. A., El-Banna, M., Price, S. M., Verot, L., Shen, M. M., Tint, G. S., Vanier, M. T., Walkley, S. U., and Lobel, P. (2004). Genetic evidence for nonredundant functional cooperativity between NPC1 and NPC2 in lipid transport. *Proceedings of the National Academy of Sciences of the United States of America*, 101(16), 5886–5891.
- Smid, B. E., Aerts, J. M. F. G., Boot, R. G., Linthorst, G. E., and Hollak, C. E. M. (2010). Pharmacological small molecules for the treatment of lysosomal storage disorders. *Expert Opin Investig Drugs*, 19(11), 1367–1379.
- Soga, M., Ishitsuka, Y., Hamasaki, M., Yoneda, K., Furuya, H., Matsuo, M., Ihn, H., Fuskai, N., Nakamura, K., Nakagata, N., Endo, F., Irie, T., and Era, T. (2015). HPGCD Outperforms HPBCD as a Potential Treatment for Niemann-Pick Disease Type C During Disease Modeling with iPS Cells. *Stem Cells*, 1075–1088.
- Son, M.-Y., Kwak, J. E., Seol, B., Lee, D. Y., Jeon, H., and Cho, Y. S. (2015). A novel human model of the neurodegenerative disease GM1 gangliosidosis using induced pluripotent stem cells demonstrates inflammasome activation. *The Journal of Pathology*, 237(1), 98–110.

- Stein, V. M., Crooks, A., Ding, W., Prociuk, M., O'Donnell, P., Bryan, C., Sikora, T., Dingemans, J., Vanier, M. T., Walkley, S. U., and Vite, C. H. (2012). Miglustat improves purkinje cell survival and alters microglial phenotype in feline Niemann-Pick disease type C. *Journal of Neuropathology and Experimental Neurology*, 71(5), 434–448.
- Suzuki, Y., Ogawa, S., and Sakakibara, Y. (2009). Chaperone therapy for neuronopathic lysosomal diseases: competitive inhibitors as chemical chaperones for enhancement of mutant enzyme activities. *Perspectives in Medicinal Chemistry*, 3, 7–19.
- Takahashi, K., Tanabe, K., Ohnuki, M., Narita, M., Ichisaka, T., Tomoda, K., and Yamanaka, S. (2007). Induction of pluripotent stem cells from adult human fibroblasts by defined factors. *Cell*, 131(5), 861–872.
- Takahashi, K., and Yamanaka, S. (2006). Induction of pluripotent stem cells from mouse embryonic and adult fibroblast cultures by defined factors. *Cell*, 126(4), 663–76.
- Tiscornia, G., Vivas, E. L., Izpisua Belmonte, J. C., and Belmonte, J. C. I. (2011). Diseases in a dish: modeling human genetic disorders using induced pluripotent cells. *Nature Medicine*, 17(12), 1570–1576.
- Tiscornia, G., Vivas, E. L., Matalonga, L., Berniakovich, I., Barragán Monasterio, M., Eguizábal, C., Gort, L., González, F., Ortiz Mellet, C., García Fernández, J. M., Ribes, A., Veiga, A., and Izpisua Belmonte, J. C. (2013). Neuronopathic Gaucher's disease: induced pluripotent stem cells for disease modelling and testing chaperone activity of small compounds. *Human Molecular Genetics*, 22(4), 633–45.
- Tolar, J., Park, I. H., Xia, L., Lees, C. J., Peacock, B., Webber, B., McElmurry, R. T., Eide, C. R., Orchard, P. J., Kyba, M., Osborn, M. J., Lund, T. C., Wagner, J. E., Daley, G. Q., and Blazar, B. R. (2011). Hematopoietic differentiation of induced pluripotent stem cells from patients with mucopolysaccharidosis type I (Hurler syndrome). *Blood*, 117(3), 839–847.
- Trilck, M., Hübner, R., Seibler, P., Klein, C., Rolfs, A., and Frech, M. J. (2013). Niemann-Pick type C1 patient-specific induced pluripotent stem cells display disease specific hallmarks. *Orphanet Journal of Rare Diseases*, 8, 144.
- Uphoff, C. C., Denkmann, S.-A., and Drexler, H. G. (2012). Treatment of mycoplasma contamination in cell cultures with Plasmocin. *Journal of Biomedicine & Biotechnology*, 267678.
- Vance, J. E., and Karten, B. (2014). Niemann-Pick C disease and mobilization of lysosomal cholesterol by cyclodextrin. *The Journal of Lipid Research*, 55(8), 1609–1621.
- Vanier, M. T. (1999). Lipid changes in Niemann-Pick disease type C brain: personal experience and review of the literature. *Neurochemical Research*, 24(4), 481–489.

- Vanier, M. T. (2010). Niemann-Pick disease type C. *Orphanet Journal of Rare Diseases*, 5, 16.
- Vanier, M. T. *Niemann-Pick diseases* in Handbook of Clinical Neurology (eds O. Dulac, M. Lasseonde. and H.B. Sarnat), 1717-1721, (Elsevier B.V., 2013).
- Vanier, M. T. (2015). Complex lipid trafficking in Niemann-Pick disease type C. *Journal of Inherited Metabolic Disease*, 38(1), 187–199.
- Vanier, M. T., Ferlinz, K., Rousson, R., Duthel, S., Louisot, P., Sandhoff, K., and Suzuki, K. (1993). Deletion of arginine (608) in acid sphingomyelinase is the prevalent mutation among Niemann-Pick disease type B patients from northern Africa. *Human Genetics*, 92(4), 325–330.
- Vanier, M. T., and Latour, P. (2015). Laboratory diagnosis of Niemann-Pick disease type C: the filipin staining test. *Methods in Cell Biology*, 126, 357–375.
- Vanier, M. T. and Patterson, M. C. *Niemann-Pick Disease Type C*, in Lysosomal Storage Disorders: A Practical Guide (eds A. Mehta and B. Winchester), 87–93, (John Wiley & Sons, Ltd, 2013).
- Vázquez, M. C., del Pozo, T., Robledo, F. a., Carrasco, G., Pavez, L., Olivares, F., González, M., Zanlungo, S., Vazquez, M. C., del Pozo, T., Robledo, F. a., Carrasco, G., Pavez, L., Olivares, F., Gonzalez, M., and Zanlungo, S. (2011). Alteration of gene expression profile in Niemann-Pick type C mice correlates with tissue damage and oxidative stress. *PLoS One*, 6(12), e28777.
- Villani, G. R., Balzano, N., Vitale, D., Saviano, M., Pavone, V., and Di Natale, P. (1999). Maroteaux-lamy syndrome: five novel mutations and their structural localization. *Biochimica et Biophysica Acta*, 1453(2), 185–192.
- Voskoboeva, E. I., Krasnopol'skaia, K. D., Peters, K., and von Figura, K. (2000). [Identification of mutations in the arylsulfatase B gene in Russian mucopolysaccharidosis type VI patients]. *Genetika*, 36(6), 837–843.
- Voskoboeva, E., Isbrandt, D., von Figura, K., Krasnopolskaya, X., and Peters, C. (1994). Four novel mutant alleles of the arylsulfatase B gene in two patients with intermediate form of mucopolysaccharidosis VI (Maroteaux-Lamy syndrome). *Human Genetics*, 93(3), 259–264.
- Wang, D., Belakhov, V., Kandasamy, J., Baasov, T., Li, S. C., Li, Y. T., Bedwell, D. M., and Keeling, K. M. (2012). The designer aminoglycoside NB84 significantly reduces glycosaminoglycan accumulation associated with MPS I-H in the Idua-W392X mouse. *Mol Genet Metab*, 105(1), 116–125.
- Watanabe, Y., Akaboshi, S., Ishida, G., Takeshima, T., Yano, T., Taniguchi, M., Ohno, K., and Nakashima, K. (1998). Increased levels of GM2 ganglioside in fibroblasts from a

- patient with juvenile Niemann-Pick disease type C. *Brain & Development*, 20(2), 95–97.
- Weintraub, H., Abramovici, A., Sandbank, U., Pentchev, P. G., Brady, R. O., Sekine, M., Suzuki, A., and Sela, B. (1985). Neurological mutation characterized by dysmyelination in NCTR-Balb/C mouse with lysosomal lipid storage disease. *Journal of Neurochemistry*, 45(3), 665–672.
- Welch, E. M., Barton, E. R., Zhuo, J., Tomizawa, Y., Friesen, W. J., Trifillis, P., Paushkin, S., Patel, M., Trotta, C. R., Hwang, S., Wilde, R. G., Karp, G., Takasugi, J., Chen, G., Jones, S., Ren, H., Moon, Y.-C. C., Corson, D., Turpoff, A. a, Campbell, J. a, Conn, M. M., Khan, A., Almstead, N. G., Hedrick, J., Mollin, A., Risher, N., Weetall, M., Yeh, S., Branstrom, A. a, Colacino, J. M., Babiak, J., Ju, W. D., Hirawat, S., Northcutt, V. J., Miller, L. L., Spatrack, P., He, F., Kawana, M., Feng, H., Jacobson, A., Peltz, S. W., and Sweeney, H. L. (2007). PTC124 targets genetic disorders caused by nonsense mutations. *Nature*, 447(7140), 87–91.
- Wilschanski, M., Yahav, Y., Yaacov, Y., Blau, H., Bentur, L., Rivlin, J., Aviram, M., Bdolah-Abram, T., Bebok, Z., Shushi, L., Kerem, B., and Kerem, E. (2003). Gentamicin-induced correction of CFTR function in patients with cystic fibrosis and CFTR stop mutations. *The New England Journal of Medicine*, 349(15), 1433–1441.
- Winchester, B. *Classification of Lysosomal Storage Diseases*, in *Lysosomal Storage Disorders: A Practical Guide* (eds A. Mehta and B. Winchester), 37–46, (John Wiley & Sons, Ltd, 2013).
- Winter, J. C. F. De. (2013). Using the Student 's t-test with extremely small sample sizes. *Practcial Assessment, Research & Evalutaion*, 18(10), 1–12.
- Wraith, J. E., Vecchio, D., Jacklin, E., Abel, L., Chadha-Boreham, H., Luzy, C., Giorgino, R., and Patterson, M. C. (2010). Miglustat in adult and juvenile patients with Niemann-Pick disease type C: Long-term data from a clinical trial. *Molecular Genetics and Metabolism*, 99(4), 351–357.
- Xie, C., Turley, S. D., and Dietschy, J. M. (1999). Cholesterol accumulation in tissues of the Niemann-pick type C mouse is determined by the rate of lipoprotein-cholesterol uptake through the coated-pit pathway in each organ. *Proceedings of the National Academy of Sciences of the United States of America*, 96(21), 11992–11997.
- Xie, X., Brown, M. S., Shelton, J. M., Richardson, J. A., Goldstein, J. L., and Liang, G. (2011). Amino acid substitution in NPC1 that abolishes cholesterol binding reproduces phenotype of complete NPC1 deficiency in mice. *Proceedings of the National Academy of Sciences of the United States of America*, 108(37), 15330–15335.
- Xu, Y.-H., Quinn, B., Witte, D., and Grabowski, G. A. (2003). Viable mouse models of acid beta-glucosidase deficiency: the defect in Gaucher disease. *The American Journal of Pathology*, 163(5), 2093–2101.

- Yang, C., Feng, J., Song, W., Wang, J., Tsai, B., Zhang, Y., Scaringe, W. A., Hill, K. A., Margaritis, P., High, K. A., and Sommer, S. S. (2007). A mouse model for nonsense mutation bypass therapy shows a dramatic multiday response to geneticin. *Proceedings of the National Academy of Sciences of the United States of America*, *104*(39), 15394–15399.
- Yu, D., Swaroop, M., Wang, M., Baxa, U., Yang, R., Yan, Y., Coksaygan, T., DeTolla, L., Marugan, J. J., Austin, C. P., McKew, J. C., Gong, D.-W., and Zheng, W. (2014). Niemann-Pick Disease Type C: Induced Pluripotent Stem Cell-Derived Neuronal Cells for Modeling Neural Disease and Evaluating Drug Efficacy. *Journal of Biomolecular Screening*, *19*(8), 1164–1173.
- Yu, X.H. H., Jiang, N., Yao, P.B. B., Zheng, X.L. L., Cayabyab, F. S., and Tang, C.K. K. (2014). NPC1, intracellular cholesterol trafficking and atherosclerosis. *Clinica Chimica Acta; International Journal of Clinical Chemistry*, *429*, 69–75.
- Yung, J. S.Y., Tam, P. K.H., and Ngan, E. S.-W. (2013). Pluripotent stem cell for modeling neurological diseases. *Experimental Cell Research*, *319*(2), 177–184.
- Zervas, M., Somers, K. L., Thrall, M. A., and Walkley, S. U. (2001). Critical role for glycosphingolipids in Niemann-Pick disease type C. *Current Biology*, *11*(16), 1283–1287.
- Zigdon, H., Meshcheriakova, A., and Futerman, A. H. (2014). From sheep to mice to cells: Tools for the study of the sphingolipidoses. *Biochimica et Biophysica Acta*, *1841*(8), 1189–1199.
- Zilberberg, A., Lahav, L., and Rosin-Arbesfeld, R. (2010). Restoration of APC gene function in colorectal cancer cells by aminoglycoside- and macrolide-induced read-through of premature termination codons. *Gut*, *59*(4), 496–507.

ANNEX

RESEARCH ARTICLE

Evaluation of Aminoglycoside and Non-Aminoglycoside Compounds for Stop-Codon Readthrough Therapy in Four Lysosomal Storage Diseases

Marta Gómez-Grau¹, Elena Garrido^{1*}, Mónica Cozar¹, Víctor Rodríguez-Sureda², Carmen Domínguez², Concepción Arenas³, Richard A. Gatti⁴, Bru Cormand¹, Daniel Grinberg^{1‡*}, Lluís Vilagellu^{1‡}

1 Departament de Genètica, Facultat de Biologia, Universitat de Barcelona, IBUB, CIBERER, Barcelona, Spain, **2** CIBBIM–Nanomedicina, Vall d'Hebron Institut de Recerca (VHIR), CIBERER, Hospital Universitari Vall d'Hebron, Barcelona, Spain, **3** Departament d'Estadística, Facultat de Biologia, Universitat de Barcelona, Barcelona, Spain, **4** David Geffen/UCLA School of Medicine, Departments of Pathology & Laboratory Medicine, and Human Genetics, Los Angeles, United States of America

‡ Current address: National Cancer Research Center (CNIO), Madrid, Spain

‡ These authors are co-last authors on this work.

* dgrinberg@ub.edu



CrossMark
click for updates

 OPEN ACCESS

Citation: Gómez-Grau M, Garrido E, Cozar M, Rodríguez-Sureda V, Domínguez C, Arenas C, et al. (2015) Evaluation of Aminoglycoside and Non-Aminoglycoside Compounds for Stop-Codon Readthrough Therapy in Four Lysosomal Storage Diseases. PLoS ONE 10(8): e0135873. doi:10.1371/journal.pone.0135873

Editor: Andrea Dardis, University Hospital S. Maria della Misericordia, Udine, ITALY

Received: March 9, 2015

Accepted: July 27, 2015

Published: August 19, 2015

Copyright: © 2015 Gómez-Grau et al. This is an open access article distributed under the terms of the [Creative Commons Attribution License](https://creativecommons.org/licenses/by/4.0/), which permits unrestricted use, distribution, and reproduction in any medium, provided the original author and source are credited.

Data Availability Statement: All relevant data are within the paper.

Funding: This study was partially funded by grants from the Spanish Ministry of Science and Innovation (SAF2010-17589, SAF2011-25431) and from the Catalan Government (2009SGR971), and by financial support from 'patient-support' associations, such as Jonah's Just Begun-Foundation to Cure Sanfilippo Inc. (USA), Association Sanfilippo Sud (France), Fundación Stop Sanfilippo (Spain), Asociación MPS España (Spain), APRAT (A-T, France), and A-T Ease

Abstract

Nonsense mutations are quite prevalent in inherited diseases. Readthrough drugs could provide a therapeutic option for any disease caused by this type of mutation. Geneticin (G418) and gentamicin were among the first to be described. Novel compounds have been generated, but only a few have shown improved results. PTC124 is the only compound to have reached clinical trials. Here we first investigated the readthrough effects of gentamicin on fibroblasts from one patient with Sanfilippo B, one with Sanfilippo C, and one with Maroteaux-Lamy. We found that ARSB activity (Maroteaux-Lamy case) resulted in an increase of 2–3 folds and that the amount of this enzyme within the lysosomes was also increased, after treatment. Since the other two cases (Sanfilippo B and Sanfilippo C) did not respond to gentamicin, the treatments were extended with the use of geneticin and five non-aminoglycoside (PTC124, RTC13, RTC14, BZ6 and BZ16) readthrough compounds (RTCs). No recovery was observed at the enzyme activity level. However, mRNA recovery was observed in both cases, nearly a two-fold increase for Sanfilippo B fibroblasts with G418 and around 1.5 fold increase for Sanfilippo C cells with RTC14 and PTC124. Afterwards, some of the products were assessed through *in vitro* analyses for seven mutations in genes responsible for those diseases and, also, for Niemann-Pick A/B. Using the coupled transcription/translation system (TNT), the best results were obtained for SMPD1 mutations with G418, reaching a 35% recovery at 0.25 µg/ml, for the p.W168X mutation. The use of COS cells transfected with mutant cDNAs gave positive results for most of the mutations with some of the drugs, although to a different extent. The higher enzyme activity recovery, of around two-fold increase, was found for gentamicin on the ARSB p.W146X mutation. Our results are promising and consistent with those of other groups. Further studies of novel

(A-T, New York, USA). RAG was partially supported by a Sponsored Research Grant for readthrough drug development from BioMarin. MGG was supported by a grant from the University of Barcelona (APIF).

Competing Interests: The authors have declared that no competing interests exist.

compounds are necessary to find those with more consistent efficacy and fewer toxic effects.

Introduction

Lysosomal storage disorders (LSDs) are a group of more than 50 genetic disorders caused by the lack of degradation of substrates within lysosomes. Most are caused by mutations in genes coding for lysosomal hydrolases. The main symptoms are bone and/or joint disease, mental retardation and/or developmental delay and visceromegalia. Lysosomal storage disorders are mainly inherited in an autosomal recessive manner, but in a few cases they are X-linked [1].

Mutations causing LSDs include missense and nonsense changes, splicing mutations, deletions, insertions, etc. Nonsense mutations can be corrected by drugs that produce the readthrough of the premature termination codon (PTC) (reviewed in Ref. [2–3]). In the present work we studied the correction of nonsense mutations in fibroblasts from patients with three LSDs: Sanfilippo syndrome types B and C, and Maroteaux-Lamy syndrome. Moreover, we also performed in vitro corrections for other mutations in the genes responsible for these diseases and, also, in the *SMPDI* gene that causes Niemann-Pick A/B disease.

Sanfilippo syndrome or mucopolysaccharidosis III (MPS III) has four subtypes (A: OMIM 252900, B: OMIM 252920, C: OMIM 252930 and D: OMIM 252940), due to mutations in four genes that result in the inability to degrade the glycosaminoglycan heparan sulfate [4]. Clinically, the four subtypes are similar, with severe central nervous system (CNS) degeneration, accompanied by mild somatic manifestations. Mucopolysaccharidosis type IIIB is characterized by deficiency in *N*-acetyl- α -glucosaminidase (Naglu, EC: 3.2.1.50) activity, which leads to lysosomal accumulation of the glycosaminoglycan (GAG) heparan sulfate (HS). The enzyme is encoded by the *NAGLU* gene (NCBI RefSeq NM_000263.4), which maps to chromosome 17 and has six exons. Mucopolysaccharidosis type IIIC is due to mutations in the *HGSNAT* gene (NCBI RefSeq NM_152419.2), which encodes acetyl-CoA: α -glucosaminide *N*-acetyltransferase (EC 2.3.1.78). The gene, located on chromosome 8p11.1, contains 18 exons [5,6]. The enzyme catalyzes acetylation of the terminal glucosamine residues of heparan sulfate prior to its hydrolysis by α -*N*-acetyl glucosaminidase [7].

Maroteaux-Lamy syndrome, or mucopolysaccharidosis (MPS) VI (OMIM 253200), is caused by impaired activity of the lysosomal enzyme *N*-acetylgalactosamine-4-sulfatase (4-sulfatase, arylsulfatase B or ARSB, EC 3.1.6.1) [4], resulting from mutations in the *ARSB* gene (NCBI RefSeq NM_00046.3). The enzyme deficiency leads to the accumulation of harmful amounts of undegraded dermatan sulfate. Symptoms include short stature, hepatosplenomegaly, dysostosis multiplex, joint stiffness, corneal clouding, cardiac abnormalities and coarse facies, without intellectual impairment.

Niemann-Pick disease (NPD) type A/B is an autosomal recessive sphingolipidosis caused by lysosomal acid sphingomyelinase (ASM, E.C. 3.1.4.12) deficiency. Type A (OMIM 257200) is a fatal infantile neurovisceral form and type B (OMIM 607616) presents a purely visceral form and survival till adulthood [8]. The acid sphingomyelinase gene (*SMPDI*; NCBI RefSeq NM_000543.4) is composed of six exons and is located on chromosome 11p15.1–11p15.4 [8].

The use of drugs that produce a readthrough of premature stop codons could be used for nonsense mutations mainly in diseases with neurological symptoms for which enzyme replacement therapy is not an option. An advantage of this strategy is that, if successful, it can be applied to any disease, provided that the molecular cause is a primary nonsense mutation (i.e.,

in which the PTC results directly from a point mutation in the DNA) [9]. In the case of neurological lysosomal storage diseases, additional advantages are the potential penetrance through the blood brain barrier, the fact that a small increase in enzyme activity is sufficient to correct the phenotype and that the approach implies an oral, non-invasive, therapy. The most extensively studied approach involves readthrough by drugs affecting the ribosomal decoding site.

In recent years, several research groups have tried to use aminoglycoside antibiotics to suppress stop codons in cells from patients bearing nonsense mutations. Positive results of treatment with gentamicin in cell culture experiments were first reported for cystic fibrosis [10]. The efficacy of this approach in vivo was first demonstrated in mdx mice using subcutaneous injection of gentamicin [11]. Since then, different aminoglycoside antibiotics have been shown to suppress premature translation termination at nonsense codons, with efficacies varying from 1% to 25% in human cell lines and animal models [12,13]. In the case of lysosomal disorders, this treatment has been assayed in human fibroblasts and animal models for some diseases [2,14–19].

Although gentamicin and geneticin have been extendedly used for this purpose, other aminoglycoside and non-aminoglycoside compounds such as amikacin [20], kanamycin B analogues [21], zidovudine, adefovir, cisplatin [22], RTC13 and 14 [23] and derivatives [24], NB54 [25] and NB84 [17] have also been tested.

High-throughput screens identified PTC124 (a.k.a. as Ataluren (Translarna), trade name of PTC Therapeutics) [26], which is a small organic molecule with no antibiotic properties that can promote readthrough of disease-causing PTCs and does not affect termination at stop codons located at the end of coding sequences. Unlike aminoglycosides, PTC124 has no serious adverse side effects. Therefore, it has great potential for treating genetic diseases. PTC124 probably functions at a different location on the ribosome than aminoglycosides, because it is part of a distinct structural class of drugs. This compound has been used in several assays for different diseases with positive effects [27–30], although negative results have also been reported [31–33]. Clinical trials of this drug are underway for patients with cystic fibrosis (phase III), Duchenne muscular dystrophy (DMD) (phase II), and other diseases [34]. A phase III study for DMD and other diseases started in 2014 (NCT02090959). Very recently, Gregory-Evans et al. [35] showed the reversion of aniridia in a mouse model of the disease through treatment with a topical application of the drug formulation named START, which contains 1% powdered Ataluren.

Readthrough efficiency inversely correlates with translation-termination efficiency, and may be influenced by different factors including the identity of the PTC and its context. It has been reported that the three stop codons are not equally susceptible to readthrough and this can vary from one species to another. In eukaryotes, the UGA stop codon is more amenable to readthrough than UAG, which is followed by UAA [36,37]. In addition, the sequence context in which the stop codon lies plays an important role in readthrough efficiency, particularly the nucleotide in position +4 [38]. However, the impact of the +4 nucleotide is also affected by its surrounding context [38].

One of the mechanisms that specifically regulates the level of PTC-bearing transcripts is nonsense-mediated decay (NMD), a quality-control process that detects and degrades such transcripts to prevent the synthesis of unstable proteins that might be deleterious for the cell. PTC readthrough compounds may increase the stability of mutant RNA by limiting NMD. In fact, several papers have reported that gentamicin and other readthrough agents inhibit NMD and thereby increase the amount of PTC-containing RNAs [39,40].

In this study, we first investigated the readthrough effects of gentamicin on fibroblasts from one patient with Sanfilippo B, one with Sanfilippo C, and one with Maroteaux-Lamy. Geneticin and five non-aminoglycoside (PTC124, RTC13, RTC14, BZ6 and BZ16) readthrough

compounds (RTCs) were also assayed for the two cases that did not respond to gentamicin. Additionally, different products were tested on seven mutations for which fibroblasts were not available using the coupled transcription/translation system (TNT) and COS cells transfected with cDNA bearing nonsense mutations. We obtained positive results for some drugs and mutations, encouraging us to continue with research on this therapeutic strategy.

Material and Methods

Mutations and patients' fibroblasts

The primary nonsense mutations analysed in this study are listed in Table 1. They all were identified in previous studies [6,41–49]. Several of them were found in Spanish patients.

Fibroblasts from a Spanish MPSVI patient (patient ML4, genotype p.W322X/c.427delG) [41], from a Spanish SFB patient (patient SFB1, genotype p.W168X/p.Q566X, named P5 in Matalonga et al. [43]), and from a French SFC patient (patient SFC13, genotype p.R384X/c.1542+4dupA) [50], were available and were used in some of the experiments.

The three *SMPD1* mutations were found in Spanish Niemann-Pick patients [46]. The other four mutations were obtained from the literature.

Ethics statement

The Bioethics Committee of the Universitat de Barcelona released a favourable bioethical statement regarding the present research. Patients were encoded to protect their confidentiality and written informed consent was obtained.

Culture and treatment of patients' fibroblasts

Fibroblasts were cultured in DMEM supplemented with 10% FBS and 1% penicillin/streptomycin (Gibco) at 37°C and 5% CO₂, in six-well plates, except for the NAGLU activity measurements, for which 100 mm plates were used.

Table 1. Studied nonsense mutations.

Gene	Disease	Mutation		Exon ¹	Stop codon ²	References
		c.DNA	Protein			
FIBROBLASTS						
<i>ARSB</i>	Maroteaux-Lamy	c.966G>A	p.W322X	5 (8)	(G) <u>UGA</u> (G)	[41]
<i>NAGLU</i>	Sanfilippo B	c.503G>A	p.W168X	2 (6)	(C) <u>UAG</u> (A)	[42]
		c.1696C>T	p.Q566X	6 (6)	(G) <u>UAG</u> (G)	[43]
<i>HGSNAT</i>	Sanfilippo C	c.1150C>T	p.R384X	12 (18)	(U) <u>UGA</u> (G)	[6]
cDNAs						
<i>ARSB</i>	Maroteaux-Lamy	c.438G>A	p.W146X	2 (8)	(A) <u>UGA</u> (C)	[44]
		c.1507C>T	p.Q503X	8 (8)	(A) <u>UAG</u> (U)	[45]
<i>SMPD1</i>	Niemann-Pick A/B	c.503G>A	p.W168X	2 (6)	(C) <u>UAG</u> (G)	[46]
		c.939C>A	p.Y313X	2 (6)	(G) <u>UAA</u> (C)	[46]
		c.1321C>T	p.R441X	4 (6)	(C) <u>UGA</u> (A)	[47]
<i>HGSNAT</i>	Sanfilippo C	c.607C>T	p.R203X	6 (18)	(U) <u>UGA</u> (G)	[48]
		c.1209G>A	p.W403X	12 (18)	(G) <u>UGA</u> (C)	[49]

¹Exon bearing the nonsense mutation (total number of exons of the corresponding gene)

²In brackets, note the nucleotides immediately 5' or 3' to the stop codon. Point mutation resulting in PTC is underlined.

For the readthrough experiments, gentamicin (300–700 $\mu\text{g/ml}$), G418 (75 $\mu\text{g/ml}$), PTC124 (20 μM), RTC13, RTC14, BZ6 and BZ16 (30 μM) were added to the medium without antibiotics. Fresh media and drugs were replaced every 24 h and cells were harvested after 3–4 days of treatment, at which point mRNA was quantified and enzyme activities were analysed. Three replicates were assayed for each condition.

For the indirect immunofluorescence studies of 4-sulfatase, WT fibroblasts and fibroblasts from the MPS VI patient ML4 [41] were grown on coverslips in 12-well plates and fixed after 6 days of treatment with increasing concentrations of gentamicin (500, 1000 and 1500 $\mu\text{g/ml}$). Anti-human ARSB and Lamp-2 (a marker of lysosomes and late endosomes) antibodies were used, as in Garrido et al. [51]. Briefly, the primary antibodies used to label the lysosomes were a sheep antibody against 4-sulfatase and the mouse anti-human Lamp-2 monoclonal antibody H4B4 (Developmental Studies Hybridoma Bank, University of Iowa, Department of Biological Sciences, Iowa City, IA, USA). The secondary antibodies were a donkey FITC anti-sheep IgG (Jackson ImmunoResearch Laboratories, Inc., West Grove, PA, USA) and goat AlexaFluor 660 antimouse IgG from Molecular Probes (Invitrogen). Images were captured with an Olympus Fluoview FV300 confocal microscope and analysed with Fluoview FV500 image software. Experiments were repeated at least three times to ensure reproducibility. Autofluorescence and secondary antibody control tests were performed.

Enzyme assays

Protein concentration was determined by the Lowry method. The activity measurements were performed in duplicate (at least) in all cases. The activity of another lysosomal enzyme (β -hexosaminidase) was measured as a control (data not shown).

Acid sphingomyelinase and acetyl-CoA: α -glucosaminide N-acetyltransferase activities were analysed using the fluorogenic substrates 6-hexadecanoylamino-4-methylumbelliferyl-phosphorylcholine and 4-methylumbelliferyl- β -D-glucosaminide (Moscerdam Substrates, Oegstgeest, The Netherlands), respectively. Measurements were performed in a Modulus Microplate Multimode Reader (Turner Biosystems, Sunnyvale, CA, USA), following the manufacturer's instructions. The 4-sulfatase activity was determined by spectrophotometric quantification of p-nitrocatechol (absorbance at 515 nm) produced by hydrolysis of the substrate p-nitrocatechol sulfate dipotassium salt (Sigma-Aldrich, St. Louis, USA).

For the α -N-acetylglucosaminidase assay, 20 μl of 200 mM sodium acetate buffer, pH 4.3, was combined with 40 μl of the fluorogenic substrate 4-methylumbelliferyl-2-acetamido-2-deoxy- α -D-glucopyranoside (Calbiochem, Merck, Darmstadt, Germany) 2 mM, and 20 μl of cell lysate was added. The mixture was incubated for 2 hours at 37°C and the reaction was stopped with 1 ml of glycine buffer 100 mM pH 10.4. Measurements were performed in a fluorometer (excitation 365 nm, emission 450 nm).

mRNA quantification

The levels of *HGSNAT* and *NAGLU* transcripts in patients' fibroblasts were analysed by qRT-PCR in a LightCycler 480 instrument (Roche Applied Sciences, Indianapolis, IN, USA). For RNA isolation, cultured patients' fibroblasts were harvested and RNA was obtained using a High Pure RNA Isolation Kit (Roche Applied Sciences), following the manufacturer's recommendations. Concentrations were determined using the NanoDrop ND-1000 spectrophotometer (NanoDrop Technologies, Wilmington, DE, USA). RNA samples were stored at -80°C until analysis. The RNA obtained was retrotranscribed using a High-Capacity cDNA Archive Kit (Applied Biosystems, Foster City, CA) and real time-PCR was performed using the LightCycler 480 II system and the Universal Probe Library (Roche Applied Science). Gene assays

were designed using Universal ProbeLibrary Assay Design Center software (Roche Applied Science). Sequence of primers and probes used are available upon request. Human-specific Taqman Gene Expression assays for *SDHA* (*succinate dehydrogenase complex*, *Hs00417200_m1*) and *HPR1* (*hypoxanthine phosphoribosyltransferase 1*, *Hs99999909_m1*) (the latter not shown) genes were used as endogenous controls to normalise the relative amounts of mRNA. These genes were selected because they were stably expressed under the experimental conditions. The Roche LightCycler 480 software was used to performed advanced relative quantification analysis of gene expression, according to the LightCycler 480 instrument operator's manual.

Nonsense-mediated RNA decay

For nonsense-mediated mRNA decay experiments, fibroblasts from SFB and SFC patients were seeded on six-well plates and cultured in the absence or presence of 1 mg/ml of cycloheximide (CHX) for 6 h. Cycloheximide, an inhibitor of protein synthesis, is one of the typical compounds used to assay for the occurrence of NMD. Total RNA was isolated and retrotranscribed as described above. A specific PCR amplification was performed to obtain fragments including mutations p.W168X (*NAGLU*) or p.R384X (*HGSNAT*), which were digested by restriction enzymes *BmpI* and *XhoI*, respectively, and the fragments were then separated by electrophoresis. Quantification of the relative intensity of the electrophoretic bands was performed using IMAGE LAB5.1 Analysis Software (Bio-Rad, Hercules, CA, USA). Amplification of the *GAPDH* cDNA was used as a control.

Site-directed mutagenesis

The nonsense mutations were introduced in the wild type full-length cDNA of the corresponding gene cloned in the pcDNA3.1 expression vector by PCR-based site-directed mutagenesis using the QuikChange II XL Site-Directed Mutagenesis Kit (Stratagene Cloning Systems, La Jolla, CA, USA), according to the manufacturer's instructions. All constructs were resequenced to ensure that no spurious mutations had been introduced.

Readthrough drugs and coupled transcription/translation assay

The TNT Quick Coupled Transcription/Translation System (Promega, Madison, WI, USA) was used for *in vitro* protein synthesis, as described by Sánchez-Alcudia et al. [32]. To assay the effect of the readthrough drugs, a range of different concentrations of G418 (0.25–10 µg/ml; Gibco, Carlsbad, CA, USA), gentamicin (2.5–20 µg/ml; Gibco), PTC124 (1.5–10 µM; Excenon Pharmatech Co., Ltd, Guangzhou City, China), RTC13 (10–40 µM) and RTC14 (10–40 µM) [23], BZ6 (10–40 µM) and BZ16 (10–40 µM) [24,52,53] were added to the coupled TNT reaction. Mutation *SMPDI* (p.Y313X) was used to choose the best concentrations for each product. Readthrough efficiency was calculated as the amount of full-length protein produced relative to the sum of the truncated protein plus the full-length protein, expressed as percentages.

COS7 cell culture and transfection

COS7 cells were a gift from the URFOA group at the Institut Hospital del Mar de Investigacions Mèdiques (IMIM), which were originally obtained from ATCC (CRL-1651). They were cultured in DMEM supplemented with 10% FBS and 1% penicillin/streptomycin (Gibco) at 37°C and 5% CO₂. For transfection with the cDNAs, COS7 cells were seeded on six-well plates. When the cells were at 80–90% confluence, 1 µg of the plasmid bearing either the wild type or the mutant cDNA (corresponding to the genes *ARSB*, *SMPDI* or *HGSNAT*) was introduced using lipofectamine 2000 (Invitrogen, Life Technologies, Paisley, UK), following the

manufacturer's instructions. As a negative control, the pcDNA3.1 empty vector was transfected. Different concentrations of G418 (50–100 µg/ml), gentamicin (500–1000 µg/ml) and PTC124 (20–60 µM) were added 4 h post-transfection. Fresh media and drugs were replaced every 24 h. Cells were harvested 48 h after treatment for *ARSB* and *SMPD1* and 72 h after treatment for *HGSNAT*, and centrifuged. The pellets were washed twice with PBS and stored at -80°C until enzyme activity analyses were performed. Two independent transfection experiments were performed for each mutation (together with the wild type construct and the negative control). The residual enzyme activity of the mutant alleles was analysed as described above. Results were expressed as a percentage of the mean activity of the wild-type construct transfected in the same experiment. The activity of the negative control was subtracted.

Statistical analyses

Statistical analyses were performed using the Student's t-test. It should be noted that this test was recently validated for extremely small sample sizes [54]. A p-value < 0.05 was predetermined as significant.

Results

Readthrough treatment of patients' fibroblasts

After 96 hours of treatment with gentamicin, ARSB activity in patient ML4 fibroblasts (bearing the p.W322X mutation) was twice (226%) to three times (282%) that of untreated fibroblasts in the 400 and 700 µg/ml conditions, respectively (Fig 1). When we compared treated to untreated cells, significant differences were only found between cells treated with gentamicin 700 µg/ml and untreated cells ($p = 0.031$). The enzyme activity achieved corresponds to 1–4% of that found in wild-type fibroblasts [41]. Also, fibroblasts of this patient were studied to detect the localisation of the mutant ARSB protein by immunofluorescence labelling. As shown in Fig 2, the amount of protein and the co-localisation with the lysosomal marker (LAMP2) was diminished in the patient compared with the WT fibroblasts. Both parameters were partially recovered by exposure to 1000 and 1500 µg/ml of gentamicin.

Fibroblasts from the Sanfilippo B and C patients showed no increase in enzyme activity upon gentamicin treatment. Thus six other readthrough compounds (G418, PTC124, RTC13, RTC14, BZ6 and BZ16) were assayed at different concentrations, but none of them led to positive recovery of enzyme activity.

In fibroblasts from these two patients, mRNA levels (of the *NAGLU* and *HGSNAT* gene, respectively) were quantified after treatment with the seven compounds mentioned above (Fig 3). Note that in these experiments the concentration of gentamicin was lower than that used for the experiments shown in Figs 1 and 2, to facilitate comparisons with results by other authors (for example, reference [32]). Treatment of Sanfilippo B fibroblasts with G418 yielded an almost two-fold increase in mRNA levels ($p = 0.025$; Fig 3A). For Sanfilippo C cells, RTC14 and PTC124 gave the best results (1.6 and 1.5-fold increase, respectively, although only the former reached significance, $p = 0.037$) (Fig 3A). When compared with WT, they reached 45–50% (Sanfilippo C, treated with PTC124 or RTC14) to 75–90% (Sanfilippo B, treated with RTC13 or G418, respectively) of WT levels (Fig 3B). The treatment of Sanfilippo B cells with RTC13 or G418 gave results that did not significantly differ from those of WT ($p = 0.086$ and $p = 0.330$, respectively). It would have been interesting to assess the level of translation of these mRNAs, but the lack of appropriate antibodies and the technical problems we had with those that were available precluded obtaining data on this issue.

To test whether the stop codon mutations could cause a decrease in mRNA levels through the nonsense-mediated decay mechanism, fibroblasts were grown in the presence of

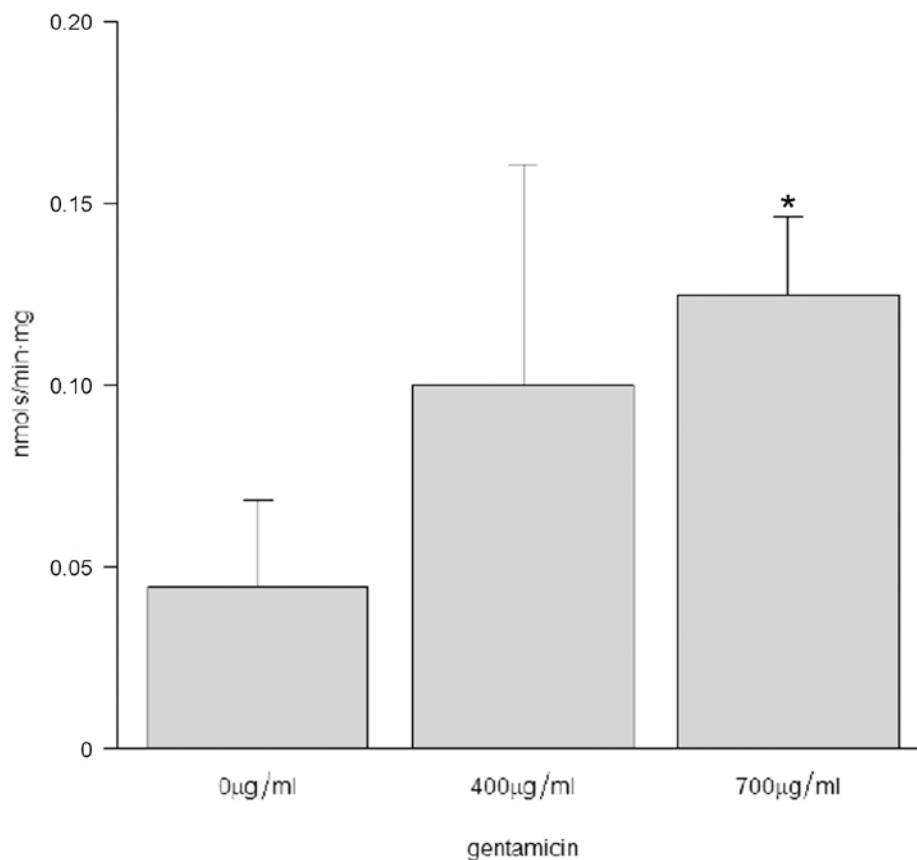


Fig 1. Effect of gentamicin treatment on ARSB activity in fibroblasts. Fibroblasts from a MPSVI patient with genotype W322X/c.427delG were treated for 96 hours at the indicated concentration. Each experiment is an average of three replicates. * $p < 0.05$, compared to 0 µg/ml (untreated).

doi:10.1371/journal.pone.0135873.g001

cycloheximide, and RT-PCR was performed. As shown in Fig 4, a significant increase in the mRNA levels of the allele bearing the stop mutation *NAGLU* p.W168X (Fig 4A and 4B) was observed after CHX treatment. For the *HGSNAT* p.R384X allele, a clear increase was also observed, with borderline significance ($p = 0.07$) (Fig 4D). The allele bearing the *NAGLU* Q566X mutation (Fig 4A and 4B) did not show any significant increase, as expected, since it lies in the last exon of the gene.

In vitro readthrough

For mutations for which fibroblasts were not available, we tested the effect of the seven different products using a mammalian-coupled TNT assay of cDNAs bearing these nonsense mutations. In the absence of treatment, truncated proteins of the expected size for each of the mutations were synthesised. Recovery of the full-length protein was observed for some of the mutants with G418 (geneticin) or gentamicin (Fig 5), while no recovery was observed with PTC124, RTC13, RTC14, BZ6 and BZ16 (not shown). In particular, for the three *SMPDI* mutations, clear recovery was observed with G418 treatment at different concentrations, while gentamicin had a lower effect on mutations p.W168X and p.Y313X and no effect on p.R441X

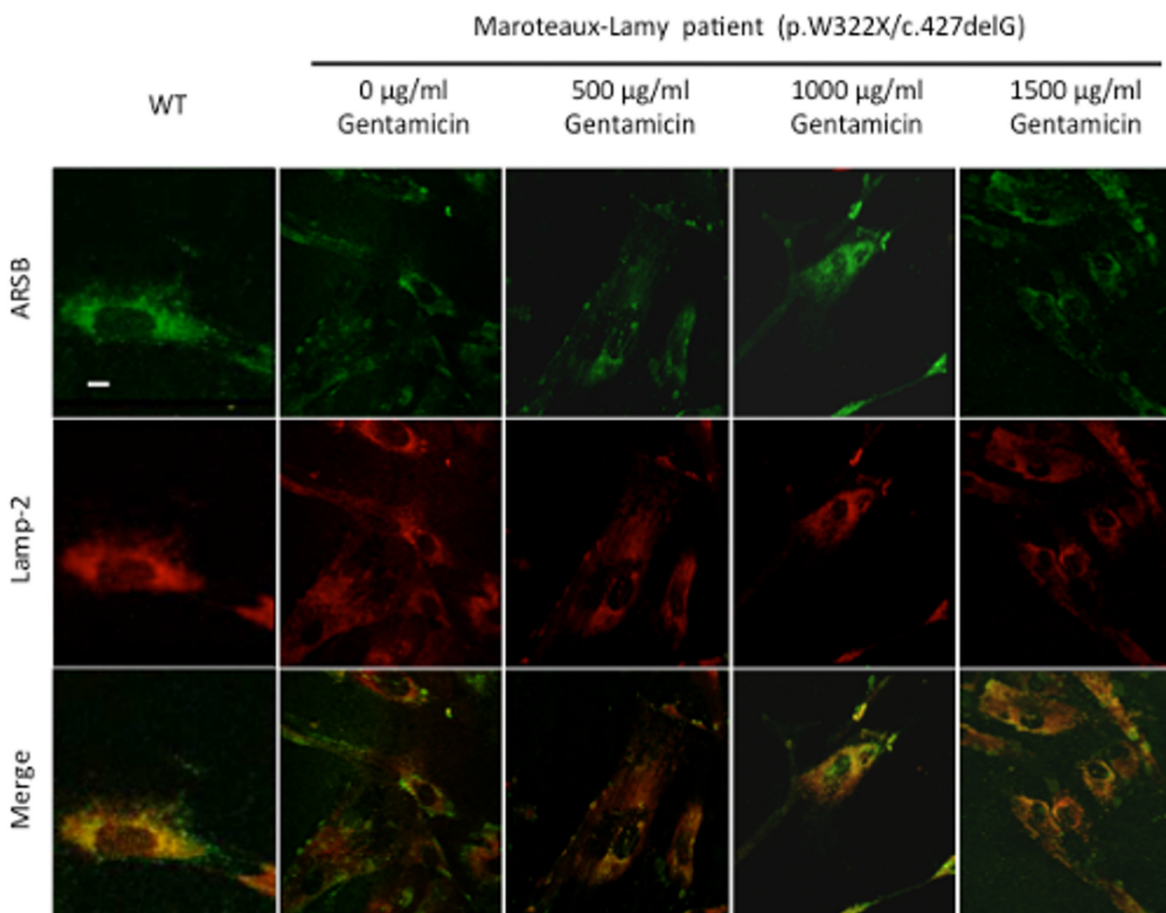


Fig 2. Confocal microscopy analysis of fibroblasts treated with gentamicin. Subcellular localization of the ARSB protein by indirect immunofluorescence in WT fibroblasts and in those from the MPSVI patient with genotype W322X/c.427delG. Fibroblasts were treated with the indicated gentamicin concentrations. ARSB protein was detected using a FITC-conjugated secondary antibody (green). Co-localization with Lamp-2 (an endogenous marker of lysosomes and late endosomes, marked in red) is shown in the overlay. The three replicates gave similar results. Magnification: 600X. The scale bar represents 20 μm .

doi:10.1371/journal.pone.0135873.g002

(Fig 5A–5C). The best results were around 35% recovery for the p.W168X mutation with 0.25 $\mu\text{g/ml}$ of G418, and around 18% recovery for mutation p.R441X after treatment with 2 $\mu\text{g/ml}$ G418 (Fig 5F). Additionally, positive results were obtained for the two *HGSNAT* mutations (p.R203X and p.W403X), the latter showing better results (Fig 5D and 5E), with recovery of around 25% with G418 at 0.5 and 1 $\mu\text{g/ml}$ (Fig 5F). Positive results with gentamicin were also observed for these two *HGSNAT* mutations, with a maximum of 16% recovery for p.W403X with 5 $\mu\text{g/ml}$ of gentamicin (Fig 5F). No recovery was found for the *ARSB* mutations (p.W146X and p.Q503X).

Enzyme activity in transfected COS cells

For mutations for which fibroblasts were not available, the possible recovery of enzyme activity was analysed in COS cells transfected with the mutated cDNA. In particular, for *SMPD1* we

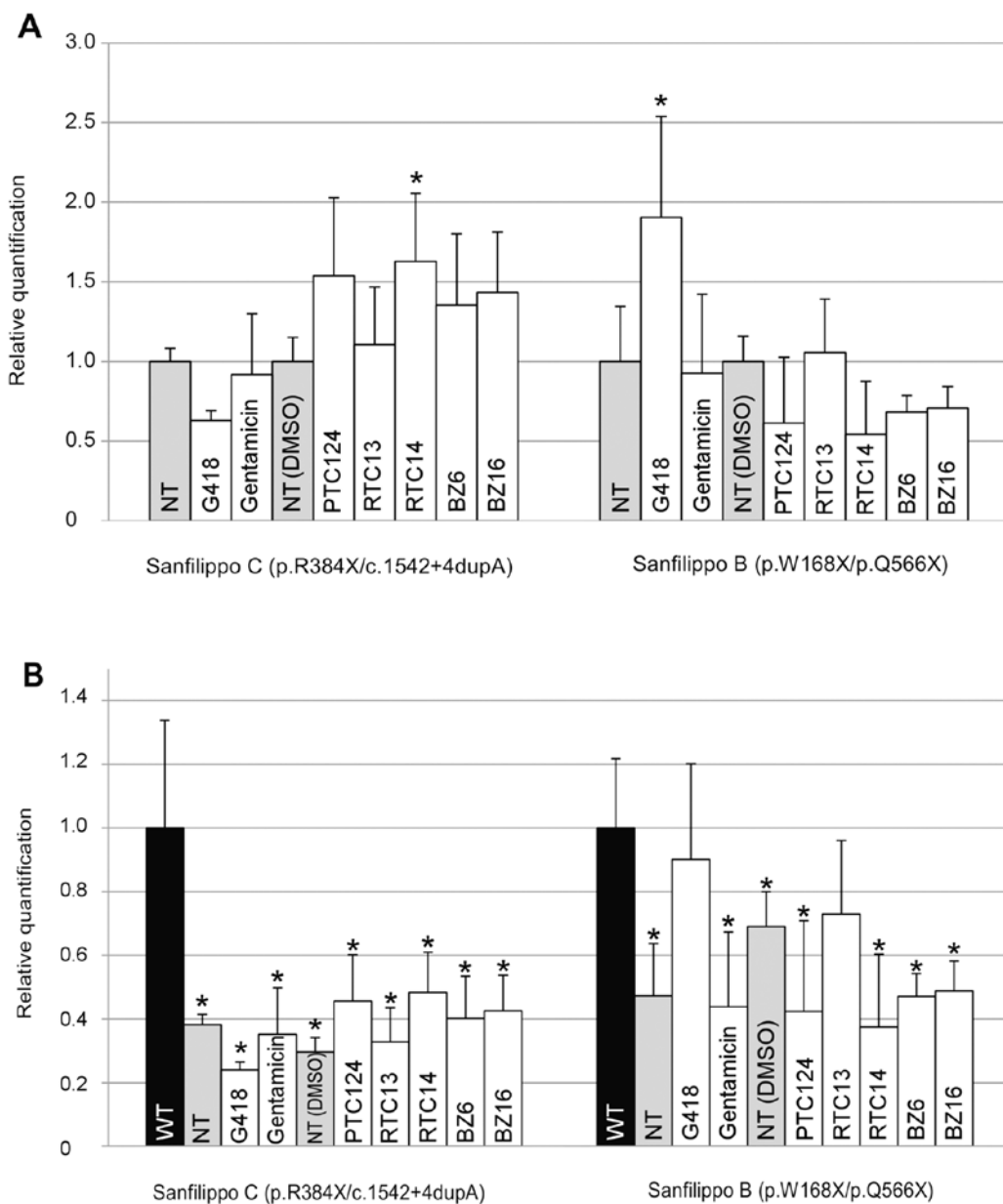


Fig 3. Quantification by qRT-PCR of HGSNAT (Sanfilippo C) and NAGLU (Sanfilippo B) mRNA levels in untreated and treated cultured fibroblasts. The concentrations of the products were G418 (75 µg/ml), gentamicin (300 µg/ml), PTC124 (20 µM), RTC13, RTC14, BZ6 and BZ16 (30 µM). (A) The Y-axis represents the results of the relative quantification of mRNA levels, normalized with respect to the untreated fibroblasts (NT), considered as 1. For PTC124, RTC13, RTC14, BZ6 and BZ16 the untreated samples included dimethyl sulfoxide (DMSO), since these products were dissolved in DMSO. (B) The Y-axis represents the results of the relative quantification of mRNA levels, normalized with respect to the wild-type fibroblasts (black bars). Data represent the mean ± SD of three experiments. Syndromes and genotypes of the different fibroblasts are indicated. * $p < 0.05$, compared to untreated cells (A) or to WT (B). (Note that: only increases in mRNA level were considered and that in part B, the relevant results are those that reached RNA levels similar to those of WT, i.e., that are not significantly different from those of WT.)

doi:10.1371/journal.pone.0135873.g003

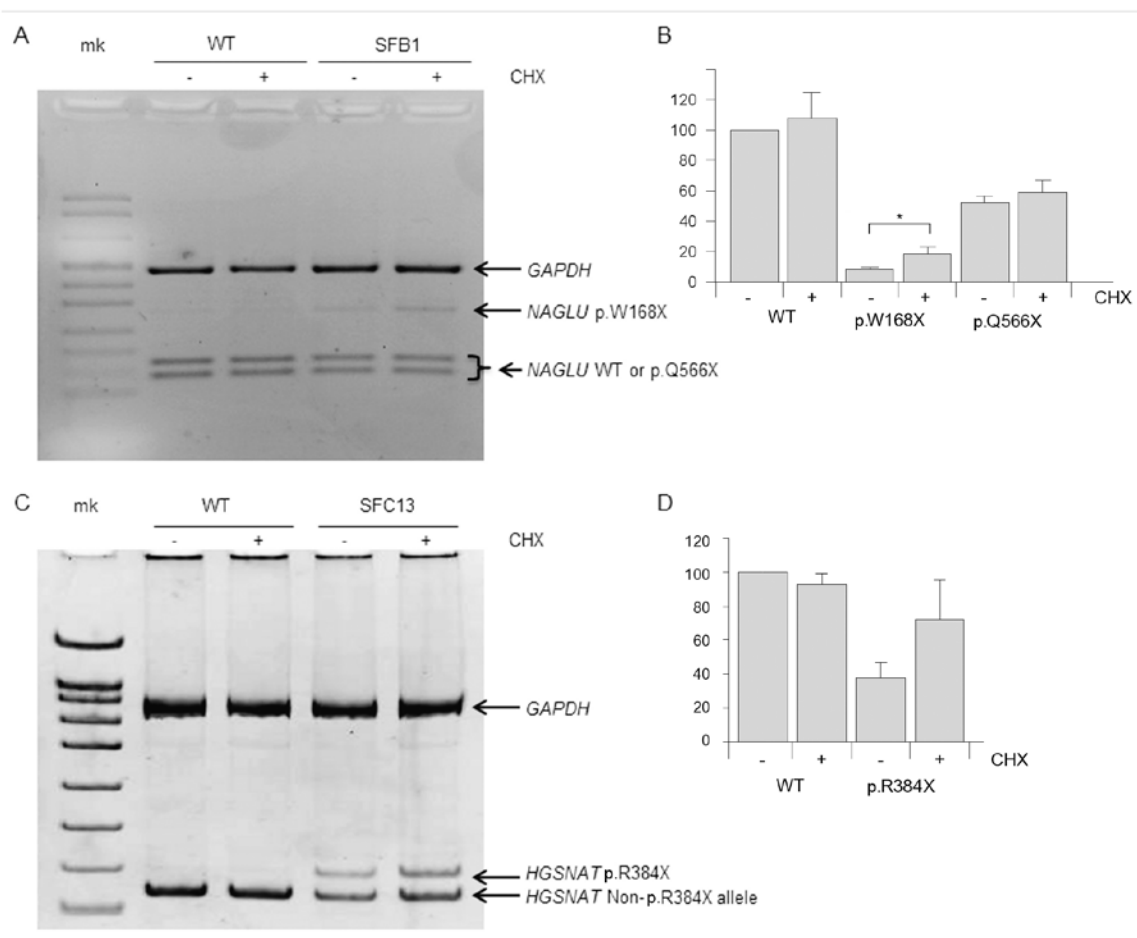


Fig 4. NMD analysis. (A) Agarose gel electrophoresis analysis of a cDNA fragment of the *NAGLU* gene (298-bp long), which includes position c.503 (corresponding to mutation p.W168*), amplified from WT fibroblasts or fibroblasts from patient SFB1 (genotype: p.W168*/p.Q566*), grown in the absence (-) or presence (+) of cycloheximide (CHX) and digested with *BmpI*. Alleles not bearing the mutation (WT or p.Q566*) were digested, yielding two fragments of 162 and 136 bp. GAPDH was used as a control gene. mk: marker. The experiment was repeated three times, one of which is shown. (B) Quantification of the relative amounts of the bands shown in A and in two additional replicates. * = $p < 0.05$. (C) Agarose gel electrophoresis analysis of a cDNA fragment of the *HGSNAT* gene (140-bp long), which includes position c.1150 (corresponding to mutation p.R384*), amplified from WT fibroblasts or fibroblasts from patient SFC13 (genotype: p.R384*/c.1542+4dupA), grown in the absence (-) or presence (+) of cycloheximide (CHX) and digested with *XhoI*. Alleles not bearing the mutation (WT or c.1542+4dupA) were digested, yielding two fragments of 121 and 19 bp (not shown in the gel). GAPDH was used as a control gene. mk: marker. The experiment was repeated three times, one of which is shown. (D) Quantification of the relative amounts of the bands shown in C and in two additional replicates.

doi:10.1371/journal.pone.0135873.g004

analysed the three mutations found in Spanish patients [46]. For *ARSB* and *HGSNAT* we decided to include two mutations from the literature for each gene, predicted to generate either a short or a long truncated protein. For this assay, only gentamicin, geneticin and PTC124 were used. The best results were obtained for the *ARSB* p.W146X mutation with gentamicin, for which an almost two-fold increase was obtained (Fig 6). A positive result for this mutation was also found with PTC124 treatment, although to a lesser extent. A moderate increase in activity (around 20 to 50%, with borderline significance) was found for the following mutations and treatments: *SMPD1* p.W168X treated with G418; *SMPD1* p.Y313X treated with

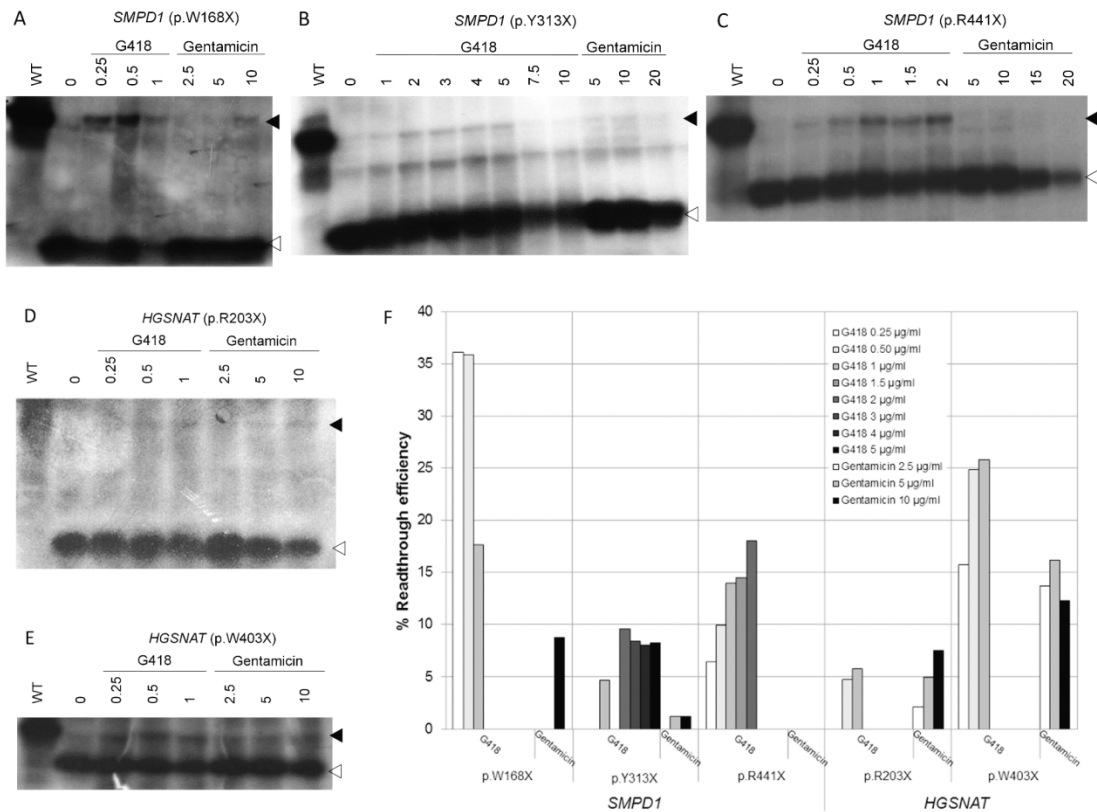


Fig 5. Effect of G418 and gentamicin on in vitro readthrough of nonsense mutations in the *SMPD1* and *HGSNAT* genes in the TNT system. The figure shows representative experiments for the indicated *SMPD1* (A-C) and *HGSNAT* (D-E) nonsense mutations. WT, wild-type construct. Black arrowhead, full-length protein. White arrowhead, truncated protein. Concentrations are in µg/ml. (F) Quantification of the full-length protein synthesized from each mutant construct. The percentage of full-length protein relative to the sum of full-length plus truncated proteins is shown for each aminoglycoside treatment and for the indicated concentration.

doi:10.1371/journal.pone.0135873.g005

gentamicin; *ARSB* p.503X treated with PTC124; and *HGSNAT* p.R203X and p.W403X treated with gentamicin (Fig 6).

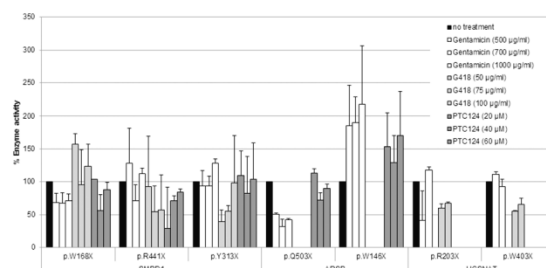


Fig 6. Effect of different readthrough compounds on the enzyme activity in COS cells transfected with cDNAs bearing the indicated nonsense mutation. The results are the mean of at least two experiments performed in duplicate. Pattern codes for compounds and concentrations are indicated in the inset.

doi:10.1371/journal.pone.0135873.g006

Discussion

Correction of nonsense mutations with small molecules that interfere with ribosomal function and alter the translation of mRNA by bypassing PTCs could be an interesting therapeutic option for monogenic diseases caused by this type of DNA mutation. Such correction has been reported as being successful for several diseases and compounds and several studies have validated this strategy using animal models. However, a critical point to be taken into account is whether the efficacy of readthrough is clinically relevant. In this regard, lysosomal storage disorders could be a good option since it has been reported that small amounts of functional protein (5–10% of enzymatic activity) may be considered therapeutically relevant in several LSDs [4]. This same principle applies for ataxia-telangiectasia [9].

Herein we first assayed gentamicin in fibroblasts from three patients, each of them affected by a different lysosomal disease: Sanfilippo B, Sanfilippo C and Maroteaux-Lamy. Only the Maroteaux-Lamy fibroblasts responded to this treatment. For the other two fibroblasts the study was extended using six additional readthrough drugs, with negative results for all compounds. Additionally, mutations for which fibroblasts were not available were analysed both by an *in vitro* transcription/translation system (TNT) and by measuring the enzyme activity in COS transfected cells.

Gentamicin is the most frequent PTC-specific compound used to date. In our study, we found a significant positive result for enzyme activity in the Maroteaux-Lamy fibroblasts. However, due to the small sample sizes, this significance should be considered with caution. This positive result prompted us to perform indirect immunofluorescence studies on these cells, which showed improved trafficking of the mutant protein. For studies at the cDNA level, gentamicin produced some recovery of the full-length protein in the TNT assay and of the enzyme activity in transfected COS cells, for some of the mutations. However, it should be noted that the main recovery of activity of ARSB p.W146X did not correlate with the TNT result for this mutation. This could be due to technical problems encountered with this construct in the TNT assays.

G418 showed good results in the TNT experiments for different mutations. Interestingly, this compound also showed good recovery of the mRNA levels for Sanfilippo B fibroblasts bearing the p.W168X/p.Q566X genotype, although no increase in enzyme activity was observed, suggesting that the missense protein generated by the readthrough was not active. This increase in mRNA levels could be due to improved mutant RNA stability as a consequence of a reduction in NMD efficacy. We were able to demonstrate that the NMD mechanism was partially responsible for the reduction in RNA levels in the alleles bearing nonsense mutations located in the NMD-competent region of the gene. Thus, a possible strategy would be treatment with readthrough drugs, together with NMD inhibitors, as suggested by Bordeira-Carrico et al. [55]. However, the toxicity of the different compounds, including G418, argues against their therapeutic potential. Some authors also found good results for G418 [23,32,56,57].

PTC124 was identified as a readthrough drug over 10 years ago and was reported as non-toxic and orally bioavailable [26]. It appeared as the most promising compound for the correction of nonsense mutations, but there was also controversy about the results. Also, it does not cross the blood–brain barrier efficiently and is a poor candidate for adjunctive readthrough therapy with replacement proteins for LSDs. In the present study, we found some recovery of ARSB activity in transfected COS cells and of RNA levels in one of the Sanfilippo C fibroblasts. The effect of PTC124 on one of the ARSB mutations studied here, p.Q503X, was previously analysed in patients' fibroblasts by Bartolomeo et al. [18], who found no recovery of activity. Whereas Peltz et al. [34], from PTC Therapeutics Inc., consider that there are multiple,

independent demonstrations of Ataluren's (PTC124) nonsense suppressing activity, other authors question this statement. McElroy et al. [33] failed to find evidence of activity for PTC124. The slight effects found in our study are consistent with those who found that this compound is, at least, not as effective as it was claimed when it was discovered. The result of the ongoing clinical trials will be very interesting.

We also assayed several compounds generated at UCLA: RTC13 and RTC14, BZ6 and BZ16 [23,24,52,53]. We found some recovery of RNA levels with RTC14 and BZ16 in Sanfilippo C fibroblasts (particularly with the former). Positive results for RTC13 and RTC14 have been found for numerous mutations in the ATM gene [23], DMD [23,58], and other genes such as collagen VII [9]. BZ16 (a derivative of RTC13) and RTC14 were also shown to increase XPC mRNA expression in skin fibroblasts from xeroderma pigmentosum (Group C) patients [24,53]. Our results are rather modest compared to those published data.

Response to this type of treatment is variable. In general, it is not a very robust response, a fact that was noted in early papers describing "nonsense suppression" in the 1960s. A possible explanation for the variability in the results is the different PTCs involved and the context surrounding them (basically, the fourth nucleotide). The UGA codon followed by a C has been reported to be the best combination for readthrough or efficiency as a STOP codon [37,38]. In the present study, only two out of the 11 mutations had this optimal combination (see Table 1). One of them, *HGSNAT* p.W403X, showed the best results in the TNT assay with gentamicin and G418, and the other one, *ARSB* p.W146X, showed the best recovery of activity in transfected COS cells after treatment with gentamicin and PTC124. Some authors suggest that besides the nucleotide in the 4th position, the first nucleotide 5' of the PTC is also important, with U being more susceptible to promote readthrough, independent of the stop codon itself [59]. In the present study, 2 out of the 11 mutations bear a U in this position (both in the *HGSNAT* gene: p.R203X and p.R384X). While they also carry the UGA stop codon (reported to be the best by several authors), none of them carry the C in the 4th position, which should make them all sub-optimal, according to Floquet et al. [53].

For one of the mutations (*ARSB* p.W322X) we showed a significant increase in protein level after gentamicin treatment, through immunofluorescence studies in fibroblasts from a patient who bore a null mutation in the other allele. This experiment also showed that the protein was in the expected location within the cell, i.e. the lysosomes, through colocalisation analyses using the lysosomal marker Lamp-2. Few studies on readthrough drugs have used this type of technique to validate the correction [23,24]. In the case of lysosomal diseases, Bartolomeo et al. [18] analysed the reduction in lysosomal size in Maroteaux-Lamy fibroblasts after treatment with PTC124. However, the data were obtained by electron microscopy and no information on the protein was available. It should be noted that, despite the increased *ARSB* protein signal that was observed in the lysosome after gentamicin treatment, we did not detect a corresponding increase in enzyme activity. It could be speculated that the protein generated by readthrough is an inactive missense variant, albeit with improved folding that allows its trafficking to the lysosome.

As a summary of the relevant findings of this study, we found positive results for *ARSB* activity and enzyme localization in Maroteaux-Lamy fibroblasts treated with gentamicin. Additionally, an increase of mRNA levels was obtained with several products in Sanfilippo B and Sanfilippo C fibroblasts, although no enzyme activity recovery was observed. Using the *in vitro* TNT system the best result was obtained for the p.W168X mutation of the *SMPD1* gene treated with G418, reaching a 35% recovery of the full-length protein. Finally, gentamicin treatment of COS cells transfected with mutant *ARSB* cDNA carrying the p.W146X mutation showed a recovery of enzyme activity of around two-fold.

In general, our results and those of others on readthrough treatment for nonsense mutations show a certain degree of recovery either in protein levels, mRNA levels or enzyme activity. The results are sometimes inconsistent between groups, mutations, compounds and techniques. However, the positive results are promising and, in some cases, they have led to clinical trials, the results of which will have important implications for the field. The small molecule readthrough (SMRT) chemicals also hold promise for systemic use, including for treatment of central nervous system involvement. Novel compounds are being generated by different groups in the search for more efficient and less toxic drugs. The fact that slight recovery of protein levels could be enough to cure these diseases, and that any good compound could be used for many diseases, is sufficient to encourage further research.

Acknowledgments

We thank B. Pérez, L.R. Desviat, G. Egea, L. Rodriguez-Pascau, and I. Canals for assistance and advice in setting up the different techniques and the Institut de Bioquímica Clínica for their collaboration. The authors are also grateful for the support of the *Centro de Investigación Biomédica en Red de Enfermedades Raras* (CIBERER), which is an initiative of the ISCIII. We are also grateful for the permanent support, from 'patient-support' associations, such as Jonah's Just Begun-Foundation to Cure Sanfilippo Inc. (USA), Association Sanfilippo Sud (France), Fundación Stop Sanfilippo (Spain), Asociación MPS España (Spain), APRAT (A-T, France), and A-T Ease (A-T, New York, USA).

Author Contributions

Conceived and designed the experiments: MGG EG BC DG LV. Performed the experiments: MGG EG MC VRS. Analyzed the data: CD CA RAG BC DG LV. Contributed reagents/materials/analysis tools: VRS CD RAG. Wrote the paper: MGG DG LV.

References

1. Boustany RM (2013) Lysosomal storage diseases—the horizon expands. *Nat Rev Neurol* 9:583–598. doi: [10.1038/nrneurol.2013.163](https://doi.org/10.1038/nrneurol.2013.163) PMID: [23938739](https://pubmed.ncbi.nlm.nih.gov/23938739/)
2. Lee HL, Dougherty JP (2012) Pharmaceutical therapies to recode nonsense mutations in inherited diseases. *Pharmacol Ther* 136:227–266. doi: [10.1016/j.pharmthera.2012.07.007](https://doi.org/10.1016/j.pharmthera.2012.07.007) PMID: [22820013](https://pubmed.ncbi.nlm.nih.gov/22820013/)
3. Keeling KM, Xue X, Gunn G, Bedwell DM (2014) Therapeutics based on stop codon readthrough. *Annu Rev Genomics Hum Genet* 15: 371–394. doi: [10.1146/annurev-genom-091212-153527](https://doi.org/10.1146/annurev-genom-091212-153527) PMID: [24773318](https://pubmed.ncbi.nlm.nih.gov/24773318/)
4. Neufeld EF, Muenzer J (2001) The mucopolysaccharidoses. In: Scriver CR, Beaudet AL, Sly WS, Valle D, eds. *The metabolic and molecular bases of inherited disease*, 8th edn, Vol. 3. New York: McGraw-Hill: 3421–3452.
5. Fan X, Zhang H, Zhang S, Bagshaw RD, Tropak MB, Callahan JW, et al. (2006) Identification of the gene encoding the enzyme deficient in mucopolysaccharidosis IIIC (Sanfilippo disease type C). *Am J Hum Genet* 79:738–744. PMID: [16960811](https://pubmed.ncbi.nlm.nih.gov/16960811/)
6. Hrebicek M, Mrazova L, Seyrantepe V, Durand S, Roslin NM, Nosková L, et al. (2006) Mutations in TMEM76* cause mucopolysaccharidosis IIIC (Sanfilippo C syndrome). *Am J Hum Genet* 79:807–819. PMID: [17033958](https://pubmed.ncbi.nlm.nih.gov/17033958/)
7. Klein U, Kresse H, von Figura K (1978) Sanfilippo syndrome type C: deficiency of acetyl-CoA:alpha-glucosaminide N-acetyltransferase in skin fibroblasts. *Proc Natl Acad Sci U S A* 75:5185–5189. PMID: [33384](https://pubmed.ncbi.nlm.nih.gov/33384/)
8. Schuchman EH and Desnick RJ (2001) Niemann-Pick disease types A and B: acid sphingomyelinase deficiencies. In: Scriver CR, Beaudet AL, Sly WS, Valle D, eds. *The metabolic and molecular bases of inherited disease*, 8th edn, Vol. 3. New York: McGraw-Hill: 3589–3610.
9. Gatti RA (2012) SMRT compounds correct nonsense mutations in primary immunodeficiency and other genetic models. *Ann N Y Acad Sci* 1250:33–40. doi: [10.1111/j.1749-6632.2012.06467.x](https://doi.org/10.1111/j.1749-6632.2012.06467.x) PMID: [22364446](https://pubmed.ncbi.nlm.nih.gov/22364446/)

10. Howard M, Frizzell RA, Bedwell DM (1996) Aminoglycoside antibiotics restore CFTR function by overcoming premature stop mutations. *Nat Med* 2:467–469. PMID: [8597960](#)
11. Barton-Davis ER, Cordier L, Shoturma DI, Leland SE, Sweeney HL (1999) Aminoglycoside antibiotics restore dystrophin function to skeletal muscles of mdx mice. *J Clin Invest* 104:375–381. PMID: [10449429](#)
12. Nudelman I, Glikin D, Smolkin B, Hainrichson M, Belakhov V, Baasov T (2010) Repairing faulty genes by aminoglycosides: development of new derivatives of geneticin (G418) with enhanced suppression of diseases-causing nonsense mutations. *Bioorg Med Chem* 18:3735–3746. doi: [10.1016/j.bmc.2010.03.060](#) PMID: [20409719](#)
13. Bidou L, Allamand V, Rousset JP, Namy O (2012) Sense from nonsense: therapies for premature stop codon diseases. *Trends Mol Med* 18:679–688. doi: [10.1016/j.molmed.2012.09.008](#) PMID: [23083810](#)
14. Keeling KM, Brooks DA, Hopwood JJ, Li P, Thompson JN, Bedwell DM (2001) Gentamicin-mediated suppression of Hurler syndrome stop mutations restores a low level of alpha-L-iduronidase activity and reduces lysosomal glycosaminoglycan accumulation. *Hum Mol Genet* 10:291–299. PMID: [11159948](#)
15. Hein LK, Bawden M, Muller VJ, Silience D, Hopwood JJ, Brooks DA (2004) alpha-L-iduronidase premature stop codons and potential read-through in mucopolysaccharidosis type I patients. *J Mol Biol* 338:453–462. PMID: [15081804](#)
16. Brooks DA, Muller VJ, Hopwood JJ (2006) Stop-codon read-through for patients affected by a lysosomal storage disorder. *Trends Mol Med* 12:367–373. PMID: [16798086](#)
17. Wang D, Belakhov V, Kandasamy J, Baasov T, Li SC, Li YT, et al. (2012). The designer aminoglycoside NB84 significantly reduces glycosaminoglycan accumulation associated with MPS I-H in the Idua-W392X mouse. *Mol Genet Metab* 105:116–125. doi: [10.1016/j.ymgme.2011.10.005](#) PMID: [22056610](#)
18. Bartolomeo R, Polishchuk EV, Volpi N, Polishchuk RS, Auricchio A (2013) Pharmacological read-through of nonsense ARSB mutations as a potential therapeutic approach for mucopolysaccharidosis VI. *J Inher Metab Dis* 36:363–371. doi: [10.1007/s10545-012-9521-y](#) PMID: [22971959](#)
19. Gunn G, Dai Y, Du M, Belakhov V, Kandasamy J, Schoeb TR, et al. (2014) Long-term nonsense suppression therapy moderates MPS I-H disease progression. *Mol Genet Metab* 111:374–381. doi: [10.1016/j.ymgme.2013.12.007](#) PMID: [24411223](#)
20. Du M, Keeling KM, Fan L, Liu X, Kovacs T, Sorscher E, et al. (2006) Clinical doses of amikacin provide more effective suppression of the human CFTR-G542X stop mutation than gentamicin in a transgenic CF mouse model. *J Mol Med (Berl)* 84:573–582.
21. Mattis VB, Rai R, Wang J, Chang CW, Coady T, Lorson CL (2006) Novel aminoglycosides increase SMN levels in spinal muscular atrophy fibroblasts. *Hum Genet* 120:589–601. PMID: [16951947](#)
22. Buck NE, Wood L, Hu R, Peters HL (2009) Stop codon read-through of a methylmalonic aciduria mutation. *Mol Genet Metab* 97:244–249. doi: [10.1016/j.ymgme.2009.04.004](#) PMID: [19427250](#)
23. Du L, Damoiseaux R, Nahas S, Gao K, Hu H, Pollard JM, et al. (2009) Nonaminoglycoside compounds induce readthrough of nonsense mutations. *J Exp Med* 206:2285–2297. doi: [10.1084/jem.20081940](#) PMID: [19770270](#)
24. Jung ME, Ku JM, Du L, Hu H, Gatti RA (2011) Synthesis and evaluation of compounds that induce readthrough of premature termination codons. *Bioorg Med Chem Lett* 21:5842–5848. doi: [10.1016/j.bmcl.2011.07.107](#) PMID: [21873052](#)
25. Nudelman I, Rebibo-Sabbah A, Cherniavsky M, Belakhov V, Hainrichson M, Chen F, et al. (2009) Development of novel aminoglycoside (NB54) with reduced toxicity and enhanced suppression of disease-causing premature stop mutations. *J Med Chem* 52:2836–2845. doi: [10.1021/jm801640k](#) PMID: [19309154](#)
26. Welch EM, Barton ER, Zhuo J, Tomizawa Y, Friesen WJ, Trifillis P, et al. (2007) PTC124 targets genetic disorders caused by nonsense mutations. *Nature* 447:87–91. PMID: [17450125](#)
27. Du M, Liu X, Welch EM, Hirawat S, Peltz SW, Bedwell DM (2008) PTC124 is an orally bioavailable compound that promotes suppression of the human CFTR-G542X nonsense allele in a CF mouse model. *Proc Natl Acad Sci U S A* 105:2064–2069. doi: [10.1073/pnas.0711795105](#) PMID: [18272502](#)
28. Finkel RS (2010) Read-through strategies for suppression of nonsense mutations in Duchenne/Becker muscular dystrophy: aminoglycosides and ataluren (PTC124). *J Child Neurol* 25:1158–1164. doi: [10.1177/0883073810371129](#) PMID: [20519671](#)
29. Goldmann T, Overlack N, Wolfrum U, Nagel-Wolfrum K (2011) PTC124-mediated translational read-through of a nonsense mutation causing Usher syndrome type 1C. *Hum Gene Ther* 22:537–547. doi: [10.1089/hum.2010.067](#) PMID: [21235327](#)
30. Tan L, Narayan SB, Chen J, Meyers GD, Bennett MJ (2011) PTC124 improves readthrough and increases enzymatic activity of the CPT1A R160X nonsense mutation. *J Inher Metab Dis* 34:443–447. doi: [10.1007/s10545-010-9265-5](#) PMID: [21253826](#)

31. Dranchak PK, Di Pietro E, Snowden A, Oesch N, Braverman NE, Steinberg SJ, et al. (2011) Nonsense suppressor therapies rescue peroxisome lipid metabolism and assembly in cells from patients with specific PEX gene mutations. *J Cell Biochem* 112:1250–1258. doi: [10.1002/jcb.22979](https://doi.org/10.1002/jcb.22979) PMID: [21465523](https://pubmed.ncbi.nlm.nih.gov/21465523/)
32. Sanchez-Alcudia R, Perez B, Ugarte M, Desviat LR (2012) Feasibility of nonsense mutation readthrough as a novel therapeutical approach in propionic acidemia. *Hum Mutat* 33:973–980. doi: [10.1002/humu.22047](https://doi.org/10.1002/humu.22047) PMID: [22334403](https://pubmed.ncbi.nlm.nih.gov/22334403/)
33. McElroy SP, Nomura T, Torrie LS, Warbrick E, Gartner U, Wood G, et al. (2013) A lack of premature termination codon read-through efficacy of PTC124 (Ataluren) in a diverse array of reporter assays. *PLoS Biol* 11:e1001593. doi: [10.1371/journal.pbio.1001593](https://doi.org/10.1371/journal.pbio.1001593) PMID: [23824517](https://pubmed.ncbi.nlm.nih.gov/23824517/)
34. Peltz SW, Morsy M, Welch EM, Jacobson A (2013) Ataluren as an agent for therapeutic nonsense suppression. *Annu Rev Med* 64:407–425. doi: [10.1146/annurev-med-120611-144851](https://doi.org/10.1146/annurev-med-120611-144851) PMID: [23215857](https://pubmed.ncbi.nlm.nih.gov/23215857/)
35. Gregory-Evans CY, Wang X, Wasan KM, Zhao J, Metcalfe AL, Gregory-Evans K (2014) Postnatal manipulation of Pax6 dosage reverses congenital tissue malformation defects. *J Clin Invest* 124:111–116. doi: [10.1172/JCI70462](https://doi.org/10.1172/JCI70462) PMID: [24355924](https://pubmed.ncbi.nlm.nih.gov/24355924/)
36. Howard MT, Shirts BH, Petros LM, Flanigan KM, Gesteland RF, Atkins JF (2000) Sequence specificity of aminoglycoside-induced stop codon readthrough: potential implications for treatment of Duchenne muscular dystrophy. *Ann Neurol* 48:164–169. PMID: [10939566](https://pubmed.ncbi.nlm.nih.gov/10939566/)
37. Manuvakhova M, Keeling K, Bedwell DM (2000) Aminoglycoside antibiotics mediate context-dependent suppression of termination codons in a mammalian translation system. *RNA* 6:1044–1055. PMID: [10917599](https://pubmed.ncbi.nlm.nih.gov/10917599/)
38. Bidou L, Hatin I, Perez N, Allamand V, Panthier JJ, Rousset JP (2004) Premature stop codons involved in muscular dystrophies show a broad spectrum of readthrough efficiencies in response to gentamicin treatment. *Gene Ther* 11:619–627. PMID: [14973546](https://pubmed.ncbi.nlm.nih.gov/14973546/)
39. Allamand V, Bidou L, Arakawa M, Floquet C, Shiozuka M, Paturneau-Jouas M, et al. (2008) Drug-induced readthrough of premature stop codons leads to the stabilization of laminin alpha2 chain mRNA in CMD myotubes. *J Gene Med* 10:217–224. PMID: [18074402](https://pubmed.ncbi.nlm.nih.gov/18074402/)
40. Bellais S, Le Goff C, Dagoneau N, Munnich A, Cormier-Daire V (2010) In vitro readthrough of termination codons by gentamycin in the Stuve-Wiedemann Syndrome. *Eur J Hum Genet* 18:130–132. doi: [10.1038/ejhg.2009.122](https://doi.org/10.1038/ejhg.2009.122) PMID: [19603067](https://pubmed.ncbi.nlm.nih.gov/19603067/)
41. Garrido E, Chabas A, Coll MJ, Blanco M, Dominguez C, Grinberg D, et al. (2007) Identification of the molecular defects in Spanish and Argentinian mucopolysaccharidosis VI (Maroteaux-Lamy syndrome) patients, including 9 novel mutations. *Mol Genet Metab* 92:122–130. PMID: [17643332](https://pubmed.ncbi.nlm.nih.gov/17643332/)
42. Coll MJ, Anton C, Chabas A (2001) Allelic heterogeneity in Spanish patients with Sanfilippo disease type B. Identification of eight new mutations. *J Inher Metab Dis* 24:83–84. PMID: [11286389](https://pubmed.ncbi.nlm.nih.gov/11286389/)
43. Matalonga L, Arias A, Coll MJ, Garcia-Villoria J, Gort L, et al. (2014) Treatment effect of coenzyme Q and an antioxidant cocktail in fibroblasts of patients with Sanfilippo disease. *J Inher Metab Dis* 37:439–446. doi: [10.1007/s10545-013-9668-1](https://doi.org/10.1007/s10545-013-9668-1) PMID: [24347096](https://pubmed.ncbi.nlm.nih.gov/24347096/)
44. Voskoboeva E, Krasnopol'skaia KD, Peters K, von Figura K (2000) Identification of mutations in the arylsulfatase B gene in Russian mucopolysaccharidosis type VI patients. *Genetika* 36:837–843. PMID: [10923267](https://pubmed.ncbi.nlm.nih.gov/10923267/)
45. Villani GR, Balzano N, Vitale D, Saviano M, Pavone V, Di Natale P (1999) Maroteaux-Lamy syndrome: five novel mutations and their structural localization. *Biochim Biophys Acta* 1453:185–192. PMID: [10036316](https://pubmed.ncbi.nlm.nih.gov/10036316/)
46. Rodríguez-Pascual L, Gort L, Schuchman EH, Vilageliu L, Grinberg D, Chabás A (2009) Identification and characterization of SMPD1 mutations causing Niemann-Pick types A and B in Spanish patients. *Hum Mutat* 30:1117–1122. doi: [10.1002/humu.21018](https://doi.org/10.1002/humu.21018) PMID: [19405096](https://pubmed.ncbi.nlm.nih.gov/19405096/)
47. Schuchman EH (1995) Two new mutations in the acid sphingomyelinase gene causing type a Niemann-pick disease: N389T and R441X. *Hum Mutat* 6:352–354. PMID: [8680412](https://pubmed.ncbi.nlm.nih.gov/8680412/)
48. Ruijter GJ, Valstar MJ, van de Kamp JM, van der Helm RM, Durand S, van Diggelen OP, et al. (2008) Clinical and genetic spectrum of Sanfilippo type C (MPS IIIC) disease in The Netherlands. *Mol Genet Metab* 93:104–111. PMID: [18024218](https://pubmed.ncbi.nlm.nih.gov/18024218/)
49. Ouesleti S, Brunel V, Ben Turkia H, Dranguet H, Miled A, Miladi N, et al. (2011) Molecular characterization of MPS IIIA, MPS IIIB and MPS IIIC in Tunisian patients. *Clin Chim Acta* 412:2326–2331. doi: [10.1016/j.cca.2011.08.032](https://doi.org/10.1016/j.cca.2011.08.032) PMID: [21910976](https://pubmed.ncbi.nlm.nih.gov/21910976/)
50. Matos L, Canals I, Dridi L, Choi Y, Prata M, et al. (2014) Therapeutic strategies based on modified U1 snRNAs and chaperones for Sanfilippo C splicing mutations. *Orphanet J Rare Dis* 9:180. doi: [10.1186/s13023-014-0180-y](https://doi.org/10.1186/s13023-014-0180-y) PMID: [25491247](https://pubmed.ncbi.nlm.nih.gov/25491247/)

51. Garrido E, Cormand B, Hopwood JJ, Chabas A, Grinberg D, Vilageliu L (2008) Maroteaux-Lamy syndrome: functional characterization of pathogenic mutations and polymorphisms in the arylsulfatase B gene. *Mol Genet Metab* 94:305–312. doi: [10.1016/j.ymgme.2008.02.012](https://doi.org/10.1016/j.ymgme.2008.02.012) PMID: [18406185](https://pubmed.ncbi.nlm.nih.gov/18406185/)
52. Du L, Jung ME, Damoiseaux R, Completo G, Fike F, Ku JM, et al. (2013) A new series of small molecular weight compounds induce read through of all three types of nonsense mutations in the ATM gene. *Mol Ther* 21:1653–1660. doi: [10.1038/mt.2013.150](https://doi.org/10.1038/mt.2013.150) PMID: [23774824](https://pubmed.ncbi.nlm.nih.gov/23774824/)
53. Kuschal C, Digiovanna JJ, Khan SG, Gatti RA, Kraemer KH (2013) Repair of UV photolesions in xeroderma pigmentosum group C cells induced by translational readthrough of premature termination codons. *Proc Natl Acad Sci U S A* 110:19483–19488. doi: [10.1073/pnas.1312088110](https://doi.org/10.1073/pnas.1312088110) PMID: [24218596](https://pubmed.ncbi.nlm.nih.gov/24218596/)
54. de Winter JCF (2013) Using the Student t-test with extremely small sample sizes. *Prac Assess Res Eval* 18:1–12.
55. Bordeira-Carrico R, Pego AP, Santos M, Oliveira C (2012) Cancer syndromes and therapy by stop-codon readthrough. *Trends Mol Med* 18:667–678. doi: [10.1016/j.molmed.2012.09.004](https://doi.org/10.1016/j.molmed.2012.09.004) PMID: [23044248](https://pubmed.ncbi.nlm.nih.gov/23044248/)
56. Lai CH, Chun HH, Nahas SA, Mitui M, Gamo KM, Du L, et al. (2004) Correction of ATM gene function by aminoglycoside-induced read-through of premature termination codons. *Proc Natl Acad Sci U S A* 101:15676–15681. PMID: [15498871](https://pubmed.ncbi.nlm.nih.gov/15498871/)
57. Floquet C, Deforges J, Rousset JP, Bidou L (2011) Rescue of non-sense mutated p53 tumor suppressor gene by aminoglycosides. *Nucleic Acids Res* 39:3350–3362. doi: [10.1093/nar/gkq1277](https://doi.org/10.1093/nar/gkq1277) PMID: [21149266](https://pubmed.ncbi.nlm.nih.gov/21149266/)
58. Kayali R, Ku JM, Khitrov G, Jung ME, Prikhodko O, Bertoni C (2012) Read-through compound 13 restores dystrophin expression and improves muscle function in the mdx mouse model for Duchenne muscular dystrophy. *Hum Mol Genet* 21:4007–4020. doi: [10.1093/hmg/dds223](https://doi.org/10.1093/hmg/dds223) PMID: [22692682](https://pubmed.ncbi.nlm.nih.gov/22692682/)
59. Floquet C, Hatin I, Rousset JP, Bidou L (2012) Statistical analysis of readthrough levels for nonsense mutations in mammalian cells reveals a major determinant of response to gentamicin. *PLoS Genet* 8:e1002608. doi: [10.1371/journal.pgen.1002608](https://doi.org/10.1371/journal.pgen.1002608) PMID: [22479203](https://pubmed.ncbi.nlm.nih.gov/22479203/)